ISSN: 2152-7385 Volume 10, Number 6, June 2019

Scientific Research Publishing

Applied Mathematics

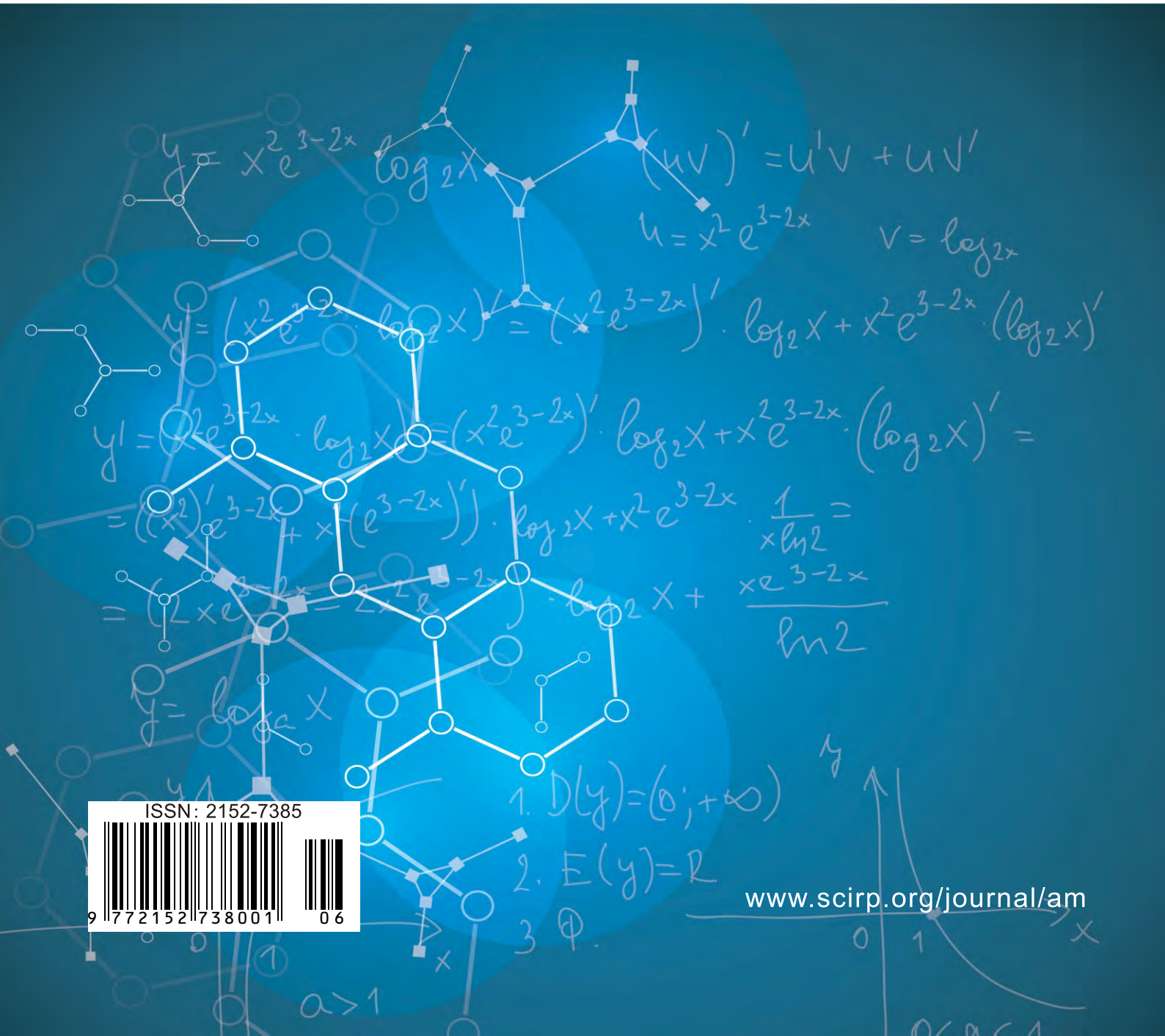

Journal Editorial Board

ISSN Print: 2152-7385 ISSN Online: 2152-7393

http://www.scirp.org/journal/am

Editorial Board

Scientific Research Publishing

Applied Mathematics, 2019, 10, 371-512
http://www.scirp.org/journal/am
ISSN Online: 2152-7393
ISSN Print: 2152-7385

Table of Contents

Volume 10 Number 6 June 2019

Applied Mathematics (AM)
Journal Information

SUBSCRIPTIONS

The *Applied Mathematics* (Online at Scientific Research Publishing, www.SciRP.org) is published monthly by Scientific Research Publishing, Inc., USA.

Subscription rates:
Print: $89 per copy.
To subscribe, please contact Journals Subscriptions Department, E-mail: sub@scirp.org

SERVICES

Advertisements
Advertisement Sales Department, E-mail: service@scirp.org

Reprints (minimum quantity 100 copies)
Reprints Co-ordinator, Scientific Research Publishing, Inc., USA.
E-mail: sub@scirp.org

COPYRIGHT

PRODUCTION INFORMATION

For manuscripts that have been accepted for publication, please contact:
E-mail: am@scirp.org

Applied Mathematics, 2019, 10, 371-382
http://www.scirp.org/journal/am
ISSN Online: 2152-7393
ISSN Print: 2152-7385

On the Deepest Fallacy in the History of Mathematics: The Denial of the Postulate about the Approximation Nature of a Simple-Iteration Method and Iterative Derivation of Cramer's Formulas

Albert Iskhakov[1], Sergey Skovpen[2]

[1]Department of Innovation Development, Joint Company "Research and Production Corporation 'Space Monitoring Systems, Information & Control and Electromechanical Complexes' named after A.G. Iosifian", Moscow, Russia
[2]Department of Ship Electricity and Automatics, Northern (Arctic) Federal University, Severodvinsk, Russia
Email: asimath@bk.ru, skovpensm@mail.ru

How to cite this paper: Iskhakov, A. and Skovpen, S. (2019) On the Deepest Fallacy in the History of Mathematics: The Denial of the Postulate about the Approximation Nature of a Simple-Iteration Method and Iterative Derivation of Cramer's Formulas. *Applied Mathematics*, **10**, 371-382.
https://doi.org/10.4236/am.2019.106027

Received: May 5, 2019
Accepted: June 14, 2019
Published: June 17, 2019

Abstract

Contrary to the opinion about approximation nature of a simple-iteration method, the exact solution of a system of linear algebraic equations (SLAE) in a finite number of iterations with a stationary matrix is demonstrated. We present a theorem and its proof that confirms the possibility to obtain the finite process and imposes the requirement for the matrix of SLAE. This matrix must be unipotent, *i.e.* all its eigenvalues to be equal to 1. An example of transformation of SLAE given analytically to the form with a unipotent matrix is presented. It is shown that splitting the unipotent matrix into identity and nilpotent ones results in Cramer's analytical formulas in a finite number of iterations.

Keywords

System of Linear Algebraic Equations (SLAE), Nilpotent Matrix, Unipotent Matrix, Eigenvalue Assignment, Finite Iterative Process, Cramer's Formulas

1. Introduction

The mathematical community considers that a simple-iteration method expressed as a linear difference equation with a stationary matrix for solving a system of linear algebraic equations (SLAE) is approximate because it does not give the exact answer for a finite number of iterations.

Examples of direct statements are:

"Iterative methods give a tool to obtain an approximate solution of a system of linear equations" (Faddeev D.K., Faddeeva V.N.) [1].

"… iterative methods that allow the roots of a system to be obtained with a given accuracy via converging infinite processes" (Demidovich B.P., Maron I.A.) [2].

"The main difference of iteration methods from direct ones consists that iteration methods give an exact solution to Equation (1) only as a limit of sequence of iterative approximations" Samarskii A.A. [3].

"Application of iterative method does not allow an exact solution to be reached …" (Strang G.) [4].

"Iterative methods for solving (1) are infinite methods which find only approximate solutions" (Rice J.R.) [5].

"… iterative methods do not frequently give an exact solution in a finite number of steps" (Demmel W.J.) [6].

"Iterative methods do not give strictly exact solution, as it is attained as a limit of a sequence of vectors" (Pirumov U.G.) [7].

"For iterative methods, *i.e.* for methods in which an exact solution can be obtained only as a result of an infinite repetition of uniform (as a rule, simple) operations …" (Verzhbitskii V.M.) [8].

"… iterative methods give a sequence of approximations which (one can hope) converges to the genuine solutions of the problem" (Watkins D.S.) [9].

"Iterative methods are approximate methods which find solutions of systems by means of infinite converging processes" (Shevtsov G.S., Kryukova O.G., Myznikova B.E.) [10].

The above statement taken from [3] has the following continuation: "The exception is methods of 'finite' iterations, which include methods of conjugate directions that, theoretically, enable the exact solution to be found in a finite number of operations for any initial guess …". This only emphasizes the authors' viewpoint that the exact solution of an SLAE cannot be obtained via iterations with a stationary matrix. In this way, these methods are contrasted with non-stationary methods that provide the exact solution in a finite number of steps. Similar reasoning can be found in other publications, for example, in [8] we read: "… the conjugate gradient method being essentially iterative should actually be referred to direct methods, because it is proved that with its help … the solution of a linear system is achieved in no more than n steps for any initial vector".

Indeed, as it can be found in numerous schoolbooks and monographs as well as in Internet, it is generally accepted to divide methods for solving SLAE into direct and iterative ones and to match them with exact and approximate methods with stationary matrix. This reflects the point of view on approximation nature of iterative methods.

These opinions can be briefly and clearly expressed for a wide audience as follows: for an analytically given second-order SLAE, the solution in the form of

Cramer's formulas cannot be obtained by a simple-iteration method.

For an arbitrary SLAE, we call this thesis the postulate about approximation nature.

2. Problem Statement

The paradox is that the postulate, which denies the possibility of obtaining a finite iterative process in a system with a stationary matrix, does not reflect the real situation for a very long time.

The fact is that in control theory, where for a linear discrete system characterized by the same equation, the method of achieving a given state in a finite number of steps has been known since the middle of the last century [10]-[19]. A brief history on finite processes, which have been called "deadbeat", is presented in [19]. For a system described in the input-output relations, the finite processes are achieved if the coefficients of the characteristic polynomial are equal to zero. For a control system defined in the state space and characterized by a matrix of coefficients, the process of moving terminates in a finite number of steps if the matrix is nilpotent. Such a matrix is obtained by transformation of the original system matrix into Frobenius form and then the row with characteristic polynomial coefficients is reduced to zero (except for sign) by adding a row of coefficients having the same values with opposite signs. These coefficients are produced in the system's feedback loop.

Generally, this method can be applied to iterative solution of an SLAE, but only in a homogeneous case, *i.e.* to reduce the error to zero for a finite number of iterations that probably was the reason of his unknown for algebraists.

Thus, it should be assumed that from the standpoint of control theory, for a homogeneous SLAE, the postulate is refuted, while for a non-homogeneous one there is no proof.

The aim of this work is to refute the postulate about approximation nature of a simple-iteration method applied to a non-homogeneous SLAE. The proof is given and accompanied by an example of obtaining an exact solution of a second-order SLAE in the form of Cramer's formulas in two iterations.

3. Methodology

To achieve the goal, we have developed an alternative method for controlling the spectrum of a matrix without transforming the matrix to the Frobenius form for which the row of the characteristic polynomial coefficients needs to be obtained except for sign. The main advantage of the method is the possibility to produce the spectrum equal to a given set of eigenvalues not only by perturbation of an autonomous matrix, but also in the case when the matrix is multiplied by a vector and added to another vector in the composition of algebraic, difference and differential equations.

Setting a zero spectrum for a difference equation gives a nilpotent matrix. The back conversion of an iterative system to algebraic one forms a unipotent matrix. The direct link between those matrix means that the condition for solving an

SLAE for a finite number of iterations is the transformation of system matrix to the form, in which all eigenvalues are equal to 1. An example is the Gauss method, where a triangular matrix with a unit diagonal (or unitriangular) is split into an identity matrix and strictly triangular matrix, which is nilpotent. In this regard, the solution process known as back substitution can be formally considered as an iterative process with a sparse matrix, which is not required to be multiplied by a vector. At each step, only one component of the solution vector is determined. In practice, this is done without any mention about the iterative nature of the process.

In the proposed method, the transformation gives a nilpotent matrix but does not change the density of the matrix of an original SLAE. Actually, the iterative procedure of solution (it may also be considered as back substitution) contains the operation of multiplying a matrix by a vector, and all the entries of the solution vector are obtained at the final step. The maximum number of steps does not exceed the order of the matrix.

4. Brief Background

The method evolution is described in more detail in [20]. The first result in the form of a two-step converging process in a second-order linear discrete system was obtained in 2001 when we were developing an advanced deadbeat control algorithm for a technical device. The purpose of the algorithm was to eliminate the transformation of the matrix to the Frobenius form, which is necessary in the well-known method and requires extra time or additional hardware. This was accomplished through a special type of a feedback in which the first difference of the state vector was used instead of the vector itself. The equation of motion expressed in such form has been formally representing a particular case of the canonical form of a two-layer iterative method.

To find eigenvalues of a matrix, a novel transformation based on the dependencies between the elements of the matrix and its spectrum has been developed. This transformation enabled the elements of the feedback vector to be found for setting desired spectrum. This was how the engineering problem of synthesizing a deadbeat controller was solved for a wide class of technical devices such as semiconductor power converters that are widely used in almost all areas of human activity.

Later it turned out that new methods allowed us to use them not only in control theory to implement control algorithms for technical systems, but also to obtain a qualitatively new effect in mathematics, which refutes the postulate about the approximation nature of a simple-iteration method for solving SLAE.

The basics of the method for transforming a matrix spectrum were expounded in [21] [22]. The method for solving a linear difference equation in a finite number of steps was presented in several journals, for example, in [23]. In this way, the possibility to find the exact solution of an SLAE by using iterative procedure with a stationary matrix has been confirmed.

In this paper, the possibility of obtaining the exact solution of an SLAE in a fi-

nite number of iterations is demonstrated for the first time. A theorem is formulated and proved. For a wide audience without a special mathematical background, the example of solving the simplest SLAE is presented for clarity and understanding. In addition, for the sake of clarity, two types of transformation are given. The first type of transformation provides a unite spectrum of the algebraic equation matrix, while the second type derives the nilpotent matrix from the canonical form of a two-layer iterative method. The result of the iterations is represented in the form of Cramer's formulas known in the school course of mathematics. This directly denies the above opinions about the impossibility of obtaining an exact solution of SLAE in a finite number of iterations.

5. Theorem and Proof

Theorem. *To find a solution of an SLAE*

$$Ax = b, \tag{1}$$

where x and b are the unknown and known vectors of k size, respectively, A is a square nonsingular matrix of k size, in a finite number of iterations, it is necessary and sufficient to reduce (1) *to the form*

$$Ex = c, \tag{2}$$

where E is a unipotent matrix with unit spectrum. Then the iterative equation

$$x(n+1) = Nx(n) + c, \tag{3}$$

where $n = 0,1,2,\cdots, E = I - N$, *I is the identity matrix, for an arbitrary initial vector* x_0, *generates the exact solution* (excluding *round-off errors*)

$$x = A^{-1}b = E^{-1}c \tag{4}$$

no more than for $m \le k$ *iterations*.

Proof. The matrix E is split into the identity matrix I and the nilpotent matrix N with the intrinsic property

$$N^k = 0. \tag{5}$$

A non-unipotent matrix does not form a nilpotent one, and, with $c = 0$, the solution to (3) given by

$$x(n) = N^n x(0) \tag{6}$$

depends on $x(0)$. This proves the necessity.

The sufficiency follows from the solution of (3) by using (5) for $n = k$:

$$x(k) = N^k x(0) + \left(I + N + \cdots + N^{k-1}\right)c = \left(I - N\right)^{-1} c = x. \tag{7}$$

Remark 1. The simple-iteration method is approximate due to the extension of the condition $\det(A) \neq 0$ to the matrix of the iteration equation, as follows from control theory and this statement is confirmed here, but this is not necessary.

Remark 2. The transformation of the difference equation to the form with nilpotent matrix, used in control theory, with $c = 0$, results in to zero in a finite

number of steps, and, with $c \neq 0$, it gives the shifted vector (as it was named in [17]) instead of the solution.

Remark 3. The specified spectrum is formed by changing the elements of a row of the matrix A itself, while in control theory, a row of the elements of the characteristic polynomial of the Frobenius matrix is changed, which is obtained by the transformation of A.

Remark 4. There exist values x_0 such that the number m equals to $1, 2, \cdots, (k-1)$, in particular, $m = k - 1$ for $x(0) = c$.

Remark 5. There exists a variety of unipotent matrices satisfying (2) so the solution (7) can be obtained by using different nilpotent matrices.

The iterative method for exact solution of an SLAE in a finite number of steps has the computational procedure of iterative methods, in the conventional sense, like the Jacobi and Seidel methods, can be called a finite-iterative method. As in control theory, it is based on setting a unit spectrum for the SLAE matrix or a zero spectrum for the matrix of the iteration equation. The main difference is the possibility to solve not only a homogeneous equation, but also a non-homogeneous one.

According to the control theory terminology, the transformation of an SLAE into the form with a unipotent matrix is provided via feedback on the first difference of the desired vector. Such a transformation is mathematically a special case of the canonical form of a one-step two-layer iterative method.

It should be emphasized that the theorem specifies only the possibility of solving SLAE in a finite number of iterations but it does not provide an algorithm for obtaining a nilpotent matrix. As noted above, the algorithm was developed in the context of solving the eigenvalue assignment problem for control the spectrum of the matrix of equation describing a specific technical device. Here, we demonstrate the application of the method that distinctly demonstrates a result in the form of an analytical solution of an SLAE in an iterative way, refuting the statements above.

6. Examples of Solving a System of Two Linear Equations

Consider (1) for $k = 2$,

$$A = \begin{bmatrix} a_{11} & a_{12} \\ a_{21} & a_{22} \end{bmatrix}, \quad b = \begin{bmatrix} b_1 \\ b_2 \end{bmatrix}, \tag{8}$$

and write the system in standard form

$$\begin{aligned} a_{11}x_1 + a_{12}x_2 &= b_1, \\ a_{21}x_1 + a_{22}x_2 &= b_2. \end{aligned} \tag{9}$$

6.1. Transformation of an SLAE to the form with a Unipotent Matrix

The objective is to transform the system (9) and obtain the equivalent system (2) with a unipotent matrix E. We write the first Equation of (9) in the form

$$a_{11}x_1 + a_{12}x_2 + h_2x_2 = b_1 + h_2x_2, \tag{10}$$

where h_2 is a constant coefficient. Substituting the second unknown

$$x_2 = \left(b_2 - a_{21}x_1\right)/a_{22} \tag{11}$$

into the right-hand side of (9) results in

$$\left(a_{11} + a_{21}h_2/a_{22}\right)x_1 + \left(a_{12} + h_2\right)x_2 = b_1 + b_2h_2/a_{22}\ . \tag{12}$$

After dividing (12) by the constant coefficient h_1, we obtain an SLAE in the form (2),

$$Ex = \begin{bmatrix} e_{11} & e_{12} \\ e_{21} & e_{22} \end{bmatrix}\begin{bmatrix} x_1 \\ x_2 \end{bmatrix} = \begin{bmatrix} \dfrac{a_{11} + \dfrac{a_{21}h_2}{a_{22}}}{h_1} & \dfrac{a_{12} + h_2}{h_1} \\ a_{21} & a_{22} \end{bmatrix}\begin{bmatrix} x_1 \\ x_2 \end{bmatrix} = \begin{bmatrix} \dfrac{b_1 + \dfrac{b_2h_2}{a_{22}}}{h_1} \\ b_2 \end{bmatrix}, \tag{13}$$

with two (not yet known) coefficients h_1 and h_2, which are used to control the spectrum, that is, to specify two characteristic numbers λ_1 and λ_2. According to the theorem, they must be equal to 1. In this case, the matrix $E = [e_{i,j}]$ of (2) satisfies the following conditions

$$\begin{aligned} &e_{11} + e_{22} = \lambda_1 + \lambda_2 = 2, \\ &e_{11}e_{22} - e_{12}e_{21} = \lambda_1\lambda_2 = 1, \end{aligned} \tag{14}$$

which leads to the following linear system

$$\begin{aligned} &\frac{a_{11} + \dfrac{a_{21}h_2}{a_{22}}}{h_1} + a_{22} = 2, \\ &\frac{a_{11} + \dfrac{a_{21}h_2}{a_{22}}}{h_1}a_{22} - \frac{a_{12} + h_2}{h_1}a_{21} = 1. \end{aligned} \tag{15}$$

We rewrite it in the normal form

$$\begin{aligned} &\left(a_{22} - 2\right)h_1 + a_{21}h_2/a_{22} = -a_{11}, \\ &h_1 = a_{11}a_{22} + a_{12}a_{21}, \end{aligned} \tag{16}$$

and find the first coefficient h_1 as the determinant of A. The second coefficient h_2 is

$$h_2 = -\left[a_{11} + \left(a_{22} - 2\right)h_1\right]a_{22}/a_{21}\ . \tag{17}$$

Substituting h_1 and h_2 into (13) makes the matrix

$$E = \begin{bmatrix} e_{11} & e_{12} \\ e_{21} & e_{22} \end{bmatrix} = \begin{bmatrix} 2 - a_{22} & \dfrac{-\left(1 - a_{22}\right)^2}{a_{21}} \\ a_{21} & a_{22} \end{bmatrix}, \quad c = \begin{bmatrix} c_1 \\ c_2 \end{bmatrix} = \begin{bmatrix} \dfrac{b_1 + \dfrac{b_2h_2}{a_{22}}}{h_1} \\ b_2 \end{bmatrix} \tag{18}$$

unipotent and defines the right-hand side of the first equation of (9).

Let us summarize the above. For the original SLAE $Ax = b$ we obtained the equivalent system of the form $Ex = c$ with the unit spectrum of E. The preparatory stage called a forward elimination in the Gauss method is completed. According to the theorem, the iterative process, with a nilpotent matrix

$$N = \begin{bmatrix} n_{11} & n_{12} \\ n_{21} & n_{22} \end{bmatrix} = I - E = \begin{bmatrix} -1 + a_{22} & \dfrac{(1-a_{22})^2}{a_{21}} \\ -a_{21} & 1 - a_{22} \end{bmatrix}, \tag{19}$$

should provide the exact solution no more than in two iterations. We have to show it.

First, we make sure the matrix (19) is nilpotent. To do this, we use (14) to calculate

$$\begin{aligned} n_{11} + n_{22} &= 0, \\ n_{11}n_{22} - n_{12}n_{21} &= 0, \end{aligned} \tag{20}$$

so the matrix (19) is really nilpotent. In the next place, using the expression (3) we execute two iterations

$$x(1) = Nx(0) + c\,, \quad x(2) = Nx(1) + c = N^2 x(0) + (I + N)c\,. \tag{21}$$

Due to the property (5), the first summand in (21) is zero. This mathematical statement says that the result does not depend on $x(0)$. The matrix factor in the second summand, due to the equality

$$I + N = (I - N)^{-1} = E^{-1} = \begin{bmatrix} a_{22} & \dfrac{(1-a_{22})^2}{a_{21}} \\ -a_{21} & 2 - a_{22} \end{bmatrix}, \tag{22}$$

is the inverse matrix of the equivalent system (2), which either has the unite spectrum. Therefore, the second iteration actually representing the product of E^{-1} by c,

$$x(2) = E^{-1}c = \begin{bmatrix} a_{22} & \dfrac{(1-a_{22})^2}{a_{21}} \\ -a_{21} & 2 - a_{22} \end{bmatrix} \begin{bmatrix} b_1 + \dfrac{b_2 h_2}{a_{22}} \\ \dfrac{h_1}{b_2} \end{bmatrix} = \begin{bmatrix} a_{22}\dfrac{b_1 + \dfrac{b_2 h_2}{a_{22}}}{h_1} & \dfrac{(1-a_{22})^2}{a_{21}} b_2 \\ -a_{21}\dfrac{b_1 + \dfrac{b_2 h_2}{a_{22}}}{h_1} & (2 - a_{22})b_2 \end{bmatrix}, \tag{23}$$

after simplifications gives an analytical solution of the SLAE in the form of Cramer's formulas

$$x(2) = x = \begin{bmatrix} \dfrac{\Delta_1}{\Delta} & \dfrac{\Delta_2}{\Delta} \end{bmatrix}^{\mathrm{T}}, \tag{24}$$

where $\Delta = a_{11}a_{22} - a_{12}a_{21}$, $\Delta_1 = a_{22}b_1 - a_{12}b_2$, $\Delta_2 = a_{11}b_2 - a_{21}b_1$.

The expression (24) represents the solution of a system known as Cramer's formulas (or Cramer's rule) in a school course of mathematics. This confirms the possibility to obtain an exact solution of an SLAE in iterative way with stationary matrix and evidently proves that the postulate is false. The form of (24) suggests that this expression can be generalized to an SLAE of an arbitrary order k and the exact solution can be found at the k-th iteration,

$$x(k) = x = \left(I + N + \cdots + N^{k-1}\right)c = (I - N)^{-1}c = \begin{bmatrix} \dfrac{\Delta_1}{\Delta} & \cdots & \dfrac{\Delta_k}{\Delta} \end{bmatrix}^{\mathrm{T}}. \tag{25}$$

In accordance with Remark 4, the exact solution can be obtained for a number of iterations not exceeding the order of the system. In this example, the exact solution is found after one iteration if we choose the initial vector $x(0)$ equal to the right-hand side c of the equivalent system. Then the solution (24) follows at the first iteration,

$$x(1)=(I+N)c=\left(\begin{bmatrix}-1+a_{22} & \dfrac{(1-a_{22})^2}{a_{21}}\\ -a_{21} & 1-a_{22}\end{bmatrix}+\begin{bmatrix}1 & 0\\ 0 & 1\end{bmatrix}\right)\cdot\begin{bmatrix}b_1+\dfrac{b_2h_2}{a_{22}}\\ h_1\\ b_2\end{bmatrix}=\begin{bmatrix}\dfrac{\Delta_1}{\Delta}\\ \dfrac{\Delta_2}{\Delta}\end{bmatrix}. \quad (26)$$

The same results can be gained by transformation of the second equation in (9) instead of the first one as it shown in [22].

6.2. Transformation of an SLAE to the Form with a Nilpotent Matrix Obtained from Canonical Form of Two-Layer Iterative Method

The transformation is that any one row of the iterative system is changed and coefficients are determined in order to obtain a given spectrum of a matrix, in this case, to be a zero spectrum. We write (1) in canonical two-layer form [3] with a single iteration parameter,

$$Ax(n)+H\left[x(n+1)-x(n)\right]=b, \quad (27)$$

and recall that the second summand in (27) plays a role of the feedback in control theory.

Taking a rank-one matrix

$$H=\begin{bmatrix}h_1 & h_2\\ 0 & 0\end{bmatrix} \quad (28)$$

whose elements play the same role as in the first example, we expand the first equation

$$a_{11}x_1(n)+a_{12}x_2(n)+h_1\left[x_1(n+1)-x_1(n)\right]+h_2\left[x_2(n+1)-x_2(n)\right]=b_1. \quad (29)$$

We write the second Equation of (9) as

$$a_{21}x_1+(a_{22}+1)x_2=x_2+b_2, \quad (30)$$

and then represent it in the indexed form

$$x_2(n+1)=a_{21}x_1(n)+(a_{22}+1)x_2(n)-b_2. \quad (31)$$

Substituting (31) into (29) leads to an iterative equation with two coefficients h_1 and h_2,

$$\begin{bmatrix}x_1(n+1)\\ x_2(n+1)\end{bmatrix}=\begin{bmatrix}n_{11} & n_{12}\\ n_{21} & n_{22}\end{bmatrix}\begin{bmatrix}x_1(n)\\ x_2(n)\end{bmatrix}+\begin{bmatrix}c_1\\ c_2\end{bmatrix}$$
$$=\begin{bmatrix}-\dfrac{a_{11}-h_1+a_{21}h_2}{h_1} & -\dfrac{a_{12}+a_{22}h_2}{h_1}\\ a_{21} & a_{22}+1\end{bmatrix}\begin{bmatrix}x_1(n)\\ x_2(n)\end{bmatrix}+\begin{bmatrix}\dfrac{b_1+b_2h_2}{h_1}\\ -b_2\end{bmatrix}. \quad (32)$$

Here, h_1 and h_2 are determined from the nilpotency condition (20). Substituting the elements of (32) into (20) gives a linear system

$$\begin{aligned} &-\frac{a_{11}-h_1+a_{21}h_2}{h_1}+a_{22}+1=0,\\ &-\frac{a_{11}-h_1+a_{21}h_2}{h_1}\left(a_{22}+1\right)+\frac{a_{12}+a_{22}h_2}{h_1}a_{21}=0 \end{aligned} \tag{33}$$

expressed in normal form

$$\begin{aligned} &\left(a_{22}+2\right)h_1-a_{21}h_2=a_{11},\\ &\left(a_{22}+1\right)h_1-a_{21}h_2=a_{11}+a_{11}a_{22}-a_{12}a_{21} \end{aligned} \tag{34}$$

whose solution is

$$\begin{aligned} &h_1=-a_{11}a_{22}+a_{12}a_{21},\\ &h_2=\left[\left(a_{22}+2\right)h_1-a_{11}\right]/a_{21}, \end{aligned} \tag{35}$$

where h_1 is the determinant (except for sign) like in the first type of transformation.

Substituting (35) into (32) make the matrix nilpotent (it is easy to check),

$$N=\begin{bmatrix} n_{11} & n_{12}\\ n_{21} & n_{22}\end{bmatrix}=\begin{bmatrix} -1-a_{22} & \dfrac{-\left(1+a_{22}\right)^2}{a_{21}}\\ a_{21} & 1+a_{22}\end{bmatrix}, \tag{36}$$

while the matrix of algebraic system becomes unipotent,

$$E=I-N=\begin{bmatrix} e_{11} & e_{12}\\ e_{21} & e_{22}\end{bmatrix}=\begin{bmatrix} 2+a_{22} & \dfrac{\left(1+a_{22}\right)^2}{a_{21}}\\ -a_{21} & -a_{22}\end{bmatrix}. \tag{37}$$

As a result, for $x(0) = c$, iterative equation with the matrix (30) gives the solution of the SLAE in the form of Cramer's formulas

$$\begin{aligned} x(1)=x=\left(N+I\right)c&=\left(\begin{bmatrix} -1-a_{22} & \dfrac{-\left(1+a_{22}\right)^2}{a_{21}}\\ a_{21} & 1+a_{22}\end{bmatrix}+\begin{bmatrix} 1 & 0\\ 0 & 1\end{bmatrix}\right)\cdot\begin{bmatrix} c_1\\ c_2\end{bmatrix}\\ &=\begin{bmatrix} -a_{22} & \dfrac{-\left(1+a_{22}\right)^2}{a_{21}}\\ a_{21} & 2+a_{22}\end{bmatrix}\cdot\begin{bmatrix} \dfrac{b_1+b_2h_2}{h_1}\\ -b_2\end{bmatrix}=\begin{bmatrix} x_1 & x_2\end{bmatrix}^{\mathrm{T}}=\begin{bmatrix} \dfrac{\Delta_1}{\Delta} & \dfrac{\Delta_2}{\Delta}\end{bmatrix}^{\mathrm{T}} \end{aligned} \tag{38}$$

after the first iteration.

7. Conclusion

In this paper, the possibility of exact solution of an SLAE by iterations with a stationary matrix has been demonstrated. Two examples are given to illustrate different approaches for finding the exact solution of a simplest SLAE by using the transformation of an original system to the form with unipotent or nilpotent matrix. It is shown that an exact solution of an SLAE is obtained in the form of

Cramer's formulas. The fallacy of the postulate about the approximation nature of a simple-iteration method has been proved. Therefore, there is a need to prepare appropriate corrections in order to include them in educational programs on methods for solving linear systems.

Conflicts of Interest

The authors declare no conflicts of interest regarding the publication of this paper.

References

[1] Fadeev, D.K. and Fadeeva, V.N. (1963) Computational Methods of Linear Algebra. Freeman, San Francisco.

[2] Demidovich, B.P. and Maron, I.A. (1981) Computational Mathematics. Mir Publishers, Moscow.

[3] Samarskii, A.A. and Nikolaev, E.S. (1978) Methods for Solving the Grid Equations. Nauka, Moscow. (In Russian)

[4] Strang, G. (1976) Linear Algebra and Its Applications. Academic Press, New York.

[5] Rice, J.R. (1981) Matrix Computations and Mathematical Software. McGraw-Hill, Inc., New York.

[6] Demmel, W.D. (1997) Applied Numerical Linear Algebra. Society for Industrial and Applied Mathematics, Philadelphia. https://doi.org/10.1137/1.9781611971446

[7] Pirumov, U.G. (2003) Numerical Methods. Dropha, Moscow. (In Russian)

[8] Verzhbitskii, V.M. (2005) Fundamentals of Numerical Methods. Vysshaya shkola, Moscow. (In Russian)

[9] Watkins, D.S. (2002) Fundamentals of Matrix Computations. 2nd Edition, John Wiley & Sons, Inc., New York. https://doi.org/10.1002/0471249718

[10] Shevtsov, G.S., Kryukova, O.G. and Myznikova, B.E. (2008) Numerical Methods of Linear Algebra. Finansy i statistika, Moscow. (In Russian)

[11] Tsypkin, Ya.Z. (1950) Discontinuous Control Theory. Part III: Transients in Discontinuous Control Systems. *Automatics and Telemechanics*, **5**, 300-319. (In Russian)

[12] Kalman, R. (1961) About the General Theory of Control Systems. In: *Proceedings of the* 1*st International Congress of IFAC*, Academy of Sciences of the USSR Publ., Moscow, Vol. 2, 521-547.

[13] Kvakernaak, H. and Sivan, R. (1977) Linear Optimal Control Systems. Mir, Moscow. (In Russian)

[14] Isermann, R. (1981) Digital Control Systems. Springer-Verlag, Berlin, Heidelberg. https://doi.org/10.1007/978-3-662-02319-8

[15] Faradzhev, R.G., Vu Ngok, P. and Shapiro, A.V. (1986) Controllability Theory for Digital Dynamic Systems. *Automatics and Telemechanics*, **1**, 5-24. (In Russian)

[16] Pervozvanskii, A.A. (1987) Course on Automatic Control Theory. Nauka, Moscow. (In Russian)

[17] Krasovskii, A.A. (1987) Reference Book on Automatic Control Theory. Nauka, Moscow. (In Russian)

[18] Demidov, N.E. (1997) Software System for Design and Research of Modified Algo-

rithms of Deadbeat Control. *Software Products and Systems*, **2**, 42-45. (In Russian)

[19] Voronov, A.A. (1979) Stability, Controllability, and Observability. Nauka, Moscow. (In Russian)

[20] Iskhakov, A.S. and Skovpen, S.M. (2019) Exact Solution of SLAE Using a Simple-Iteration Method. *Rostov Scientific Journal*, **1**, 334-433. (In Russian)

[21] Iskhakov, A., Pospelov, V. and Skovpen, S. (2012) Non-Frobenius Spectrum-Transformation Method. *Applied Mathematics*, **3**, 1471-1479. https://doi.org/10.4236/am.2012.330206

[22] Iskhakov, A. and Skovpen, S. (2015) A Direct Transformation of a Matrix Spectrum. *Advances in Linear Algebra & Matrix Theory*, **5**, 109-128. https://doi.org/10.4236/alamt.2015.53011

[23] Iskhakov, A. and Skovpen, S. (2018) Exact Solution of a Linear Difference Equation in a Finite Number of Steps. *Applied Mathematics*, **9**, 287-290. https://doi.org/10.4236/am.2018.93022

Applied Mathematics, 2019, 10, 383-396
http://www.scirp.org/journal/am
ISSN Online: 2152-7393
ISSN Print: 2152-7385

A Mathematical Model Reveals That Both Randomness and Periodicity Are Essential for Sustainable Fluctuations in Stock Prices

Motohisa Osaka

Department of Basic Science, Nippon Veterinary and Life Science University, Musashino, Tokyo, Japan
Email: osaka@nms.ac.jp

How to cite this paper: Osaka, M. (2019) A Mathematical Model Reveals That Both Randomness and Periodicity Are Essential for Sustainable Fluctuations in Stock Prices. *Applied Mathematics*, **10**, 383-396.
https://doi.org/10.4236/am.2019.106028

Received: May 13, 2019
Accepted: June 14, 2019
Published: June 17, 2019

Abstract

Is it true that there is an implicit understanding that Brownian motion or fractional Brownian motion is the driving force behind stock price fluctuations? An analysis of daily prices and volumes of a particular stock revealed the following findings: 1) the logarithms of the moving averages of stock prices and volumes have a strong positive correlation, even though price and volume appear to be fluctuating independently of each other, 2) price and volume fluctuations are messy, but these time series are not necessarily Brownian motion by replacing each daily value by 1 or –1 when it rises or falls compared to the previous day's value, and 3) the difference between the volume on the previous day and that on the current day is periodic by the frequency analysis. Using these findings, we constructed differential equations for stock prices, the number of buy orders, and the number of sell orders. These equations include terms for both randomness and periodicity. It is apparent that both randomness and periodicity are essential for stock price fluctuations to be sustainable, and that stock prices show large hill-like or valley-like fluctuations stochastically without any increasing or decreasing trend, and repeat themselves over a certain range.

Keywords

Stock Price, Volume, Brownian Motion, Randomness

1. Introduction

It is generally considered difficult to forecast the behavior of stock prices, and thus many methods have been proposed. For example, fundamental analysis and technical analysis are widely used approaches. Fundamental analysis involves investigating any data that can be expected to impact the price of a stock. The

advantage of this method is that the estimation is objective because the selected economic indicators such as future growth, return on equity, and profit margins are inputted into a particular relational expression to predict the stock price. However, because there is often a time lag prior to the release of economic indicators, one drawback of this approach is that the economic indicators may be outdated. In contrast, technical analysis focuses only on the trading and price history of a stock. The principle underlying technical analysis is that the market price reflects all available information that could affect the stock market. As a result, there is no need to take new economic developments into account because they are already priced into a given security. Technical analysts generally believe that prices move in trends, and that history tends to repeat itself. However, these trends may be a product of chance, and there may actually be a chance that large hill-like or valley-like fluctuations are also considered to be trends. It seems that the market fluctuates based on psychological aspects. There are two major types of technical analysis: chart patterns and technical indicators. Chart patterns are a subjective form of analysis wherein technicians attempt to identify areas of support and resistance on a chart by observing specific patterns. These patterns, identified based on experience and behavioral economics, are designed to predict where prices are headed following a breakout or breakdown from a specific price point. Technical indicators are a statistical form wherein technicians apply various mathematical formulas to prices and volumes. The most common technical indicators are moving averages, which smooth price data to make it easier to spot trends.

Difficulties arise in terms of predicting stock prices because daily changes in stock prices seem to be quite random. In particular, fluctuations in stock prices are considered to follow Brownian motion, fluctuating independently of past stock prices. The notion of using a Brownian motion process to explain the behavior of stock prices was first proposed by Black *et al.* [1]. A Brownian motion process has the property of independent increments. This means that the present price does not affect future prices. However, the present stock price may influence the stock price at some time in the future. Hence, a Brownian motion process is not suitable for explaining stock price movements. Subsequently, a fractional Brownian motion process, which exhibits the property of long-range dependence, was proposed [2]. Meanwhile, it is also considered that there is a relationship between stock price and volume [3] [4]. Volume is an important aspect of technical analysis because it is used to confirm trends and chart patterns. Any price motion up or down with relatively high volume is seen as a stronger, more relevant move than a similar move with weak volume. Data that are available to general investors include time series of stock prices and volumes. As pointed out in the past, the trend of the stock price itself is random [5], and using this data alone, it is completely unpredictable how the price will change in the near future. However, since volume is a measure of how much interest sellers and buyers have in the stock, volume data provide a better understanding of stock price fluctuations.

There is already a famous stochastic differential equation that attempts to mathematically elucidate the transition of one bond and one or more stock prices [1], but the purpose of this study is to reveal the driving force behind sustainable fluctuations in the price of an arbitrary stock using a mathematical model. The rest of this paper is organized as follows. Sections 2 and 3 clarify the relationship between stock prices and volumes, Section 4 presents a model of the proposed relationship, Sections 5 and 6 present an interpretation of the simulation, and Section 7 discusses the effectiveness of the model by comparing the results of the simulation with real data.

2. Characteristics of the Real Data

It is possible to obtain time-series data (e.g., closing prices and volumes) in relation to stock prices for free via the Internet. Although it is acceptable to use data from any source, because the author lives in Japan, data for 50 stocks on the First Section of the Tokyo Stock Exchange were used. It is considered that the results will not lose generality outside Japan.

As an example, time-series data on the stock price of the Takeda Pharmaceutical Company Limited, one of the leading pharmaceutical companies in Japan, was examined.

Figure 1(a) shows the fluctuations in closing prices (abbreviated to prices hereafter) (p_i; i = 1, 2, …, 9012) from 4 January 1983 to 20 March 2019. **Figure 1(b)** shows the difference, Dp_i, between p_{i+1} and p_i (i = 1, 2, …, 9011). **Figure 1(c)** shows the fluctuations in volume (v_i; i = 1, 2, …, 9012). **Figure 1(d)** shows that the difference, Dv_i, between v_{i+1} and v_i (i = 1, 2, …, 9011) appears to be fluctuating periodically. **Figure 1(e)** shows the fluctuations in $Dp_i/\log_e(v_i)$ (i = 1, 2, …, 9011). Since this is an indicator of how much the volume affects the change in stock prices compared with the previous day, I have introduced it anew. If Dp_i is ≥ 0, Bp_i is represented as 1 (i = 1, 2, …, 9011), otherwise Bp_i is represented as −1. **Figure 1(f)** shows the fluctuations in Bp_i (i = 1, 2, …, 9011). Bp_i indicates whether the price is rising or falling. The frequency of Bp_i = 1 is 0.5461. If Dv_i is ≥ 0, Bv_i is represented as 1 (i = 1, 2, …, 9011), otherwise Bv_i is represented as −1. Bv_i indicates whether the volume is rising or falling. The frequency of Bv_i = 1 is 0.4924. **Figure 1(g)** shows the fluctuations in Bv_i (i = 1, 2, …, 9011). From the frequency analysis of Dp_i and Dv_i, it can be seen that the power of Dp_i is almost 0 compared with the power of Dv_i, and Dp_i has no characteristic period, but Dv_i has a period of one to three days (see **Figure 2**). **Figure 3** shows the autocorrelation function of p_i, $Rpp(\tau)$ (=E[$p_i \cdot p_{i+\tau}$]), the autocorrelation function of v_i, $Rvv(\tau)$ (=E[$v_i \cdot v_{i+\tau}$]), and the cross-correlation function, $Rpv(\tau)$ (=E[$p_i \cdot v_{i+\tau}$]), where τ represents the time lag in days. Although $Rpp(\tau)$ and $Rpv(\tau)$ are very small compared with $Rvv(\tau)$, and are almost zero, **Figure 3** indicates that there is a significant correlation between v_i and v_{i+1}. The moving averages are computed: Mp_i, the mean with a window of length 101 that includes the element in the current position, p_i, and 100 elements backward, and Mv_i, the mean with a window of length 101 that includes the element in the current position, v_i, and 100 ele-

ments backward. These are then converted to logarithms: $LMp_i = \log_e(Mp_i)$ and $LMv_i = \log_e(Mv_i)$. Figure 4 shows the relationship between LMv_i and LMp_i. The relationship is significant, with a correlation coefficient of 0.7312 (at the 0.05 significance level).

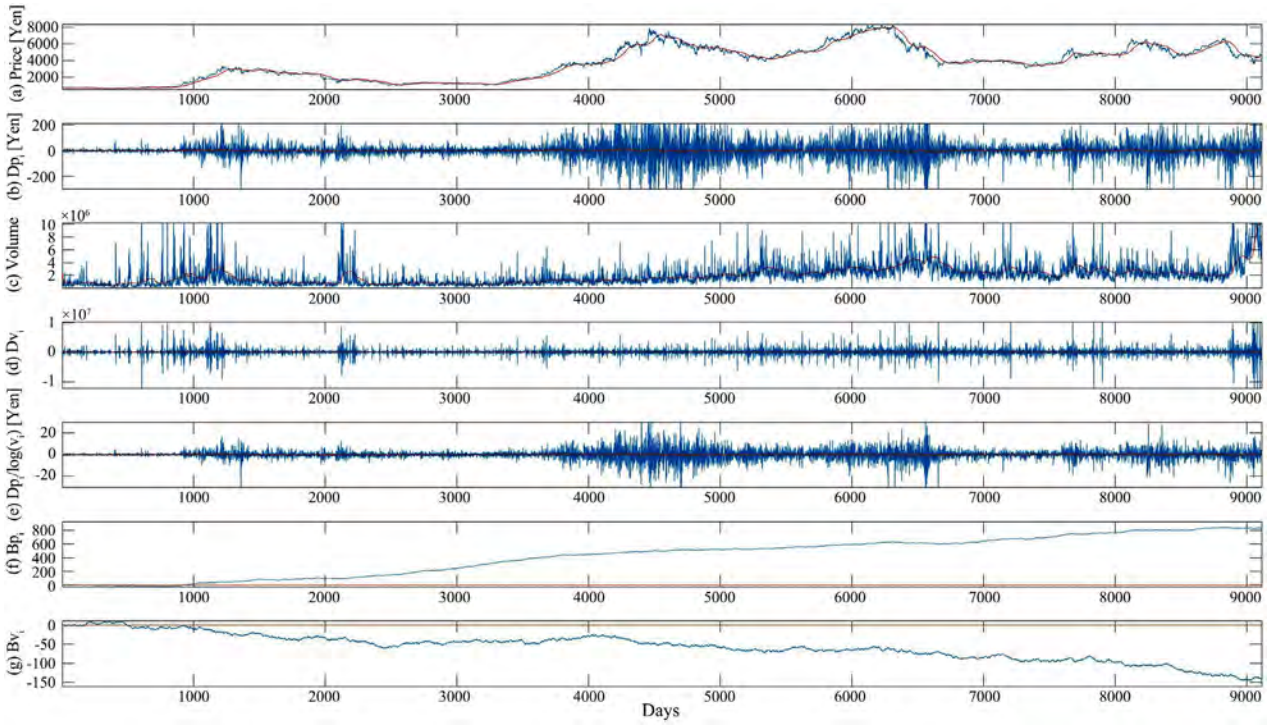

Figure 1. (a) Stock prices (p_i; i =1, 2, …, 9012) from 4 January 4 1983 to 20 March 2019; (b) The difference, Dp_i, between p_{i+1} and p_i (i =1, 2, …, 9011); (c) Volumes (v_i; i = 1, 2, …, 9012); (d) The difference, Dv_i, between v_{i+1} and v_i (i = 1, 2, …, 9011); (e) $Dp_i/\log_e(v_i)$ (i = 1, 2, …, 9011). If Dp_i is ≥ 0, Bp_i is represented as 1 (i = 1, 2, …, 9011), otherwise Bp_i is represented as –1; (f) Bp_i (i = 1, 2, …, 9011). If Dv_i is ≥0, Bv_i is represented as 1 (i = 1, 2, …, 9011), otherwise Bv_i is represented as –1; (g) Bv_i (i = 1, 2, …, 9011). The red lines in (a)-(e) represent the moving averages.

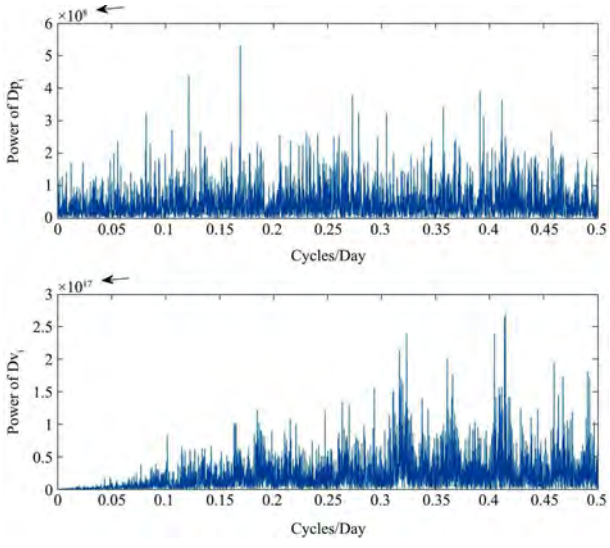

Figure 2. Frequency analysis of Dp_i and Dv_i. The two arrows indicate that the power of Dp_i is extremely small compared with the power of Dv_i.

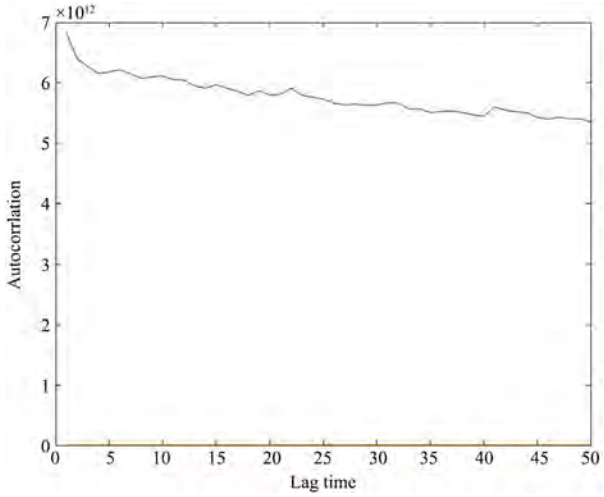

Figure 3. The autocorrelation function of p_i, $R_{pp}(\tau)$ (=E[$p_i p_{i+\tau}$]) (yellow line), the autocorrelation function of v_i, $R_{vv}(\tau)$ (=E[$v_i v_{i+\tau}$]) (blue line), and the cross-correlation function, $R_{pv}(\tau)$ (=E[$p_i v_{i+\tau}$])(yellow line); τ represents the time lag in days.

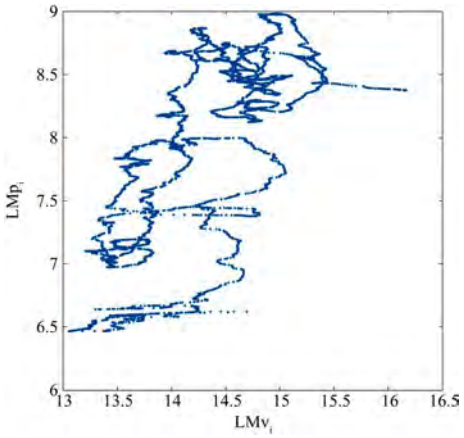

Figure 4. Plots of LMv_i and LMp_i. LMv_i is the logarithm of moving averages of v_i, while LMp_i is the logarithm of moving averages of p_i.

The following findings are based on the information presented in **Figures 1-4**.

1) Comparing **Figure 1(a)** and **Figure 1(c)**, it can be seen that there are days when the volume has increased before a rise in the stock price, but it appears that the price is not always linked to a change in the volume.

2) Comparing **Figure 1(b)** and **Figure 1(d)**, it can be seen that Dp_i and Dv_i appear to fluctuate independently. Close observation of the fluctuations in price and volume reveals that Dv_i appears to change periodically. **Figure 2** shows that Dv_i has a period of one to three days. **Figure 3** shows that the present price is not correlated with the past stock price, and the stock price is not correlated with the volume, although the present volume is related to the volume over several days, especially that of the previous day.

3) **Figure 1(f)** and **Figure 1(g)** show that Bp_i and Bv_i do not return to the origin again after having done so several times near the beginning (18 times for Dp_i

and 22 times for Dv_i). It is understandable that a return to the origin is unlikely in the case of Brownian motion processes because of the arc sine law of last returns, but even if Bp_i and Bv_i follow a Brownian motion process, the number of returns to the origin is at most 22 and the probability of this occurrence is low (0.1820), as shown in the theorem presented in the Appendix. Therefore, neither Bp_i nor Bv_i may be considered to follow a Brownian motion process.

4) **Figure 1(e)** shows that, for example, even if Dp_i rises by only a little, $Dp_i/\log_e(v_i)$ will rise sharply when the volume is small. That is, $Dp_i/\log_e(v_i)$ represents the degree of interest in the stock.

5) Since **Figure 4** shows that LMp_i and LMv_i have a significant positive correlation, it follows that there is a positive correlation between the transition of prices and the transition of its volumes from the logarithm of moving average of 101 days in total.

The following points can be used to construct a mathematical model from the above findings.

a) From (2), fluctuations in price and volume seem to be random and independent, but Dv_i appears to change periodically.

b) From (5), LMp_i and LMv_i have a significant positive correlation.

3. Behavioral Psychology of Investors Affecting Stock Prices

A high volume of turnover means that there are numerous buyers and sellers who are interested in the stock. It has become clear that the average price over the long term (101 days in the above example) is significantly correlated with the average volume during the same period. Therefore, it is essential to know the investors' mindsets because the volume reflects the interest of buyers and sellers in the stock. Since Bv_i indicates whether the volume is rising or falling, it reflects rising or falling interest on the part of buyers and sellers.

The prospect theory of behavioral finance suggests that investors who are overly preoccupied with the negative effects of losses in comparison to an equivalent amount of gains tend to take a short-term view of an investment [6]. This leads those investors to pay far too much attention to the short-term volatility of their stock portfolios. Thus, in general, investors tend to limit their losses by selling their stocks, being overly preoccupied with their latest losses, even though the price of their stock may have subsequently risen.

The gambler's fallacy occurs when, during a series of coin tosses, the gambler thinks that a tail is due following a series of heads. This idea is often used in behavioral economics. In relation to investment, it is easy to become susceptible to the gambler's fallacy. For example, when prices rise over several successive days, many investors will come to believe that, even if there is no rational reason to think so, they will soon fall again. They have various criteria that they use in their decision-making, and even if they are not actually selling, there is a significant possibility that this feeling will affect their judgment. Investors think that the stock price will go up as they go down on a daily basis, and if the stock is bought, it will often happen that the stock price will go down further and lose.

In summary, investors tend to sell in the short term to secure a slight profit because they dislike losses in accordance with the loss avoidance aspect of prospect theory. Meanwhile, they tend to think that prices that are continuing to rise should fall soon, based on the gambler's fallacy. However, there is also a tendency to think that prices will continue to rise. Then, the buying and selling behavior will be repeated periodically to some extent. This summary can be used to construct a mathematical model based on the following conditions. There are random fluctuations in relation to stock prices, the number of buy orders, and the number of sell orders. In particular, the number of buy orders and the number of sell orders fluctuate periodically.

4. Mathematical Model

Stock prices, the number of buy orders, and the number of sell orders are represented by P, B, and S, respectively. Figure 5 shows the interactions among P, B, and S. The formulations of these relationships are as follows:

$$\frac{\mathrm{d}P}{\mathrm{d}t} = a\left(B-S\right) - r_1 \cdot RND_1 \cdot P + t_1 \cdot sign\left(RND_4 - t_2\right), \tag{1}$$

$$\frac{\mathrm{d}B}{\mathrm{d}t} = b\left(1 - r_2 \cdot RND_2 \cdot \sin\left(2\pi ft\right)\right) \cdot P - B, \tag{2}$$

$$\frac{\mathrm{d}S}{\mathrm{d}t} = c\left(1 - r_3 \cdot RND_3 \cdot \sin\left(2\pi ft\right)\right) \cdot P - S, \tag{3}$$

where a, b, c, r_1, r_2, r_3, t_1, t_2, and f are positive constants. $sign(x)$ is 1 if $x > 0$, 0 if $x = 0$, and −1 if $x < 0$. RND_1, RND_2, RND_3, and RND_4 are uniformly distributed random numbers in the interval (0, 1), each of which changes every time step on solving these differential equations by using ode45 of MATLAB®. In equation (1), $B - S$ represents the volume. If $t_1 \cdot sign\left(RND_4 - t_2\right) > 0$, prices are increasing, if $t_1 \cdot sign\left(RND_4 - t_2\right) = 0$, prices display no trend, and if $t_1 \cdot sign\left(RND_4 - t_2\right) < 0$, prices are decreasing. In Equations (1), (2), and (3), $-r_1 \cdot RND_1 \cdot P$, $-B$, and $-S$ are necessary to prevent these variables from diverging to infinity. A preliminary study indicated that RND_1, RND_2, RND_3, and RND_4 are required for P, B, and S to fluctuate randomly in various changes, similar to real data. This finding suggests that continuous up-and-down changes are the result of the randomness of prices.

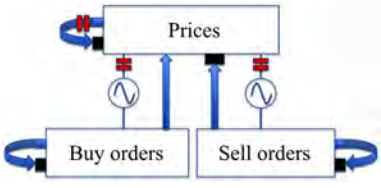

Figure 5. Relationships among prices, buy orders, and sell orders. Arrows represent promotion, while blocked arrows represent suppression. The red lines represent random noise. A wave in the circle between prices and buy orders (or sell orders) indicates that the effect of promoting or suppressing the buy orders (or sell orders) on the stock price changes periodically.

5. Results

The parameters are set as follows: $a = 0.2$, $b = 2$, $c = 1$, $r_1 = 0.4$, $r_2 = 2$, $r_3 = 4$, and $f = 0.2$.

5.1. $t_1 = 0$, $t_2 = 0$

Regardless of $t_1 \cdot sign\left(RND_4 - t_2\right) = 0$, there are a couple of significant rises in prices, as if there was a trend (see Figure 6). However, the prices do not increase constantly. It can be seen from Figure 6(f) and Figure 6(g) that the number of times Bp_i and Bv_i cross the origin is extremely small. Figure 7 shows the relationship between LMv_i and LMp_i. The relationship is significant with a correlation coefficient of 0.7452 (at the 0.05 significance level).

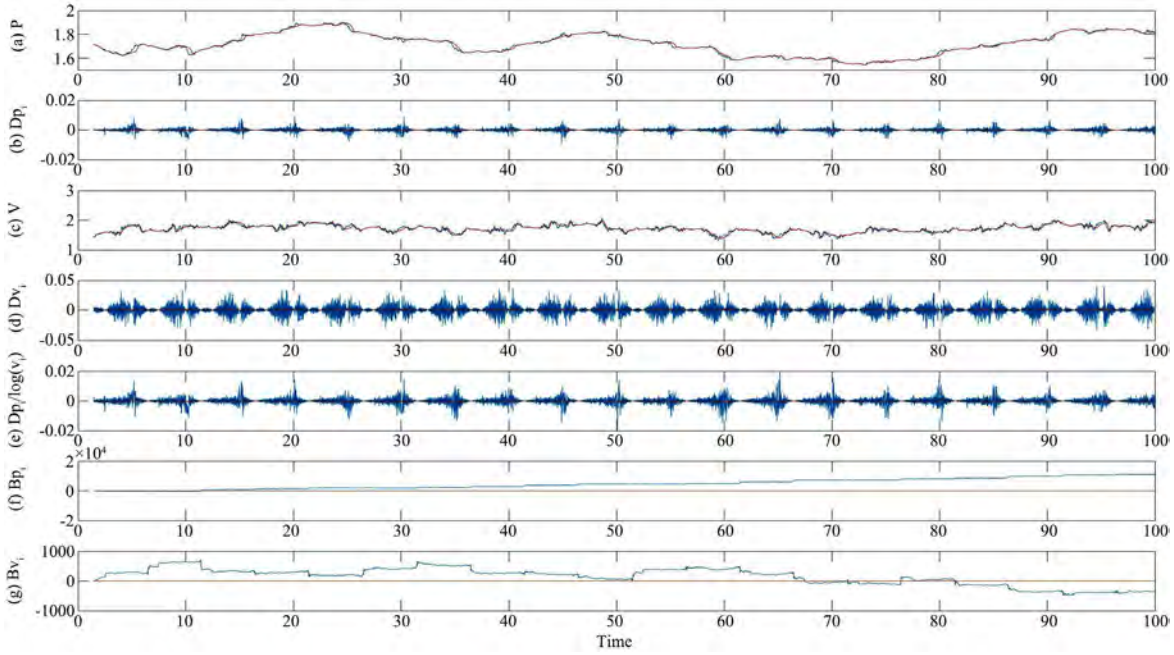

Figure 6. Plots of $P(=p_i)$, Dp_i, $V(=v_i)$, Dv_i, $Dp_i/\log_e(v_i)$, Bp_i, and Bv_i, which are calculated at $t_1 = 0$, $t_2 = 0$. The red lines in (a)-(e) represent the moving averages.

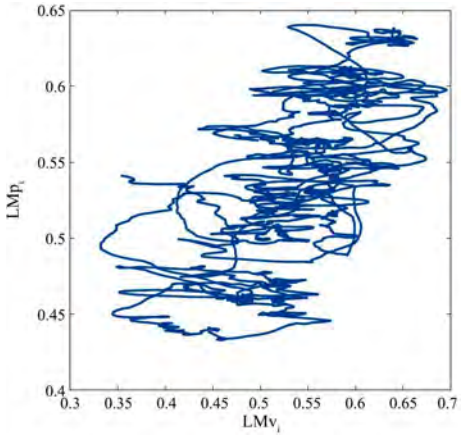

Figure 7. Plots of LMv_i and LMp_i, which are calculated at $t_1 = 0$, $t_2 = 0$.

5.2. $t_1 = 0.001, 0.005$, or $0.01, t_2 = 0$

As $t_2 = 0$, $t_1 \cdot sign\left(RND_4 - t_2\right) > 0$. When $0.001 < t_1 < 0.005$, prices do not necessarily show an upward trend. When $t_1 = 0.01$, prices show a constant upward trend (see Figure 8). Thus, Bp_i and Bv_i are constantly increasing. Figure 9 shows the relationship between LMp_i and LMv_i. The relationship is significant with a correlation coefficient of 0.8778 (at the 0.05 significance level). The correlation between price and volume is stronger for the condition $t_1 = 0.01$, $t_2 = 0$ than for the condition $t_1 = 0$, $t_2 = 0$.

5.3. $t_1 = 0.01$; $t_2 = 0.25, 0.5$, or 0.75

When $t_2 = 0.25$, $t_1 \cdot sign\left(RND_4 - t_2\right) > 0$ with probability of 0.75. When $t_2 = 0.5$, $t_1 \cdot sign\left(RND_4 - t_2\right) > 0$ with probability of 0.5. When $t_2 = 0.75$, $t_1 \cdot sign\left(RND_4 - t_2\right) > 0$ with probability of 0.25, in other words, $t_1 \cdot sign\left(RND_4 - t_2\right) < 0$ with probability of 0.75. When $t_2 = 0.25$, prices show an upward trend. When $t_2 = 0.5$, price fluctuations show various patterns. When $t_2 = 0.75$, prices are constantly decreasing (see Figure 10).

6. Mathematical Analysis

The parameters are the same as in Section **5.1**, namely, $a = 0.2$, $b = 2$, $c = 1$, $r_1 = 0.4$, $r_2 = 2$, $r_3 = 4$, $f = 0.2$, $t_1 = 0$, and $t_2 = 0$. Then the prices do not increase constantly, and are confined within a certain range. This can be confirmed by mathematical analysis as follows. The volume, $B - S$, is represented by V.

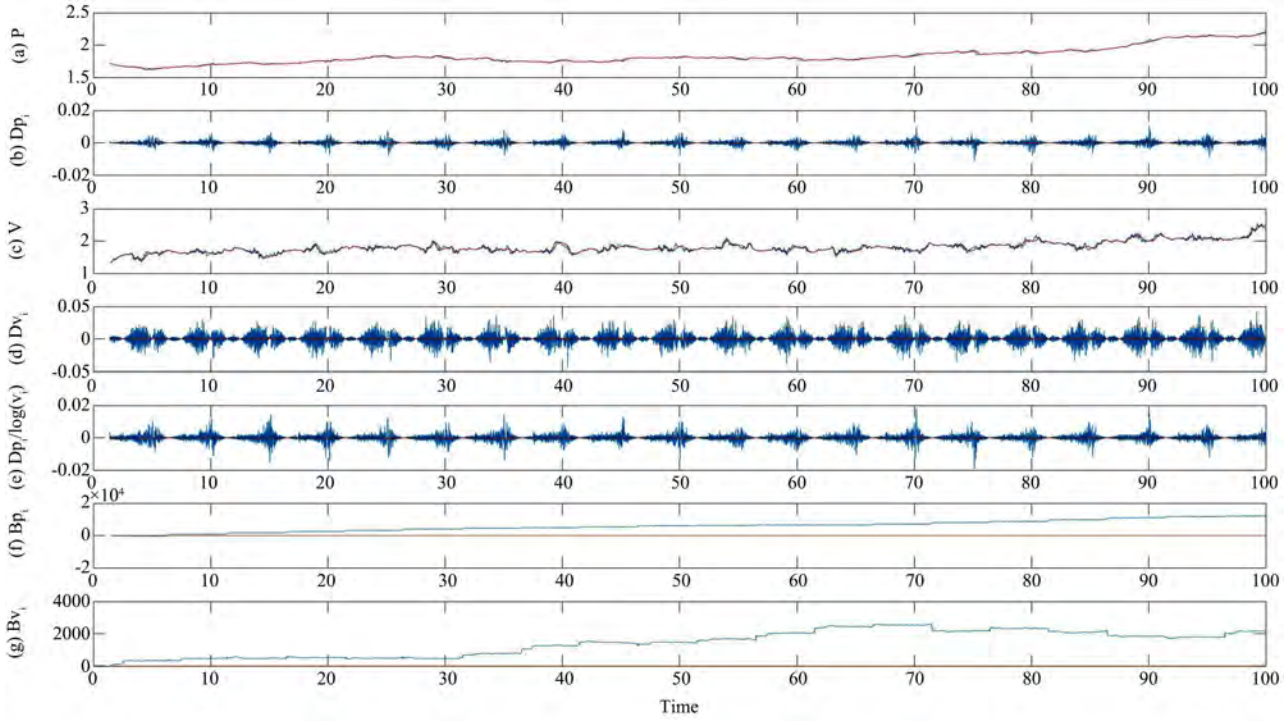

Figure 8. Plots of $P(=p_i)$, Dp_i, $V(=v_i)$, Dv_i, $Dp_i/\log_e(v_i)$, Bp_i, and Bv_i, which are calculated at $t_1 = 0.01$, $t_2 = 0$. The red lines in (a)-(e) represent the moving averages.

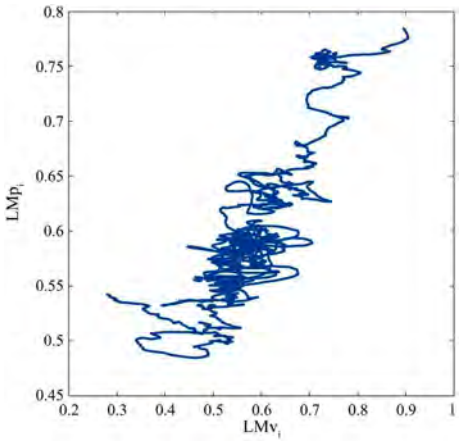

Figure 9. Plots of LMv_i and LMp_i, which are calculated at $t_1 = 0.01$, $t_2 = 0$.

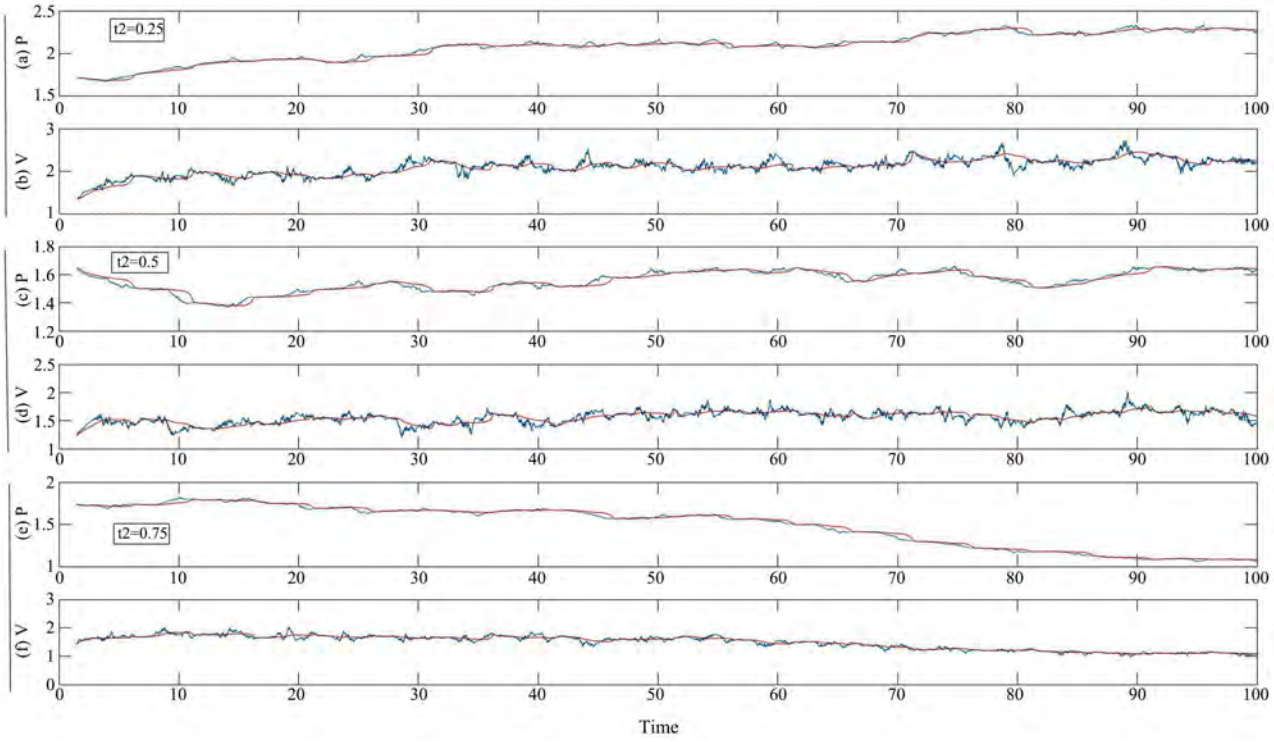

Figure 10. Plots of P and V, which are calculated at $t_1 = 0.01$, $t_2 = 0.25$, 0.5, or 0.75.

As $t_1 = 0$, Equation (1) is expressed as follows.

$$\frac{\mathrm{d}P}{\mathrm{d}t} = 0.2 \cdot V - r_1 \cdot RND_1 \cdot P \tag{4}$$

Equation (2) minus Equation (3) is expressed as follows.

$$\frac{\mathrm{d}V}{\mathrm{d}t} = \left(1 - 4 \cdot \left(RND_2 - RND_3\right) \cdot \sin\left(2\pi ft\right)\right) \cdot P - V \tag{5}$$

here $r_1 \cdot RND_1, RND_2 - RND_3, \left(RND_2 - RND_3\right) \cdot \sin\left(2\pi ft\right)$ are denoted as α, β, and γ, respectively. Since these parameters include random numbers or time variables, these parameters are considered below once as constants. Then Equa-

tions (4) and (5) are considered to be ordinary differential equations.

$$\frac{\mathrm{d}}{\mathrm{d}t}\begin{pmatrix} P \\ V \end{pmatrix} = \begin{pmatrix} -\alpha & 0.2 \\ 1-4\gamma & -1 \end{pmatrix}\begin{pmatrix} P \\ V \end{pmatrix} \tag{6}$$

The characteristic polynomial of Equation (6) is given by

$$\lambda^2 + (1+\alpha)\lambda + \alpha + 0.8\gamma - 0.2 = 0. \tag{7}$$

$$\lambda = \frac{-(1+\alpha) \pm \sqrt{(1+\alpha)^2 - 4(\alpha + 0.8\gamma - 0.2)}}{2} \tag{8}$$

If $-\alpha - 0.8\gamma + 0.2 > 0, \gamma < (1-5\alpha)/4$. Then, one of the two eigenvalues is positive and the other is negative. Since α is distributed uniformly in (0, 0.4), $-1/4 < (1-5\alpha)/4 < 1/4$.

If $\gamma < -1/4$, one of the two eigenvalues is always positive.

As $\gamma\left(=\left(RND_2 - RND_3\right)\cdot\sin(2\pi ft)\right)$ is $\beta\cdot\sin(2\pi ft)$, $\beta\cdot\sin(2\pi ft) < -1/4$. Now, $-1 < \beta < 1$.

If $\sin(2\pi ft) > 0$,

$$\beta < -\frac{1}{4\sin(2\pi ft)} \le -\frac{1}{4} \tag{9}$$

If $\sin(2\pi ft) < 0$,

$$\beta > -\frac{1}{4\sin(2\pi ft)} \ge \frac{1}{4} \tag{10}$$

As RND_2 and RND_3 are distributed uniformly in (0, 1), the probability density function, $f(\beta)$, of β ($=RND_2 - RND_3$) is expressed as shown in Figure 11. The probability of $\beta < -1/4$ is 9/32, and the probability of $\beta > 1/4$ is 9/32. The total time of $\sin(2\pi ft) > 0$ is 50% in any observation time. Similarly, the total time of $\sin(2\pi ft) < 0$ is 50% in any observation time. Hence, the total time of $\gamma < -1/4$ is at most 9/32 in any observation time. Conversely, if $\gamma > 1/4$, the two eigenvalues are always negative real numbers or complex numbers with negative real parts. In the same way as $\gamma < -1/4$, the total time of $\gamma > 1/4$ is at most 9/32 in any observation time. In the remaining time, when $-1/4 < \gamma < 1/4$, there are various combinations of the two eigenvalues: one positive and the other negative

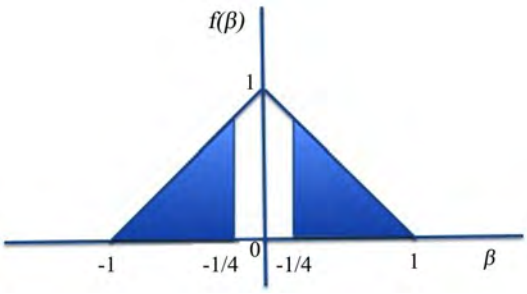

Figure 11. Probability density function, $f(\beta)$, of β ($=RND_2 - RND_3$). The area of each blue triangle is 9/32.

real numbers, two negative real numbers, and two complex numbers with negative real parts. In no cases do two positive real eigenvalues or two complex eigenvalues with positive real parts occur. P does not diverge to infinity or converge to zero because the two eigenvalues are not always positive real numbers (or complex numbers whose real parts are positive numbers) and not always negative real numbers. Hence, P fluctuates within a certain range.

7. Discussion

In this study, the relationship between the price and trading volume of a stock is examined. Fluctuations in prices and volumes seem to be random and independent, but LMp_i and LMv_i have a significant positive correlation. In particular, Dv_i appears to change periodically, based on frequency analysis. The present volume is related to the volume over the last few days, especially the previous day. A preliminary study indicated that RND_1, RND_2, RND_3, and RND_4 are required for P, B, and S to fluctuate daily in the same manner as real data. These findings suggest that fluctuations in stock prices are characterized by both randomness and periodicity. Although there is a tacit understanding that continual fluctuations in stock prices are the result of Brownian motion, Kong *et al.* reported the possibility that fractional Brownian motion is the driving force [2]. However, Brownian motion seems unlikely to be the only driving force based on the results for Bp_i and Bv_i obtained in Section **2**. The prospect theory of behavioral finance suggests that investors who are overly preoccupied with the negative effects of losses tend to limit their losses by selling their stocks. Investors who have fallen into the gambler's fallacy sell their stocks in the belief that prices are due to fall if they have been rising. However, when the stock price rises further, they then try to buy it back, thinking it will continue to rise. Thus, there is repeated buying and selling over a short period without sound underlying reasons. This is why stock prices include a periodic factor. Thus, the differential equations consist of a component for randomness, as well as one for periodicity (see **Figure 5**).

The prices of an arbitrary stock generally display up-and-down motions, but are generally confined within a certain range. Although technical analysts believe that prices generally move in trends and that history tends to repeat itself, the findings in Section **5.1** indicate that stock prices show large hill-like or valley-like fluctuations stochastically without any increasing or decreasing trend, and repeat themselves over a certain range. This seems to be natural at first glance, but the question arises as to what is the driving force.

From Section **5**, it can be seen that the stock price increases almost monotonically if the change in the price of a certain stock is accompanied by an increasing trend without noise (as well as a decreasing trend). However, in reality, it seems that randomness mixes with this increasing or decreasing trend. Thus, stock prices can fluctuate unpredictably depending on the degree of this mixing, making it difficult to predict stock prices. From Section **5.2**, it can be seen that if a noise-free increasing or decreasing trend is added to stock prices, LMp_i and

LMv_i have a stronger positive correlation. Then, since the prices increase almost monotonically, they become predictable. In other words, if all of the information, including external factors, affecting stock prices is known, stock prices can be predicted. Otherwise, they are generally unpredictable.

8. Conclusion

The analysis of daily prices and volumes of a certain stock revealed the following findings: 1) price and volume fluctuations are random, 2) the difference between the volume on the previous day and that on the current day is periodic. Based on these findings, the differential equations of stock prices, the number of buy orders, and the number of sell orders were constructed. From simulation by these equations it is clear that both randomness and periodicity are essential for stock price fluctuations to be sustainable. In the future, I would like to clarify the conditions of the parameters in the mathematical model under which stock prices will continue to fluctuate within a certain range. This finding will reveal which parameters have a strong influence in order to make the stock price fluctuate continuously within the certain range.

Acknowledgements

We thank Geoff Whyte, MBA, from Edanz Group (www.edanzediting.com/ac) for editing a draft of this manuscript.

Conflicts of Interest

The author declares no conflicts of interest regarding the publication of this paper.

References

[1] Black, F. and Scholes, M. (1973) The Pricing of Options and Corporate Liabilities. *Journal of Political Economy*, **81**, 637-654. https://doi.org/10.1086/260062

[2] Kong, X., Jing, B. and Li, C. (2013) Is the Driving Force of a Continuous Process a Brownian Motion or Fractional Brownian Motion. *Journal of Mathematical Finance*, **3**, 454-464. https://doi.org/10.4236/jmf.2013.34048

[3] Amihud, Y. and Mendelson, H. (1989) Market Microstructure and Price Discovery in the Tokyo Stock Exchange. *Japan and the World Economy*, **1**, 341-370. https://doi.org/10.1016/0922-1425(89)90013-3

[4] Chan, W.S. and Tse, Y.K. (1993) Price-volume Relation in Stocks: A Multiple Time Series Analysis on the Singapore Market. *Asia Pacific Journal of Management*, **10**, 39-56. https://doi.org/10.1007/bf01732223

[5] Iwaki, H. and Luo, L. (2013) An Empirical Study of Option Prices under the Hybrid Brownian Motion Model. *Journal of Mathematical Finance*, **3**, 329-334. https://doi.org/10.4236/jmf.2013.32033

[6] Pan, Z. (2019) A Review of Prospect Theory. *Journal of Human Resource and Sustainability Studies*, **7**, 98-107.

Appendix

Theorem (normal approximation)

The length of paths is $2n$. Suppose that n is large and α is a fixed positive number. The probability, $f(\alpha)$, that fewer than $\alpha \cdot \sqrt{2n}$ changes of sign occur tends to

$$f(\alpha) = \sqrt{\frac{2}{\pi}} \cdot \int_0^{\alpha} \exp\left(-\frac{s^2}{2}\right) \mathrm{ds} \quad \text{as } n \to \infty \tag{11}$$

Applied Mathematics, 2019, 10, 397-418
http://www.scirp.org/journal/am
ISSN Online: 2152-7393
ISSN Print: 2152-7385

Global Transmission Dynamics of a Schistosomiasis Model and Its Optimal Control

Mouhamadou Diaby[1], Mariama Sène[2], Abdou Sène[3]

[1]Laboratoire d'Analyse Numérique et d'Informatique (LANI), UFR SAT, Université Gaston Berger de Saint-Louis, Saint-Louis, Sénégal
[2]UFR AGRO, Université Gaston Berger de Saint-Louis, Saint-Louis, Sénégal
[3]LANI, Pôle STN MAI (Mathématiques Appliquées et Informatique), Université Virtuelle du SENEGAL, Dakar-Fann, Sénégal
Email: diabloss84@yahoo.fr, mariama-sene.wade@ugb.edu.sn, abdou.sene@uvs.edu.sn

How to cite this paper: Diaby, M., Sène, M. and Sène, A. (2019) Global Transmission Dynamics of a Schistosomiasis Model and Its Optimal Control. *Applied Mathematics*, **10**, 397-418.
https://doi.org/10.4236/am.2019.106029

Received: March 9, 2019
Accepted: June 14, 2019
Published: June 17, 2019

Abstract

Drug treatment, snail control, cercariae control, improved sanitation and health education are the effective strategies which are used to control the schistosomiasis. In this paper, we consider a deterministic model for schistosomiasis transmission dynamics in order to explore the role of the several control strategies. The global stability of a schistosomiasis infection model that involves mating structure including male schistosomes, female schistosomes, paired schistosomes and snails is studied by constructing appropriate Lyapunov functions. We derive the basic reproduction number $\mathcal{R}_0$ for the deterministic model, and establish that the global dynamics are completely determined by the values of $\mathcal{R}_0$. We show that the disease can be eradicated when $\mathcal{R}_0 \leq 1$; otherwise, the system is persistent. In the case where $\mathcal{R}_0 > 1$, we prove the existence, uniqueness and global asymptotic stability of an endemic steady state. Sensitivity analysis and simulations are carried out in order to determine the relative importance of different control strategies for disease transmission and prevalence. Next, optimal control theory is applied to investigate the control strategies for eliminating schistosomiasis using time dependent controls. The characterization of the optimal control is carried out via the Pontryagins Maximum Principle. The simulation results demonstrate that the insecticide is important in the control of schistosomiasis.

Keywords

Schistosomiasis Models, Nonlinear Dynamical Systems, Global Stability, Reproduction Number, Optimal Control, Sensitivity Analysis

1. Introduction

Schistosomiasis (also known as bilharzia, bilharziasis or snail fever) is a vec-

tor-borne disease caused by infection of the intestinal or urinary venous system by trematode worms of the genus Schistosoma. More than 220.8 million people required preventive treatment worldwide in 2017, out of which more than 102.3 million people were reported to have been treated [1]. Schistosomiasis is prevalent in tropical and subtropical areas, especially in poor communities without access to safe drinking water and adequate sanitation. Of the 207 million people with schistosomiasis, 85% live in Africa [1]. Of the tropical diseases, only malaria accounts for a greater global burden than schistosomiasis [2]. Therefore, it is vital to prevent and control the schistosomiasis transmission.

Schistosoma requires the use of two hosts to complete its life cycle: the definitive hosts and the intermediate snail hosts. In definitive hosts, schistosoma has two distinct sexes. Mature male and female worms pair and migrate either to the intestines or the bladder where eggs production occurs. One female worm may lay an average of 200 to 2000 eggs per day for up to twenty years. Most eggs leave the bloodstream and body through the intestines. Some of the eggs are not excreted, however, and can lodge in the tissues. It is the presence of these eggs, rather than the worms themselves, that causes the disease. These eggs pass in urine or feces into fresh water into miracidia which infect the intermediate snail hosts. In snail hosts, parasites undergo further asexual reproduction, ultimately yielding large numbers of the second free-living stage, the cercaria. Free-swimming cercariae leave the snail host and move through the aquatic or marine environment, often using a whip-like tail, though a tremendous diversity of tail morphology is seen. Cercariae are infective to the second host and turn it into single schistosoma, and infection may occur passively (e.g., a fish consumes a cercaria) or actively (the cercaria penetrates the fish) and terminates the life cycle of the parasite.

Many effective strategies are used in the real world, such as: based on preventive treatment, snail control, cercariae control, improved sanitation and health education. The WHO strategy for schistosomiasis control focuses on reducing disease through periodic, targeted treatment with praziquantel. This involves regular treatment of all people in at-risk groups [1]. Over the past few decades, different mathematical models [3] [4] [5] [6] have been constructed to describe the transmission dynamics involving two-sex problems. In [3] [4] [5], a mathematical model is developed for a schistosomiasis infection that involves pair-formation models and studied the existence, uniqueness and the stabilities of exponential solutions. We note that in [4] [5] authors formulate three forms of pair-formation functions (also known as mating functions) that are the harmonic mean function, the geometric mean function and the minimum function. In [7], Xu *et al.* have proposed a multi-strain schistosome model with mating structure. Their goal was to study the effect of drug treatment on the maintenance of schistosome genetic diversity. However, in their model they only consider the adult parasite populations. Castillo-Chavez *et al.* [3] have considered a time delay model but also do not include the snails dynamics. But it is important to take into account the snail dynamics as it is shown in the life cycle of schisto-

soma. In fact, the parasite offspring is produced directly by infected snails but not by paired parasites as is related in [6]. Recently, Qi *et al.* [6] have formulated a deterministic mathematical model to study the transmission dynamics of schistosomiasis with a linear mating function incorporating these snail dynamics. This paper gave the expression of a threshold number (and not the basic reproduction number) with a local stability analysis of the disease free equilibrium. The sensitivity analysis of this threshold number is also discussed.

However, no work has been done to investigate the global stability of the equilibria which is more in interest. Here, we take this deterministic schistosomiasis model with mating structure [6] and we propose a complete mathematical analysis. A stability analysis is provided to study the epidemiological consequences of control strategies. We compute the basic reproduction number and we show that when it is less or equal to one then the disease free equilibrium (DFE) is the unique equilibrium of the system and it is globally asymptotically stable, while when the basic reproduction number is greater than one then there is a unique endemic equilibrium which is globally asymptotically stable in the whole space minus the stable manifold of the DFE. A sensitivity analysis of the endemic equilibrium is performed giving a more interest interpretation of the control strategies. Optimal control is a branch of mathematics developed to find optimal ways to control a dynamic system [8] [9]. There are few papers that apply optimal control to schistosomiasis models. Here we propose and analyze one such optimal control problem, where the control function represents the fraction of snails individuals (X_s and X_i) that will be submitted to treatment. The objective is to find the optimal treatment strategy through insecticide campaigns that minimizes the number of snails individuals as well as the cost of interventions. This paper is organized as follows. Model formulation is carried out and the basic properties are shown in the next section. In Section 3, we determine the basic reproductive number $\mathcal{R}_0$ of the model and also establish local and global stability of the disease-free equilibrium. In the end of this section we show that the disease is uniformly persistent when $\mathcal{R}_0 > 1$. Section 4 is devoted to prove the global asymptotic stability of the endemic equilibrium. In Section 5, a sensitivity analysis of the basic reproductive number and of the endemic equilibrium are explored. The goal is to identify the most sensitive parameter allowing decreasing the disease prevalence. In Section 6 we propose and analyze an optimal control problem. A general conclusion is given in the last section.

2. Mathematical Model

The model that we consider has been presented in [6]. It describes the time evolution of a population divided in three parasites sub-populations and two intermediate snail host sub-populations. The state variables of the model are:

- $X_m(t)$ the male schistosoma population size.
- $X_f(t)$ the female schistosoma population size.
- $X_p(t)$ the pair schistosoma population size.

- $X_s(t)$ the susceptible (uninfected) snail host population size.
- $X_i(t)$ the infected snail host population size.

The time evolution of the different populations is governed by the following system of equations:

$$\begin{cases} \dfrac{\mathrm{d}X_m}{\mathrm{d}t} = k_m X_i - \left(\mu_m + \epsilon_m\right) X_m - \rho X_f, \\ \dfrac{\mathrm{d}X_f}{\mathrm{d}t} = k_f X_i - \left(\mu_f + \epsilon_f\right) X_f - \rho X_f, \\ \dfrac{\mathrm{d}X_p}{\mathrm{d}t} = \rho X_f - \left(\mu_p + \epsilon_p\right) X_p, \\ \dfrac{\mathrm{d}X_s}{\mathrm{d}t} = \Lambda - \left(\mu_s + \epsilon_s\right) X_s - \beta X_p X_s, \\ \dfrac{\mathrm{d}X_i}{\mathrm{d}t} = \beta X_p X_s - \left(\mu_s + \epsilon_s + \alpha_s\right) X_i. \end{cases} \tag{1}$$

The different parameters are:

- k_m and k_f are the recruitment rates of male schistosoma and female schistosoma respectively.
- μ_m, μ_f, μ_p, and μ_s denote the natural death rate for male, female, pair and snail hosts respectively. α_s is the disease-induced death rate of snail hosts.
- ρ represents the effective mating rate.
- Λ is the recruitment rate of snail hosts.
- β is the transmission rate from pairs parasite to susceptible snails.
- ϵ_m, ϵ_f, ϵ_p and ϵ_s are the elimination rates of male shistosoma, female schistosoma, paired schistosoma and snails respectively. These elimination rates represent the control strategies.

As it has been done in [6], we shall denote

$$\mu_m + \epsilon_m = \mu_{m\epsilon}, \quad \mu_f + \epsilon_f = \mu_{f\epsilon},$$

$$\mu_p + \epsilon_p = \mu_{p\epsilon}, \quad \mu_s + \epsilon_s = \mu_{s\epsilon}.$$

2.1. Basic Properties

In this section, we give some basic results concerning solutions of system (1) that will be subsequently used in the proofs of the stability results.

Proposition 1 *The set* $\Gamma = \left\{X_m \geq X_f \geq 0, X_p \geq 0, X_s \geq 0, X_i \geq 0\right\}$ *is a positively invariant set for system* (1).

Proof. The vector field given by the right-hand side of system (1) points inward on the boundary of Γ. For example, if $X_s = 0$, then, $\dot{X}_s = \Lambda > 0$. In an analogous manner, the same can be shown for the other system components.

Proposition 2 *All solutions of system* (1) *are forward bounded.*

Proof. Let us define $N_X = X_m + X_f + X_p$ and $N_Y = X_s + X_i$. Using system (1), we have $\dfrac{\mathrm{d}N_Y}{\mathrm{d}t} = \Lambda - \mu_{s\epsilon} N_Y - \alpha_s X_i \leq \Lambda - \mu_{s\epsilon} N_Y$. This implies that the set

$\left\{N_Y \le \frac{\Lambda}{\mu_{s\epsilon}}\right\}$ is positively invariant and attracts all the solutions of (1).

We also have:

$$\begin{aligned}\frac{\mathrm{d}N_X}{\mathrm{d}t} &= \left(k_m + k_f\right)X_i - \mu_{m\epsilon}X_m - \left(\mu_{f\epsilon} + \rho\right)X_f - \mu_{p\epsilon}X_p \\ &\le \left(k_m + k_f\right)\frac{\Lambda}{\mu_{s\varepsilon}} - \min\left\{\mu_{m\epsilon}, \mu_{f\epsilon}, \mu_{p\epsilon}\right\}N_X - \rho X_f.\end{aligned}$$

Hence, the set $\left\{N_X \le \frac{\left(k_m + k_f\right)\Lambda}{\mu_{s\epsilon}\gamma}\right\}$, where $\gamma = \min\left\{\mu_{m\epsilon}, \mu_{f\epsilon}, \mu_{p\epsilon}\right\}$, is positively invariant set and attracts all the solutions of (1).

Therefore all feasible solutions of system (1) enter the region

$$\Omega = \left\{\left(X_m, X_f, X_p, X_s, X_i\right) \in \mathbb{R}_+^5 : X_s + X_i \le \frac{\Lambda}{\mu_{s\epsilon}}, \right.$$
$$\left. X_m + X_f + X_p \le \frac{\left(k_m + k_f\right)\Lambda}{\mu_{s\epsilon}\gamma}\right\},$$

and the set Ω is a compact positively invariant set for system (1). It is then sufficient to consider solutions in Ω.

3. The Basic Reproduction Number and the Disease-Free Equilibrium

The disease-free equilibrium of system (1) is

$\mathcal{E}^0 = \left(0,0,0,X_s^0,0\right) = \left(0,0,0,\frac{\Lambda}{\mu_{s\epsilon}},0\right)$. Using the notations of [10] for the model system (1), the matrices F and V for the new infection terms and the remaining transfer terms are, respectively, given by

$$F = \begin{pmatrix} 0 & 0 & 0 & 0 \\ 0 & 0 & 0 & 0 \\ 0 & 0 & 0 & 0 \\ 0 & 0 & \beta\frac{\Lambda}{\mu_{s\epsilon}} & 0 \end{pmatrix} \text{ and } V = \begin{pmatrix} -k_m & \mu_{m\epsilon} & \rho & 0 \\ 0 & \rho + \mu_{f\epsilon} & 0 & -k_f \\ 0 & -\rho & \mu_{p\epsilon} & 0 \\ 0 & 0 & & \mu_{s\epsilon} + \alpha_s \end{pmatrix}$$

The basic reproduction number $\mathcal{R}_0$ is equal to the spectral radius of the matrix FV^{-1}, a simple computation gives:

$$\mathcal{R}_0 = \frac{\beta\rho k_f \Lambda}{\mu_{s\epsilon}\mu_{p\epsilon}\left(\mu_{f\epsilon} + \rho\right)\left(\mu_{s\epsilon} + \alpha_s\right)} = \frac{\beta\rho k_f X_s^0}{\mu_{p\epsilon}\left(\mu_{f\epsilon} + \rho\right)\left(\mu_{s\epsilon} + \alpha_s\right)}.$$

One can remark that there is a mistake in the formula for $\mathcal{R}_0$ provided in [6].

The basic reproductive number for system (1) measures the average number of new infections generated by a single infected individual in a completely susceptible population.

As it is well known (see, for instance, [10]), the local asymptotic stability of

the disease-free equilibrium is completely determined by the value of $\mathcal{R}_0$ compared to unity, *i.e.*, The disease-free equilibrium $\mathcal{E}^0$ of the system (1) is locally asymptotically stable if $\mathcal{R}_0 < 1$ and unstable if $\mathcal{R}_0 > 1$.

Hence $\mathcal{R}_0$ determines whether the disease will be prevalent in the given population or will go extinct.

Next, we discuss the global stability of infection-free equilibrium by using suitable Lyapunov function and LaSalle invariance principle for system (1). In recent years, the method of Lyapunov functions has been a popular technique to study global properties of population models. However, it is often difficult to construct suitable Lyapunov functions.

Theorem 3 *The disease-free equilibrium* $\mathcal{E}^0$ *of system* (1) *is globally asymptotically stable* (*GAS*) *on the nonnegative orthant* $\mathbb{R}^5_+$ *whenever* $\mathcal{R}_0 \le 1$.

Proof. We shall use the following notations: $x = \left(X_m, X_f, X_p, X_s, X_i\right)$, and $X_s^0 = \dfrac{\Lambda}{\mu_{s\epsilon}}$. To show the global stability of infection-free equilibrium of system (1), we use the following candidate Lyapunov function:

$$V(x) = \frac{\mu_{s\epsilon} + \alpha_s}{k_f} X_f + \frac{\left(\mu_{s\epsilon} + \alpha_s\right)\left(\mu_{f\epsilon} + \rho\right)}{k_f \rho} X_p + \int_{X_s^0}^{X_s} \frac{X_\tau - X_s^0}{X_\tau} \mathrm{d}X_\tau + X_i \quad (2)$$

This function satisfies: $V(x) \ge 0$ for all $x \in \Omega$, and $V(x) = 0$ if and only if $x = \left(X_m, 0, 0, X_s^0, 0\right)$.

Taking the time derivative of the function V (defined by 2), along the solutions of system (1), we obtain

$$\begin{aligned}\dot{V} &= \left(1 - \frac{X_s^0}{X_s}\right)\left(\Lambda - \mu_{s\epsilon} X_s - \beta X_s X_p\right) + \left(\beta X_s X_p - \left(\mu_{s\epsilon} + \alpha_s\right) X_i\right) \\ &\quad + \frac{\mu_{s\epsilon} + \alpha_s}{k_f}\left(k_f X_i - \left(\mu_{f\epsilon} + \rho\right)\right) X_f + \frac{\left(\mu_{s\epsilon} + \alpha_s\right)\left(\mu_{f\epsilon} + \rho\right)}{k_f \rho}\left(\rho X_f - \mu_{p\epsilon} X_p\right)\end{aligned}$$

Using $\Lambda - \mu_{s\epsilon} X_s^0 = 0$, we get

$$\begin{aligned}\dot{V} &= \left(1 - \frac{X_s^0}{X_s}\right)\left(-\mu_{s\epsilon} X_s + \mu_{s\epsilon} X_s^0\right) + \left[\beta X_s^0 X_p - \frac{\left(\mu_{s\epsilon} + \alpha_s\right)\left(\mu_{f\epsilon} + \rho\right)}{k_f \rho} \mu_{p\epsilon} X_p\right] \\ &= \mu_{s\epsilon} X_s^0 \left(1 - \frac{X_s^0}{X_s}\right)\left(1 - \frac{X_s}{X_s^0}\right) + \frac{\beta\Lambda}{\mu_{s\epsilon}}\left[1 - \frac{\left(\mu_{s\epsilon} + \alpha_s\right)\left(\mu_{f\epsilon} + \rho\right)\mu_{m\epsilon}\mu_{p\epsilon}}{k_f \rho \Lambda \beta}\right] X_p \\ &= \mu_{s\epsilon} X_s^0 \left(1 - \frac{X_s^0}{X_s}\right)\left(1 - \frac{X_s}{X_s^0}\right) + \frac{\beta\Lambda}{\mu_{s\epsilon}}\left[1 - \frac{1}{\mathcal{R}_0}\right] X_p \\ &= -\frac{\mu_{s\epsilon}}{X_s}\left(X_s^0 - X_s\right)^2 + \frac{\beta\Lambda}{\mu_{s\epsilon}}\left[1 - \frac{1}{\mathcal{R}_0}\right] X_p\end{aligned} \quad (3)$$

Hence, $\dot{V} \le 0$ if $\mathcal{R}_0 \le 1$, and

$$\Omega \bigcap \left\{\dot{V} = 0\right\} = \begin{cases} \left\{x \in \Omega : x = \left(X_m, X_f, 0, X_s^0, X_i\right)\right\} & \text{if } \mathcal{R}_0 < 1 \\ \left\{x \in \Omega : x = \left(X_m, X_f, X_p, X_s^0, X_i\right)\right\} & \text{if } \mathcal{R}_0 = 1 \end{cases}$$

We will show that the largest invariant set $\mathcal{L}$ contained in $\Omega \bigcap \left\{\dot{V} = 0\right\}$ is

reduced to the disease-free equilibrium $\mathcal{E}^0$.

Let $x=\left(X_m, X_f, X_p, X_s, X_i\right)\in\mathcal{L}$ and $x(t)=\left(X_m(t), X_f(t), X_p(t), X_s(t), X_i(t)\right)$ the solution of (1) issued from this point. By invariance of $\mathcal{L}$, we have $X_s(t)\equiv X_s^0$ which implies $\dot{X}_s(t)=0=\Lambda-\mu_s X_s(t)-\beta X_p(t)X_s(t)=\Lambda-\mu_s X_s^0-\beta X_p(t)X_s^0$ and hence $X_p(t)=0$ for all *t*. But, $X_p(t)\equiv 0$ implies that $\dot{X}_p(t)=0$ for all *t* which implies, using system (1), that $X_f(t)=0$ for all *t*. In the same way, it can be proved that $X_i(t)=0$ for all *t*. Reporting in the first equation of system (1), one obtains that, in $\mathcal{L}$,

$$\dot{X}_m(t)=-\mu_{m\epsilon}X_m(t)\quad\forall t$$

Thus the solution of (1) issued from $x=\left(X_m, X_f, X_p, X_s, X_i\right)\in\mathcal{L}$ is given by $x(t)=\left(X_m e^{-\mu_{m\epsilon}t}, 0, 0, X_s^0, 0\right)$ which clearly leaves Ω and hence $\mathcal{L}$ for $t<0$ if $X_m\neq 0$. Therefore $\mathcal{L}=\left\{\mathcal{E}^0\right\}$ and hence $\mathcal{E}^0$ is a globally asymptotically stable equilibrium state for system (1) on the compact set Ω thanks to LaSalle invariance principle [11], (one can also see [12], Theorem 3.7.11, page 346). Since the set Ω is an attractive set, the DFE is actually GAS on the non-negative orthant $\mathbb{R}_+^5$.

Biologically speaking, Theorem 3 implies that schistosomiasis may be eliminated from the community if $\mathcal{R}_0\leq 1$. One can remark that $\mathcal{R}_0$ does not depend on $\mu_{m\epsilon}=\mu_m+\epsilon_m$. Hence it is not helpful to try to control the male schistosoma population and then one can take $\epsilon_m=0$. Therefore the only way to eliminate schistosomiasis is to increase the killing rates of female schistosoma (ϵ_f), paired schistosoma (ϵ_p) and snails (ϵ_s) in order to have $\mathcal{R}_0\leq 1$.

In the rest of this section, we show that the disease persists when $\mathcal{R}_0>1$. The disease is endemic if the infected fraction of the population persists above a certain positive level. The endemicity of a disease can be well captured and analyzed through the notion of uniform persistence. System (1) is said to be uniformly persistent in Ω if there exists constant $c>0$, independent of initial conditions in $\mathring{\Omega}$ (the interior of Ω), such that all solutions $\left(X_m(t), X_f(t), X_p(t), X_s(t), X_i(t)\right)$ of system (1) satysfy

$$\liminf_{t\to\infty} X_m(t)\geq c,\quad \liminf_{t\to\infty} X_f(t)\geq c,\quad \liminf_{t\to\infty} X_p(t)\geq c,$$

$$\liminf_{t\to\infty} X_s(t)>c,\quad \liminf_{t\to\infty} X_i(t)\geq c,$$

provided $\left(X_m(0), X_f(0), X_p(0), X_s(0), X_i(0)\right)\in\mathring{\Omega}$, (see [13] [14]).

Theorem 4 *System* (1) *is uniformly persistent in* Ω *if and only if* $\mathcal{R}_0>1$.

Proof. When $\mathcal{R}_0\leq 1$, the infection-free equilibrium $\mathcal{E}^0$ is globally asymptotically stable which precludes any sort of persistence and hence $\mathcal{R}_0>1$ is a necessary condition for persistence. In order to show that $\mathcal{R}_0>1$ is a sufficient condition for uniform persistence, it suffices to verify conditions (1) and (2) of Theorem 4.1 in [15] (one can also see [16], Theorem 3.5).

We use the notations of [15] with $\mathscr{X}=\Omega$ and $\mathscr{Y}=\partial\Omega$. Let M be the largest invariant compact set in $\mathscr{Y}$. We have already seen that $M=\left\{\mathcal{E}^0\right\}$, and so M is isolated. To show that $\mathcal{W}^s(M)$ (the stable set of M) is contained in

$\mathscr{Y} = \partial\Omega$, we use the following function:

$$\mathcal{F} = \frac{\mu_{s\epsilon} + \alpha_s}{k_f} X_f + \frac{(\mu_{s\epsilon} + \alpha_s)(\mu_{f\epsilon} + \rho)}{k_f \rho} X_p + X_i$$

The time derivative of $\mathcal{F}$ along the solutions of system (1) is given by

$$\begin{aligned}\dot{\mathcal{F}} &= \beta X_s X_p - \frac{(\mu_{s\epsilon} + \alpha_s)(\mu_{f\epsilon} + \rho)}{k_f \rho} \mu_{p\epsilon} X_p \\ &= \left(\beta X_s - \frac{(\mu_{s\epsilon} + \alpha_s)(\mu_{f\epsilon} + \rho)}{k_f \rho} \mu_{p\epsilon} \right) X_p \\ &= \frac{\mu_{p\epsilon}(\mu_{s\epsilon} + \alpha_s)(\mu_{f\epsilon} + \rho)}{k_f \rho} \left(\beta X_s \frac{k_f \rho}{\mu_{p\epsilon}(\mu_{s\epsilon} + \alpha_s)(\mu_{f\epsilon} + \rho)} - 1 \right) X_p \\ &= \frac{\mu_{p\epsilon}(\mu_{s\epsilon} + \alpha_s)(\mu_{f\epsilon} + \rho)}{k_f \rho} \left(\mathcal{R}_0 \frac{X_s}{X_s^0} - 1 \right) X_p\end{aligned}$$

Since $\mathcal{R}_0 > 1$, we have $\dot{\mathcal{F}} > 0$ for $X_p > 0$ and $\frac{X_s^0}{\mathcal{R}_0} < X_s \le X_s^0$. Therefore $\dot{\mathcal{F}} > 0$ in a neighborhood N of $\mathcal{E}^0$ relative to $\Omega \setminus \partial\Omega$. This implies that any solution starting in N must leave N at finite time and hence the stable set of M, $W^s(M)$ is contained in $\partial\Omega$.

4. Endemic Equilibrium and Its Stability

Endemic equilibrium points are steady-state solutions where the disease persists in the population (all state variables are positive).

In this case system (1) has an endemic equilibrium point given by

$$\mathcal{E}_h = \begin{cases} X_m^* = \mu_{p\epsilon}\mu_{s\epsilon} \dfrac{\rho(k_m - k_f) + k_m \mu_{f\epsilon}}{\beta \rho k_f \mu_{m\epsilon}} (\mathcal{R}_0 - 1), \\ X_f^* = \dfrac{k_f \Lambda}{(\mu_{s\epsilon} + \alpha_s)(\rho + \mu_{f\epsilon})} \left(1 - \dfrac{1}{\mathcal{R}_0}\right), \quad X_p^* = \dfrac{(\mathcal{R}_0 - 1)\mu_{s\epsilon}}{\beta}, \\ X_s^* = \dfrac{\Lambda}{\mathcal{R}_0 \mu_{s\epsilon}}, \quad X_i^* = \dfrac{\Lambda}{\mu_{s\epsilon} + \alpha_s} \left(1 - \dfrac{1}{\mathcal{R}_0}\right). \end{cases}$$

This equilibrium has a biological sense only when $\mathcal{R}_0 > 1$.

Theorem 5 *If $\mathcal{R}_0 > 1$, the unique endemic equilibrium $\mathcal{E}_h$ is globally asymptotically stable.*

Proof. In order to investigate the global stability of the endemic equilibrium, we consider the following function defined on $\Omega_1 = \{x \in \Omega : X_f > 0, X_p > 0, X_s > 0 \text{ and } X_s > 0\}$:

$$\begin{aligned}W(x) = \frac{(\mu_{s\epsilon} + \alpha_s)}{k_f} \int_{X_f}^{X_f^*} \frac{u - X_f^*}{u} du + \frac{(\mu_{s\epsilon} + \alpha_s)(\mu_{f\epsilon} + \rho)}{k_f \rho} \int_{X_p}^{X_p^*} \frac{u - X_p^*}{u} du \\ + \int_{X_s}^{X_s^*} \frac{u - X_s^*}{u} du + \int_{X_i}^{X_i^*} \frac{u - X_i^*}{u} du\end{aligned}$$

This function satisfies: $W(x) \geq 0$ for all $x \in \Omega_1$, and $W(x) = 0$ if and only if $(X_f, X_p, X_s, X_i) = (X_f^*, X_p^*, X_s^*, X_i^*)$. The time derivative of W with respect to the solutions of system (1) is

$$\begin{aligned}
\dot{W} &= \left(1-\frac{X_s^*}{X_s}\right)\left(\Lambda - \mu_{s\epsilon} X_s - \beta X_s X_p\right) \\
&\quad + \left(1-\frac{X_i^*}{X_i}\right)\left(\beta X_s X_p - (\mu_{s\epsilon} + \alpha_s) X_i\right) \\
&\quad + \frac{(\mu_{s\varepsilon} + \alpha_s)}{k_f}\left(1-\frac{X_f^*}{X_f}\right)\left(k_f X_i - (\mu_{f\epsilon} + \rho) X_f\right) \\
&\quad + \frac{(\mu_{s\epsilon} + \alpha_s)(\mu_{f\epsilon} + \rho)}{k_f \rho}\left(1-\frac{X_p^*}{X_p}\right)\left(\rho X_f - \mu_{p\epsilon} X_p\right) \\
&= (\Lambda - \mu_{s\epsilon} X_s)\left(1-\frac{X_s^*}{X_s}\right) + \beta X_s^* X_p - \beta X_s X_p - \frac{X_i^*}{X_i}\beta X_s X_p \\
&\quad + (\mu_{s\epsilon} + \alpha_s) X_i^* + \beta X_s X_p - (\mu_{s\epsilon} + \alpha_s) X_i - (\mu_{s\epsilon} + \alpha_s)\frac{X_f^*}{X_f} X_i \\
&\quad + \frac{(\mu_{s\epsilon} + \alpha_s)(\mu_{f\epsilon} + \rho)}{k_f \rho} X_f^* - (\mu_{s\epsilon} + \alpha_s) X_i - \frac{(\mu_{s\epsilon} + \alpha_s)(\mu_{f\epsilon} + \rho)}{k_f} X_f \\
&\quad - \frac{(\mu_{s\epsilon} + \alpha_s)(\mu_{f\epsilon} + \rho)}{k_f \rho} \mu_{p\epsilon} X_p + (\mu_{s\epsilon} + \alpha_s) X_i \\
&\quad - \frac{(\mu_{s\epsilon} + \alpha_s)(\mu_{f\epsilon} + \rho)}{k_f} X_f - \frac{(\mu_{s\epsilon} + \alpha_s)(\mu_{f\epsilon} + \rho)}{k_f \rho} \mu_{p\epsilon} X_p \\
&\quad + \frac{(\mu_{s\epsilon} + \alpha_s)(\mu_{f\epsilon} + \rho)}{k_f \rho} \frac{X_p^*}{X_p} \mu_{p\epsilon} X_p + \frac{(\mu_{s\epsilon} + \alpha_s)(\mu_{f\epsilon} + \rho)}{k_f} X_f \\
&\quad - \frac{(\mu_{s\epsilon} + \alpha_s)(\mu_{f\epsilon} + \rho)}{k_f \rho} \frac{X_p^*}{X_p} X_f
\end{aligned}$$

Thus,

$$\begin{aligned}
\dot{W} &= (\Lambda - \mu_{s\epsilon} X_s)\left(1-\frac{X_s^*}{X_s}\right) + \beta X_s^* X_p - \frac{X_i^*}{X_i}\beta X_s X_p + (\mu_{s\epsilon} + \alpha_s) X_i^* \\
&\quad - (\mu_{s\epsilon} + \alpha_s)\frac{X_f^*}{X_f} X_i + \frac{(\mu_{s\epsilon} + \alpha_s)(\mu_{f\epsilon} + \rho)}{k_f} X_f^* \\
&\quad - \frac{(\mu_{s\epsilon} + \alpha_s)(\mu_{f\epsilon} + \rho)}{k_f \rho} \mu_{p\epsilon} X_p - \frac{(\mu_{s\epsilon} + \alpha_s)(\mu_{f\epsilon} + \rho)}{k_f} \frac{X_p^*}{X_p} X_f \\
&\quad + \frac{(\mu_{s\epsilon} + \alpha_s)(\mu_{f\epsilon} + \rho)}{k_f \rho} \frac{X_p^*}{X_p} \mu_{p\epsilon} X_p.
\end{aligned}$$

Using the equilibrium relations ($\mathcal{EQ}$)

$$\mathcal{EQ} = \begin{cases} \Lambda - \mu_{s\epsilon} X_s^* = \beta X_s^* X_p^*, \quad \beta\Lambda - \mu_{s\epsilon} X_s^* = (\mu_{s\epsilon} + \alpha_s) X_i^*, \\ \rho X_f^* = \mu_{p\epsilon} X_p^*, \quad k_f X_i^* = (\mu_{s\epsilon} + \rho) X_f^*. \end{cases}$$

It follows that

$$\begin{aligned}\dot{W} &= \left(\Lambda-\mu_{s\epsilon}X_s\right)\left(1-\frac{X_s^*}{X_s}\right)+\beta X_s^* X_p-\left(\mu_{s\epsilon}+\alpha_s\right)\frac{X_i^*}{\beta X_s^* X_p^*}\frac{X_i^*}{X_i}\beta X_s X_p\\ &\quad+\left(\mu_{s\epsilon}+\alpha_s\right)X_i^*-\left(\mu_{s\epsilon}+\alpha_s\right)\frac{X_i^*}{X_i^*}\frac{X_f^*}{X_f}X_i+\left(\mu_{s\epsilon}+\alpha_s\right)X_i^*\\ &\quad-\left(\mu_{s\epsilon}+\alpha_s\right)X_i^*\frac{X_p^*}{X_p}-\left(\mu_{s\epsilon}+\alpha_s\right)\frac{X_i^*}{X_f^*}\frac{X_p^*}{X_p}X_f+\left(\mu_{s\epsilon}+\alpha_s\right)X_i^*\frac{X_p}{X_p^*}\frac{X_p^*}{X_p}\\ &=\left(\Lambda-\mu_{s\epsilon}X_s\right)\left(1-\frac{X_s^*}{X_s}\right)+\beta X_s^* X_p+\left(\mu_{s\epsilon}+\alpha_s\right)X_i^*\left[\frac{X_p^*}{X_p}\frac{X_f}{X_f^*}-\frac{X_p^*}{X_p}\right]\\ &\quad-\left(\mu_{s\epsilon}+\alpha_s\right)X_i^*\left[\frac{X_i^*}{X_i}\frac{X_s}{X_s^*}\frac{X_p}{X_p^*}+\frac{X_i}{X_i^*}\frac{X_f^*}{X_f}+\frac{X_p^*}{X_p}\frac{X_f}{X_f^*}-2\right]\end{aligned}$$

$$\begin{aligned}&=\left(\Lambda-\mu_{s\epsilon}X_s\right)\left(1-\frac{X_s^*}{X_s}\right)+\left(\mu_{s\epsilon}+\alpha_s\right)\frac{X_i^*}{X_p^*}X_p+\left(\mu_{s\epsilon}+\alpha_s\right)X_i^*\left[\frac{X_p^*}{X_p}\frac{X_p}{X_p^*}-\frac{X_p}{X_p^*}\right]\\ &\quad-\left(\mu_{s\epsilon}+\alpha_s\right)X_i^*\left[\frac{X_s^*}{X_s}+\frac{X_i^*}{X_i}\frac{X_s}{X_s^*}\frac{X_p}{X_p^*}+\frac{X_i}{X_i^*}\frac{X_f^*}{X_f}+\frac{X_p^*}{X_f}\frac{X_p}{X_f^*}-4\right]\\ &\quad+\left(\mu_{s\epsilon}+\alpha_s\right)X_i^*\frac{X_s^*}{X_s}-2\left(\mu_{s\epsilon}+\alpha_s\right)X_i^*.\end{aligned}$$

This implies that

$$\begin{aligned}\dot{W} &= \left(\Lambda-\mu_{s\epsilon}X_s-\left(\mu_{s\epsilon}+\alpha_s\right)X_i^*\right)\left(1-\frac{X_s^*}{X_s}\right)\\ &\quad+\left(\mu_{s\epsilon}+\alpha_s\right)X_i^*\left[\frac{X_p^*}{X_p}\frac{X_p}{X_p^*}-\frac{X_p}{X_p^*}+\frac{X_p}{X_p^*}-1\right]\\ &\quad-\left(\mu_{s\epsilon}+\alpha_s\right)X_i^*\left[\frac{X_s^*}{X_s}+\frac{X_i^*}{X_i}\frac{X_s}{X_s^*}\frac{X_p}{X_p^*}+\frac{X_i}{X_i^*}\frac{X_f^*}{X_f}+\frac{X_p^*}{X_f}\frac{X_p}{X_f^*}-4\right]\end{aligned}$$

And since $\left(\mu_{s\epsilon}+\alpha_s\right)X_i^*=\Lambda-\mu_{s\epsilon}X_s^*$, it follows that

$$\begin{aligned}\dot{W} &= \mu_{s\epsilon}X_s^*\left(1-\frac{X_s^*}{X_s}\right)\left(1-\frac{X_s}{X_s^*}\right)\\ &\quad-\left(\mu_{s\epsilon}+\alpha_s\right)X_i^*\left[\frac{X_s^*}{X_s}+\frac{X_i^*}{X_i}\frac{X_s}{X_s^*}\frac{X_p}{X_p^*}+\frac{X_i}{X_i^*}\frac{X_f^*}{X_f}+\frac{X_p^*}{X_f}\frac{X_p}{X_f^*}-4\right]\end{aligned}$$

From the AM-GM inequality (which says that the algebraic mean is not smaller than the geometric mean), we have

$$\frac{X_s^*}{X_s}+\frac{X_i^*}{X_i}\frac{X_s}{X_s^*}\frac{X_p}{X_p^*}+\frac{X_i}{X_i^*}\frac{X_f^*}{X_f}+\frac{X_p^*}{X_f}\frac{X_p}{X_f^*}-4\geq 0$$

$$\left(1-\frac{X_s^*}{X_s}\right)\left(1-\frac{X_s}{X_s^*}\right)\leq 0.$$

Then, $\dot{W} \le 0$ on Ω_1 for $\mathcal{R}_0 > 1$. Hence, W is a Lyapunov function on Ω_1. Moreover, $\dot{W} = 0$ if and only if $X_f = X_f^*$, $X_p = X_p^*$, $X_s = X_s^*$, and $X_i = X_i^*$.

To obtain the largest invariant set $\mathcal{L}$ within the region $\left\{x \in \Omega_1 : \dot{W} = 0\right\}$, note that the trajectory of $X_m(t)$ with an initial condition in $\mathcal{L}$ must be a solution of:

$$\frac{\mathrm{d}X_m}{\mathrm{d}t} = k_m X_i^* - \mu_{m\epsilon} X_m - \rho X_f^*$$

Consequently, we have that

$$X_m(t) = \frac{k_m X_i^* - \rho X_f^*}{\mu_{m\epsilon}} + \mathrm{e}^{-(\mu_{m\epsilon}+\epsilon_m)t}\left(X_m(0) - \frac{k_m X_i^* - \rho X_f^*}{\mu_{m\epsilon}}\right) \quad \forall t$$

Since $X_m(t)$ must not leave the domain $\mathcal{L}$ for all t, it follows that

$$X_m(t) = \frac{k_m X_i^* - \rho X_f^*}{\mu_{m\epsilon}} \quad \forall t$$

Hence, the largest invariant set $\mathcal{L}$ contained in $\left\{x \in \Omega_1 : \dot{W} = 0\right\}$ is reduced to $\{\mathcal{E}_h\}$, and therefore by LaSalle's principle [11], $\mathcal{E}_h$ is globally asymptotically stable over Ω_1.

5. Sensitivity Analysis and Numerical Simulations

Sensitivity analysis and simulations are important to determine how best we can reduce the effect of schistosomiasis, by studying the relative importance of different factors responsible for its transmission and prevalence. Generally speaking, initial disease transmission is directly related to the basic reproduction number, and the disease prevalence is directly related to the endemic equilibrium state $\mathcal{E}_h$, and more specifically to the magnitude of X_i^*, X_m^*, X_f^*, X_p^*. We perform the analysis by deriving the sensitivity indices of the basic reproduction number to the parameters using both local and global methods.

5.1. Local Sensitivity Analysis of $\mathcal{R}_0$

We calculate the sensitivity indices of the reproductive number, $\mathcal{R}_0$, and the endemic equilibrium point, $\mathcal{E}_h$, to the parameters in the model. we can derive an analytical expression for its sensitivity to each parameter using the normalized forward sensitivity index as described by Chitnis *et al.* [17].

The normalized forward sensitivity index of a variable to a parameter is a ratio of the relative change in the variable to the relative change in the parameter. When a variable is a differentiable function of the parameter, the sensitivity index may be alternatively defined using partial derivatives.

Definition 1 *The normalised forward sensitivity index of a variable p that depends differentiable on a parameter q is defined as*:

$$\Upsilon_q^p = \frac{\partial p}{\partial q} \times \frac{q}{p}$$

Sensitivity analysis is commonly used to determine the robustness of model predictions to parameter values (since there are usually errors in data collection and presumed parameter values). Here we use it to discover parameters that have a high impact on $\mathcal{R}_0$, and $\mathcal{E}_h$, and should be targeted by intervention strategies.

The sensitivity analysis of $\mathcal{R}_0$ has already been done in [6]. We just correct here the expressions of the flexibilities of $\mu_{s\epsilon}$, $\mu_{f\epsilon}$, and $\mu_{p\epsilon}$ on the basic reproduction number $\mathcal{R}_0$ (the mistakes in [6] are due to the error in the expression of $\mathcal{R}_0$). The right expressions are:

$$\Upsilon_{\mu_{s\epsilon}}^{\mathcal{R}_0} = \frac{\partial \mathcal{R}_0}{\partial \mu_{s\epsilon}} \times \frac{\mu_{s\epsilon}}{\mathcal{R}_0} = -\frac{2\mu_{s\epsilon} + \alpha_s}{\mu_{s\epsilon} + \alpha_s}$$

$$\Upsilon_{\mu_{f\epsilon}}^{\mathcal{R}_0} = \frac{\partial \mathcal{R}_0}{\partial \mu_{f\epsilon}} \times \frac{\mu_{f\epsilon}}{\mathcal{R}_0} = -\frac{\mu_{f\epsilon}}{\mu_{f\epsilon} + \rho}$$

$$\Upsilon_{\mu_{p\epsilon}}^{\mathcal{R}_0} = \frac{\partial \mathcal{R}_0}{\partial \mu_{p\epsilon}} \times \frac{\mu_{p\epsilon}}{\mathcal{R}_0} = -1$$

However the conclusions are not affected: the authors remarked that $\left|\Upsilon_{\mu_{f\epsilon}}^{\mathcal{R}_0}\right| < 1 = \left|\Upsilon_{\mu_{p\epsilon}}^{\mathcal{R}_0}\right| < \left|\Upsilon_{\mu_{s\epsilon}}^{\mathcal{R}_0}\right|$, and so the most sensitive parameter most sensitive parameter is $\mu_{s\epsilon}$ the death rate of snails, followed by $\mu_{p\epsilon}$ the death rate of pair schistosoma. The least sensitive parameter is $\mu_{f\epsilon}$ the death rate of female single schistosoma. Therefore the most efficient way to reduce the value of $\mathcal{R}_0$ is to reduce the snail host population.

Sensitivity analysis of $\mathcal{E}_h$

Since in general it is not easy to reduce the value of $\mathcal{R}_0$ to be less than one and hence to eradicate the disease, one of the control strategy goal could be to reduce the disease prevalence. To this end, we perform a sensitivity analysis of the endemic equilibrium state. Sensitivity analysis of the endemic equilibrium has usually been used to determine the relative importance of different parameters responsible for equilibrium disease prevalence. Equilibrium disease prevalence is related to the magnitude of $\left(X_m^*, X_f^*, X_p^*, X_i^*\right)$, and specifically to the magnitude of X_i^*.

The sensitivity indices of X_i^*, to the parameters, $\mu_{s\epsilon}$, $\mu_{f\epsilon}$ and $\mu_{p\epsilon}$ are given by

$$\Upsilon_{\mu_{s\epsilon}}^{X_i^*} = \frac{\partial X_i^*}{\partial \mu_{s\epsilon}} \times \frac{\mu_{s\epsilon}}{X_i^*} = \frac{\mu_{s\epsilon}\left(\beta\rho k_f \Lambda_s + \mu_{p\epsilon}\left(\mu_{f\epsilon} + \rho\right)\left(\alpha_s + \mu_{s\epsilon}\right)^2\right)}{\left(\alpha_s + \mu_{s\epsilon}\right)\left(\mu_{p\epsilon}\mu_{s\epsilon}\left(\mu_{f\epsilon} + \rho\right)\left(\alpha_s + \mu_{s\epsilon}\right) - \beta\rho k_f \Lambda_s\right)}$$

$$\Upsilon_{\mu_{f\epsilon}}^{X_i^*} = \frac{\partial X_i^*}{\partial \mu_{f\epsilon}} \times \frac{\mu_{f\epsilon}}{X_i^*} = \frac{\mu_{s\epsilon}\left(\beta\rho k_f \Lambda_s + \mu_{p\epsilon}\left(\mu_{f\epsilon} + \rho\right)\left(\alpha_s + \mu_{s\epsilon}\right)^2\right)}{\left(\alpha_s + \mu_{s\epsilon}\right)\left(\mu_{p\epsilon}\mu_{s\epsilon}\left(\mu_{f\epsilon} + \rho\right)\left(\alpha_s + \mu_{s\epsilon}\right) - \beta\rho k_f \Lambda_s\right)}$$

$$\Upsilon_{\mu_{p\epsilon}}^{X_i^*} = \frac{\partial X_i^*}{\partial \mu_{p\epsilon}} \times \frac{\mu_{p\epsilon}}{X_i^*} = \frac{\mu_{p\epsilon}\mu_{s\epsilon}\left(\mu_{f\epsilon} + \rho\right)\left(\alpha_s + \mu_{s\epsilon}\right)}{\mu_{p\epsilon}\mu_{s\epsilon}\left(\mu_{f\epsilon} + \rho\right)\left(\alpha_s + \mu_{s\epsilon}\right) - \beta\rho k_f \Lambda_s}$$

It follows that

$$\frac{\Upsilon_{\mu_{s\epsilon}}^{X_i^*}}{\Upsilon_{\mu_{f\epsilon}}^{X_i^*}} = \frac{\beta\rho k_f \Lambda_s}{\mu_{f\epsilon}\mu_{p\epsilon}\left(\alpha_s + \mu_{s\epsilon}\right)^2} + \frac{\mu_{f\epsilon} + \rho}{\mu_{f\epsilon}}$$

$$\frac{\Upsilon_{\mu_{f\epsilon}}^{X_i^*}}{\Upsilon_{\mu_{p\epsilon}}^{X_i^*}} = \frac{\mu_{f\epsilon}}{\mu_{f\epsilon} + \rho}$$

$$\frac{\Upsilon_{\mu_{s\epsilon}}^{X_i^*}}{\Upsilon_{\mu_{p\epsilon}}^{X_i^*}} = \frac{\beta\rho k_f \Lambda_s}{\mu_{p\epsilon}\left(\mu_{f\epsilon} + \rho\right)\left(\alpha_s + \mu_{s\epsilon}\right)^2} + 1$$

This implies that

$$\left|\Upsilon_{\mu_{f\epsilon}}^{X_i^*}\right| < \left|\Upsilon_{\mu_{p\epsilon}}^{X_i^*}\right| < \left|\Upsilon_{\mu_{s\epsilon}}^{X_i^*}\right|$$

We note that the most sensitive parameter for X_i^* is $\mu_{s\epsilon}$ the death rate of host snails followed by $\mu_{p\epsilon}$ the death rate of pair parasites and $\mu_{f\epsilon}$ the death rate of female parasites.

5.2. Global Sensitivity Analysis of $\mathcal{R}_0$

In this subsection we propose the global sensitivity analysis of the model parameter to determine how much the parameters affect the output of the model. Global sensitivity analysis is a collection of more robust procedures, modifying groups of parameters simultaneously, with a specific goal to recognize the impacts of interactions between various parameters. LHS is at present the most productive and refined statistical techniques [18] and Blower presented it of the field of disease modelling in 1994. We use the technique of Latin Hypercube Sampling, which belong to the monte Carlo class of sampling methods [19]. LHS allows for an efficient analysis of parameter variations across simultaneous uncertainty ranges in each parameter. For each parameter, a probability density function is defined and stratified into N equiproportional serial intervals [20]. Here, for each input parameter we have assumed a uniform distribution across the ranges listed in **Table 1** due to the absence of data on the distribution function. We then calculated $\mathcal{R}_0$ as the model output using $n = 1000$ sets of sampled parameters. We used the partial rank correlation coefficient (PRCC) to assess the significance of each parameter with respect to $\mathcal{R}_0$. **Figure 1** illustrates the results for the range of parameters in **Table 1**. The sign of the correlation coefficient indicates the direction of the relationship and the value of the correlation indicates the strength of the relationship between input parameters and model output. The global sensitive analysis confirm the local conclusions by showing the influence of the death rate to the model output $\mathcal{R}_0$. The death rate $\mu_{s\epsilon}$ have negative PRCC values, all above 0.5 indicating high significance to $\mathcal{R}_0$ with indirect proportional relationship, that is, an increase in $\mu_{s\epsilon}$ increases $\mathcal{R}_0$. This suggests that this parameter need to be estimated with precision ignored to accurately capture the transmission dynamics of schistosomiasis. The model output is also sensitive to $\mu_{p\epsilon}$ and $\mu_{f\epsilon}$ with PRCC negative indicating a decrease in $\mathcal{R}_0$.

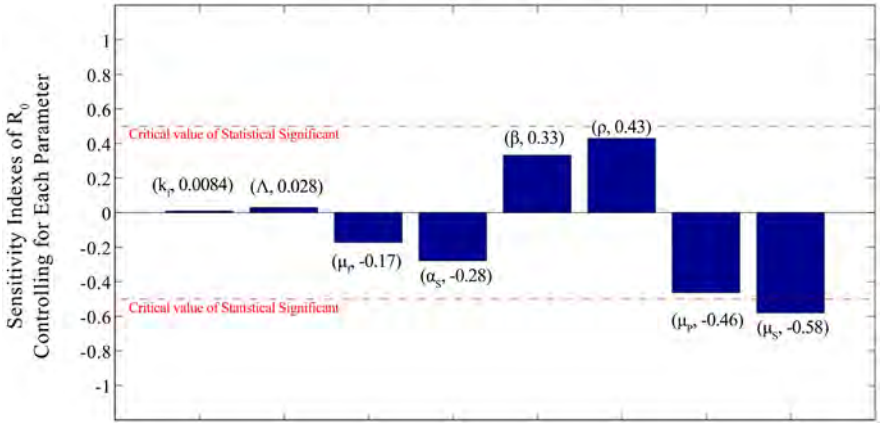

Figure 1. Sensitivity indexes of $\mathcal{R}_0$ in terms of the model parameters disposed in order of increasing magnitude.

Table 1. Numerical values of the parameters of model system.

Parameter	Description	Sample value	Range
Λ	recruitment rate of snail hosts	150 per year	100 - 200
k_m	recruitment rate of single male	145 per year	-
k_f	recruitment rate of single female	100 per year	-
μ_m	elimination rate of single male	0.1 per year	0.01 - 0.2
μ_p	elimination rate of single pair	0.02 per year	0.001 - 0.05
μ_f	elimination rate of single female	0.2 per year	0.1 - 0.5
μ_s	elimination rate of snail hosts	0.1 per year	0.01 - 0.2
α_s	disease-induced death rate of snail hosts	0.5 per year	0.1 - 0.9
β	transmission rate from pairs to susceptible snails	1.8×10^{-4} per year	10×10^{-4} - 25×10^{-4}
ρ	the effective mating rate 0.467 per year	0.467 per year	0.1 - 0.5

6. Optimal Control

In this section, we aim to place the system (1) thereof in an optimal control setting, in order to be able to calculate the optimal intervention strategies. The optimal control represents the most effective way of controlling the disease that can be adopted by authorities in response to its outbreak. We now modify our model (1) with time-dependent treatment effort $u(t)$ as control for the system. The variable $u(t)$ represents the amounts of insecticide that is continuously applied during a considered period, as a measure to fight the disease:

$u(t) \equiv$ level of insecticide campaigns at time t

Our model with snails treatment can be described with the following differential equations:

$$\begin{cases} \dfrac{\mathrm{d}X_m}{\mathrm{d}t} = k_m X_i - \left(\mu_m + \epsilon_m\right) X_m - \rho X_f, \\ \dfrac{\mathrm{d}X_f}{\mathrm{d}t} = k_f X_i - \left(\mu_f + \epsilon_f\right) X_f - \rho X_f, \end{cases} \tag{4}$$

$$\begin{cases} \dfrac{\mathrm{d}X_p}{\mathrm{d}t} = \rho X_f - \left(\mu_p + \epsilon_p\right) X_p, \\ \dfrac{\mathrm{d}X_s}{\mathrm{d}t} = \Lambda - \left(\mu_s + \epsilon_s\right) X_s - \beta X_p X_s, \\ \dfrac{\mathrm{d}X_i}{\mathrm{d}t} = \beta X_p X_s - \left(\mu_s + \epsilon_s + \alpha_s + u(t)\right) X_i. \end{cases}$$

The control variable $u(t)$ is a bounded, Lebesgue integrable function that is considered in relative terms, varying from 0 to 1. The goal is to maximize the following objective function

$$J(u) = \min_u \int_0^T \left(c_s X_s(t) + c_i X_i(t) + \frac{1}{2} c_u u(t)^2 \right) \mathrm{d}t$$

subject to the system differential Equations (4), where c_s, c_i and c_u are the positive balancing constants. We seek to find an optimal control u^* such that

$$J(u^*) = \min_u \{ J(u) \}$$

where the control set is defined as
$\mathcal{U} = \{ u : [0,T] \to [0,1], u \text{ is Lebesgue measurable} \}$. Here, the running costs of susceptible snails are given by $c_s X_s(t)$, while term $c_i X_i(t)$ determines the costs of infected snails. Notice that $\frac{1}{2} c_u u(t)^2$ is the cost of eliminating a fraction $N_Y = \left(X_s(t) + X_i(t)\right)$ of the snails population. The choice of the cost function as linear in the number of susceptible and infected and quadratic in the control is as generally done [21] [22] [23].

6.1. The Optimality System

This system satisfies standard conditions for the existence of an optimal control and thus by using Pontryagins Maximum Principle as stated in [24] [25], we derive the necessary conditions for our optimal control and corresponding states. The Hamiltonian H for the control problem is as follows:

$$\begin{aligned} H = {} & c_s X_s(t) + c_i X_i(t) + \frac{1}{2} c_u u(t)^2 + \lambda_1(t) \frac{\mathrm{d}X_m}{\mathrm{d}t} + \lambda_2(t) \frac{\mathrm{d}X_f}{\mathrm{d}t} \\ & + \lambda_3(t) \frac{\mathrm{d}X_p}{\mathrm{d}t} + \lambda_4(t) \frac{\mathrm{d}X_s}{\mathrm{d}t} + \lambda_5(t) \frac{\mathrm{d}X_i}{\mathrm{d}t} \end{aligned}$$

The adjoint variables $\lambda_i \left(i = 1,2,3,4,5\right)$ are the solution of the following system:

$$\begin{cases} \dfrac{\mathrm{d}\lambda_1}{\mathrm{d}t} = \mu_m \lambda_1(t), \\ \dfrac{\mathrm{d}\lambda_2}{\mathrm{d}t} = -\lambda_2(t)\left(-\mu_f - \rho\right) + \rho\lambda_1(t) - \rho\lambda_3(t), \\ \dfrac{\mathrm{d}\lambda_3}{\mathrm{d}t} = \mu_p \lambda_3(t) - \beta\lambda_4(t) X_s(t) - \beta\lambda_5(t) X_s(t), \\ \dfrac{\mathrm{d}\lambda_4}{\mathrm{d}t} = -c_s - \beta\lambda_4(t) X_p(t) - \beta\lambda_5(t) X_p(t), \\ \dfrac{\mathrm{d}\lambda_5}{\mathrm{d}t} = -c_i - k_f \lambda_2(t) - \lambda_4(t)\left(-\alpha_s - \mu_s - u(t)\right) - \lambda_5(t)\left(-\alpha_s - \mu_s - u(t)\right). \end{cases} \quad (5)$$

with the boundary conditions $\lambda_i(T)=0$.

By using Pontryagins Maximum Principle and the existence result for the optimal control from Fleming and Rishel [8], we obtain

Theorem 6 *There exists an optimal strategy* $u^* \in \mathcal{U}$ *such that*

$$J(u^*)=\min_{u\in\mathcal{U}}\{J(u)\},$$

given by

$$u^*=\min\left\{1,\max\left\{0,\frac{\lambda_4 X_i+\lambda_5 X_i}{c_u}\right\}\right\}$$

where $\lambda_i\ (i=1,2,3,4,5)$ *are the solutions of* (5).

Proof. Here the control and the state variables are nonnegative values. The necessary convexity of the objective functional in u is satisfied for this minimising problem. The control variable set $u\in\mathcal{U}$ is also convex and closed by definition. In addition, the integrand of $J(u)$ with respect to control variables u^* is convex and it is easy to verify the Lipschitz property of the state system with respect to the state variables. Together with a priori boundedness of the state solutions, the existence of an optimal control has been given by in [8] (see corollary 4.1).

System (5) is obtained by differentiating the Hamiltonian function. Furthermore, by equating to zero the derivatives of the Hamiltonian with respect to the control, we obtain

$$\frac{\partial H}{\partial t}=c_u(t)-\lambda_4(t)X_i(t)-\lambda_5 X_i(t)=0$$

$$\Rightarrow u^*(t)=\frac{\lambda_4(t)X_i(t)+\lambda_5 X_i(t)}{c_u}$$

Using the property of the control space, we obtain

$$u^*(t)=\begin{cases}0, & \text{if } \dfrac{l_4(t)X_i(t)+l_5X_i(t)}{c_u}\le 0\\[2ex] \dfrac{\lambda_4(t)X_i(t)+\lambda_5X_i(t)}{c_u}, & \text{if } \dfrac{l_4(t)X_i(t)+l_5X_i(t)}{c_u}\in(0,1)\\[2ex] 1, & \text{if } \dfrac{l_4(t)X_i(t)+l_5X_i(t)}{c_u}\ge 1.\end{cases}$$

Those can be rewritten in compact notation

$$u^*=\min\left\{1,\max\left\{0,\frac{\lambda_4 X_i+\lambda_5 X_i}{c_u}\right\}\right\}$$

6.2. Numerical Examples

The numerical simulations are completed utilizing Matlab and making use of parameter values in [6] to verify the effectiveness of our new model by comparing the disease progression before and after introducing the optimal control variables $u(t)$. For that, first we solve system (4) with a guess for the controls over

the time interval $[0,T]$ using a forward fourth-order Runge-Kutta scheme and the transversality conditions $\lambda_i(T)=0, i=1,\cdots,5$. Then, system (5) is solved by a backward fourth-order Runge-Kutta scheme using the current iteration solution of (4).

The control is updated by using a convex combination of the previous control. The iteration is stopped when the values of the unknowns at the previous iteration are very close to the ones at the present iteration. For more details see, e.g., [25].

We represent the solution curves of the five state variables both in the presence and absence of the control. When viewing the graphs, remember that each of the individuals with control is marked by dashed blue lines. The individuals without control are marked by red lines. It is observed that the application of optimal control reduces a quite larger number of schistosoma (male, female, pair) and snails in the absence of the control. This is occurring as the application of pesticide control reduces the snails population significantly as seen in **Figure 2** and **Figure 3**. Again from the **Figures 4-6** it is easy to see that the schistosoma population also much affected due to the use of the insecticide control.

We have considered the schistosomiasis infection in an endemic population (when $\mathcal{R}_0$). In **Figures 4-6**, we observe that the fraction of schistosoma (male, female, pair) is lower when control is considered. More precisely, at the end of 15 years, the total number of male, female and pair schistosoma is 10^5, 0.1×10^5

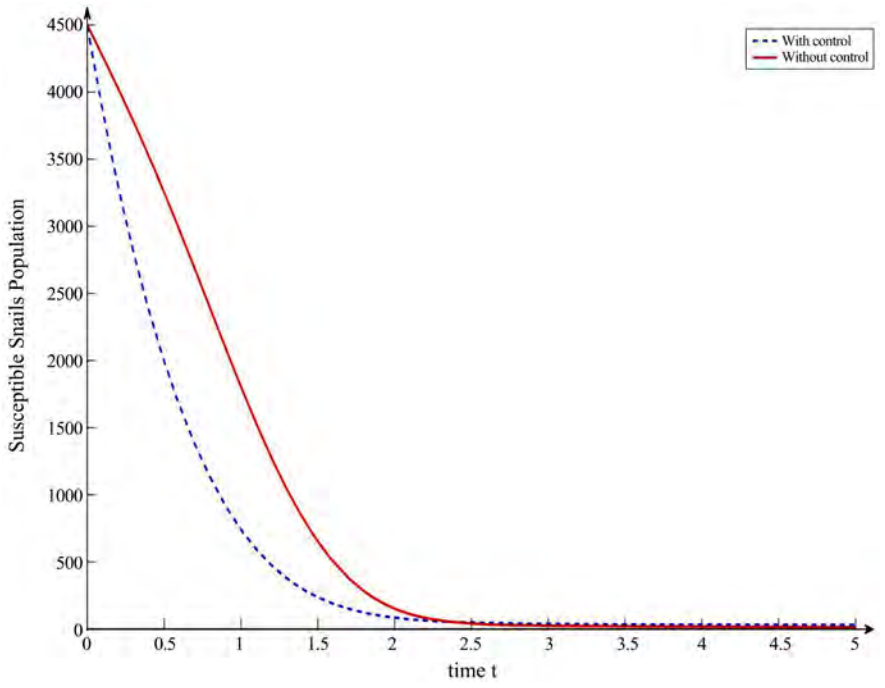

Figure 2. The evolution of susceptible snails with and without control. The state is solved forward time with initial conditions $IC(0)=(50000;30000;25000;4500;2500)$ while the adjoint system is solved backward in time (in years) with terminal condition $TC=(0;0;0;0;0)$ where $T=5$ and $(c_s,c_i,c_u)=(1,1,0.5)$.

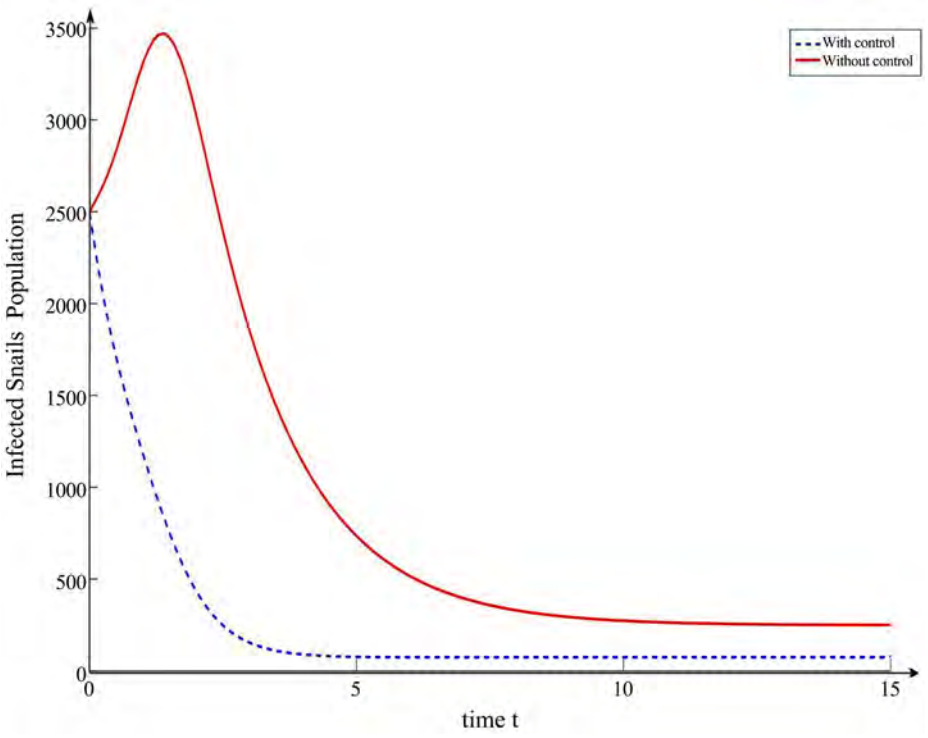

Figure 3. The evolution of infected snails with and without control. The state is solved forward time with initial conditions $IC(0)=(50000;30000;25000;4500;2500)$ while the adjoint system is solved backward in time in (in years) with terminal condition $TC=(0;0;0;0;0;0)$ where $T=15$ and $(c_s,c_i,c_u)=(1,1,0.5)$.

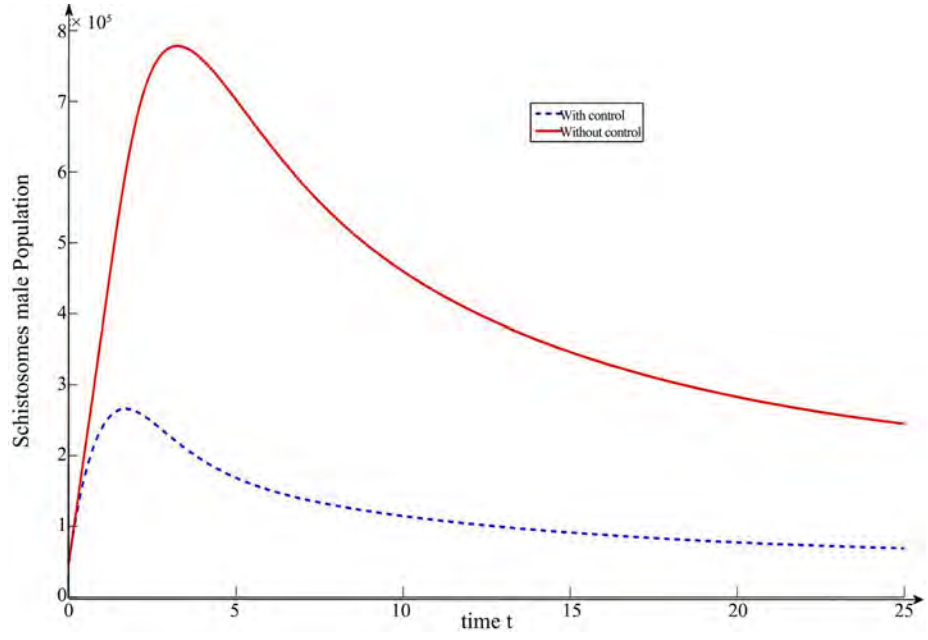

Figure 4. The evolution of male schistosoma with and without control. The state is solved forward time with initial conditions $IC(0)=(50000;30000;25000;4500;2500)$ while the adjoint system is solved backward in time (in years) with terminal condition $TC=(0;0;0;0;0;0)$ where $T=25$ and $(c_s,c_i,c_u)=(1,1,0.5)$.

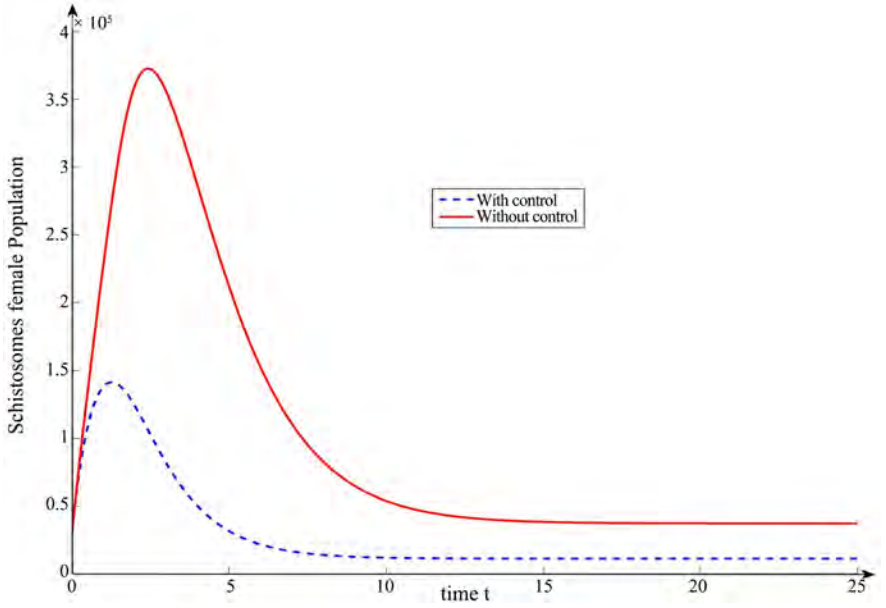

Figure 5. The evolution of female schistosoma with and without control. The state is solved forward time with initial conditions $IC(0)=(50000;30000;25000;4500;2500)$ while the adjoint system is solved backward in time (in years) with terminal condition $TC=(0;0;0;0;0;0)$ where $T=25$ and $(c_s,c_i,c_u)=(1,1,0.5)$.

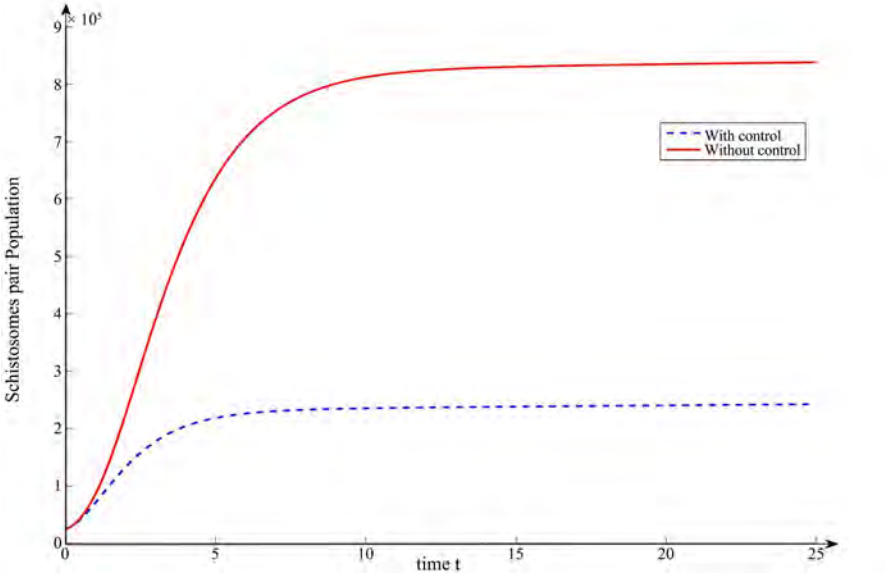

Figure 6. The evolution of pair schistosoma with and without control. The state is solved forward time with initial conditions $IC(0)$ = (50000; 30000; 25000; 4500; 2500) while the adjoint system is solved backward in time (in years) with terminal condition TC = (0; 0; 0; 0; 0; 0) where T = 25 and (c_s, c_i, c_u) = (1, 1, 0.5).

and 2×10^5 respectively when control is considered, and 3.5×10^5, 0.5×10^5 and 8×10^5 respectively without control. The schistosoma can survive for very long periods in a dry state, often for more than a few years, that's why in the stage without control evolution of the number of schistosoma (male, female, pair)

take higher levels, once controlled, the number of schistosoma doesn't develop as shown in Figures 4-6.

In Figure 2, we remark that the number of susceptible snails is more important than in the case without control, this is due to the aim of our approach which focuses on the reduction of the number of susceptible and infected snails population, so in the case without control the number of susceptible snails decrease is less and goes to its stable state, because it also applied a control on schistosoma by the elimination rates (ϵ_m, ϵ_f, ϵ_p).

In Figure 3, it's the evolution of infected snails which is presented, the major case of our approach, and the graph below shows the effectiveness of the study done in this work. As given above, the numerical simulations suggested 10 years as minimal duration for treatment. We see that if there are control the infected snails population begins to sharply decrease from the very beginning day of treatment and gradually decreases as time goes on.

Acknowledgements

This research was carried out with financial support of CEA-MITIC for postdoc project in Université Gaston Berger de SAINT-LOUIS.

Conflicts of Interest

The authors declare no conflicts of interest regarding the publication of this paper.

References

[1] Schistosomiasis. http://www.who.int/mediacentre/factsheets/fs115/en/

[2] Savioli, L., Stansfield, S., Bundy, D.A., Mitchell, A., Bhatia, R., Engels, D., Montresor, A., Neira, M. and Shein, A.M. (2002) Schistosomiasis and Soil-Transmitted Helminth Infections: Forging Control Efforts. *Transactions of the Royal Society of Tropical Medicine and Hygiene*, **96**, 577-579. https://doi.org/10.1016/S0035-9203(02)90316-0

[3] Castillo-Chavez, C., Feng, Z. and Xu, D. (2008) A Schistosomiasis Model with Mating Structure and Time Delay. *Mathematical Biosciences*, **211**, 333-341. https://doi.org/10.1016/j.mbs.2007.11.001

[4] Hadeler, K., Waldstätter, R. and Wörz-Busekros, A. (1988) Models for Pair Formation in Bisexual Populations. *Journal of Mathematical Biology*, **26**, 635-649. https://doi.org/10.1007/BF00276145

[5] Schmitz, S.-F.H. and Castillo-Chavez, C. (2000) A Note on Pair-Formation Functions. *Mathematical and Computer Modelling*, **31**, 83-91. https://doi.org/10.1016/S0895-7177(00)00025-X

[6] Qi, L. and Cui, J.-A. (2013) A Schistosomiasis Model with Mating Structure. *Abstract and Applied Analysis*, **2013**, Article ID: 741386. https://doi.org/10.1155/2013/741386

[7] Xu, D., Curtis, J., Feng, Z. and Minchella, D.J. (2005) On the Role of Schistosome mating Structure in the Maintenance of Drug Resistant Strains. *Bulletin of Mathematical Biology*, **67**, 1207-1226. https://doi.org/10.1016/j.bulm.2005.01.007

[8] Fleming, W.H. and Rishel, R.W. (2012) Deterministic and Stochastic Optimal Control. Springer Science & Business Media, Berlin, Heidelberg.

[9] Gamkrelidze, R., Pontrjagin, L.S. and Boltjanskij, V.G. (1964) The Mathematical Theory of Optimal Processes. Macmillan Company, New York.

[10] Van den Driessche, P. and Watmough, J. (2002) Reproduction Numbers and Sub-Threshold Endemic Equilibria for Compartmental Models of Disease Transmission. *Mathematical Biosciences*, **180**, 29-48. https://doi.org/10.1016/S0025-5564(02)00108-6

[11] LaSalle, J. (1976) The Stability of Dynamical Systems, Regional Conference Series in Applied Mathematics. Society for Industrial and Applied Mathematics, Philadelphia, PA.

[12] Bhatia, N.P. and Szegö, G.P. (1967) Dynamical Systems: Stability Theory and Applications. In: *Lecture Notes in Mathematics*, Springer, Berlin, Heidelberg, New York. https://doi.org/10.1007/BFb0080630

[13] Thieme, H.R. (1992) Epidemic and Demographic Interaction in the Spread of Potentially Fatal Diseases in Growing Populations. *Mathematical Biosciences*, **111**, 99-130. https://doi.org/10.1016/0025-5564(92)90081-7

[14] Butler, G., Freedman, H. and Waltman, P. (1986) Uniformly Persistent Systems. *Proceedings of the American Mathematical Society*, **96**, 425-430. https://doi.org/10.2307/2046588

[15] Hofbauer, J. and So, J.W.-H. (1989) Uniform Persistence and Repellors for Maps. *Proceedings of the American Mathematical Society*, **107**, 1137-1142. https://doi.org/10.2307/2047679

[16] Lin, X. and So, J.W.-H. (1993) Global Stability of the Endemic Equilibrium and Uniform Persistence in Epidemic Models with Subpopulations. *The ANZIAM Journal*, **34**, 282-295. https://doi.org/10.1017/S0334270000008900

[17] Chitnis, N., Hyman, J.M. and Cushing, J.M. (2008) Determining Important Parameters in the Spread of Malaria through the Sensitivity Analysis of a Mathematical Model. *Bulletin of Mathematical Biology*, **70**, 1272-1296. https://doi.org/10.1007/s11538-008-9299-0

[18] Blower, S.M. and Dowlatabadi, H. (1994) Sensitivity and Uncertainty Analysis of Complex Models of Disease Transmission: An HIV Model, as an Example. *International Statistical Review/Revue Internationale de Statistique*, **66**, 229-243. https://doi.org/10.2307/1403510

[19] Marino, S., Hogue, I.B., Ray, C.J. and Kirschner, D.E. (2008) A Methodology for Performing Global Uncertainty and Sensitivity Analysis in Systems Biology. *Journal of Theoretical Biology*, **254**, 178-196. https://doi.org/10.1016/j.jtbi.2008.04.011

[20] Wu, J., Dhingra, R., Gambhir, M. and Remais, J.V. (2013) Sensitivity Analysis of Infectious Disease Models: Methods, Advances and Their Application. *Journal of the Royal Society Interface*, **10**, Article ID: 20121018. https://doi.org/10.1098/rsif.2012.1018

[21] Lee, S., Chowell, G. and Castillo-Chávez, C. (2010) Optimal Control for Pandemic Influenza: The Role of Limited Antiviral Treatment and Isolation. *Journal of Theoretical Biology*, **265**, 136-150. https://doi.org/10.1016/j.jtbi.2010.04.003

[22] Okosun, K.O., Ouifki, R. and Marcus, N. (2011) Optimal Control Analysis of a Malaria Disease Transmission Model that Includes Treatment and Vaccination with Waning Immunity. *Biosystems*, **106**, 136-145. https://doi.org/10.1016/j.biosystems.2011.07.006

[23] Tchuenche, J., Khamis, S., Agusto, F. and Mpeshe, S. (2011) Optimal Control and Sensitivity Analysis of an Influenza Model with Treatment and Vaccination. *Acta biotheoretica*, **59**, 1-28. https://doi.org/10.1007/s10441-010-9095-8

[24] Pontryagin, L.S., Boltyanskii, V., Gamkrelidze, R. and Mishchenko, E.F. (1962) the Mathematical Theory of Optimal Processes. Interscience, New York.

[25] Lenhart, S. and Workman, J.T. (2007) Optimal Control Applied to Biological Models. CRC Press, Boca Raton, FL.

Applied Mathematics, 2019, 10, 419-434
http://www.scirp.org/journal/am
ISSN Online: 2152-7393
ISSN Print: 2152-7385

Homotopy Analysis Method for Solving Initial Value Problems of Second Order with Discontinuities

Waleed Al-Hayani, Rasha Fahad

Department of Mathematics, College of Computer Science and Mathematics, Mosul University, Mosul, Iraq
Email: *waleedalhayani@uomosul.edu.iq, waleedalhayani@yahoo.es

How to cite this paper: Al-Hayani, W. and Fahad, R. (2019) Homotopy Analysis Method for Solving Initial Value Problems of Second Order with Discontinuities. *Applied Mathematics*, **10**, 419-434.
https://doi.org/10.4236/am.2019.106030

Received: March 30, 2019
Accepted: June 14, 2019
Published: June 17, 2019

Abstract

In this paper, the standard homotopy analysis method was applied to initial value problems of the second order with some types of discontinuities, for both linear and nonlinear cases. To show the high accuracy of the solution results compared with the exact solution, a comparison of the numerical results was made applying the standard homotopy analysis method with the iteration of the integral equation and the numerical solution with the Simpson rule. Also, the maximum absolute error, $\|\cdot\|_2$, the maximum relative error, the maximum residual error and the estimated order of convergence were given. The research is meaningful and I recommend it to be published in the journal.

Keywords

Homotopy Analysis Method, Initial Value Problems, Heaviside Step Function, Dirac Delta Function, Simpson Rule

1. Introduction

Liao Shijun [1] [2] [3] proposed in 1992 in his Ph.D. dissertation a new and fruitful method (Homotopy Analysis Method (HAM)) for solving linear and nonlinear (ordinary differential, partial differential, integral, etc.) equations. It has been shown that this method yields a rapid convergence of the solutions series to linear and nonlinear deterministic.

In recent literature, Al-Hayani and Casasùs [4] [5] applied the Adomian decomposition method (ADM) to the initial value problems (IVPs) with discontinuities. Ji-Huan [6] used the homotopy perturbation method (HPM) solving for nonlinear oscillators with discontinuities.

In the consulted bibliography we have not found any results of the application of the HAM to differential problems with discontinuities. For this reason, this paper systematically analyzes its application to IVPs of ODEs of second order with independent non-continuous term. We have treated functions with a discontinuous derivative, with some of Heaviside step function and with Dirac delta function.

In what follows, we give a brief review of the HAM.

2. Basic Idea of HAM

In this article, we apply the HAM to the discussed problem. To show the basic idea, we consider the following differential equation

$$\mathcal{N}\left[u(x)\right]=k(x), \tag{2.1}$$

where $\mathcal{N}$ is a nonlinear operator, x denotes independent variable, $u(x)$ is an unknown function, and $k(x)$ is a known analytic function. For simplicity, we ignore all boundary or initial conditions, which can be treated in the similar way. By means of generalizing the traditional homotopy method, Liao [1] [2] [3] constructs the so-called zero-order deformation equation

$$(1-q)\mathcal{L}\left[\phi(x;q)-u_0(x)\right]=qhH(x)\left\{\mathcal{N}\left[\phi(x;q)\right]-k(x)\right\}, \tag{2.2}$$

where $q\in[0,1]$ is an embedding parameter, $h\neq 0$, is a non-zero auxiliary parameter $H(x)\neq 0$ is an auxiliary function, $\mathcal{L}$ is an auxiliary linear operator, $u_0(x)$ is an initial guess of $u(x)$ and $\phi(x;q)$ is an unknown function. It is important to note that one has great freedom to choose auxiliary objects such as h and $\mathcal{L}$ in the HAM. Obviously when $q=0$ and $q=1$, both

$$\phi(x;0)=u_0(x) \text{ and } \phi(x;1)=u(x) \tag{2.3}$$

hold. Thus as q increases from 0 to 1, the solution $\phi(x;q)$ varies from the initial guess $u_0(x)$ to the solution $u(x)$. Expanding $\phi(x;q)$ in Taylor series with respect to q, one has

$$\phi(x;q)=u_0(x)+\sum_{m=1}^{+\infty}u_m(x)q^m, \tag{2.4}$$

where

$$u_m=\frac{1}{m!}\frac{\partial^m\phi(x;q)}{\partial q^m}\bigg|_{q=0}, \tag{2.5}$$

If the auxiliary linear operator, the initial guess, the auxiliary parameter h, and the auxiliary function are so properly chosen, then the series (2.4) converges at $q=1$ and one has

$$\phi(x;1)=u_0(x)+\sum_{m=1}^{+\infty}u_m(x), \tag{2.6}$$

which must be one of the original non-linear equation, as proved by Liao [1] [2] [3]. If $h=-1$, Equation (2.2) becomes

$$(1-q)\mathcal{L}\left[\phi(x;q)-u_0(x)\right]+q\left\{\mathcal{N}\left[\phi(x;q)-k(x)\right]\right\}=0, \tag{2.7}$$

which is used mostly in the HPM [6] [7].

According to Equation (2.5), the governing equations can be deduced from the zeroth-order deformation Equations (2.2). We define the vectors

$$\boldsymbol{u}_i=\left\{u_0(x),u_1(x),\cdots,u_i(x)\right\}. \tag{2.8}$$

Differentiating Equation (2.2) m times with respect to the embedding parameter q and then setting $q=0$ and finally dividing them by $m!$, we have the so-called mth-order deformation equation

$$\mathcal{L}\left[u_m(x)-\mathcal{X}_m u_{m-1}(x)\right]=h\mathcal{R}_m\left(\boldsymbol{u}_{m-1}\right), \tag{2.9}$$

where

$$\mathcal{R}_m\left(\boldsymbol{u}_{m-1}\right)=\frac{1}{(m-1)!}\frac{\partial^{m-1}\left\{\mathcal{N}\left[\phi(;q)\right]-k(x)\right\}}{\partial q^{m-1}}\bigg|_{q=0}, \tag{2.10}$$

and

$$\mathcal{X}_m=\begin{cases}0, & m\le 1,\\ 1, & m>1.\end{cases} \tag{2.11}$$

It should be emphasized that $u_m(x)$ $(m\ge 1)$ are governed by the linear equation (2.9) with the linear boundary conditions that come from the original problem, which can be easily solved by symbolic computation softwares such as Maple and Mathematica.

3. HAM Applied to an IVP of the Second Order

Consider the general IVP of the second order [4]:

$$\begin{aligned}&u''+g(u,u')+k^2u=\lambda f(x,u,u'),\ 0\le x\le T,\\ &u(0)=\alpha,\ u'(0)=\beta,\end{aligned} \tag{3.1}$$

where k,λ,α and β are real constants, g is a (possibly) nonlinear function of u,u' and f is a function with some discontinuity.

To sole Equation (3.1) by means of the standard HAM, we choose the initial approximations

$$u(0)=\alpha,\ u'(0)=\beta, \tag{3.2}$$

and the linear operator

$$\mathcal{L}\left[\phi(x;q)\right]=\frac{\partial^2\phi(x;q)}{\partial x^2}, \tag{3.3}$$

with the property

$$\mathcal{L}\left[c_1+c_2x\right]=0, \tag{3.4}$$

where c_1 and c_2 are constants of integration. Furthermore, Equation (3.1) suggests that we define the nonlinear operator as

$$\mathcal{N}\left[\phi(x;q)\right]=\frac{\partial^2\phi(x;q)}{\partial x^2}+g\left(\phi(x;q),\frac{\partial\phi(x;q)}{\partial x}\right)+k^2\phi(x;q)$$
$$-\lambda f\left(x,\phi(x;q),\frac{\partial\phi(x;q)}{\partial x}\right), \tag{3.5}$$

Using the above definition, we construct the zeroth-order deformation equation as in (2.2) and (2.3) and the mth-order deformation equation for $m\geq 1$ is

$$\mathcal{L}\left[u_m(x)-\mathcal{X}_m u_{m-1}(x)\right]=hR_m\left(\boldsymbol{u}_{m-1}\right), \tag{3.6}$$

with the initial conditions

$$u_m(0)=0,\ u_m'(0)=0, \tag{3.7}$$

where

$$R_m\left(\boldsymbol{u}_{m-1}\right)=u_{m-1}''+g\left(u_{m-1},u_{m-1}'\right)+k^2u_{m-1}-\lambda f\left(x,u_{m-1},u_{m-1}'\right) \tag{3.8}$$

Now, the solution of the mth-order deformation Equation (3.6) for $m\geq 1$ is

$$u_m(x)=\mathcal{X}_m y_{m-1}(x)+h\int_0^x\int_0^x R_m\left(\boldsymbol{u}_{m-1}\right)\mathrm{d}x\mathrm{d}x, \tag{3.9}$$

Thus, the approximate solution in a series form is given by

$$u(x)=u_0(x)+\sum_{m=1}^{+\infty}u_m(x). \tag{3.10}$$

3.1. Linear Case

Let $g(u,u')=u'$, $\alpha=0$ and $\beta=1$.

Case 3.1.1 If we take $\lambda=10,k=10$ and the function $f(x,u)$ is continuous, but not differentiable, for example

$$f(x,u)=\begin{cases}x-\dfrac{1}{2}, & x\geq\dfrac{1}{2}\\ -x+\dfrac{1}{2}, & x<\dfrac{1}{2}\end{cases} \tag{3.11}$$

From Equation (3.9) the first iterations are then determined in the following recursive way:

$$u_0(x)=x,$$

$$u_1(x)=\begin{cases}\dfrac{1}{3}hx^2(55x-6), & x<\dfrac{1}{2}\\ \dfrac{1}{12}h\left(180x^3+36x^2-30x+5\right), & x\geq\dfrac{1}{2}\end{cases},$$

$$u_2(x)=\begin{cases}\dfrac{275}{3}h^2x^5-\dfrac{145}{12}h^2x^4+\dfrac{1}{3}hx^3(55+53h)-2hx^2(1+h), & x<\dfrac{1}{2}\\ 75h^2x^5+\dfrac{115}{4}h^2x^4+hx^3\left(15-\dfrac{77}{3}h\right)+hx^2\left(3+\dfrac{271}{12}h\right)\\ \quad-\dfrac{5}{2}hx\left(1+\dfrac{35}{12}h\right)+\dfrac{5}{12}h\left(1+\dfrac{17}{8}h\right), & x\geq\dfrac{1}{2}\end{cases}$$

$$\vdots$$

and so on, in this manner the rest of the iterations can be obtained. Thus, the approximate solution in a series form when $h=-1$ is

$$u(x)=u_0(x)+\sum_{m=1}^{15}u_m(x)=\begin{cases}p_1(x), & x<\dfrac{1}{2}\\ p_2(x), & x\geq\dfrac{1}{2}\end{cases} \tag{3.12}$$

where

$$\begin{aligned}p_1(x)=x+2x^2-19x^3-\frac{143}{12}x^4+\frac{5843}{60}x^5+\frac{2819}{120}x^6-\frac{592757}{2520}x^7-\frac{252943}{20160}x^8\\ +\frac{19842881}{60480}x^9-\frac{34234343}{1814400}x^{10}-\frac{5918629957}{19958400}x^{11}+\frac{3114021419}{79833600}x^{12}\\ +\frac{52956448313}{283046400}x^{13}-\frac{1516727357143}{43589145600}x^{14}-\frac{18911788595719}{217945728000}x^{15}\\ +\frac{41681620300291}{2092278988800}x^{16}+\frac{10930256954423}{355687428096}x^{17}-\frac{18736423525}{2280047616}x^{18}\\ -\frac{32512931860625}{3801409387776}x^{19}+\frac{1790227609375}{691165343232}x^{20}+\frac{25453049921875}{13304932857216}x^{21}\\ -\frac{35542462890625}{54882848036016}x^{22}-\frac{2509960937500}{7172190368343}x^{23}\\ +\frac{25589599609375}{194200846896672}x^{24}+\frac{33294677734375}{631152752414184}x^{25}\\ -\frac{4241943359375}{186476949576918}x^{26}-\frac{193786621093750}{27691827012172323}x^{27}\\ +\frac{1964569091796875}{581528367255618783}x^{28}+\frac{1907348632812500}{1533120240946631337}x^{29}\end{aligned}$$

and

$$\begin{aligned}p_2(x)=-\frac{284894489701085211138596665947}{22634910703973637003631656960 0}\\ +\frac{21783072633769906956915570 83}{19512854055149687072096256 00}x\\ +\frac{11865728863595729706480 17}{36678297096146028331008 0}x^2-\frac{33376213227737153324107}{18524392472801024409 60}x^3\\ -\frac{78674566012860119002187}{3503708621552410951680}x^4+\frac{70417020638210378913643 99}{74453808207988732723200}x^5\\ +\frac{54989559357595903086356 3}{9306726025998591590400}x^6-\frac{33087191796820586109271}{1416240916999785676 80}x^7\\ -\frac{392978766117540050705}{5149669709083115 52}x^8+\frac{2456170645710279487}{7376767051530240}x^9\\ +\frac{41780926473659473181}{811444375668326400}x^{10}-\frac{306846492148853223323}{998290120065638400}x^{11}\\ -\frac{17826687959696195557}{1331053493420851200}x^{12}+\frac{504004732035392079 79}{254466109036339200}x^{13}\\ -\frac{549653451307296101}{8096648923883520 0}x^{14}-\frac{1044971689229281329 17}{1113289227033984000}x^{15}\\ +\frac{44252896760138813 27}{5089321807267840 0}x^{16}+\frac{17404262491512559}{511943651315712}x^{17}\end{aligned}$$

$$-\frac{23600088137477575}{4991450600328192}x^{18}-\frac{20901216917575625}{2155399122868992}x^{19}$$
$$+\frac{682160726359375}{391890749612544}x^{20}+\frac{5546125344453125}{2514632310013824}x^{21}$$
$$-\frac{96575453125000}{216101214141813}x^{22}-\frac{644336083984375}{1420093692931914}x^{23}$$
$$+\frac{3135924072265625}{22721499086910624}x^{24}+\frac{212506103515625}{5680374771727656}x^{25}$$
$$-\frac{17364501953125}{18461218008114882}x^{26}-\frac{209045410156250}{11867925862359567}x^{27}$$
$$+\frac{1125335693359375}{193842789085206261}x^{28}+\frac{1907348632812500}{1873813627823660523}x^{29}$$

This series has the closed form as $m\to\infty$

$$u_{Exact}(x)=\begin{cases}p_3(x), & x<\frac{1}{2}\\ p_4(x), & x\geq\frac{1}{2}\end{cases} \tag{3.13}$$

where

$$p_3(x)=\frac{307\sqrt{399}}{57000}\mathrm{e}^{-\frac{1}{2}x}\sin\left(\frac{\sqrt{399}}{2}x\right)-\frac{51}{1000}\mathrm{e}^{-\frac{1}{2}x}\cos\left(\frac{\sqrt{399}}{2}x\right)+\frac{51}{1000}-\frac{1}{10}x,$$

$$p_4(x)=\frac{307\sqrt{399}}{57000}\mathrm{e}^{-\frac{1}{2}x}\sin\left(\frac{\sqrt{399}}{2}x\right)-\frac{51}{1000}\mathrm{e}^{-\frac{1}{2}x}\cos\left(\frac{\sqrt{399}}{2}x\right)-\frac{51}{1000}+\frac{1}{10}x$$
$$+\frac{1}{500}\mathrm{e}^{-\frac{1}{2}x+\frac{1}{4}}\cos\left(\frac{\sqrt{399}}{4}(2x-1)\right)-\frac{199\sqrt{399}}{199500}\mathrm{e}^{-\frac{1}{2}x+\frac{1}{4}}\sin\left(\frac{\sqrt{399}}{4}(2x-1)\right),$$

which is exactly the exact solution for the case 3.1.1.

In Table 1 show a comparison of the numerical results applying the **HAM** ($m=15$), Iteration of the Integral Equation **(IIE) (3.9)**, and the numerical solution of **(3.9)** with Simpson rule **(SIMP)** with the exact solution **(3.13).** Twenty points have been used in the Simpson rule**.** In Table 2 we list the Maximum Absolute Error **(MAE)**, $\|\cdot\|_2$, the Maximum Relative Error **(MRE)**, the Maximum Residual Error **(MRR),** obtained by the **HAM** with the exact solution **(3.13)** on the interval $[0,1]$. The Estimated Order of Convergence **(EOC)** for different values of the constant k are given in Table 3.

Figure 1 represents both the exact solution $u_{Exact}(x)$ and our approximation by HAM ($m=14$) within the interval $0\leq t\leq 1$.

For $k\geq 13$, the application of the HAM requires approximants of order $m>15$ if we want to arrive beyond the discontinuity (at $x=\frac{1}{2}$).

Case 3.1.2 Taking $\beta=1,k=1,\lambda=1$ and

$$f(x,u,u')=H(x-1)=\begin{cases}0, & \text{if } x<1\\ 1, & \text{if } x\geq 1,\end{cases} \tag{3.14}$$

The Heaviside step function at $x=1$. We now successively obtain

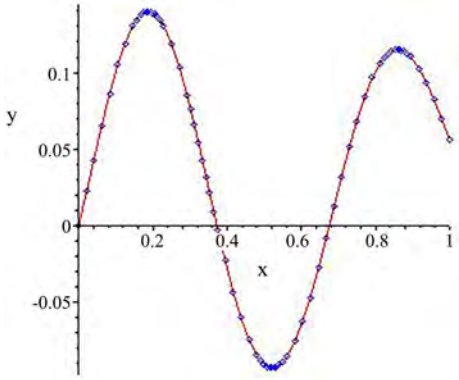

Figure 1. Continuous line: $u_{Exact}(x), +: \text{HAM}, \lambda = 10, k = 10$.

Table 1. Numerical results for the case 3.1.1.

x	$u_{Exact}(x)$	HAM	IIE	SIMP
0.0	0.000000000	0.000000000	0.000000000	0.000000000
0.1	0.100782334	0.100782334	0.100782334	0.100782334
0.2	0.138716799	0.138716799	0.138716799	0.138716799
0.3	0.077844715	0.077844715	0.077844715	0.077844715
0.4	−0.027921565	−0.027921565	−0.027921565	−0.027921565
0.5	−0.090520718	−0.090520718	−0.090520718	−0.090520718
0.6	−0.064945725	−0.064945725	−0.064945723	−0.064945723
0.7	0.023844667	0.023844566	0.023844678	0.023844678
0.8	0.100898402	0.100896153	0.100898714	0.100898714
0.9	0.108664846	0.108638517	0.108670237	0.108670234
1.0	0.055691769	0.055659061	0.055736683	0.055736417

Table 2. MAE, $\|\cdot\|_2$, MRE and MRR for the case 3.1.1.

m	MAE	$\|\cdot\|_2$	MRE	MRR
12	1.104E−01	1.474E−02	1.983E−00	89.418E−00
13	1.541E−02	1.889E−03	2.767E−01	16.061E−00
14	1.360E−03	1.408E−04	2.443E−02	2.222E−00
15	6.803E−05	1.732E−05	9.487E−04	1.940E−01

Table 3. EOC for the case 3.1.1.

k	$x = 0.4$	$x = 0.6$
10	1.0660	1.0778
11	1.0628	1.0824
12	1.0459	1.0923

$$u_0(x)=x,$$

$$u_1(x)=\begin{cases}\frac{1}{6}hx^3+\frac{1}{2}hx^2, & x<1\\ \frac{1}{6}hx^3+hx-\frac{1}{2}h, & x\geq 1\end{cases},$$

$$u_2(x)=\begin{cases}\frac{1}{120}h^2x^5+\frac{1}{12}h^2x^4+\frac{1}{3}hx^3\left(\frac{1}{2}+h\right)+\frac{1}{2}hx^2(1+h), & x<1\\ \frac{1}{120}h^2x^5+\frac{1}{24}h^2x^4+\frac{1}{3}hx^3\left(\frac{1}{2}+h\right)+hx\left(\frac{2}{3}h+1\right)-\frac{1}{2}h\left(1+\frac{3}{4}h\right), & x\geq 1\end{cases},$$

$$\vdots$$

and so on, in this manner the rest of the iterations can be obtained. Thus, the approximate solution in a series form when $h=-1$ is

$$u(x)=u_0(x)+\sum_{m=1}^{9}u_m(x)=\begin{cases}p_5(x), & x<1\\ p_6(x), & x\geq 1\end{cases} \tag{3.15}$$

where

$$\begin{aligned}p_5(x)=x&-\frac{1}{2}x^2+\frac{1}{24}x^4-\frac{1}{120}x^5+\frac{1}{5040}x^7-\frac{1}{40320}x^8+\frac{1}{1814400}x^{10}\\&+\frac{1}{5702400}x^{11}+\frac{1}{17740800}x^{12}+\frac{1}{124540416}x^{13}+\frac{1}{1779148800}x^{14}\\&+\frac{1}{48432384000}x^{15}+\frac{1}{2615348736000}x^{16}+\frac{1}{355687428096000}x^{17}\end{aligned}$$

and

$$\begin{aligned}p_6(x)=&\frac{4581894569957}{6974263296000}-\frac{294371651437}{653837184000}x+\frac{23051120003}{58118860800}x^2\\&-\frac{355931929}{6227020800}x^3-\frac{215859517}{11496038400}x^4+\frac{251909}{38016000}x^5\\&-\frac{422017}{870912000}x^6-\frac{80707}{914457600}x^7+\frac{11293}{541900800}x^8\\&-\frac{463}{304819200}x^9+\frac{401}{2612736000}x^{10}+\frac{211}{798336000}x^{11}\\&+\frac{19}{348364800}x^{12}+\frac{113}{18681062400}x^{13}+\frac{71}{174356582400}x^{14}\\&+\frac{1}{62270208000}x^{15}+\frac{1}{2988969984000}x^{16}+\frac{1}{355687428096000}x^{17}\end{aligned}$$

This series has the closed form as $m\to\infty$

$$u_{Exact}(x)=\begin{cases}\frac{2\sqrt{3}}{3}e^{-\frac{1}{2}x}\sin\left(\frac{1}{2}\sqrt{3}x\right), & x<1\\ \frac{2\sqrt{3}}{3}e^{-\frac{1}{2}x}\sin\left(\frac{\sqrt{3}}{2}x\right)-\frac{\sqrt{3}}{3}e^{-\frac{1}{2}x+\frac{1}{2}}\sin\left(\frac{\sqrt{3}}{2}(-1+x)\right)\\ \quad -e^{-\frac{1}{2}x+\frac{1}{2}}\cos\left(\frac{\sqrt{3}}{2}(-1+x)\right)+1, & x\geq 1,\end{cases} \tag{3.16}$$

which is exactly the exact solution for the case 3.1.2.

In Table 4 show a comparison of the numerical results applying the **HAM** ($m=9$), Iteration of the Integral Equation **(IIE) (3.9),** and the numerical solution of **(3.9)** with Simpson rule **(SIMP)** with the exact solution **(3.16)**. In Table 5 we list the **MAE**, $\|\cdot\|_2$, the **MRE**, and the **MRR**, obtained by the **HAM** with the exact solution **(3.16)** on the interval $[0,1]$. The EOC for different values of the constant k are given in Table 6.

Figure 2 represents both the exact solution $u_{Exact}(x)$ and our approximation by HAM ($m=9$) within the interval $0 \le t \le 2$.

Case 3.1.3 Taking $\beta=1, k=1, \lambda=1$ and $f(x,u,u')=\delta(x-1)$, the Dirac delta function at $x=1$. We now successively obtain

$$u_0(x)=x,$$

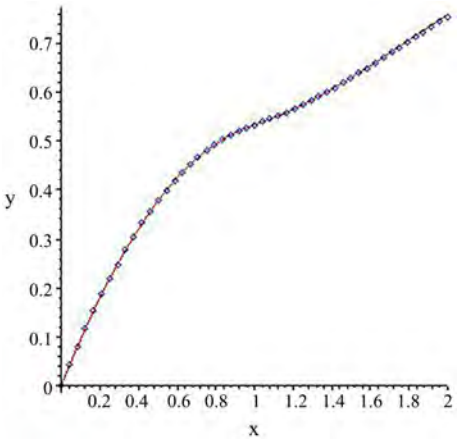

Figure 2. Continuous line: $u_{Exact}(x)$, +: HAM, $\lambda=1, k=1$.

Table 4. Numerical results for the case 3.1.2.

x	$u_{Exact}(x)$	HAM	IIE	SIMP
0.0	0.000000000	0.000000000	0.000000000	0.000000000
0.2	0.180064002	0.180064002	0.180064002	0.180064002
0.4	0.320981642	0.320981642	0.320981642	0.320981642
0.6	0.424757139	0.424757141	0.424757139	0.424757139
0.8	0.494373476	0.494373527	0.494373472	0.494373472
1.0	0.533507195	0.533507735	0.533507144	0.533507144
1.2	0.564939072	0.564942862	0.564938646	0.564938646
1.4	0.606393480	0.606413454	0.606390844	0.606390844
1.6	0.654555758	0.654641161	0.654542809	0.654542808
1.8	0.706469719	0.706780754	0.706416357	0.706416354
2.0	0.759579476	0.760577057	0.7593881936	0.759388182

Table 5. MAE, $\|\cdot\|_2$, MRE and MRR for the case 3.1.2.

m	MAE	$\|\cdot\|_2$	MRE	MRR
5	2.214E−01	8.262E−02	2.914E−01	3.091E−00
6	7.122E−02	2.471E−02	9.377E−02	1.313E−00
7	1.955E−02	6.370E−03	2.573E−02	4.573E−01
8	4.684E−03	1.446E−03	6.167E−03	1.351E−01
9	9.976E−04	2.933E−04	1.313E−03	3.471E−02

Table 6. EOC for the case 3.1.2.

k	$x=0.9$	$x=1.1$
1	1.0871	1.1001
2	1.1081	1.1300

$$u_1(x)=-\frac{1}{6}h\left(-x^3-3x^2+6H(x-1)x-6H(x-1)\right)$$

$$u_2(x)=-\frac{1}{120}h\left(-hx^5-10hx^4-20x^3(2h+1)+20hH(x-1)x^3\right.$$
$$\left.-60x^2(h+1)+60H(x-1)x(h+2)-40H(x-1)(2h+3)\right)$$

$$\vdots$$

and so on, in this manner the rest of the iterations can be obtained. Thus, the approximate solution in a series form when $h=-1$ is

$$\begin{aligned}u(x)&=u_0(x)+\sum_{m=1}^{8}u_m(x)\\&=H(x-1)\left(-\frac{9030495007}{6227020800}+\frac{858929737}{479001600}x-\frac{2734477}{15966720}x^2\right.\\&\quad-\frac{5271359}{21772800}x^3+\frac{653741}{8709120}x^4-\frac{14383}{4838400}x^5-\frac{7477}{3628800}x^6\\&\quad+\frac{293}{725760}x^7-\frac{71}{4838400}x^8-\frac{71}{8709120}x^9+\frac{23}{21772800}x^{10}\\&\quad\left.+\frac{17}{79833600}x^{11}+\frac{1}{95800320}x^{12}+\frac{1}{6227020800}x^{13}\right)\\&\quad+\left(x-\frac{1}{2}x^2+\frac{1}{24}x^4-\frac{1}{120}x^5+\frac{1}{5040}x^7-\frac{1}{40320}x^8-\frac{1}{362880}x^9\right.\\&\quad-\frac{1}{604800}x^{10}-\frac{1}{1900800}x^{11}-\frac{29}{479001600}x^{12}-\frac{1}{311351040}x^{13}\\&\quad\left.-\frac{1}{12454041600}x^{14}-\frac{1}{1307674368000}x^{15}\right)\end{aligned}\tag{3.17}$$

This series has the closed form as $m\to\infty$

$$u_{Exact}(x)=\frac{2\sqrt{3}}{3}\left[H(x-1)\mathrm{e}^{\frac{1}{2}-\frac{1}{2}x}\sin\left(\frac{\sqrt{3}}{2}(x-1)\right)+\mathrm{e}^{-\frac{1}{2}x}\sin\left(\frac{\sqrt{3}}{2}x\right)\right]\tag{3.18}$$

which is exactly the exact solution for the case 3.1.3.

In Table 7 we list the **MAE,** $\|\cdot\|_2$, the **MRE,** and the **MRR,** obtained by the **HAM** with the exact solution **(3.18)** on the interval $[0,2]$. The EOC are 1.0984 at $x=0.9$ and 1.1156 at $x=1.1$.

Figure 3 gives both the exact solution $u_{Exact}(x)$ and our approximation by HAM ($m=8$) within the interval $0 \le t \le 2$.

3.2. Non-Linear Case

Let $\alpha=0, \beta=1, \lambda=10$ and $k=1$.

Case 3.2.1 Taking $g(u,u')=uu'$, and

$$f(x,u,u')=\begin{cases}0, & \text{if } x<\dfrac{1}{2}\\ 1, & \text{if } x\ge\dfrac{1}{2}\end{cases} \tag{3.19}$$

Using the Adomian polynomials [8] [9] for calculation the nonlinear term uu' is given by

$$g(u,u')=uu'=\sum_{i=0}^{n}u_i u'_{n-i},\ n\ge i,\ n=0,1,2,\cdots \tag{3.20}$$

We now successively obtain

$$u_0(x)=x,$$

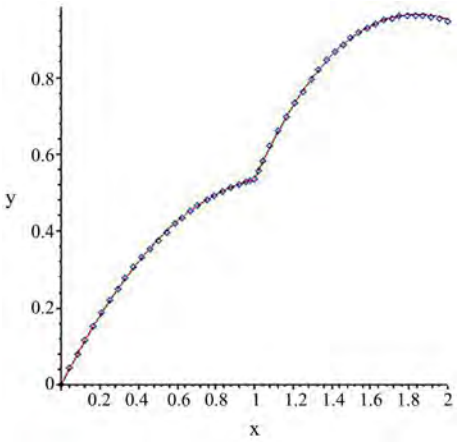

Figure 3. Continuous line: $u_{Exact}(x)$, +: HAM, $\lambda=1, k=1$.

Table 7. MAE, $\|\cdot\|_2$, MRE and MRR for the case 3.1.3.

m	MAE	$\|\cdot\|_2$	MRE	MRR
5	2.105E−01	7.952E−02	2.210E−01	2.786E−00
6	6.923E−02	2.418E−02	7.266E−02	1.231E−00
7	1.924E−02	6.295E−03	2.019E−02	4.402E−01
8	4.644E−03	1.436E−03	4.874E−03	1.322E−01
9	9.928E−04	2.922E−04	1.042E−03	3.428E−02

$$u_1(x)=\begin{cases}\frac{1}{3}hx^3, & x<\frac{1}{2}\\ \frac{1}{12}h\left(4x^3-60x^2+60x-15\right), & x\geq\frac{1}{2}\end{cases},$$

$$u_2(x)=\begin{cases}\frac{1}{12}h^2x^5+\frac{1}{3}hx^3(h+1), & x<\frac{1}{2}\\ \frac{1}{12}h^2x^5-\frac{5}{3}h^2x^4+\frac{1}{3}hx^3\left(1+\frac{17}{2}h\right)-5hx^2\left(1+\frac{5}{4}h\right) & \\ \quad+5hx\left(1+\frac{25}{24}h\right)-\frac{5}{4}h(1+h), & x\geq\frac{1}{2}\end{cases},$$

$$\vdots$$

and so on, in this manner the rest of the iterations can be obtained. Thus, the approximate solution in a series form when $h=-1$ is

$$u(x)=u_0(x)+\sum_{m=1}^{7}u_m(x)=\begin{cases}p_7(x), & x<\frac{1}{2}\\ p_8(x), & x\geq\frac{1}{2}\end{cases}, \tag{3.21}$$

where

$$p_7(x)=x-\frac{1}{3}x^3+\frac{1}{12}x^5-\frac{11}{504}x^7+\frac{211}{36288}x^9-\frac{6221}{3991680}x^{11}+\frac{260833}{622702080}x^{13}$$

and

$$\begin{aligned}p_8(x)=&\frac{131015952083}{98099527680}-\frac{846993899}{181665792}x+\frac{1362271259}{185794560}x^2-\frac{202153183}{37158912}x^3\\&+\frac{44111605}{6193152}x^4-\frac{37786871}{7741440}x^5-\frac{156205}{165888}x^6+\frac{4167853}{645120}x^7\\&-\frac{18511}{2016}x^8+\frac{431939}{64512}x^9-\frac{3502817}{1451520}x^{10}+\frac{267623}{725760}x^{11}\\&-\frac{520067}{23950080}x^{12}+\frac{260833}{622702080}x^{13}\end{aligned}$$

In Table 8 show a comparison of the numerical results applying the **HAM** ($m=7$), Iteration of the Integral Equation **(IIE) (3.9)**, and the numerical solution of **(3.9)** with Simpson rule **(SIMP)** with the numeric solution (rkf45) $u_N(x)$. In Table 9 we list the **MAE**, the **MRE**, and the **MRR**, obtained by the **HAM** with the numeric solution (rkf45) $u_N(x)$ on the interval $[0,1]$.

Figure 4 represents both the numeric solution (rkf45) $u_N(x)$ with a very small error and our approximation by HAM ($m=7$) within the interval $0\leq t\leq 1$.

Case 3.2.2 Taking $g(u,u')=u^2$, and

$$f(x,u,u')=\begin{cases}0, & \text{if } x<1\\ 1, & \text{if } x\geq 1\end{cases} \tag{3.22}$$

Using the Adomian polynomials [8] [9] for calculation the nonlinear term u^2 is given by

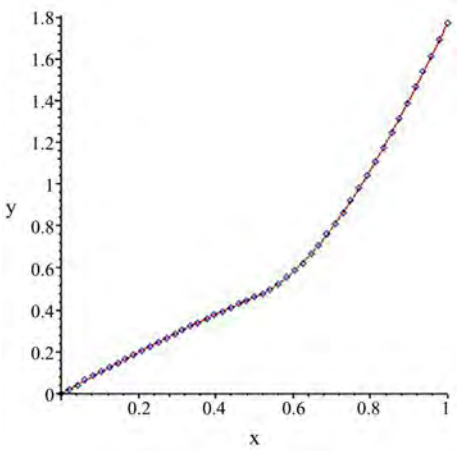

Figure 4. Continuous line: $u_N(x), +: \text{HAM}, \lambda = 10, k = 1$.

Table 8. Numerical results for the case 3.2.1.

x	rkf45	HAM	IIE	SIMP
0.0	0.000000000	0.000000000	0.000000000	0.000000000
0.1	0.099667499	0.099667497	0.099667497	0.099667497
0.2	0.197359727	0.197359723	0.197359723	0.197359723
0.3	0.291197840	0.291197838	0.291197838	0.291197838
0.4	0.379485700	0.379485702	0.379485702	0.379485702
0.5	0.460777633	0.460777635	0.460777632	0.460777632
0.6	0.583008128	0.583008017	0.583007978	0.583007978
0.7	0.789366837	0.789366701	0.789366561	0.789366561
0.8	1.068091674	1.068091572	1.068091282	1.068091282
0.9	1.402735913	1.402734083	1.402735383	1.402735385
1.0	1.773297313	1.773238159	1.773299771	1.773299790

Table 9. MAE, MRE and MRR for the case 3.2.1.

m	MAE	MRE	MRR
4	9.966E−03	5.620E−03	1.969E−00
5	9.854E−05	6.217E−05	1.329E−01
6	5.806E−04	3.274E−04	2.288E−01
7	5.915E−05	3.336E−05	4.510E−02

$$g(u,u') = u^2 = \sum_{i=0}^{n} u_i u_{n-i}, \quad n \geq i, \quad n = 0,1,2,\cdots \tag{3.23}$$

we now successively obtain

$$u_0(x) = x,$$

$$u_1(x) = \frac{1}{12}h\left(x^4 + 2x^3\right) - 5hH(x-1)\left(x^2 - 2x + 1\right),$$

$$\begin{aligned} u_2(x) = &-\frac{1}{2520}hH(x-1)\left(1260hx^5 - 3150hx^4 + 18900hx^2 - 31500hx\right. \\ &\left. + 12600x^2 + 14490h - 25200x + 12600\right) + \frac{1}{2520}h\left(10hx^7 + 35hx^6\right. \\ &\left. + 21hx^5 + 210hx^4 + 420hx^3 + 210x^4 + 420x^3\right), \end{aligned}$$

$$\vdots$$

and so on, in this manner the rest of the iterations can be obtained. Thus, the approximate solution in a series form when $h = -1$ is

$$\begin{aligned} u(x) &= u_0(x) + \sum_{m=1}^{8} u_m(x) \\ &= H(x-1)\left(\frac{41629462050061}{11263435223040} - \frac{2498253046769}{563171761152}x - \frac{18764031409}{4704860160}x^2\right. \\ &\quad + \frac{1761739129}{274450176}x^3 - \frac{502232959}{181621440}x^4 + \frac{1677121153}{242161920}x^5 - \frac{10243801115}{581188608}x^6 \\ &\quad + \frac{341190523}{13453440}x^7 - \frac{150931763}{6209280}x^8 + \frac{11334138401}{670602240}x^9 - \frac{2673838147}{304819200}x^{10} \\ &\quad + \frac{2650717003}{79833600}x^{11} - \frac{1572737}{1905120}x^{12} + \frac{88586453}{1089728640}x^{13} + \frac{213052381}{8717829120}x^{14} \\ &\quad - \frac{6247867}{605404800}x^{15} + \frac{71250341}{58118860800}x^{16} + \frac{48109}{823350528}x^{17} \\ &\quad \left. - \frac{1322521}{59281238016}x^{18} + \frac{74645}{140792940288}x^{19} + \frac{157891}{1126343522304}x^{20}\right) \\ &\quad + \left(x - \frac{1}{6}x^3 - \frac{1}{12}x^4 + \frac{1}{120}x^5 + \frac{1}{72}x^6 + \frac{19}{5040}x^7 - \frac{1}{960}x^8\right. \\ &\quad - \frac{299}{362880}x^9 - \frac{43}{362880}x^{10} + \frac{3239}{39916800}x^{11} + \frac{869}{21772800}x^{12} \\ &\quad + \frac{8201}{6227020800}x^{13} - \frac{53}{10644480}x^{14} - \frac{2150341}{1307674368000}x^{15} \\ &\quad + \frac{1660739}{10461394944000}x^{16} + \frac{20675}{79041650688}x^{17} + \frac{11819}{209227898880}x^{18} \\ &\quad - \frac{12799}{750895681536}x^{19} - \frac{743}{56458321920}x^{20} - \frac{803}{252975550464}x^{21} \\ &\quad \left. - \frac{73}{252975550464}x^{22}\right) \end{aligned} \tag{3.24}$$

In Table 10 we list the **MAE**, the **MRE**, and the **MRR**, obtained by the **HAM** with the numeric solution (rkf45) $u_N(x)$ on the interval $[0,2]$.

Figure 5 represents both the numeric solution (rkf45) $u_N(x)$ with a very small error and our approximation by HAM ($m = 8$) within the interval $0 \le t \le 2$.

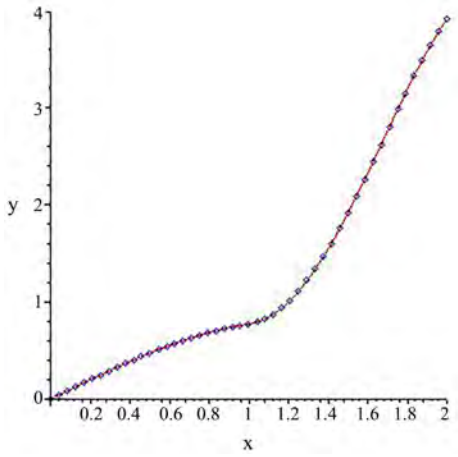

Figure 5. Continuous line: $u_N(x), +$: HAM, $\lambda = 10, k = 1$.

Table 10. MAE, MRE and MRR for the case 3.2.2.

m	MAE	MRE	MRR
4	6.298E−02	1.606E−02	3.926E−00
5	1.036E−02	2.642E−03	1.123E−00
6	2.845E−03	7.921E−04	4.894E−01
7	2.916E−03	7.436E−04	1.788E−01
8	6.366E−04	1.623E−04	5.743E−02

4. Conclusions

In this work, the HAM has been successfully applied to solve IVPs of second order with discontinuities. The size of the jump (given by λ) does not affect the convergence of the method, which behaves equally well on both sides of the discontinuity. In this IVPs, the application by the HAM with *k*, does not converge even for small values of the parameter like λ.

The proposed scheme of the HAM has been applied directly without any need for transformation formulae or restrictive assumptions. The solution process by the HAM is compatible with the method in the literature providing analytical approximation such as ADM. The approach of the HAM has been tested by employing the method to obtain approximate-exact solutions of the linear case. The results obtained in all cases demonstrate the reliability and the efficiency of this method.

Conflicts of Interest

The authors declare no conflicts of interest regarding the publication of this paper.

References

[1] Liao, S.J. (1992) The Proposed Homotopy Analysis Technique for the Solution of Nonlinear Problems. Doctoral Dissertation, Ph.D. Thesis, Shanghai Jiao Tong Uni-

versity, Shanghai.

[2] Liao, S.J. (1999) An Explicit, Totally Analytic Approximation of Blasius' Viscous Flow Problems. *International Journal of Non-Linear Mechanics*, **34**, 759-778. https://doi.org/10.1016/s0020-7462(98)00056-0

[3] Liao, S.J. (2003) Beyond Perturbation: Introduction to the Homotopy Analysis Method. CRC Press, Boca Raton.

[4] Casasús, L. and Al-Hayani, W. (2002) The Decomposition Method for Ordinary Differential Equations with Discontinuities. *Applied Mathematics and Computation*, **131**, 245-251. https://doi.org/10.1016/s0096-3003(01)00142-4

[5] Al-Hayani, W. and Casasús, L. (2006) On the Applicability of the Adomian Method to Initial Value Problems with Discontinuities. *Applied Mathematics Letters*, **19**, 22-31. https://doi.org/10.1016/j.aml.2005.03.004

[6] He, J.-H. (2004) The Homotopy Perturbation Method for Nonlinear Oscillators with Discontinuities. *Applied Mathematics and Computation*, **151**, 287-292. https://doi.org/10.1016/s0096-3003(03)00341-2

[7] He, J.-H. (2003) Homotopy Perturbation Method: A New Nonlinear Analytical Technique. *Applied Mathematics and Computation*, **135**, 73-79. https://doi.org/10.1016/s0096-3003(01)00312-5

[8] Adomian, G. (1986) Nonlinear Stochastic Operator Equations. Academic Press, New York.

[9] Wazwaz, A.M. (2000) A New Algorithm for Calculating Adomian Polynomials for Nonlinear Operators. *Applied Mathematics and Computation*, **111**, 53-69. https://doi.org/10.1016/s0096-3003(99)00063-6

Applied Mathematics, 2019, 10, 435-447
http://www.scirp.org/journal/am
ISSN Online: 2152-7393
ISSN Print: 2152-7385

Interaction of Nonstationary Waves on Cylindrical Body

Safarov Ismoil Ibrohimovich[1], Kulmuratov Nurillo Rakhimovich[2], Teshayev Muhsin Khudoyberdiyevich[3*], Kuldashov Nasriddin Urinovich[1]

[1]Tashkent Institute of Chemistry and Technology, Tashkent, Republic of Uzbekistan
[2]Navoi State Mining and Metallurgical Institute, Navoi, Republic of Uzbekistan
[3]Bukhara Engineering-Technological Institute, Bukhara, Republic of Uzbekistan

Email: *muhsin_5@mail.ru

How to cite this paper: Ibrohimovich, S.I., Rakhimovich, K.N., Khudoyberdiyevich, T.M. and Urinovich, K.N. (2019) Interaction of Nonstationary Waves on Cylindrical Body. *Applied Mathematics*, **10**, 435-447.
https://doi.org/10.4236/am.2019.106031

Received: March 29, 2019
Accepted: June 14, 2019
Published: June 17, 2019

Abstract

In this paper, the case of the interaction of a flat compression pulse with a layered cylindrical body in an infinite homogeneous and isotropic elastic medium is studied. The problem by the methods of integral Fourier transforms is solved. The inverse transform numerically by the Romberg method is calculated. With a time of toast and a decrease in momentum, the accuracy is not less than 2%. Taking into account the diffracted waves the results are obtained.

Keywords

Compression Impulses, Fourier Transform, Romberg Method, Heaviside Function, Reflections, Diffraction

1. Introduction

Various issues related to the interaction of bodies with a continuous medium (the creation of effective mathematical models is, theoretical and experimental methods for the study of non-stationary problems of dynamics) are described in monographs [1] [2] [3] [4] [5]. We have to deal with these questions when solving a wide variety of tasks. Their successful solution is associated with the further harmonic interaction of various sciences: aerodynamics, the theory of elasticity and plasticity, soil mechanics and underground structures, and others. The range of tasks for solving which is necessary to take into account the influence of the environment on the behavior of structures, structures and systems is continuously expanding: problems of pipe transport, defect scope, calculation of elements of nuclear reactors, seismic effects and others. Despite the great successes

achieved recently in this area, many problems still remain unresolved. The problems of unsteady interaction of deformable bodies with elastic media and with the ground are especially poorly studied. In the future, it is necessary to pay more attention to the following issues: building more accurate schemes (models) of the interaction of waves (of varying intensity) and bodies with deformable barriers; development and creation of computing systems based on modern computers for solving applied dynamics problems.

The problems of the no stationary dynamics of a homogeneous isotropic linearly elastic medium in cylindrical coordinates are given in the work of C. Chree [6]. Some problems of the dynamics of elastic cylindrical bodies are given in [7] [8]. In [9] [10], using the Laplace transform in time, the problem of radial oscillations of a thick-walled sphere immersed in an infinite elastic medium was investigated by specifying the uniform unsteady pressure. The stress-strain state of a hollow elastic cylinder surrounded and filled with acoustic or elastic media, under the action of non-stationary loads applied on the side surfaces, was investigated in [11] [12].

Some issues related to the diffraction of no stationary waves on cavities and absolutely rigid obstacles are considered in the works of A.N. Guzz, V.D. Kubenko and M.A. Cherevko [13] and Y.H. Pao and C.C. Mowa [14]. Works devoted to these problems are partially cited in the reviews of A.G. Gorshkov [15]. A general approach to solving plane diffraction problems in elastic media, based on the method of boundary integral equations, was developed by G.D. Manos and D.E. Beskos [16], D.M. Cole, D.D. Kosloff and J.B. Minster [17].

The influence of various factors on the behavior of a smooth infinitely long thin cylindrical shell during the diffraction of a plane shock wave on it (a plane problem) was studied by many authors [18]-[23]. The interaction of a plane mobile shock wave with a thin-walled structure consisting of coaxial cylindrical shells was considered in [24] [25]. Recently, considerable attention has been paid to the problems of non-stationary dynamics associated with the calculation of engineering structures for the action of seismic loads. The works of K. Fujita [26] are devoted to determining the response of some types of structures to seismic effects (Harouma and G.W. Housnera [27]). The creation of universal algorithms for calculating piecewise-homogeneous cylindrical bodies under the influence of non-stationary loads is an actual unsolved problem.

2. Statement and Methods for Solving the Problem of the Interaction of Non-Stationary Waves with a Cylindrical Body with a Liquid

The problem of the action of non-stationary waves on layered cylindrical bodies with radius R_k is considered. The motion vector of the medium is connected with the potentials φ_N and $\boldsymbol{\psi}_k$ by means of the formulas

$$\boldsymbol{u}_k = grad\,\varphi_k + rot\left(\boldsymbol{\psi}_k\right)\ \left(k = 1, 2, \cdots, N\right).$$

Suppose that the elastic medium is in plane strain conditions in the plane. In

polar coordinates r,θ, the basic ratios of the plane problem are

$$u_{rk}=\frac{\partial\varphi_k}{\partial r}+\frac{1}{r}\frac{\partial\psi_k}{\partial\theta},\ u_{\theta k}=\frac{1}{r}\frac{\partial\varphi_k}{\partial\theta}-\frac{\partial\psi_k}{\partial r}$$

$$\sigma_{rrk}=\frac{\lambda_k}{c_{1k}}\frac{\partial^2\varphi_k}{\partial t^2}+2\mu_k\left(\frac{\partial^2\varphi_k}{\partial r^2}+\frac{1}{r}\frac{\partial^2\psi_k}{\partial r\partial\theta}-\frac{1}{r^2}\frac{\partial\psi_k}{\partial\theta}\right)$$

$$\sigma_{\theta\theta k}=\rho_k\frac{\partial^2\varphi_k}{\partial t^2}-2\mu_k\left(\frac{\partial^2\varphi_k}{\partial r^2}+\frac{1}{r}\frac{\partial^2\psi_k}{\partial r\partial\theta}-\frac{1}{r^2}\frac{\partial\psi_k}{\partial\theta}\right)$$

$$\sigma_{r\theta k}=\rho_k\frac{\partial^2\psi_k}{\partial t^2}+2\mu_k\left(\frac{1}{r}\frac{\partial^2\varphi_k}{\partial r\partial\theta}-\frac{1}{r^2}\frac{\partial\varphi_k}{\partial\theta}-\frac{\partial^2\psi_k}{\partial r^2}\right)$$

here λ_k and μ_k the Lame elastic constants of the k-th layer; ρ_k—density of the material of the k-th layer; $\sigma_{rrk},\sigma_{\theta\theta k},\sigma_{r\theta k}$—components of the stress tensor of the *k*-th layer.

Non-stationary stress waves $\sigma_{xx}^{(i)}$ and $\sigma_{xy}^{(i)}$, whose front is parallel to the longitudinal axis of the cylinder, fall on a layered cylinder (**Figure 1**).

The basic equations of the theory of elasticity for this problem of plane strain in displacement potentials are reduced to the following:

$$\begin{aligned}\nabla^2\varphi_j&=\frac{1}{c_{pj}^2}\frac{\partial^2\varphi_j^{\kappa}}{\partial t^2};\quad (j=1,2,\cdots,N)\\ \nabla^2\psi_j&=\frac{1}{c_{\rho j}^2}\frac{\partial^2\psi_j}{\partial t^2}.\end{aligned}\tag{1}$$

where U_j and ψ_j are the displacement potentials of the *j*-th layer, c_{pj} and $c_{\beta j}$—are the phase velocities of the extension and shear waves of the *j*-th layer.

Suppose that time t is counted from the moment when the incident pulse touches the surface of the external $(N-1)$-th cylinder at point $r=r_N$, $\theta=0$. Until that moment, peace remains. In accordance with the foregoing, the task of finding the field of diffracted waves and the stress-strain state caused by the incident pulse [17]

$$\begin{aligned}\sigma_{xx}^{(i)}&=\sigma_0 H\left(\hat{t}\right),\\ \sigma_{xy}^{(i)}&=\sigma_0\frac{\nu_N}{1-\nu_N}H\left(\hat{t}\right),\ \hat{t}=t-\left(x+r_N\right)/C_{PN}\end{aligned}\tag{2}$$

σ_0—the amplitude of the incident waves; $H\left(\hat{t}\right)$—the unit Heaviside function, reduces to solving differential Equations (1). Boundary conditions on the contact of two cylindrical surfaces should be equal to displacement and tension

$$r=a_\kappa:\quad \sigma_{rr\kappa}=\sigma_{rr(\kappa+1)};\quad \sigma_{r\theta\kappa}=\sigma_{r\theta(\kappa+1)};\quad \sigma_{rz\kappa}=\sigma_{rz(\kappa+1)};$$

$$u_\kappa=u_{\kappa+1};\quad \vartheta_\kappa=\vartheta_{\kappa+1};\ w_\kappa=w_{\kappa+1}.$$

At infinity ($r\to\infty$), the perturbations must die out. If φ_N and ψ_N—diverging waves, then

$$\varphi_N\to 0,\psi_N\to 0\ \text{ at }\ \sqrt{x^2+y^2+z^2}\to\infty.$$

The problem is solved under the following zero initial conditions [19]:

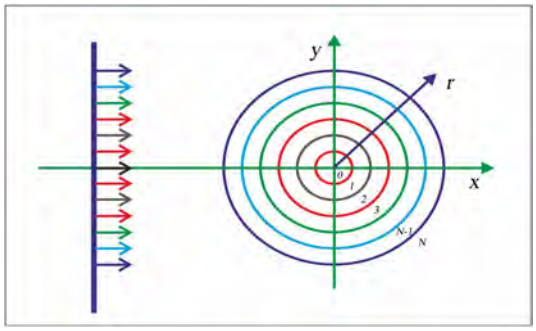

Figure 1. The effect of non-stationary waves on a layered body.

$$\begin{aligned} &\frac{\partial \phi_j}{\partial r}+\frac{1}{r}\frac{\partial \psi_j}{\partial \theta}\bigg|_{t=0}=\frac{\partial}{\partial t}\left(\frac{\partial \phi_j}{\partial r}+\frac{1}{r}\frac{\partial \psi_j}{\partial \theta}\right)\bigg|_{t=0}=0, \\ &\frac{1}{r}\frac{\partial \psi_j}{\partial \theta}-\frac{\partial \phi_j}{\partial r}=\frac{\partial}{\partial t}\left(\frac{1}{r}\frac{\partial \psi_j}{\partial \theta}-\frac{\partial \phi_j}{\partial r}\right)\bigg|_{t=0}=0, \end{aligned} \tag{3}$$

where $j=1,2,\cdots,N$; $Nt = j$—is the number of cylindrical layers; $j=N$ —environment.

It is required to determine the dynamic stress-strain state of the cylinder and its environment caused by the incident voltage pulse (2).

3. Solution Methods

To solve the plane problem, the integral Laplace transform (or Fourier transform) over time t is often used. When applying the integral Laplace transform for a function $f(t)$ that is integral in the sense of Lebegue on any open interval $0<t<T$, is expressed by the formula

$$f^L(s)=\int_0^\infty \mathrm{e}^{-st} f(t)\mathrm{d}t = L\left[f(t)\right]$$

The function $f^L(s)$ is usually called the image (transform ant), the function of the $f(t)$—original. The inversion of the Laplace transform is determined by the formula

$$f(t)=\frac{1}{2\pi i}\int_{\gamma-i\infty}^{\gamma+i\infty} \mathrm{e}^{st} f^L(s)\mathrm{d}s = L^{-1}\left[f^L(s)\right],$$

where the integral is taken along the path to the right of the singularities of the integrand. Using the Laplace transform problem, the interaction of non-stationary waves with a layered cylindrical body is a time-consuming task. Under the integral function is complex and has a complex form. Therefore, to find the exact expression of the original and bring to the numerical calculation is almost impossible. This method is applied in the work of V.D. Kubenko [1] for the problem of interaction of non-stationary waves of the cavity and obtained some particular solutions. Therefore, to solve this problem, the Fourier integral transform is used [28].

Integral Fourier transform. The stress field caused by the forces (2) satisfies

the wave Equation (1), *i.e.* every cylindrical layer satisfies it. To solve the above problem, apply the t-integral Fourier transform with respect to time

$$\phi^F(\xi)=\frac{1}{\sqrt{2\pi}}\int_{-\infty}^{+\infty}\phi(\Omega)\ell^{-i\xi\Omega}\mathrm{d}\Omega;\quad \phi(\Omega)=\frac{1}{\sqrt{2\pi}}\int_{-\infty}^{+\infty}\phi^F(\xi)\ell^{i\xi\Omega}\mathrm{d}\xi \tag{4}$$

Using zero initial conditions, we obtain the depicted problem

$$\begin{aligned}&\frac{1}{r}\frac{\partial}{\partial r}\left(r\frac{\partial\phi_j^F}{\partial r}\right)+\frac{1}{r^2}\frac{\partial^2\phi_j^F}{\partial\theta^2}+\frac{\Omega^2}{C_{P_j}^2}\bar{\phi}_j^F=0,\\&\frac{1}{r}\frac{\partial}{\partial r}\left(r\frac{\partial\bar{\psi}_j^F}{\partial r}\right)+\frac{1}{r^2}\frac{\partial^2\bar{\psi}_j^F}{\partial\theta^2}+\frac{\Omega^2}{C_{P_j}^2}\bar{\psi}_j^F=0,\end{aligned} \tag{5}$$

where Ω —Fourier transforms parameter; φ_j^F,ψ_j^F —image of the Fourier transform of functions $\varphi_j(t)$ and $\psi_j(t)$ respectively. Then the solution of Equations (4) and (5) will be

$$\begin{aligned}&\phi_j^F(r,\theta,\Omega)=\bar{\phi}_j^F(r,\Omega)\cos n\theta;\\&\psi_j^F(r,\theta,\Omega)=\bar{\psi}_j^F(r,\Omega)\sin n\theta\end{aligned} \tag{6}$$

here

$$\begin{aligned}&\bar{\phi}_j^F(r,\Omega)\\&=\begin{cases}A_nH_n^{(1)}\left(\Omega r/C_{PN}\right),\ r\ge r_N,\\A_{nj}H_n^{(1)}\left(\Omega r/C_{Pj}\right)+B_{nj}H^{(2)}\left(\Omega r/C_{Pj}\right),\ r_0\le 2\le r_N\ (j=1,2,\cdots,N-1),\\A_{n0}I_n\left(\Omega r/C_{SN}\right),\ 0\le r\le r_0;\end{cases}\end{aligned} \tag{7}$$

$$\bar{\psi}_j^F(r,\Omega)=\begin{cases}C_{nJ}H_n^{(1)}\left(\Omega r/C_{Sj}\right)+L_{nJ}H_n^{(2)}\left(\Omega r/C_{Sj}\right),\ r_0\le r\le r_N,\\C_nH_n^{(1)}\left(\Omega r/C_{SN}\right),\ r\ge r_N,\\C_{n0}I_n\left(\Omega r/C_{S0}\right),\ r_n\le r\le r.\end{cases} \tag{8}$$

Coefficients $A_{n0},A_{nj},A_{nN},B_{nj},C_{nj},C_{nN}$ —determined from the boundary conditions (7)-(8), which are placed on the contact of two cylindrical surfaces. Boundary conditions at $r=R_n$ taking into account the incident waves (1) take the form

a) $\sigma_{rrN}^F+\sigma_{rrN}^{(i)F}=\sigma_{rr(N-1)}^F$,
b) $\sigma_{r\theta N}^F+\sigma_{r\theta N}^{(i)F}=\sigma_{r\theta(N-1)}^F$,
v) $u_{rN}^F+u_{rN}^{(i)F}=u_{r(N-1)}^F$,
g) $u_{\theta N}^F+u_{\theta N}^{(i)F}=u_{\theta(N-1)}^F$,

where

a) $\sigma_{rrN}^{(i)F}(\Omega)=\sigma_{01}^{(P)}\sum_{n=0}^{\infty}(-1)^n\in_n I_n\left(\Omega r/C_{PN}\right)\cos n\theta$;
b) $\sigma_{rrN}^F(\Omega)=\sigma_{rrN}^F\left(\cos^2\theta+\in_N\sin^2\theta\right)$;
v) $\sigma_{r\theta N}^F=-\sigma_{rr}^F\left[(1-E_N)/2\right]\sin 2\theta$;
g) $u_{rN}^F=u_{rN}^F\cos\theta$;
d) $u_{\theta N}^F=u_{\theta N}^F\sin\theta$;
$\sigma_{01}^{(P)}=\sigma_0\mathrm{e}^{-N\Omega/C_{PN}}$.

Substituting (5) and (6) into the boundary conditions (7) and (8), we obtain a

system of complex algebraic equations with $(4j+3)$ unknowns in the form

$$[Z]\{g\}=\{P\}, \tag{9}$$

$$[Z]=\begin{pmatrix} [Z_1] & & 0 \\ & [Z_2] & \\ & & [Z_{(N-1)}] \\ 0 & & [Z_N] \end{pmatrix}$$

$[Z_j]$—4 × 4 matrix, the elements of which are of the nth order first and second kind Bessel and Henkel functions; $\{g\}$—Vector columns of unknown coefficients; $\{P\}-\{0,0,\cdots,0,P_{1N},P_{2N},P_{3N},P_{4N}\}^{\mathrm{T}}$—vector columns characterizing the falling loads, where $P_{1N},P_{2N},P_{3N},P_{4N}$ corresponds to $\sigma_{rrN}^{(i)F},\sigma_{r\theta N}^{(i)F},u_{rN}^{(i)F},u_{\theta N}^{(i)F}$. Let the stepped waves interact with a cylindrical hole when $r=r_0$ and a stress-free hole $\left(\sigma_{rr}\big|_{r=a}=\sigma_{r\theta}\big|_{r=a}=0\right)$. The only voltage that does not vanish at $r=r_0$, is the ring voltage $\sigma_{\theta\theta n}/\sigma_0$. Applying the Fourier transform to the equation of motion and the boundary conditions [5], we obtain the expression for ring stresses at $\sigma_{rr}=\sigma_0 H(t)\cos nt$, $\sigma_{r\theta}=\tau_0 H(t)\sin\theta$:

$$\sigma_{\theta\theta n}^{*}=\frac{\sigma_{\theta\theta n}(r_{01}\theta,t)}{\sigma}=\frac{1}{2\pi}\int_{-\infty}^{\infty}\frac{\Delta_1(r_0\Omega)\mathrm{e}^{i\Omega t}}{\Omega_1\left[\Delta_2\Delta_3+\Delta_4\Delta_5\right]}\mathrm{d}\Omega, \tag{10}$$

$$\Delta_1(r_{01}\Omega)=(\Delta_3+\tau_0 E)\left[2\Omega H_{n-1}^{(1)}(\Omega)-\left(\left(2n^2+2n\right)+\Omega^2\right)H_n^{(1)}(\Omega)\right]$$

$$+\left[\tau_0\Delta_2-\Delta_4\right]\left[2n(n+1)H_n^{(1)}\left((C_{P1}/C_{S1})\Omega\right)+\frac{2C_P n\Omega}{C_{S1}}H_{n-1}^{(1)}\left(\frac{C_P}{C_S}\Omega\right)\right].$$

Expression $\Delta_k\,(k=1,2,3,4,5)$ given in [20]. The improper integral (10) is solved numerically using the developed algorithms [21]. Practically, the calculation (10) on a computer can be carried out as follows. Since infinite numerical integration is unthinkable, the integral (10) is replaced by

$$\sigma_{\theta\theta n}^{*}=\frac{1}{2\pi}\int_{\omega_a}^{\omega_b}\frac{\Delta_1(r_{01}\Omega_1)}{\Omega_1\left[\Delta_2\Delta_3+\Delta_4\Delta_5\right]}\mathrm{e}^{-i\Omega t}\mathrm{d}\Omega. \tag{11}$$

Values of the limits of integration ω_a,ω_b are selected depending on the type of incident pulse. Numerical values of spectral density $\sigma_{rr}^{(i)F}(\Omega)$ from (9) of the final incident pulse; only in a small frequency range is significantly different from zero. Limits of integration ω_a,ω_b should be selected in accordance with this range and taking into account the required accuracy. At the same time, the question remains open as to what error the neglect of the contribution of integrals of the type (10), within the limits of integration of $-\infty$ to ω_a and from ω_b to ∞. The numerical summation of the infinite sum (10) is, of course, also impossible. However, it was shown in [22] that for sufficiently large n (the n-order of the Bessel and Henkel functions), we can construct an asymptotic representation of the general term of this sum. As a result, it becomes possible to either estimate the error of the transition from an infinite to a finite sum, or approximate summation of an infinite sum. In view of the above, we keep in (10)

an infinite sum. The calculation by the considered method is reduced to the construction of two calculation algorithms: coefficients $Z_{ke}(\Omega)(k,e=1,2)$ (11) and integral (10). The first and second algorithms do not depend on the type of mathematical model of the object.

4. Calculation Algorithm

Magnitude $\sigma_{\theta\theta n}/\sigma_0$ from (11) is calculated on a computer as follows. All numeric parameters required for calculations are specified. The following notation is introduced: $x_1=\Omega$, $x_2=n_1\Omega$, where $n_1=C_{P1}/C_{S1}$; $\Omega=\omega\alpha/C_{P1}$. For two values $x_k(k=1,2)$ Bessel function is determined $I_n(\xi)$ и $N_n(\xi)(n=1,2,\cdots,10)$. These arrays are calculated by the formula

$$u_n(\xi)=\frac{2(n-1)}{\xi}u_{n-1}(\xi)-u_{n-2}(\xi),\ u_n(\xi)=I_n(\xi),N_n(\xi) \tag{12}$$

As shown in [23], the absolute value of the Bessel function decreases rapidly with increasing index, starting from the moment when the index exceeds the argument. In this case, the direct use of formula (12) does not lead to the goal. Nevertheless, the calculation by (12) is possible, if by the recurrence formula

$$\overline{I}_n(\xi)=\frac{2(n-1)}{\xi}\overline{I}_{n+1}(\xi)-\overline{I}_{n+2}(\xi) \tag{13}$$

in the direction of decreasing index (from $n=N$ to $n=0$), an auxiliary function is calculated $\overline{I}_n(\xi)$. To calculate the integral (11) of the integrand function

$$\chi_1(r_0,\Omega,t)=\left(\Delta_1(r_0,\Omega_1)/\Omega_1(\Delta_2\Delta_3+\Delta_4\Delta_5)\right)\mathrm{e}^{i\Omega t}$$

can be integrated numerically by writing it in the form

$$\chi_1(r_0,\Omega,t)=x_1(r_0,\Omega,t)-ix_2(r_0,\Omega,t).$$

The falling pulse $\sigma_{xx}^{(i)}(\Omega)$ [23] is described by the expression

$$\sigma_{xx}^{(i)}(\Omega)=f_1(\Omega,t)-if_2(\Omega,t),$$

where $f_1(\Omega,t)$, $f_2(\Omega,t)$—real functions. Using Euler's formula for $\ell xp(i\Omega t)$, dividing (18) into real and imaginary (19) parts, after some transformations we get

$$\sigma_{\theta\theta n}^{*}=\frac{1}{\sqrt{2\pi}}\int_{-\infty}^{\infty}\left[x_1(\Omega,t)-ix_2(\Omega,t)\right]\mathrm{d}\Omega \tag{14}$$

Dividing the integral (14) into two terms

$$\sigma_{\theta\theta n}=\frac{1}{\sqrt{2\pi}}\int_{-\infty}^{0}\left[x_1(\Omega,t)-ix_2(\Omega,t)\right]\mathrm{d}\Omega+\frac{1}{\sqrt{2\pi}}\int_{0}^{\infty}\left[x_1(\Omega,t)-ix_2(\Omega,t)\right]\mathrm{d}\Omega. \tag{15}$$

And replacing the variable in the first integral Ω on $-\Omega$, will have

$$\sigma_{\theta\theta n}=\frac{1}{\sqrt{2\pi}}\int_{0}^{\infty}\left[x_1(\Omega,t)-x_1(-\Omega,t)\right]-i\left[x_2(\Omega,t)-x_2(-\Omega,t)\right]\mathrm{d}\Omega. \tag{16}$$

Since (16) is the inverse Fourier transform and contains the real value in the left-hand side [24], the relation

$$x_1(\Omega,t)=-x_1(-\Omega,t);x_2(\Omega,t)=-x_2(-\Omega,t). \tag{17}$$

Considering it, from (17) we finally get

$$\sigma^*_{\theta\theta n}=\frac{\sqrt{2}}{\pi}\int_{\omega_a}^{\omega_b}\left[x_1(\Omega,t)+ix_2(\Omega,t)\right]\mathrm{d}\Omega.$$

The value of integral (17) can be found numerically using the Romberg method [9] [10]. The basic algorithm of this method is given in the first chapter. When calculating the integral using the Romberg method, one has to repeatedly calculate the integrand. The inverse Fourier transform for some image, the original of which is known in advance, showed that with an integration step length of 0.01, the error of the procedure does not exceed 0.3% - 0.5%.

Numerical results are presented for the ring voltage at $r=r_0$, caused by the incident flat shock wave with a stepped distribution of voltage over time. Numerical results were obtained for $\nu=0.25$: $C_{S1}/C_{P1}=0.5$; $\theta=0^\circ$ и 90°. To determine the integral (17) of the boundary of the integral ω_a and ω_b have chosen $\left[10^{-4}-N\right], N=1,2,3,4,5$, a step $h=0.1,0.01,0.001$. At $N=5$ and $N=6$ the value of the ring voltage differs from the previous one by the fifth decimal place. Change $\sigma^*_{\theta\theta}$ depending on the τ at various $n=0,1,2,3,4,5$ shown in **Figure 2**, **Figure 3** and **Figure 4**. The results of our numerical calculations were compared with known results [20]. The values obtained differ by approximately 30% at n = 0.1: the maximum ring stress at $h=0.01$ and $\theta=90$ is 2.962/3.0; and on work [11] [12]—3.28/3.0 ($\tau\approx 4.71$).

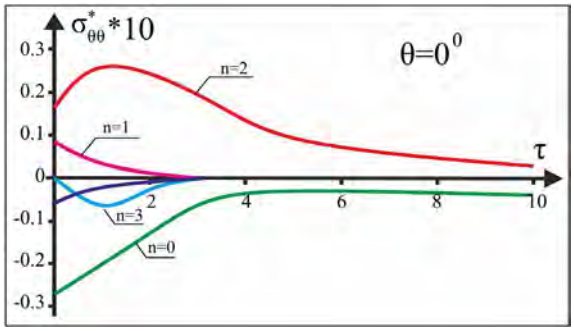

Figure 2. The dependence of ring stresses on time, with different *n*.

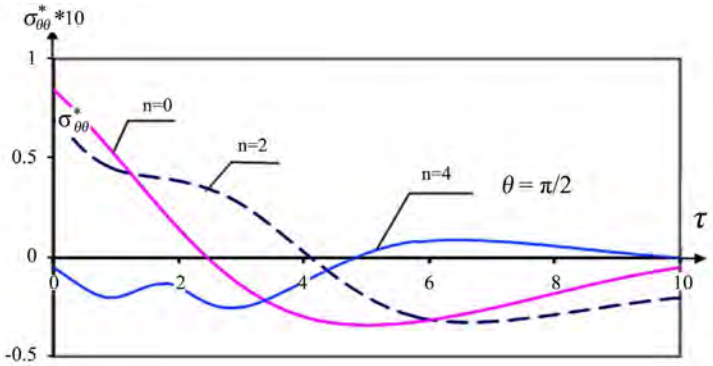

Figure 3. The dependence of ring stresses on time, with different *n*.

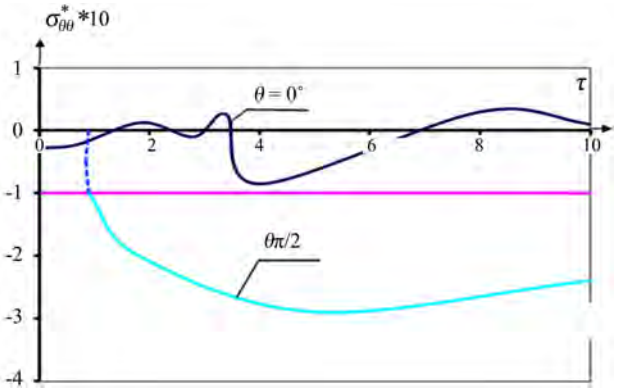

Figure 4. The dependence of the ring voltage on time τ.

5. Diffraction of Non-Stationary Waves on a Cylindrical Body

Let the inner boundary $(r = r_0)$ free from voltage, and on contact with the environment, the condition of equality of displacements and stresses (7) [25] [26]. After the Fourier transform, we obtain the cylindrical Bessel Equations (13) and (16), the solution of which has the form (7) and (8). In our problem there will be six arbitrary constants, which are determined from the boundary conditions (8). Here are some of them:

$$\sigma_{rr_2} = 2\mu_2 r^{-2} \sum_{k=1}^{2} \sum_{n=0}^{\infty} \int_{-\infty}^{+\infty} \left[C_{nk} \varepsilon_{1n}^{(k)} + D_{nk} \varepsilon_{2n}^{(k)} \right] e^{i\Omega\tau} d\Omega,$$

$$\sigma_{\theta\theta_2} = 2\mu_2 r^{-2} \sum_{k=1}^{2} \sum_{n=0}^{\infty} \int_{-\infty}^{+\infty} \left[C_{nk} \varepsilon_{3n}^{(k)} + D_{nk} \varepsilon_{4n}^{(k)} \right] e^{i\Omega\tau} d\Omega,$$

$$\sigma_{r\theta_2} = 2\mu_2 r^{-2} \sum_{k=1}^{2} \sum_{n=0}^{\infty} \int_{-\infty}^{+\infty} \left[C_{nk} \varepsilon_{5n}^{(k)} + D_{nk} \varepsilon_{6n}^{(k)} \right] e^{i\Omega\tau} d\Omega,$$

$$\sigma_{rr_1} = 2\mu_1 r^{-2} \sum_{k=1}^{2} \sum_{n=1}^{\infty} \int_{-\infty}^{+\infty} \left[A_n \delta_n^{(1)} + B_n \delta_n^{(2)} \right] e^{i\Omega\tau} d\Omega,$$

where C_{nk}, D_{nk}, A_n, B_n —arbitrary constants: $C_{nk} = \sigma_{kn}^{(c)} / \Delta_n$, $D_{nk} = \sigma_{kn}^{(D)} / \Delta_n$, $A_n = \delta_n^{(A)} / \Delta_n$, $B_n = \sigma_n^{(B)} / \Delta_n$; $\sigma_{kn}^{(k)}$ and Δ_n —square complex matrices (6×6). The remaining elements of the stress tensor are written similarly (17)

$$\begin{aligned} &C_{nk} = \operatorname{Re} C_{nk} + i \operatorname{Im} C_{nk}, \; D_{nk} = \operatorname{Re} D_{nk} + i \operatorname{Im} D_{nk}, \\ &A_n = \operatorname{Re} A_n + i \operatorname{Im} A_n, \; B_n = \operatorname{Re} B_n + i \operatorname{Im} B_n, \\ &\delta_n^{(e)} = \operatorname{Re} \delta_n^{(e)} + i \operatorname{Im} \delta_n^{(e)}, \; e = 1, 2, \; \varepsilon_{mn}^{(k)} = \operatorname{Re} \varepsilon_{mn}^{(k)} + i \operatorname{Im} \varepsilon_{mn}^{(k)}, \\ &e^{i\Omega t} = \cos \Omega t + i \sin \Omega t, \; m = 1, 2, 3, 4, 5 \end{aligned} \tag{18}$$

Substituting (18) into (17), after some transformations, we obtain the stress tensor

$$\sigma_{ji} = \sum_{k=1}^{2} \sum_{n=0}^{\infty} \int_{\omega_a}^{\omega_b} \operatorname{Re} \sigma'_{ij} d\Omega. \tag{19}$$

All these procedures are stored in the memory of the machine. A universal algorithm for calculating integrals of type (19) has been developed. The results of the calculations are shown in **Figure 5** with

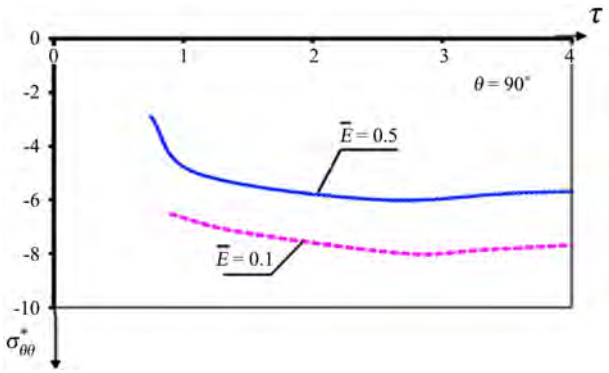

Figure 5. The dependence of the ring voltage of time τ.

$$\theta = 90^{\circ}\left(\nu_1 = 0.2; \nu_2 = 0.25; r_0/r_1 = 0.5; E_1/E_2 = 0.1; \eta = 0.1\right)$$

The obtained data are compared with known results [25] [26]. When integrating the limit $\omega_a = 10^{-4}, \omega_b = 4, h = 10^{-2}$ the results of my calculation are different from the data on ≈20%. Similar results were obtained for cylindrical shells in an elastic medium. The equation of motion of cylindrical shells has the form [27], and the circumferential stress $\sigma^*_{\theta\theta}$ in the shell but here $C_{n2} = D_{n2} = 0$. Change in peripheral voltage $\sigma^*_{\theta\theta}\left(\theta = 90^{\circ}, r = r_0\right)$ depending on the τ shown in **Figure 6**, where 1 is the results of [28], 2 are mine for given $\left(h/r = 0.04; h = \left(r_1 - r_0\right)/2\right)$. Similar results were obtained in [28], but the authors believe that $\in_1 = h^2/12R^2 = 0$, those. They take into account the bending moment. In the case of elastic cylindrical bodies, the determination of the stress-strain state of an object and its environment under the action of non-stationary waves is based on building a sequence of incident pulses from stationary components, where each pulse is a change in time of unsteady voltage in the incident wave.

Figure 7 shows the change in circumferential voltage $\sigma^*_{\theta\theta}$ $\left(\theta = 90^{\circ}, r = r_0, r = r_0 + \left(r_1 - r_0\right)/2, r = r_1\right)$, depending on the τ.

The difference between the stresses on the outer and inner surfaces reaches ≈15% - 20%, and the difference between the stresses on the middle and inner surfaces ≈10% $\left(r_0/r_1 = 0.5\right)$. Calculations show that when $\tau = 12\alpha/C_{P_1}$ the results of this study are approaching the exact static value $\sigma^*_{\theta\theta} = 8.13$. The dependence of the circumferential voltage on τ presented in **Figure 8**. It is seen that the maximum stress and displacement significantly depend on $\overline{\eta}$ and $\overline{E}$.

6. Diffraction of Elastic Non-Stationary Waves in a Two-Layer Cylindrical Body

Let a non-stationary step load (1) fall on an elastic two-layer cylindrical body for $t > 0$. A hard contact condition is set at the borders of the contact. The stress tensor in each layer is written as

$$\sigma_{ij}^{(k)}\left(r_1\theta_1 t\right) = \frac{1}{\pi}\sum_{n=0}^{\infty}\int_{\omega_a}^{\omega_b} \mathrm{Re}\,\sigma_{nij}^{\prime(k)}\left(r_1\theta_1\Omega\right)\mathrm{d}\Omega, \quad k = 1,2,3. \tag{20}$$

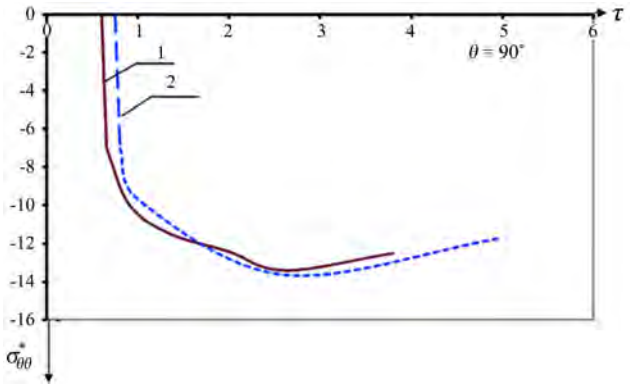

Figure 6. The dependence of the ring voltage of the middle surface of the layer on τ.

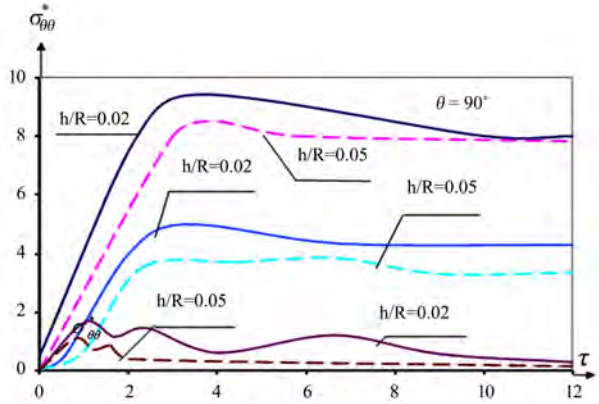

Figure 7. The dependence of the dimensionless ring stress on τ at various h/R.

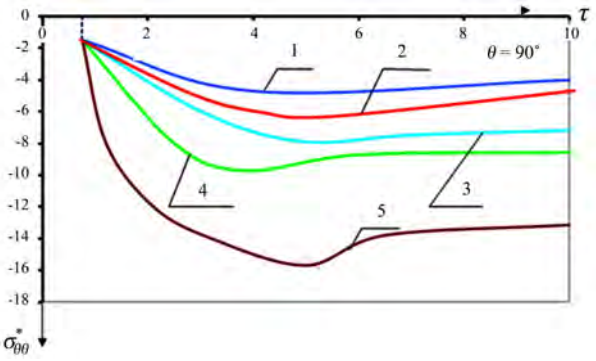

Figure 8. The dependence of the annular stress of the inner surface of the cylindrical layer on the time: 1—granite-concrete; 2—sandstone concrete; 3—soft concrete.

Stress tensor $\sigma_{ij}^{(k)}$ represents the functions of Bessel and Hankel of the first and second kind of the n-th order. Integral (20) is calculated according to the developed algorithm of the first chapter. The decision was limited to five members of the series (20), since the retention of the next members of the series has almost no effect on the results. For example, holding ten members (20) changes the voltage value by less than 2% - 3%. The following parameters were used in the calculations.: $r_0/r_2 = 0.2$; $r_1/r_2 = 0.6$; $\nu_1 = 0.2$; $\nu_2 = 0.25$; $\nu_3 = 0.2$; $E_1/E_2 = 0.3$; $E_3/E_2 = 0.1$; $\rho_1/\rho_2 = 0.3$; $\rho_3/\rho_2 = 0.1$.

7. Conclusions

1) In this paper, a method and algorithm are proposed for solving the problem of no stationary interaction of elastic waves on multilayer cylindrical bodies.

2) A new approach to solving dynamic problems of bodies interacting with the environment, based on the methods of Fourier and the Romberg method, is proposed.

3) It has been established that with the same loading characteristics in the material of the outer layer of a two-layer body, stress waves with the same parameters are formed at the initial moments of time.

Conflicts of Interest

The authors declare no conflicts of interest regarding the publication of this paper.

References

[1] Kubenko, V.D. (1979) Non-Stationary Interaction of Structural Elements with the Environment. Nauk. Dumka, Kiev, 182 p.

[2] Safarov, I.I., Akhmedov, M. and Umarov, A. (2017) Own Vibrations of Toroidal Shell with Flowing Liquid. Lambert Academic Publishing, Saarbrücken, 177 p.

[3] Safarov, I.I., Teshaev, M.Kh. and Boltaev, Z.I. (2017) Distribution of Harmonic Waves in Expansion Plastic and Cylindrical Viscoelastic Bodies. Open Science Publishing, Raleigh, 218 p.

[4] Safarov, I.I. (1992) Collisions and Waves in Dissipatively Non-Fertile Environments and Constructions. Fan, Tashkent, 250 p.

[5] Safarov, I.I., Akhmedov, M.Sh. and Buronov, S. (2017) Method of Finite Elements in the Calculations of Pipelines. Lambert Academic Publishing, Saarbrücken, 225 p.

[6] Chree, C. (1889) The Equations of an Isotropic Elastic Solid in Polar and Cylindrical Coordinates. Their Solution and Application. *Transactions of the Cambridge Philosophical Society*, **14**, 251-369.

[7] Mente, M. (1963) Dynamic Stresses and Displacement in the Vicinity of a Cylindrical Discontinuity Surface from a Plane Harmonic Shear Wave. *Applied Mechanics*, *Translation from English*, **30**, 117-126.

[8] Safarov, I.I. and Umarov, A.O. (2014) The Impact of Longitudinal and Transverse Waves on Cylindrical Layers with Liquid. *Bulletin of Perm University. Mathematics, Mechanics*, *Informatics*, **3**, 69-75.

[9] Safarov, I.I., Akhmedov, M.Sh. and Umarov, A.O. (2014) Dynamic Stresses and Mixing near a Cylindrical Reinforced Cavity from a Plane Harmonic Wave. *Monthly Scientific Journal "Prospero"* (*Novosibirsk*), No. 3, 57-61.

[10] Safarov, I.I., Boltaev, Z.I. and Umarov, A. (2017) Own Waves in Infinite Viscoelastic Cylindrical Panel from Variable Thickness. *World Wide Journal of Multidisciplinary Research and Development*, **3**, 287-294.

[11] Safarov, I.I., Teshaev, M.X., Akhmedov, M.Sh. and Boltaev, Z.I. (2017) Distribution Free Waves in Viscoelastic Wedge with and Arbitrary Angle Tops. *Applied Mathematics*, **8**, 736-745. http://www.scirp.org/journal/am
https://doi.org/10.4236/am.2017.85058

[12] Safarov, I.I., Teshaev, M.Kh., Boltaev, Z.I. and Nuriddinov, B.Z. (2017) Of Own and

Forced Vibrations of Dissipative Inhomogeneous Mechanical Systems. *Applied Mathematics*, **8**, 1001-1015. https://doi.org/10.4236/am.2017.87078

[13] Guz, A.N., Kubenko, V.D. and Cherevko, M.A. (1978) Diffraction of Elastic Waves. Naukova Dumka, Kiev, 307 p.

[14] Pao, Y.H. and Mowa, C.C. (1973) Diffraction of Elastic Waves and Dynamic Stress Concentrations. Crane, New York, 694 p. https://doi.org/10.1115/1.3423178

[15] Safarov, I.I., Teshayev, M.Kh., Boltayev, Z.I. and Akhmedov, M.Sh. (2017) Damping Properties of Vibrations of Three-Layer VIscoelastic Plate. *International Journal of Theoretical and Applied Mathematics*, **3**, 191-198. https://doi.org/10.11648/j.ijtam.20170306.13

[16] Manos, G.D. and Beskos, D.E. (1981) Dynamic Stress Concentration Studies by Bourtidary Integrals and Laplase Transform. *International Journal for Numerical Methods in Engineering*, **17**, 573-599. https://doi.org/10.1002/nme.1620170407

[17] Safarov, I.I. and Boltayev, Z.I. (2017) Propagation of Natural Waves in Extended Cylindrical Viscoelastic Panels. *International Journal of Emerging Engineering Research and Technology*, **5**, 37-40.

[18] Safarov, I.I., Boltaev, Z.I. and Axmedov, M.Sh. (2015) Setting the Linear Oscillations of Structural Heterogeneity Viscoelastic Lamellar Systems with Point Relations. *Applied Mathematics*, **6**, 228-234. https://doi.org/10.4236/am.2015.62022

[19] Safarov, I.I., Marasulov, A., Akhmedov, M.Sh. and Shodiyev, Z.O. (2017) Voltage Deformable State Parallel Arrangement of Cylindrical Pipe with a Liquid under Harmonic Loads. *Case Studies Journal*, **6**, 36-47.

[20] Safarov, I.I., Akhmedov, M.Sh. and Rajabov, O. (2017) About the Natural Oscillations Viscoelastic Toroidal Shell with the Flowing Fluid. *World Wide Journal of Multidisciplinary Research and Development*, **3**, 295-309.

[21] Safarov, I.I. and Boltaev, Z.I. (2018) Propagation of Natural Waves on Plates of a Variable Cross Section. *Open Access Library Journal*, **5**, 1-29.

[22] Safarov, I.I., Teshaev, M.Kh., Nuriddinov, B.Z. and Boltayev, Z.I. (2017) Of Own and Forced Vibrations of Dissipative Inhomogeneous Mechanical Systems. *Applied Mathematics*, **8**, 1001-1015. https://doi.org/10.4236/am.2017.87078

[23] Safarov, I.I., Teshaev, M.Kh. and Boltaev, Z.I. (2018) Own Vibrations of Bodies Interacting with Unlimited Deformable Environment. *Open Access Library Journal*, **5**, e4432. https://doi.org/10.4236/oalib.1104432

[24] Safarov, I.I., Teshaev, M.Kh. and Akhmedov, M.S. (2018) Free Oscillations of a Toroidal Viscoelastic Shell with a Flowing Liquid. *American Journal of Mechanics and Applications*, **6**, 37-49. https://doi.org/10.11648/j.ajma.20180602.11

[25] Safarov, I.I., Boltaev, Z.I. and Axmedov, M.Sh. (2014) Loose Waves in Viscoelastic Cylindrical Wave Guide with Radial Crack. *Applied Mathematics*, **5**, 3518-3524. https://doi.org/10.4236/am.2014.521329

[26] Fujita, K. (1981) A Seismic Response Analysis of a Cylindrical Liquid Storage Tank. *Bulletin of the JSME*, **24**, 1029-1036. https://doi.org/10.1299/jsme1958.24.1029

[27] Haroum, M.A. and Housner, G.W. (1981) Earthquake Response of Deformable Liquid Storage Tanks. *Journal of Applied Mechanics, Transactions ASME*, **48**, 411-418. https://doi.org/10.1115/1.3157631

[28] Safarov, I.I. and Teshaev, M.Kh. (2018) Vibration Protection of Mechanical Systems Consisting of Solid and Deformable Bodies. *European Journal of Engineering Research and Science*, **3**, 18-28. https://doi.org/10.24018/ejers.2018.3.9.860

Applied Mathematics, 2019, 10, 448-467
http://www.scirp.org/journal/am
ISSN Online: 2152-7393
ISSN Print: 2152-7385

Mediative Sugeno's-TSK Fuzzy Logic Based Screening Analysis to Diagnosis of Heart Disease

Nitesh Dhiman, Mukesh Kumar Sharma

Department of Mathematics, C.C.S. University, Meerut, India
Email: drmukeshsharma@gmail.com

How to cite this paper: Dhiman, N. and Sharma, M.K. (2019) Mediative Sugeno's-TSK Fuzzy Logic Based Screening Analysis to Diagnosis of Heart Disease. *Applied Mathematics*, **10**, 448-467.
https://doi.org/10.4236/am.2019.106032

Received: May 10, 2019
Accepted: June 21, 2019
Published: June 24, 2019

Abstract

Fuzzy logic is an approach which deals with the incomplete information to handle the imperfect knowledge. In the present research paper we have proposed a new approach that can handle the imperfect knowledge, in a broader way that we will consider the unfavourable case also as the intuitionistic fuzzy logic does. The mediative fuzzy logic is an extensive approach of intuitionistic fuzzy logic, which provides a solution, when there is a contradiction in the expert knowledge for favourable as well as unfavourable cases. The purpose of the present paper is to design a mediative fuzzy inference system based Sugeno-TSK model for the diagnosis of heart disease. Our proposed method is the extension of Sugeno-TSK fuzzy logic controller in the form of Sugeno-TSK mediative fuzzy logic controller.

Keywords

Fuzzy Logic, Intuitionistic Fuzzy Logic, Mediative Fuzzy Logic, Sugeno's Fuzzy Controller, Fuzzy Rule, Firing Level, Heart Disease

1. Introduction

Uncertainty affects all the decision of experts and appears in different forms. Uncertainty is an objective fact or just a subjective impression which is closely related to individual person. The choice of an appropriate uncertainty calculus may depend on the cause of uncertainty, quantity and quality of information available, type of information processing required by the respective uncertainty calculus and the language required by the final observer. The concept of information is fully connected with concept of uncertainty. The most fundamental aspect of this connection is that uncertainty involved in any problem-solving

situation is a result of some information deficiency, which may be incomplete, imprecise, fragmentary, vague, contradictory and not reliable information. Fuzzy approximate reasoning [1] [2] allows handling such type of uncertainty. Fuzzy logic proposed by L. A. Zadeh in 1965 [3] [4] covers the uncertainty with the help of membership function only. Fuzzy logic provides a mathematical theory to handle the uncertainty associated with the human decision with the help of its membership function. In 1986 the concept of intuitionistic fuzzy sets was proposed by K. Atanassov [5] [6], which deals with membership function, non-membership function and hesitation part which has the property to incorporate the uncertainty of the information. Intuitionistic fuzzy sets are the generalization of fuzzy sets. IFSs proffer a new criterion to represent impartial knowledge and therefore, to present in a more adequate manner for may real world problems. In 2014 Hajek [7] gave the methods for the defuzzification in the inference system for the Takagi-Sugeno type so that we can observe the crisp values for the outputs.

Many real life applications have given the evidence that intuitionistic fuzzy sets are better than the traditional fuzzy logic. In this list we may also mention some more aspects [8] [9] that may give better results than traditional fuzzy logic *i.e.* type-I, type-II, interval valued fuzzy sets and vague sets, interval valued vague sets etc. but the intuitionistic fuzzy sets cover the uncertainty caused by membership, non-membership and the hesitation part. Castillo etc. [10] in 2003 gave a new method for the inference for the fuzzy inference based on intuitionistic fuzzy logic that is in this work he explained the importance of favorable and unfavorable cases. Again in 2007 [11] used this concept for plant monitoring system and gave a scheme for the diagnosis of the defects. In 2007 Melin [12] used the mediative fuzzy logic for the contradictory knowledge management and explained how the logic is better than previous ones. Montiel etc. [13] in 2008 gave the concept of mediative fuzzy logic that is a new approach for handling the contradiction in the decision. So we can construct an intuitionistic fuzzy logic controller similar to the fuzzy logic controller given by Jang etc. [14] in neuro-fuzzy and soft computing. 1979 Sanchez [15] used the fuzzy logic and fuzzy relation for medical diagnosis in 2001 Supriya [16] used the extension of fuzzy sets in the form of intuitionistic fuzzy sets in medical diagnosis but What happens if the knowledge base rule changes with the perception of experts give a contradictory, non-contradictory and the incomplete information or the combination of these situations? Intuitionistic fuzzy sets are inadequate to explain these situations. To deal such situations, which inference system be used. Montiel [17] etc. in 2009 gave an algorithm which is able to deal with kind of information for controlling population size, which may be inconsistent, incomplete and contradiction exists. This is a mediate solution. Mediative fuzzy logic can bring down to the intuitionistic and fuzzy logic based on the affirmations and denials are established. In 2018 Iancu [18] used the mediative fuzzy logic in the heart disease using the Mamdani fuzzy inference rule for single input and single output. In our work we have extended this by using Sugeno's-TSK fuzzy infe-

rence system with two inputs and one output. By using this inference system we have developed an algorithm and on the basis of this algorithm we have constructed eight hundred and eighty five rules, from these rules here we have given the fifty rules and their crisp outputs and the firing level.

In this present research paper we have designed a meditative fuzzy inference system in **Figure 1** for Sugeno's-TSK fuzzy controller for the diagnosis of heart disease. The present research paper is divided into six sections. In the second section we have taken some basic definitions on mediative fuzzy logic, contradiction fuzzy sets and intuitionstic fuzzy numbers. In section third of the research paper we have developed an algorithm which is based on Sugeno's-TSK controller using mediative fuzzy logic. The algorithm contains all the steps which we have proposed for our method including the block diagram. In section four of the research paper we have categorized the outputs and make the membership and non-membership for the stages of the risk about the sickness. In section five we have computed the values of the outputs using the defuzzification methods and the firing level of the observed during that output. In the last section conclusion of the research paper is given.

2. Basic Definitions

2.1. Meditative Fuzzy Logic

Intuitionistic Fuzzy Sets: let X be an universal set then IFSs (instuitionistic fuzzy sets) A^I in X is defined as

$$A^I = \left\langle \left(x, \mu_{A^I}(x), \upsilon_{A^I}(x) : x \in X \right) \right\rangle \tag{1}$$

where

$$\mu_{A^I}(x) : X \to [0,1] \text{ and } \upsilon_{A^I}(x) : X \to [0,1], \text{ with, } 0 \le \mu_{A^I}(x) + \upsilon_{A^I}(x) \le 1 \tag{2}$$

are called membership and non membership functions respectively. And for all IFSs A^I in X,

$$\pi_{A^I}(x) = 1 - \mu_{A^I}(x) - \upsilon_{A^I}(x) \tag{3}$$

where,

$$0 \le \pi_{A^I}(x) \le 1 \tag{4}$$

hesitation part of x in A^I is called intuitionistic fuzzy index or we can say the hesitation part.

Total IFS output of an intuitionistic fuzzy system, calculated by the linear relation between FS_μ and FS_υ, which are traditional output of system with using membership and non membership values respectively, as

$$IFS = (1 - \pi) FS_\mu + \pi FS_\upsilon \tag{5}$$

We may observe if $\pi = 0$ then it will reduce as the output of a traditional fuzzy system, but for other values of π different from zero we will get the different outputs for the intuitionistic fuzzy systems. The advantage of this method for finding the IFS output of an intuitionistic system, is that we can use methodolo-

gy based on membership functions representing the fuzzy systems for computing FS_{μ} and FS_{υ}.

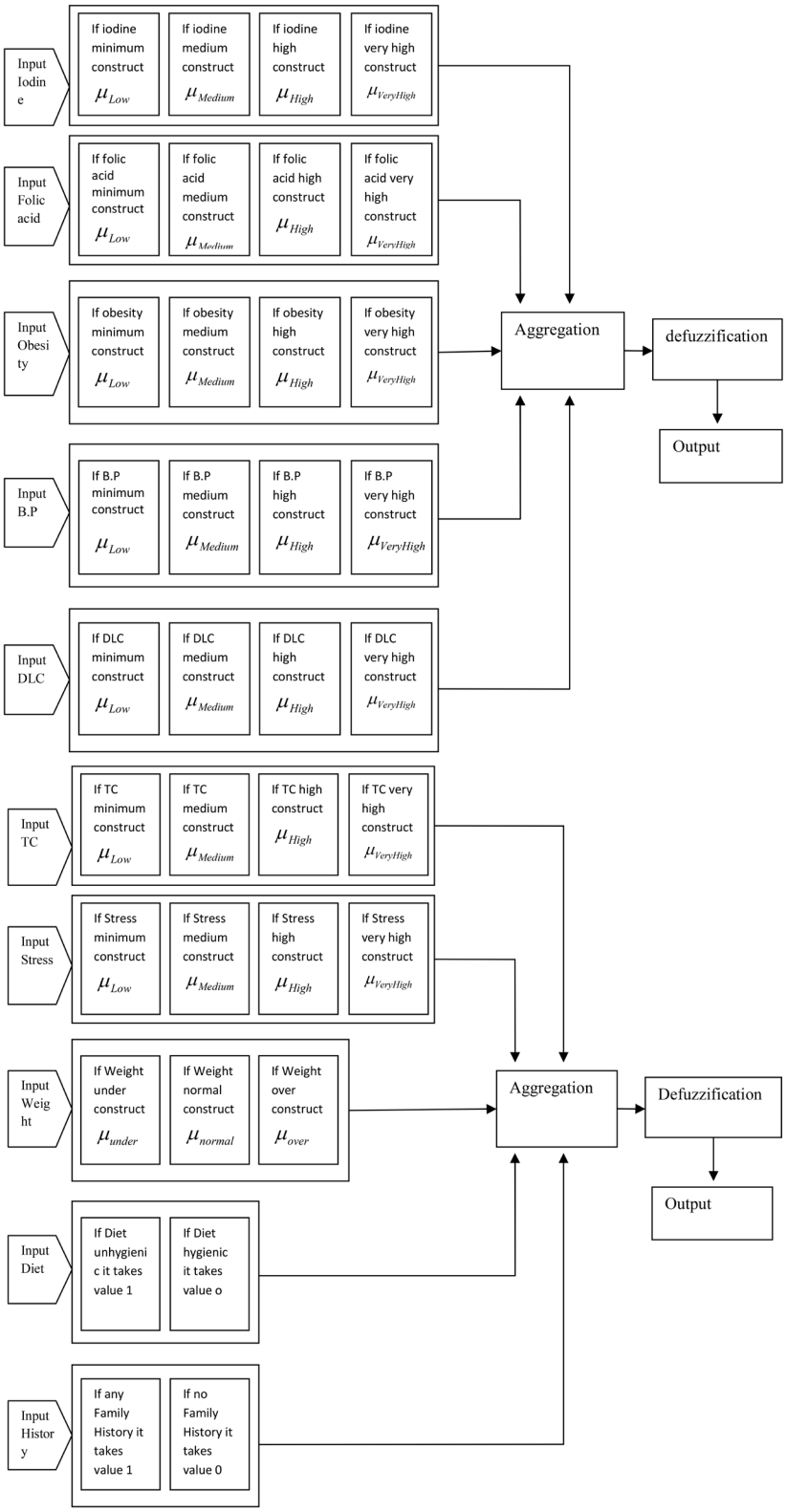

Figure 1. Computing framework of fuzzy inference system.

2.2. Contradiction Fuzzy Set

A contradiction fuzzy set C in X is given by

$$\zeta_c(x) = \min\left(\mu_c(x), \upsilon_c(x)\right), \tag{6}$$

where $\mu_c(x)$ represents the agreement membership function, and $\upsilon_c(x)$ non-agreement membership function. We will use the agreement and non-agreement membership functions in place of membership and non-membership functions in the analysis of our study, because we think these names are more appropriate for handling the uncertainty with the help of intuitionistic fuzzy sets. On the basis of these contradiction fuzzy sets, Montiel *et al.* [8], proposed the following three expressions

$$MFS = \left(1-\pi-\frac{\zeta}{2}\right)FS_{\mu} + \left(\pi+\frac{\zeta}{2}\right)FS_{\upsilon} \tag{7}$$

$$MFS = \min\left((1-\pi)FS_{\mu} + \pi FS_{\upsilon}, 1-\frac{\zeta}{2}\right) \tag{8}$$

$$MFS = \left((1-\pi)FS_{\mu} + \pi FS_{\upsilon}\right)\left(1-\frac{\zeta}{2}\right) \tag{9}$$

2.3. Intuitionistic Fuzzy Number

Let an intuitionistic fuzzy set A^I in X defines as $A^I = \left\langle \left(x, \mu_{A^I}(x), \upsilon_{A^I}(x) : x \in X\right)\right\rangle$ Then A^I is called intuitionistic fuzzy number if:

1) A^I is normal.

2) A^I is convex

3) Membership and non membership functions are path wise continuous.

a) Triangular instuitionistic fuzzy number in R, is defined with their membership and non membership grade as

$$\mu_{A^I}(x) = \begin{cases} \dfrac{x-a}{b-a} & \text{if } a \le x < b \\ \dfrac{c-x}{c-b} & \text{if } b \le x \le c \\ 0 & \text{if } x > c \text{ and } x < a \end{cases} \quad \text{and} \quad \upsilon_{A^I}(x) = \begin{cases} \dfrac{b-x}{b-a^*} & \text{if } a^* \le x < b \\ \dfrac{c^*-x}{c^*-b} & \text{if } b \le x \le c^* \\ 1 & \text{if } x < a^* \text{ and } x > c^* \end{cases}$$

where $a^* < a < b < c < c^*$ on real line.

b) Trapezoidal intuitionistic fuzzy number in R, is defined with their membership and non membership grade as

$$\mu_{A^I}(x) = \begin{cases} \dfrac{x-a}{b-a} & \text{if } a \le x < b \\ 1 & \text{if } b \le x \le c \\ \dfrac{d-x}{d-c} & \text{if } c < x \le d \\ 0 & \text{if } x > d \text{ and } x < a \end{cases} \quad \text{and} \quad \upsilon_{A^I}(x) = \begin{cases} \dfrac{b-x}{b-a^*} & \text{if } a^* \le x < b \\ 1 & \text{if } b \le x \le c \\ \dfrac{d^*-x}{d^*-c} & \text{if } c < x \le d^* \\ 0 & \text{if } x > d^* \text{ and } x < a \end{cases}$$

where $a^* < a < b < c < d < d^*$ on real line.

2.4. Fuzzy Implication

Czogala and Leski [19] analyzing a set of eight implications (Kleene-Dienes, Reichenbach, Lukasiewicz, Godel, Rescher-Gaines, Goguen, Zadeh, Fodor) concluded that the Lukasiewicz implication,

$$I_L(x,y) = \min(1, 1-x+y) \tag{10}$$

2.5. Firing Level

Processing of the fuzzification means that we have to assign a membership as well as non-membership grade to each input value to make it intuitionistic fuzzy set. Let $x_\circ \in U$ is fuzzified into $\overline{x_\circ}$ according to the relations:

$$\mu_{\overline{x_\circ}}(x) = \begin{cases} 1 & \text{if } x = x_\circ \\ 0 & \text{else} \end{cases}, \quad \upsilon_{\overline{x_\circ}}(x) = \begin{cases} 0 & \text{if } x = x_\circ \\ 1 & \text{else} \end{cases}$$

The μ-firing level and ν-firing level of an intuitionistic fuzzy set A^I with $x_\circ$ as crisp input are $\mu_{A^I}(x_\circ)$ and $\upsilon_{A^I}(x_\circ)$ respectively.

3. Proposed Algorithm for Planned Sugeno's—TSK Meditative System

In disease diagnosis, we often find illogical information that comes from different inference system that does not concede. In case when the classical logic, fuzzy logic or intuitionistic fuzzy logic do not work, then we need to apply meditative fuzzy logic. That will give the better results considering the favorable, unfavorable and the situation where neither the membership nor non-membership help for getting the better results but also the agreement and non-agreement membership function. In this present research paper we will develop a methodology using Sugeno's fuzzy inference system based on meditative fuzzy logic. We will develop Sugeno's-TSK meditative fuzzy logic controller and make fuzzy rule base with using two parameters as input variables which variations may cause heart disease in the form of one output value for the diagnosis of heart disease. We have proposed the algorithm as follows:

Step 1: Suppose we have a fuzzy inference rule for conditional and unqualified proposition as hypothetical syllogism which is the generalization of inference for hypothetical syllogism for classical logic. In the present research paper we will use the inference rule for fuzzy logic for conditional fuzzy proposition in the extended form of intuitionistic fuzzy logic. That is for conditional and unqualified proposition the inference rule R is: if X_1 is A_1 and X_2 is A_2 then Y is B. Because we are working with a rule with two inputs, so for the intuitionistic fuzzy set, in case of A_1 using μ—firing level I_{μ_1} for the membership will be denoted by α_1 and ν—firing level I_{υ_1} for the non-membership for A_2 will be denoted by β_1 and μ—firing level for I_{μ_2} and ν—firing level I_{ν_2} corresponds to rule R will be denoted by α_2 and β_2 respectively. Firing level for membership and non-membership will be given by setting Here we have two input values, we give some input to both the input variable, and we get the value of firing level corresponds to membership and non membership function.

Namely α_1 and β_1 for first input and α_2 and β_2 for second input respectively. This rule is represented by lukasiewicz implication and conclusion is inferred using Sugeno's TSK Fuzzy Model.

Step 2: Using Sugeno's fuzzy inference model with two input variables and one output variable *i.e.* an inference for conditional and qualified proposition we will get the firing level for the two antecedents that will result in one consequence for the membership and non-membership. Find $I_\mu = \min\left(I_{\mu_1}, I_{\mu_2}\right)$ for membership for the functions and the non-membership $l_\upsilon = \min\left(l_{\upsilon_1}, l_{\upsilon_2}\right)$ for the factors causing the stages of the disease, by setting $\alpha = \min\left(\alpha_1, \alpha_2\right)$ and $\beta = \min\left(\beta_1, \beta_2\right)$.

Step 3: After the step second we need to calculate the values for the intuitionistic fuzzy index in the form of hesitation part and contradiction that is in the form of agreement and disagreement by taking ζ = minimum of α and β, and $\pi = 1-(\alpha+\beta)$. The values of α and β will be taken from step 2.

Step 4: For the final Membership Fuzzy System output, the values obtained in step 3 in the form of the conclusions B^μ and B^ν as follows:

$$\begin{aligned} \mu_{B^\mu}(y) &= I_L\left(\alpha, \mu_B(y)\right), \quad \forall y \in Y \\ &= \min\left(1-\alpha+\mu_B(y), 1\right) \\ y^\mu &= defuzz\left(B^\mu\right) \end{aligned} \tag{11}$$

$$\begin{aligned} \mu_{B^\nu}(y) &= I_L\left(\beta, \mu_B(y)\right), \quad \forall y \in Y \\ &= \min\left(1-\beta+\mu_B(y), 1\right) \\ y^\mu &= defuzz\left(B^\nu\right) \end{aligned} \tag{12}$$

Will be defuzzified into the values for membership fuzzy output and non-membership fuzzy output as y^μ and y^υ, respectively by using the defuzzification method of Middle of Maxima and Middle of Minima techniques.

Step 5: Finally for getting the output after the final step from Sugeno's-TSK fuzzy inference system, we will get membership fuzzy system output by the formula

$$Z = \left[1-\left(1-(\alpha+\beta)\right)+\frac{1}{2}\min(\alpha,\beta)\right]y^\mu + \left[\left(1-(\alpha+\beta)\right)+\frac{1}{2}\min(\alpha,\beta)\right]y^\nu \tag{13}$$

3.1. Factors Effects Heart Disease: (Input Variables)

There are so many factors which affect heart disease but here we have considered the following ten most affecting factors in our study (Table 1).

3.2. Fuzzification of the Factors

First we will fuzzify the above factors according to the given range of the data in the form of membership and non-membership functions as follows:

3.2.1. Iodine

The recommended daily allowance for iodine [150 mcg/day] for adult, this input

is divided into four category low, medium, high and very high. Defined by intuitionistic fuzzy sets, by their μ membership values and υ non membership values, as given below:

$$\mu_{\text{low}}(x)=\begin{cases}1 & \text{if } x\le 110\\ \dfrac{135-x}{25} & \text{if } 110<x\le 135\end{cases},$$

$$\mu_{\text{medium}}(x)=\begin{cases}\dfrac{x-125}{10} & \text{if } 125\le x\le 135\\ 1 & \text{if } x=135\\ \dfrac{170-x}{35} & \text{if } 135\le x\le 170\end{cases}$$

$$\mu_{\text{high}}(x)=\begin{cases}\dfrac{x-165}{30} & \text{if } 165\le x\le 195\\ 1 & \text{if } x=195\\ \dfrac{220-x}{25} & \text{if } 195\le x\le 220\end{cases},$$

$$\mu_{\text{very high}}(x)=\begin{cases}\dfrac{x-210}{30} & \text{if } 210\le x\le 240\\ 1 & \text{if } x>240\end{cases}$$

Non membership values

$$\upsilon_{\text{low}}(x)=\begin{cases}\dfrac{x-125}{20} & \text{if } 125\le x\le 145\\ 1 & \text{if } x>145\end{cases},$$

$$\upsilon_{\text{medium}}(x)=\begin{cases}1 & \text{if } x<116\\ \dfrac{135-x}{19} & \text{if } 116\le x\le 135\\ 0 & \text{if } x=135\\ \dfrac{x-139}{45} & \text{if } 135\le x\le 180\\ 1 & \text{if } x>180\end{cases}$$

Table 1. Input factors which effects heart disease.

Input Factors	1) Iodine
	2) Folic acid
	3) Obesity
	4) B.P (Blood Pressure)
	5) DLC (Density Lipoprotein Cholesterol)
	6) TC (Total cholesterol)
	7) Stress
	8) Weight
	9) Diet
	10)Family history
Rules	Two input-one output

$$\upsilon_{\text{high}}(x)=\begin{cases}1 & \text{if } x\le 145\\ \dfrac{195-x}{50} & \text{if } 145\le x\le 195\\ 0 & \text{if } x=195\\ \dfrac{x-195}{25} & \text{if } 195\le x\le 220\\ 1 & \text{if } x>220\end{cases},$$

$$\upsilon_{\text{very high}}(x)=\begin{cases}1 & \text{if } x<195\\ \dfrac{225-x}{30} & \text{if } 195\le x\le 225\end{cases}$$

3.2.2. Folic Acid

Folic acid normal blood reference is around [2 - 20 mg/ml], this input is also divided into four category low, medium, high and very high. Defined by intuitionistic fuzzy sets, by their μ membership values and υ non membership values, are given below:

$$\mu_{\text{low}}(x)=\begin{cases}1 & \text{if } x\le 6\\ \dfrac{10-x}{4} & \text{if } 6\le x\le 10\end{cases},\quad \mu_{\text{medium}}(x)=\begin{cases}\dfrac{x-8}{4} & \text{if } 8\le x\le 12\\ 1 & \text{if } x=12\\ \dfrac{15-x}{3} & \text{if } 12\le x\le 15\end{cases}$$

$$\mu_{\text{high}}(x)=\begin{cases}\dfrac{x-14}{6} & \text{if } 14\le x\le 20\\ 1 & \text{if } x=20\\ \dfrac{25-x}{5} & \text{if } 20\le x\le 25\end{cases},\quad \mu_{\text{very high}}(x)=\begin{cases}\dfrac{x-18}{12} & \text{if } 18\le x\le 30\\ 1 & \text{if } x>30\end{cases}$$

Non membership values

$$\upsilon_{\text{low}}(x)=\begin{cases}\dfrac{x-8}{4} & \text{if } 8\le x\le 12\\ 1 & \text{if } x>12\end{cases},\quad \upsilon_{\text{medium}}(x)=\begin{cases}1 & \text{if } x<7\\ \dfrac{12-x}{5} & \text{if } 7\le x\le 12\\ 0 & \text{if } x=12\\ \dfrac{x-12}{6} & \text{if } 12<x\le 18\\ 1 & \text{if } x>18\end{cases}$$

$$\upsilon_{\text{high}}(x)=\begin{cases}1 & \text{if } x<12\\ \dfrac{20-x}{8} & \text{if } 12\le x\le 20\\ 0 & \text{if } x=20\\ \dfrac{x-20}{8} & \text{if } 20\le x\le 28\\ 1 & \text{if } x>28\end{cases},\quad \upsilon_{\text{very high}}(x)=\begin{cases}1 & \text{if } x<26\\ \dfrac{32-x}{6} & \text{if } 26\le x\le 32\end{cases}$$

3.2.3. Obesity

Normal range of obesity for heart disease is around [18.5 - 24.9 kg/m^2], obesity

input variable has 4 values low, medium, high and very high as intitutionistic fuzzy set by their membership and non membership values, are given below as:

$$\mu_{\text{low}}(x)=\begin{cases}1 & \text{if } x<11\\ \dfrac{16-x}{5} & \text{if } 11\le x\le 16\end{cases},$$

$$\mu_{\text{medium}}(x)=\begin{cases}\dfrac{x-14.5}{5} & \text{if } 14.5\le x\le 19.5\\ 1 & \text{if } x=19.5\\ \dfrac{22.5-x}{3} & \text{if } 19.5\le x\le 22.5\end{cases}$$

$$\mu_{\text{high}}(x)=\begin{cases}\dfrac{x-21}{2.5} & \text{if } 21\le x\le 23.5\\ 1 & \text{if } x=23.5\\ \dfrac{26.5-x}{3} & \text{if } 23.5\le x\le 26.5\end{cases},$$

$$\mu_{\text{very high}}(x)=\begin{cases}\dfrac{x-24.5}{4.1} & \text{if } 24.5\le x\le 28.6\\ 1 & \text{if } x>28.6\end{cases}$$

Non membership values

$$\upsilon_{\text{low}}(x)=\begin{cases}\dfrac{x-12.5}{6.3} & \text{if } 12.5\le x\le 18.8\\ 1 & \text{if } x>18.8\end{cases},$$

$$\upsilon_{\text{medium}}(x)=\begin{cases}1 & \text{if } x<13.5\\ \dfrac{19.5-x}{6} & \text{if } 13.5\le x\le 19.5\\ 0 & \text{if } x=19.5\\ \dfrac{x-19.5}{5.12} & \text{if } 19.5\le x\le 24.6\\ 1 & \text{if } x>24.6\end{cases}$$

$$\upsilon_{\text{high}}(x)=\begin{cases}1 & \text{if } x<19\\ \dfrac{23.5-x}{4.5} & \text{if } 19<x<23.5\\ 0 & \text{if } x=23.5\\ \dfrac{x-23.5}{4.2} & \text{if } 23.5<x\le 27.6\\ 1 & \text{if } x>27.6\end{cases},$$

$$\upsilon_{\text{very high}}(x)=\begin{cases}1 & \text{if } x<26.5\\ \dfrac{30.2-x}{3.7} & \text{if } 26.5\le x\le 30.2\end{cases}$$

3.2.4. Blood Pressure

The range of blood pressure for heart disease for adult is [80 - 120]; this input has four linguistic values and their membership and non membership values are given below:

$$\mu_{\text{low}}(x)=\begin{cases}1 & \text{if } x<110\\ \dfrac{130-x}{20} & \text{if } 110\le x\le 130\end{cases},$$

$$\mu_{\text{medium}}(x)=\begin{cases}\dfrac{x-122}{13} & \text{if } 122\le x\le 135\\ 1 & \text{if } x=135\\ \dfrac{151-x}{16} & \text{if } 135\le x\le 151\end{cases}$$

$$\mu_{\text{high}}(x)=\begin{cases}\dfrac{x-138}{8} & \text{if } 138\le x\le 145\\ 1 & \text{if } x=148\\ \dfrac{176-x}{30} & \text{if } 146\le x\le 176\end{cases},$$

$$\mu_{\text{very high}}(x)=\begin{cases}\dfrac{x-144}{30} & \text{if } 144\le x\le 174\\ 1 & \text{if } x>174\end{cases}$$

Non membership values

$$\upsilon_{\text{low}}(x)=\begin{cases}\dfrac{x-122}{20} & \text{if } 112\le x\le 132\\ 1 & \text{if } x>132\end{cases},$$

$$\upsilon_{\text{medium}}(x)=\begin{cases}1 & \text{if } x<195\\ \dfrac{135-x}{15.5} & \text{if } 195\le x\le 135\\ 0 & \text{if } x=135\\ \dfrac{x-135}{21} & \text{if } 135\le x\le 156\\ 1 & \text{if } x>156\end{cases}$$

$$\upsilon_{\text{high}}(x)=\begin{cases}1 & \text{if } x<132\\ \dfrac{148-x}{16} & \text{if } 132\le x\le 148\\ 0 & \text{if } x=148\\ \dfrac{x-148}{30} & \text{if } 148\le x\le 178\\ 1 & \text{if } x>178\end{cases},$$

$$\upsilon_{\text{very high}}(x)=\begin{cases}1 & \text{if } x<164.5\\ \dfrac{182.6-x}{16.1} & \text{if } 164.5\le x\le 182.6\end{cases}$$

3.2.5. 1) Cholesterol (Density Lipoprotein Cholesterol)

The quantity of density lipoprotein cholesterol for adult for good heart is around [180 - 250 mg/deciliter]. The DLC input factor also categories into four parts

$$\mu_{\text{low}}(x)=\begin{cases}1 & \text{if } x<149\\ \dfrac{192-x}{43} & \text{if } 149\le x\le 192\end{cases},$$

$$\mu_{\text{medium}}(x)=\begin{cases}\dfrac{x-180}{30} & \text{if } 180\le x\le 210\\ 1 & \text{if } x=210\\ \dfrac{245-x}{35} & \text{if } 210\le x\le 245\end{cases}$$

$$\mu_{\text{high}}(x)=\begin{cases}\dfrac{x-222}{38} & \text{if } 222\le x\le 260\\ 1 & \text{if } x=260\\ \dfrac{302-x}{42} & \text{if } 260\le x\le 302\end{cases},$$

$$\mu_{\text{very high}}(x)=\begin{cases}\dfrac{x-275}{65} & \text{if } 275\le x\le 340\\ 1 & \text{if } x>340\end{cases}$$

Non membership values

$$\upsilon_{\text{low}}(x)=\begin{cases}\dfrac{x-170}{35} & \text{if } 170\le x\le 205\\ 1 & \text{if } x<205\end{cases},$$

$$\upsilon_{\text{medium}}(x)=\begin{cases}1 & \text{if } x<168\\ \dfrac{210-x}{42} & \text{if } 168\le x\le 210\\ 0 & \text{if } x=210\\ \dfrac{x-210}{64} & \text{if } 210<x\le 274\\ 1 & \text{if } x>274\end{cases}$$

$$\upsilon_{\text{high}}(x)=\begin{cases}1 & \text{if } x<196\\ \dfrac{260-x}{64} & \text{if } 196\le x\le 260\\ 0 & \text{if } x=260\\ \dfrac{x-260}{55} & \text{if } 260<x\le 315\\ 1 & \text{if } x>315\end{cases},$$

$$\upsilon_{\text{very high}}(x)=\begin{cases}1 & \text{if } x<268\\ \dfrac{317-x}{49} & \text{if } 268\le x\le 317\end{cases}$$

3.2.5. 2) Cholesterol (Total)

It has normal range for adult is [200 - 239 mg/deciliter]. The Total cholesterol also divided into four linguistic values with membership and non membership functions are shown below:

$$\mu_{\text{low}}(x)=\begin{cases}1 & \text{if } x<160\\ \dfrac{180-x}{20} & \text{if } 160\le x\le 180\end{cases},\quad \mu_{\text{medium}}(x)=\begin{cases}\dfrac{x-170}{25} & \text{if } 170\le x\le 195\\ 1 & \text{if } x=195\\ \dfrac{220-x}{25} & \text{if } 195\le x\le 220\end{cases}$$

$$\mu_{\text{very high}}(x)=\begin{cases}\dfrac{x-245}{20} & \text{if } 245\le x\le 265\\ 1 & \text{if } x>265\end{cases},$$

$$\mu_{\text{high}}(x)=\begin{cases}\dfrac{x-215}{21} & \text{if } 215\le x\le 236\\ 1 & \text{if } x=236\\ \dfrac{250-x}{14} & \text{if } 236\le x\le 250\end{cases}$$

Non membership values

$$\upsilon_{\text{low}}(x)=\begin{cases}\dfrac{x-172}{20} & \text{if } 172\le x\le 192\\ 1 & \text{if } x>192\end{cases},$$

$$\upsilon_{\text{medium}}(x)=\begin{cases}1 & \text{if } x<168\\ \dfrac{195-x}{27} & \text{if } 168\le x\le 195\\ 0 & \text{if } x=195\\ \dfrac{x-195}{35} & \text{if } 195\le x\le 230\\ 1 & \text{if } x>230\end{cases}$$

$$\upsilon_{\text{high}}(x)=\begin{cases}1 & \text{if } x<206\\ \dfrac{236-x}{30} & \text{if } 206\le x\le 236\\ 0 & \text{if } x=236\\ \dfrac{x-236}{25} & \text{if } 236\le x\le 261\\ 1 & \text{if } x>261\end{cases},$$

$$\upsilon_{\text{very high}}(x)=\begin{cases}1 & \text{if } x<240\\ \dfrac{260-x}{20} & \text{if } 240\le x\le 260\end{cases}$$

3.2.6. Stress

This parameter may be categorized into four categories. The four categories will be divided into low, medium, high and very high respectively with their membership and non membership values denoted as:

$$\mu_{\text{low}}(x)=\begin{cases}1 & \text{if } x<10\\ \dfrac{14-x}{4} & \text{if } 10\le x\le 14\end{cases},\quad \mu_{\text{medium}}(x)=\begin{cases}\dfrac{x-12}{2} & \text{if } 12\le x\le 14\\ \dfrac{18-x}{4} & \text{if } 14\le x\le 18\end{cases}$$

$$\mu_{\text{high}}(x)=\begin{cases}\dfrac{x-16}{2} & \text{if } 16\le x\le 18\\ \dfrac{22-x}{4} & \text{if } 18\le x\le 22\end{cases},\quad \mu_{\text{very high}}(x)=\begin{cases}\dfrac{24-x}{4} & \text{if } 20\le x\le 24\\ 1 & \text{if } x>24\end{cases}$$

Non membership values

$$\upsilon_{\text{low}}(x)=\begin{cases}\dfrac{11-x}{5} & \text{if } 11\le x\le 16\\ 1 & \text{if } x>16\end{cases},$$

$$\upsilon_{\text{medium}}(x)=\begin{cases}1 & \text{if } x<11\\ \dfrac{14-x}{3} & \text{if } 11\le x\le 14\\ \dfrac{x-14}{5} & \text{if } 14\le x\le 19\\ 1\end{cases}$$

$$\upsilon_{\text{high}}(x)=\begin{cases}1 & \text{if } x<14\\ \dfrac{18-x}{4} & \text{if } 14\le x\le 18\\ \dfrac{x-18}{6} & \text{if } 18\le x\le 24\\ 1 & \text{if } x>24\end{cases},$$

$$\upsilon_{\text{very high}}(x)=\begin{cases}1 & \text{if } x<18\\ \dfrac{22-x}{4} & \text{if } 18\le x\le 22\end{cases}$$

3.2.7. Weight

This parameter may be categorized into three categories. The three categories are under weight, normal weight and overweight with membership and non membership values shown below as:

$$\mu_{\text{under}}(x)=\begin{cases}1 & \text{if } x<40\\ \dfrac{60-x}{20} & \text{if } 40\le x\le 60\end{cases},$$

$$\mu_{\text{normal}}(x)=\begin{cases}\dfrac{x-55}{10} & \text{if } 55\le x\le 65\\ \dfrac{80-x}{15} & \text{if } 65\le x\le 80\end{cases},\quad \mu_{\text{over}}(x)=\begin{cases}\dfrac{x-75}{15} & \text{if } 75\le x\le 90\\ 1 & \text{if } x>90\end{cases}$$

Non membership

$$\upsilon_{\text{under}}(x)=\begin{cases}\dfrac{x-50}{15} & \text{if } 50\le x\le 65\\ 1 & \text{if } x>65\end{cases},$$

$$\upsilon_{\text{normal}}(x)=\begin{cases}1 & \text{if } x<40\\ \dfrac{60-x}{25} & \text{if } 40\le x\le 60\\ \dfrac{x-60}{25} & \text{if } 60\le x\le 85\end{cases},$$

$$\upsilon_{\text{over}}(x)=\begin{cases}1 & \text{if } x<70\\ \dfrac{95-x}{25} & \text{if } 70\le x\le 95\\ 0 & \text{if } x>95\end{cases}$$

3.2.8. Diet

This parameter may be categorized into two 2 linguistic values hygienic and unhygienic.

3.2.9. Family History

This parameter may be classified into two categories *i.e.* yes and No. If the patient this input also categories into two linguistic values yes (if patient have heart disease or stroke in his/her family) and no (if patient have no family history for heart disease).

3.2.10. Smoking

This parameter will be classified into two linguistic variable value smoker and non smoker.

3.3. Fuzzy Rule Base

From the inference developed by us for sugeno's-TSK fuzzy controller by using the factors which we have used in our research paper, the total eight hundred eighty five rules will be formed. From the following eight hundred eighty five rules, we have taken fifty rules. The criterion for choosing fuzzy rules for our work is that the critical changes in the heart disease have been taken and the others not affecting more have been omitted.

R_1: IF Iodine is low and folic acid is medium THEN result is stage 2

R_2: IF iodine is medium and obesity is low THEN result is stage 2

R_3: IF iodine is medium and obesity is medium THEN result is stage 1

R_4: IF iodine is high and B.P is medium THEN result is stage 3

R_5: IF iodine is medium and cholesterol (total) is very high THEN result is stage 4

R_6: IF folic acid is low and obesity is high THEN result is stage 3

R_7: IF folic acid is medium and obesity is low THEN result is stage 2

R_8: IF folic acid is medium and B.P is medium THEN result is stage 1

R_9: IF folic acid is high and obesity is high THEN result is stage 3

R_{10}: IF folic acid is very high and obesity is low THEN result is stage 4

R_{11}: IF obesity is low and B.P is low THEN result is stage 2

R_{12}: IF obesity is medium and cholesterol (total) is medium THEN result is stage 1

R_{13}: IF obesity is high and diet is unhygienic THEN result is stage 3

R_{14}: IF obesity is very high and family history is yes/1 THEN result is stage 4

R_{15}: IF obesity is very high and cholesterol (dlc) is very high THEN result is stage 4

R_{16}: IF B.P is low and weight is under THEN result is stage 2

R_{17}: IF B.P is medium and diet is hygienic THEN result is stage 1

R_{18}: IF B.P is high and cholesterol (total) is high THEN result is stage 3

R_{19}: IF B.P is very high and folic acid is very high THEN result is stage 4

R_{20}: IF B.P is very high and iodine is high THEN result is stage 4

R_{21}: IF cholesterol (dlc) is low and stress is low THEN result is stage 2

R_{22}: IF cholesterol (dlc) is medium and iodine is medium THEN result is stage 1

R_{23}: IF cholesterol (dlc) is high and diet is unhygienic THEN result is stage 3

R_{24}: IF cholesterol (dlc) is high and weight is over THEN result is stage 3

R_{25}: IF cholesterol (dlc) is very high and family history is yes/1 THEN result is stage 4

R_{26}: IF cholesterol (total) is low and iodine is medium THEN result is stage 2

R_{27}: IF cholesterol (total) is medium and folic acid is medium THEN result is stage 1

R_{28}: IF cholesterol (total) is high and stress is high THEN result is stage 3

R_{29}: IF cholesterol (total) is very high and B.P is high THEN result is stage 4

R_{30}: IF cholesterol (total) is very high and diet is unhygienic THEN result is stage 4

R_{31}: IF stress is low and iodine is low THEN result is stage 2

R_{32}: IF stress is medium and folic acid is medium THEN result is stage 1

R_{33}: IF stress is high and iodine is low THEN result is stage 3

R_{34}: IF stress is high and weight is over THEN result is stage 3

R_{35}: IF stress is very high and diet is unhygienic THEN result is stage 4

R_{36}: IF diet is hygienic and B.P is medium THEN result is stage 1

R_{37}: IF diet is hygienic and weight is under THEN result is stage 2

R_{38}: IF diet is unhygienic and folic acid is high THEN result is stage 3

R_{39}: IF diet is unhygienic and cholesterol (dlc) is high THEN result is stage 3

R_{40}: IF diet is unhygienic and cholesterol (dlc) is very high THEN result is stage 4

R_{41}: IF weight is under and iodine is low THEN result is stage 2

R_{42}: IF weight is under and cholesterol (total) is normal THEN result is stage 2

R_{43}: IF weight is normal and B.P is medium THEN result is stage 1

R_{44}: IF weight is over and stress is high THEN result is stage 3

R_{45}: IF weight is over and folic acid is very high THEN result is stage 4

R_{46}: IF family history is yes/1 and cholesterol (dlc) is low THEN result is stage 2

R_{47}: IF family history is yes/1 and weight is under THEN result is stage 2

R_{48}: IF family history is yes/1 and folic acid is high THEN result is stage 3

R_{49}: IF family history is yes/1 and B.P is very high THEN result is stage 4

R_{50}: IF family history is yes/1 and obesity is very high THEN result is stage 4

3.4. Fuzzy Inference System

The fuzzy inference system [10] is a popular computing framework based on the concept of fuzzy logic, fuzzy rule base system and fuzzy reasoning. The basic structure of the inference system consists of three conceptual components; a database which defines the membership functions used in fuzzy rules, a rule base and a reasoning procedure. In the research paper we have constructed an Suge-

no's-TSK inference system based on the meditative fuzzy logic.

4. Fuzzy Output Variables

The last step of our proposed algorithm is to get the output in the fuzzy form. First we will obtain the aggregation of the factors and after getting aggregation of we will obtain the fuzzy form of our output. Then the output values obtained from the inference of the input in the form of fuzzy propositions can be classified into four categories. The four categories may be in the combination of qualified, unqualified, conditional and unconditional fuzzy propositions. In the four categories inference from input variables will be divided into four stages. The classification of the stages will be based on the stages to obtain the stages of risk to the patient which are namely classified as stage 1, stage 2, stage 3 and stage 4 and these will take values on the scaling from 1 to 5. Stage 1 patient considered as low risk for heart disease, Stage 2 denotes medium risk, stage 3 denote high risk and stage 4 denotes very high risk for heart disease to the patient. The functions for the output values are shown by using intuitionistic fuzzy numbers.

For membership values

$$\mu_{\text{stage1}}(x)=\begin{cases}1 & \text{if } x<1.35\\ \dfrac{2-x}{0.65} & \text{if } 1.35\le x\le 2\end{cases},\quad \mu_{\text{stage2}}(x)=\begin{cases}\dfrac{1.8-x}{0.8} & \text{if } 1.8\le x\le 2.6\\ 1 & \text{if } x=2.6\\ \dfrac{3.4-x}{0.8} & \text{if } 2.6\le x\le 3.4\end{cases}$$

$$\mu_{\text{stage3}}(x)=\begin{cases}\dfrac{3.2-x}{0.7} & \text{if } 3.2\le x\le 3.9\\ 1 & \text{if } x=3.9\\ \dfrac{4.6-x}{0.7} & \text{if } 3.9\le x\le 4.6\end{cases},\quad \mu_{\text{stage4}}(x)=\begin{cases}\dfrac{x-4.3}{0.4} & \text{if } 4.3\le x\le 4.7\\ 1 & \text{if } x>4.7\end{cases}$$

Non membership functions

$$\upsilon_{\text{stage1}}(x)=\begin{cases}\dfrac{x-1.6}{0.8} & \text{if } 1.6\le x\le 2.8\\ 1 & \text{if } x>2.8\end{cases},\quad \upsilon_{\text{stage2}}(x)=\begin{cases}1 & \text{if } x<1.6\\ \dfrac{x-1.6}{1} & \text{if } 1.6\le x\le 2.6\\ 0 & \text{if } x=2.6\\ \dfrac{x-2.6}{0.8} & \text{if } 2.6\le x\le 3.4\\ 1 & \text{if } x>3.4\end{cases}$$

$$\upsilon_{\text{stage3}}(x)=\begin{cases}1 & \text{if } x<2.9\\ \dfrac{3.9-x}{1.5} & \text{if } 2.9\le x\le 3.9\\ 0 & \text{if } x=3.9\\ \dfrac{x-3.9}{1} & \text{if } 3.9\le x\le 4.9\\ 1 & \text{if } x>4.9\end{cases},\quad \upsilon_{\text{stage4}}(x)=\begin{cases}1 & \text{if } x<4.1\\ \dfrac{4.8-x}{0.7} & \text{if } 4.1\le x\le 4.8\end{cases}$$

5. Numerical Results and Interpretations

Table 2. Results and interpretations.

Rules	Firing level	Output	Rules	Firing level	Output
R_1	1	2.6	R_{26}	0.443831	2.589
R_2	0.25	2.55	R_{27}	0.41	1.038
R_3	0.195	3.064	R_{28}	0.3284	3.89416
R_4	0.194	3.7073	R_{29}	0.4274	3.08616
R_5	0.2324	4.59	R_{30}	0.16	3.2324
R_6	1	3.9	R_{31}	1	2.6
R_7	0.3204	1.44524	R_{32}	0.4744	1.8
R_8	0.4159	1.8599575	R_{33}	0.25	3.9
R_9	0.2869	3.5255	R_{34}	0.3031	3.9
R_{10}	0.027884	0.7822	R_{35}	0.0625	2.7125
R_{11}	1	2.6	R_{36}	0.1659	2.838
R_{12}	0.41	1.689	R_{37}	0.2244	2.6
R_{13}	0.028	3.316	R_{38}	0.1256	3.9
R_{14}	0.1369	3.03938	R_{39}	0.0625	3.9
R_{15}	0.1476	4.235	R_{40}	0.005776	2.251
R_{16}	1	2.6	R_{41}	1	2.6
R_{17}	0.1659	2.118	R_{42}	0.16	2.6
R_{18}	0.2351	3.9	R_{43}	0.25	2.6
R_{19}	0.215389	2.54	R_{44}	0.3301	3.9
R_{20}	0.2782	2.97	R_{45}	0.128089	3.97
R_{21}	0.28	1.020625	R_{46}	0.0784	2.528
R_{22}	0.3094	0.615	R_{47}	1	2.6
R_{23}	0.676	3.9	R_{48}	0.1156	3.9
R_{24}	0.5284	3.9	R_{49}	0.2913	3.29568
R_{25}	0.5776	4.14152	R_{50}	0.1369	3.73162

6. Conclusion

Fuzzy logic provides a platform to handle the uncertainty associated with human cognizance. The cognizance may be due to reasoning or thinking of the human being. But when the information may be incomplete, vague, fragmentarily reliable that is not fully reliable, there exists contradictory remark about the information then we are not in the position to deal it with fuzzy logic. In the present research paper we will use the inference rule for fuzzy logic for conditional fuzzy proposition in the extended form of intuitionistic fuzzy logic for the input factors which have been shown in Table 1 (effects the heart diseases). That is for conditional and unqualified proposition the inference rule R is: if X_1 is A_1

and X_2 is A_2 then Y is B. In this present paper we have evaluated the firing level and output which have been shown in Table 2 with a rule which included two inputs, so for the meditative fuzzy logic. In the present research paper we have also shown the superiority of meditative fuzzy logic on the previous traditional and intuitional logics. In the present paper we have extended and improved the system by using Sugeno's-TSK model with the help of meditative fuzzy logic. On the basis of output we can categorize the risk stages. The output of the reasoning system corresponds to the category of sickness.

Acknowledgements

The first author is grateful to University Grant Commission for the financial assistance.

Conflicts of Interest

The authors declare no conflicts of interest regarding the publication of this paper.

References

[1] Zadeh, L.A. (1975) The Concept of a Linguistic Variable and Its Application to Approximate Reasoning. *Information Sciences*, **8**, 199-249. https://doi.org/10.1016/0020-0255(75)90036-5

[2] Zadeh, L.A. (1979) A Theory of Approximate Reasoning. In: *Machine Intelligence*, John Wiley & Sons, New York, 149-194.

[3] Zadeh, L.A. (1965) Fuzzy Sets. *Inform Control*, **8**, 338-356. https://doi.org/10.1016/S0019-9958(65)90241-X

[4] Zadeh, L.A. (1978) Fuzzy Sets as a Basis for a Theory of a Possibility. *Fuzzy Sets and Systems*, **1**, 2-28. https://doi.org/10.1016/0165-0114(78)90029-5

[5] Atanassov, K. (1986) Intuitionistic Fuzzy Sets. *Fuzzy Sets and Systems*, **20**, 87-96. https://doi.org/10.1016/S0165-0114(86)80034-3

[6] Atanassov, K. (1989) More or Intuitionistic Fuzzy Sets. *Fuzzy Sets and Systems*, **33**, 37-46. https://doi.org/10.1016/0165-0114(89)90215-7

[7] Hajek, P. and Olej, V. (2014) Defuzzification Methods in Intuitionistic Fuzzy Inference Systems of Takagi-Sugeno Type. 11*th International Conference on Fuzzy Systems and Knowledge Discovery*, Xiamen, 19-21 August 2014, 532. https://doi.org/10.1109/FSKD.2014.6980838

[8] Mendel, J. (2007) Type-2 Fuzzy Sets and Systems. An Overview. *IEEE Computational Intelligence Magazine*, **2**, 20-29. https://doi.org/10.1109/MCI.2007.380672

[9] Akram, M., Shahzad, S., Butt, A. and Khaliq, A. (2013) Intuitionistic Fuzzy Logic Control for Heater Fans. *Mathematics in Computer Science*, **7**, 367-378. https://doi.org/10.1007/s11786-013-0161-x

[10] Castillo, O. and Melin, P. (2003) A New Method for Fuzzy Inference in Intuitionstic Fuzzy Systems. In: *Proceedings of the International Conference NAFIPS*, IEEE Press, Chicago, 20-25.

[11] Castillo, O., Alanis, A., Garcia, M. and Arias, H. (2007) An Intuitionistic Fuzzy System for Time Series Analysis in Plant Monitoring and Diagnosis. *Applied Soft*

Computing, **7**, 1227-1233. https://doi.org/10.1016/j.asoc.2006.01.010

[12] Melin, P., *et al.* (2007) Mediative Fuzzy Logic: A New Approach for Contradictory Knowledge Management. *Soft Computing*, **12**, 251-256.

[13] Montiel, O., Castillo, O., Melin, P. and Sepulveda, R. (2008) Mediative Fuzzy Logic: A New Approach for Contradictory Knowledge Management. *Soft Computing*, **12**, 251-256. https://doi.org/10.1007/s00500-007-0206-7

[14] Jang, J.-S.R., Sun, C.T. and Mizutani, E. (1997) Neuro-Fuzzy and Soft Computing. Pearson Education, Singapore, 19.

[15] Sanchez, E. (1979) Medical Diagnosis and Composite Fuzzy Relation. In: Gupta, M.M., Ragade, R.K. and Yeager, R.R., Eds., *Advances in Fuzzy Sets and Applications*, North-Holland, New York, 437-447.

[16] Kumar, D.S., Biswas, R. and Roy, A. (2001) An Application of Intutiosnistic Fuzzy Sets in Medical Diagnosis. *Fuzzy Sets and Systems*, **117**, 209-213. https://doi.org/10.1016/S0165-0114(98)00235-8

[17] Montiel, O., Castillo, O., Melin, P. and Sepulveda, M. (2009) Mediative Fuzzy Logic for Controlling Population Size in Evolutionary Algorithms. *Intelligent Information Management*, **1**, 108-119. https://doi.org/10.4236/iim.2009.12016

[18] Iancu, I. (2018) Heart Diseases Diagnosis Based on Mediative Fuzzy Logic. *Artificial Intelligence in Medicine*, **89**, 51-60. https://doi.org/10.1016/j.artmed.2018.05.004

[19] Czogala, E. and Leski, J. (2001) On Equivalence of Approximate Reasoning Results Using Different Interpolations of Fuzzy If-Then Rules. *Fuzzy Sets and Systems*, **11**, 279-296. https://doi.org/10.1016/S0165-0114(98)00412-6

Applied Mathematics, 2019, 10, 468-484
http://www.scirp.org/journal/am
ISSN Online: 2152-7393
ISSN Print: 2152-7385

Diffraction of Surface Harmonic Viscoelastic Waves on a Multilayer Cylinder with a Liquid

Safarov Ismoil Ibrohimovich[1], Kulmuratov Nurillo Rakhimovich[2], Teshayev Muhsin Khudoyberdiyevich[3*], Kuldashov Nasriddin Urinovich[1]

[1]Tashkent Institute of Chemistry and Technology, Tashkent, Republic of Uzbekistan
[2]Navoi State Mining and Metallurgical Institute, Navoi, Republic of Uzbekistan
[3]Bukhara Engineering-Technological Institute, Bukhara, Republic of Uzbekistan

Email: *muhsin_5@mail.ru

How to cite this paper: Ibrohimovich, S., Rakhimovich, K.N., Khudoyberdiyevich, T.M. and Urinovich, K.N. (2019) Diffraction of Surface Harmonic Viscoelastic Waves on a Multilayer Cylinder with a Liquid. *Applied Mathematics*, **10**, 468-484.
https://doi.org/10.4236/am.2019.106033

Received: April 1, 2019
Accepted: June 21, 2019
Published: June 24, 2019

Abstract

An infinitely long circular cylinder, consisting generally of a finite number of coaxial viscoelastic layers, surrounded by a deformable medium is considered. The dynamic stress—the deformed state of a piecewise-homogeneous cylindrical layer from a harmonic wave is investigated. The numerical results of stress, depending on the wavelength are obtained.

Keywords

Viscoelasticity, Fluid, Frequency, Longitudinal and Transverse Wave, Shell, Plane Strain

1. Introduction

During seismic impacts, modern underground pipelines operate under conditions of not only static but also dynamic loads, which are accompanied by large damage and even failure of the whole system [1]-[6]. In the case of a sufficiently long cavity, the impact perpendicular to its longitudinal axis, the environment surrounding the cavity and the lining are in conditions of plane deformation, and the task of determining the stress state of the array and lining reduces to a flat problem of the dynamic theory of elasticity (and whether visco-elasticity) [7] [8] [9] [10]. In [11], the problem of stress concentration in an infinite linearly elastic cavity near a circular cavity with the propagation of longitudinal harmonic waves was solved. The solution of the diffraction problem for a harmonic transverse wave was obtained in [12]. This paper investigates the interaction of cylindrical stress waves with a cylinder, which in the general case consists of a fi-

nite number of coaxial viscoelastic layers. Due to the fact that long-term seismic waves, as a rule, exceed the characteristic dimensions of the cross section designs (for example, diameter D), therefore, when solving diffraction problems, it is necessary to consider long-wave effects ($\frac{D}{\lambda}<1$, λ is the wavelength). With longer wavelengths ($\frac{D}{\lambda}=0.04\div 0.16$) maximum coefficients of dynamic concentrations turned out to be 5% - 10% more than with the corresponding bi-axial static loaded ($\lambda\to\infty$) [13]. At $\frac{D}{\lambda}>0.16$ dynamic stress concentrations are significantly lower than static. In [14], it was shown that the difference in dynamic stress concentrations in the case of a rigid inclusion and cavity can be attributed to the possibility of propagation of generalized Rayleigh-type waves on a concave free cylindrical surface of the cavity. A significant contribution to the calculation of flexible pipelines was made in [15] [16], which investigated such important issues as accounting without a backing zone and determining the stability of underground pipelines. There are a large number of authors who have applications in other branches of technology who can be successfully applied to the calculation of underground pipelines. These works are devoted to the study of the stress distribution in plastic, weakened by a reinforced bore, operating under plane strain conditions. The most significant research in this area can be attributed to the work that solved the problem in stretching a plate in which a ring is embedded or soldered.

2. Problem Statement and Basic Relations

In this paper, the interaction of a cylindrical stress wave by parallel-layered elastic layers with a liquid is investigated. It is assumed that the linear source in **Figure 1** is a continuous source of dilatation (or transverse) stress waves with an angular velocity ω and amplitude φ_0 (or ψ_0), and the layered package is a thick-walled and thin-walled layers of the cylinder. In describing the movement of thin-walled elements, the equations of the theory of such shells are used, which are based on the Kirchhoff-Love hypotheses. For thin-walled layers, the original equations are the linear theory of elasticity. The numbering of the layers is the product in ascending order of their radii from $k=1$ to $k=N$ (**Figure 1**). The value characterizing the properties and the state of the elements correspond to the values $j=1,2,\cdots,N$, where K is the elastic layer enclosed between K-1 and K-m layers. The environmental parameters are denoted by the indices $K=N$ (**Figure 1**). Under the assumption of a generalized plane-deformed state, the equation of motion in displacements has the form [1]

$$\left(\tilde{\lambda}_j+2\tilde{\mu}_j\right)grad\left(div\left(\boldsymbol{u}_j\right)\right)-\tilde{\mu}rot\left(rot\left(\boldsymbol{u}_j\right)\right)+\boldsymbol{b}_j=\rho_j\frac{\partial^2\boldsymbol{u}_j}{\partial t^2}. \quad (1)$$

where λ_j and μ_j ($j=1,2,\cdots,N$, $j=N$ —relate to the environment, $j=1,2,\cdots,N-1$—to layer) operator moduli of elasticity [13]

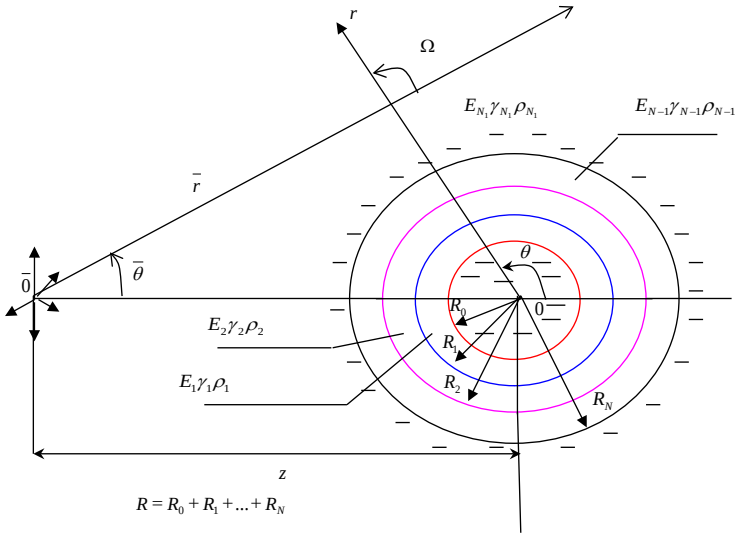

Figure 1. The design scheme of layered cylindrical bodies in a deformable medium.

$$\tilde{\lambda}_j f(t) = \lambda_{0j}\left[f(t) - \int_{-\infty}^{t} R_{\lambda}^{(i)}(t-\tau) f(\tau)\mathrm{d}\tau \right]$$

$$\tilde{\mu}_j f(t) = \mu_{0j}\left[f(t) - \int_{-\infty}^{t} R_{\mu}^{(i)}(t-\tau) f(\tau)\mathrm{d}\tau \right];$$

$\boldsymbol{b}_j$ —Volume force density vector ($b_j = 0$); $f(t)$ —some function; ρ_j —density of materials, $R_{\mu}^{(i)}(t-\tau)$ and $R_{\lambda}^{(i)}(t-\tau)$ —relaxation core, λ_{oj}, μ_{oj} —instantaneous elastic moduli of viscoelastic material, $\boldsymbol{u}_j(u_{rj}, u_{\theta j})$ —displacement vector which depends on r, θ, t. At pressures up to 100 MPa, the movement of the fluid in is satisfactorily described by the wave velocity of the particle particles [14]

$$\Delta\varphi_0 = \frac{1}{C_o^2}\frac{\partial^2\varphi_0}{\partial t^2}. \tag{2}$$

where $\Delta = \frac{\mathrm{d}^2}{\mathrm{d}r^2} + \frac{\mathrm{d}}{r\mathrm{d}r} + \frac{\mathrm{d}^2}{r^2\mathrm{d}\theta^2}$; C_o—acoustic velocity of sound in a fluid. Potential φ_0 and the fluid velocity vector are dependent $\boldsymbol{V} = grad\varphi_0$. Fluid pressure $r = R_0$ is determined using the linearized Cauchy-Lagrange integral $P = -\rho_o C_0 \frac{\partial\varphi_0}{\partial t}$ —fluid pressure on the wall of the cylindrical layer and ρ_o-fluid density Under the condition of continuous flow of fluid, the normal component of the velocity of the fluid and the layer on the surface of their contact $r = R_0$ must be equal

$$\left.\frac{\partial\varphi_0}{\partial r}\right|_{r=R_0} = \left.\frac{\partial u_{r1}}{\partial t}\right|_{r=R_0}. \tag{3}$$

where u_{r1} —moving the layer along the normal. On the contact of two bodies $r = R_j$ equal displacements and stresses (fixed contact condition)

$$u_{rj} = u_{r(j+1)};\ \sigma_{rrj} = \sigma_{rr(j+1)};\ u_{\theta j} = u_{\theta(j+1)};\ \sigma_{r\theta j} = \sigma_{r\theta(j+1)} \tag{4}$$

Note that in the case of sliding ground contact over the pipe surface, the last Equation in (4) takes the form [16]:

$$\sigma_{r\theta j} = 0 .$$

where $\sigma_{nn}^{(j)}$ and $\sigma_{ns_1}^{(j)}$—radial and tangential stresses in the *j*-th viscoelastic body; $u_n^{(j)}$ and $u_{s_1}^{(j)}$—radial and tangential displacement of the *j*-th body. The solution of the wave Equation (1) in the displacement potentials satisfies at infinity $r \to \infty$ the Summerfield radiation condition [14]:

$$\lim_{r\to\infty} \varphi_N = 0, \lim_{r\to\infty} \left(\sqrt{r}\right)^{\kappa} \left(\frac{\partial \varphi_N}{\partial r} + i\alpha_N \varphi_N \right) = 0 , \tag{5}$$

$$\lim_{r\to\infty} \psi_N = 0, \lim_{r\to\infty} \left(\sqrt{r}\right)^{\kappa} \left(\frac{\partial \psi_N}{\partial r} + i\beta_N \psi_N \right) = 0 .$$

As $r \to \infty$, natural oscillations by the first and third conditions (5) are not fulfilled, therefore, the shortened Sommerfeld conditions at infinity are set, which in detail in [14] was considered.

If in place the equation of motion (1) is used cylindrical shells, then the equation of motion of shells in a flat formulation is:

$$\begin{aligned} &\frac{\partial^2 u}{\partial \theta^2} + \frac{\partial W}{\partial \theta} = -\frac{R^2}{B} X_1 \\ &\frac{\partial u}{\partial \theta} + b^2 \left(\frac{\partial^4 W}{\partial \theta^4} + 2\frac{\partial^2 V}{\partial \theta^2} + W \right) + W = \frac{R^2}{B} X_2 \end{aligned} \tag{6}$$

where u and W- longitudinal and transverse displacements respectively:

$$X_1 = -\sigma_{r\theta}\big|_{r=R_0+h_c/2} - \rho_c h_c \frac{\partial^2 u}{\partial t^2}; \quad X_2 = -\sigma_{rr}\big|_{r=R_0+h_c/2} - \rho_c h_c \frac{\partial^2 W}{\partial t^2};$$

$$b^2 = \frac{h_c^2}{12R_0^2}, \quad B = \frac{E_c h_c}{1-\nu_c^2}.$$

$$b^2 = \frac{h_c^2}{12R_0^2}, \quad B = \frac{E_c h_c}{1-\nu_c^2}.$$

Shell radius R_0, ρ_c—shell density, ν_c—shells Puasson ratio, h_c—shell thickness, E_c—shell elastic modulus, σ_{rr} and $\sigma_{r\theta}$—normal and tangent components of the reaction from the environment.

The contact between the shell and the environment can be hard or sliding:

$$u\big|_{r=R_0+h_c/2} = u_\theta\big|_{r=R_0+h_c/2}, \; W\big|_{r=R_0+h_c/2} = u_r\big|_{r=R_0+h_c/2} \tag{7}$$

Consider a longitudinal wave generated by a longitudinal source of expansion waves located at $\overline{O}$ (**Figure 1**). The displacement potentials of the incident expansion wave can be represented as [15]

$$\varphi_N^P = \varphi_{NO} i\pi H_0^{(1)}\left(\alpha_N \overline{r}\right) \mathrm{e}^{-i\omega t} . \tag{8}$$

where $H_0^{(1)}$—is the divergent functions of Henkel (the first kind of zero order); φ_{NO}—expansion wave amplitude; α_N—compression wave number; $\alpha_N^2 = \omega^2 / c_\alpha^2$, $c_\alpha^2 = \left(\lambda_N + 2\mu_N\right)/\rho_N$, ω—circular frequency. In the absence of an

incident wave (6), the natural oscillations of a reinforced bore located in a viscoelastic medium are considered.

3. Solution Methods

The problem is solved in displacement potentials, for this we present the displacement vector in the form:

$$\boldsymbol{u}_j = grad\left(\varphi_j\right) + rot\left(\boldsymbol{\psi}_j\right), \quad \left(j = 1, 2, \cdots, N\right)$$

where φ_j —longitudinal wave potential; $\boldsymbol{\psi}_j\left(\psi_{rj}, \psi_{\theta j}\right)$ —vector potential of transverse waves.

The basic equations of the theory of visco elasticity (1) for this problem of plane strain are reduced to the following equation

$$\begin{aligned}
&\left(\lambda_{oj} + 2\mu_{oj}\right)\nabla^2\varphi_j - \lambda_{oj}\int_{-\infty}^{t} R_{\lambda}^{(j)}\left(t-\tau\right)\nabla^2\varphi_j \mathrm{d}\tau \\
&-2\mu_{oj}\int_{-\infty}^{t} R_{\mu}^{(j)}\left(t-\tau\right)\nabla^2\varphi_j \mathrm{d}\tau = \rho_j \frac{\partial^2\varphi_j}{\partial t^2} \\
&\mu_{oj}\nabla^2\boldsymbol{\psi}_j - \mu_{oj}\int_{-\infty}^{t} R_{\mu}^{(j)}\left(t-\tau\right)\nabla^2\boldsymbol{\psi}_j \mathrm{d}\tau = \rho_j \frac{\partial^2\boldsymbol{\psi}_j}{\partial t^2}
\end{aligned} \tag{9}$$

where $\nabla^2 = \frac{\partial^2}{\partial r^2} + \frac{1}{r}\frac{\partial}{\partial r} + \frac{1}{r^2} + \frac{\partial^2}{\partial\theta^2}$ —differential operators in cylindrical coordinates and ν_j — Poisson's ratio.

At infinity, $r \to \infty$ potentials of longitudinal and transverse waves with $j = N$ satisfy the Summerfield radiation condition (5).

The solution of Equation (9) can be sought in the form:

$$\varphi_j\left(r,\theta,t\right) = \sum_{k=1}^{\infty} q_{kj}^{(\varphi)}\left(r,\theta\right)\mathrm{e}^{-i\omega t}; \quad \psi_j\left(r,\theta,t\right) = \sum_{k=1}^{\infty} q_{kj}^{(\psi)}\left(r,\theta\right)\mathrm{e}^{-i\omega t}. \tag{10}$$

where $q_{kj}^{(\varphi)}\left(r,\theta\right)$ and $q_{kj}^{(\psi)}\left(r,\theta\right)$ —complex function which is solving the following Equations (10)

$$\begin{aligned}
&\nabla^2 q_{kj}^{(\varphi)}\left(r,\theta\right) + \alpha_j^2 q_{kj}^{(\varphi)} = 0, \quad \nabla^2 q_{kj}^{(\psi)}\left(r,\theta\right) + \beta_j^2 q_{kj}^{(\psi)} = 0, \\
&\nabla^2 q_{k0}^{(\varphi)}\left(r,\theta\right) + \alpha_0^2 q_{k0}^{(\varphi)} = 0,\ j = 1, 2, \cdots, N
\end{aligned} \tag{11}$$

where $\alpha_j^2 = \frac{\rho\omega^2}{\lambda_{oj}\left(1-\overline{\lambda}_{oj}\right) + 2\mu_{oj}\left(1-\overline{\mu}_{oj}\right)}$, $\beta_j^2 = \frac{\rho\omega^2}{\mu_{oj}\left(1-\overline{\mu}_{oj}\right)}$, $\alpha_0^2 = \frac{\omega^2}{C_0^2}$

$$\overline{\lambda}_{oj} = a_{\lambda j}\left(\omega\right) + ib_{\lambda j}\left(\omega\right), \quad \overline{\mu}_{oj} = a_{\lambda\mu}\left(\omega\right) + ib_{\mu j}\left(\omega\right),$$

$$a_{\lambda j}\left(\omega\right) = \int_0^{\infty} R_{\lambda j}\left(\tau\right)\sin\left(\omega\tau\right)\mathrm{d}\tau, \quad b_{\lambda j}\left(\omega\right) = \int_0^{\infty} R_{\mu j}\left(\tau\right)\cos\left(\omega\tau\right)\mathrm{d}\tau.$$

The solution of Equation (9) with regard to (11) is expressed in terms of Henkel functions of the 1st and 2-nd kind of the nth order:

$$\phi_j = \sum_{n=0}^{\infty}\left[A_{nj}H_n^{(1)}\left(\alpha_j r\right) + A_{nj}'H_n^{(2)}\left(\alpha_j r\right)\right]\cos\left(n\theta\right)\mathrm{e}^{-i\omega t}$$

$$\psi_j = \sum_{n=0}^{\infty}\left[B_{nj}H_n^{(1)}(\beta_j r)+B'_{nj}H_n^{(2)}(\beta_j r)\right]\sin(n\theta)\mathrm{e}^{-i\omega t};\ j=1,2,\cdots,N-1$$

$$\phi_N = \sum_{n=0}^{\infty}\left[C_{nN}H_n^{(1)}(\alpha_N r)+D_{nN}H_n^{(2)}(\alpha_N r)\right]\cos(n\theta)\mathrm{e}^{-i\omega t} \quad (12)$$

$$\psi_N = \sum_{n=0}^{\infty}\left[M_{nN}H_n^{(1)}(\beta_N r)+L_{nN}H_n^{(2)}(\beta_N r)\right]\sin(n\theta)\mathrm{e}^{-i\omega t}$$

$$\phi_0 = \sum_{n=0}^{\infty}\left[K_{n0}J_n(\alpha_0 r)+K'_{n0}N_n(\alpha_0 r)\right]\cos(n\theta)\mathrm{e}^{-i\omega t}$$

where $A_{nj}, A'_{nj}, B_{nj}, B'_{nj}, C_{nj}, D_{nj}, L_{nN}, M_{nN}, K_{nN}$ and K'_{nN} —decomposition coefficients, which are determined by the corresponding boundary conditions; $H_n^{(1)}(\alpha_j r)$ and $H_n^{(2)}(\alpha_j r)$—respectively, the Henkel function of the 1st and 2nd kind of the nth order $H_n^{(1),(2)}(\alpha r) = J_n(\alpha r) \pm iN_n(\alpha r)$.

Solution (12) with $j = N$ satisfies at infinity $r \to \infty$ the Somerfield radiation condition (5) and is represented as:

$$\phi_N = \sum_{m=0}^{\infty} C_{nN}H_n^{(1)}(\alpha_N r)\cos(m\theta)\mathrm{e}^{-i\omega t};$$

$$\psi_N = \sum_{m=0}^{\infty} M_{nN}H_n^{(1)}(\beta_N r)\sin(n\theta)\mathrm{e}^{-i\omega t}.$$

Solving problem (2) with $r \to 0$ satisfies the condition of limiting the force factors [10] and it follows that $K'_n = 0$

$$\phi_0 = \sum_{n=0}^{\infty} K_{n0}J_n(\alpha_0 r)\cos(n\theta)\mathrm{e}^{-i\omega t}$$

The full potential can be determined by imposing the potentials of the incident and reflected waves. Thus, the displacement potentials will be

$$\phi_N = \varphi_N^{(p)} + \varphi_N,\ \Psi_N = \psi_N,\ \phi_j = \varphi_j,\ \Psi_j = \psi_j,\ \phi_0 = \varphi_0 \quad (13)$$

To determine the stress-strain state, it is first necessary to express the incident wave through wave functions (13). Using the geometric construction in **Figure 1** and moving from the coordinates $\bar{r}, \bar{\theta}$ to coordinates r, θ in the area of $r \le r_N$

$$\phi_N^{(p)} = \phi_0 i\pi\sum_{n=1}^{\infty}\left[(-1)^n E_n J_n(\alpha_N r)H_n^{(1)}(\alpha_N z)\right]\cos(n\theta)\mathrm{e}^{-i\omega t}.$$

where $E_n = \begin{cases}1, & n=0\\ 2, & n\ge 1\end{cases}$, J_n—cylindrical Bessel function of the first kind.

It follows that voltages and offsets can easily be expressed in terms of displacement potentials [15]

$$u_{rj} = \frac{\partial\varphi_j}{\partial r} + \frac{1}{r}\frac{\partial\psi_j}{\partial\theta};\ u_{\theta j} = \frac{1}{r}\frac{\partial\varphi_j}{\partial\theta} - \frac{\partial\psi_j}{\partial r}, \quad (14)$$

$$\sigma_{rrj} = \bar{\lambda}\nabla^2\phi_j + 2\bar{\mu}_j\left[\frac{\partial^2\phi_j}{\partial r^2} + \frac{\partial}{\partial r}\left(\frac{1}{r}\frac{\partial\psi_j}{\partial\theta}\right)\right];$$

$$\sigma_{\theta\theta j}=\overline{\lambda}\nabla^2\phi_j+2\overline{\mu}_j\left[\frac{1}{r}\left(\frac{\partial\phi_j}{\partial r}+\frac{1}{r}\frac{\partial^2\phi_j}{\partial\theta^2}\right)+\frac{1}{r}\left(\frac{1}{r}\frac{\partial\psi_j}{\partial\theta}-\frac{\partial^2\psi_j}{\partial r\partial\theta}\right)\right];$$

$$\sigma_{r\theta j}=\overline{\mu}\left\{2\left[\frac{1}{r}\frac{\partial^2\phi_j}{\partial\theta\partial r}-\frac{1}{r^2}\frac{\partial\phi_j}{\partial\theta}\right]+\left[\frac{1}{r^2}\frac{\partial^2\psi_j}{\partial\theta^2}-r\frac{\partial}{\partial r}\left(\frac{1}{r}\frac{\partial\psi_j}{\partial r}\right)\right]\right\}$$

Displacement and stresses for the case of a compression wave falling on a layer ψ it turns out.

Substituting (13) into (14) after considering (11), we obtain the following expression for displacement and stress:

$$u_{rN}=r^{-1}\sum_{n=0}^{\infty}\left[\phi_0E_ni^nE_{51}^{(1N)}\left(\alpha_Nr\right)+C_{nN}E_{51}^{(3N)}\left(\alpha_Nr\right)+M_{nN}E_{52}^{(3N)}\left(\beta_Nr\right)\right]\cos\left(n\theta\right)\mathrm{e}^{i\omega t}$$

$$u_{\theta N}=r^{-1}\sum_{n=0}^{\infty}\left[\phi_0E_ni^nE_{61}^{(1N)}\left(\alpha_Nr\right)+C_{nN}E_{61}^{(3N)}\left(\alpha_Nr\right)+M_{nN}E_{62}^{(3N)}\left(\beta_Nr\right)\right]\cos\left(n\theta\right)\mathrm{e}^{-i\omega t}$$

$$u_{rj}=r^{-1}\sum_{n=0}^{\infty}\left[A_{nj}E_{51}^{(3j)}\left(\alpha_jr\right)+A_{nj}^{1}E_{61}^{(4j)}\left(\alpha_jr\right)+B_{nj}E_{52}^{(3j)}\left(\beta_jr\right)+B_n^1E_{52}^{(4j)}\right]\cos\left(n\theta\right)\mathrm{e}^{-i\omega t}$$

$$u_{\theta j}=r^{-1}\sum_{n=0}^{\infty}\left[A_{nj}E_{61}^{(3j)}\left(\alpha_jr\right)+A_{nj}^{1}E_{61}^{(4j)}\left(\alpha_jr\right)+B_{nj}E_{62}^{(3j)}\left(\beta_jr\right)+B_{nj}^{1}E_{62}^{(4j)}\left(\beta_jr\right)\right]\sin\left(n\theta\right)\mathrm{e}^{-i\omega t}\tag{15}$$

$$\sigma_{rrN}=2\mu_{0N}\left(1-M_{kN}\right)r^{-2}\sum_{n=0}^{\infty}\phi_0E_ni^nE_{11}^{(1N)}\left(\alpha_Nr\right)+C_{nN}E_{11}^{(3N)}\left(\alpha_Nr\right)+M_{nN}E_{12}^{(3N)}\left(\beta_Nr\right)\cos\left(n\theta\right)\mathrm{e}^{-i\omega t}$$

$$\sigma_{\theta\theta N}=2\mu_{0N}\left(1-M_{kN}\right)r^{-2}\sum_{n=0}^{\infty}\left[\phi_0E_ni^nE_{21}^{(1N)}\left(\alpha_Nr\right)+C_{nN}E_{21}^{(3N)}\left(\alpha_Nr\right)+M_{nN}E_{22}^{(3N)}\left(\beta_Nr\right)\right]\cos\left(n\theta\right)\mathrm{e}^{-i\omega t}$$

$$\sigma_{r\theta N}=2\mu_{0N}\left(1-M_{kN}\right)r^{-2}\sum_{n=0}^{\infty}\left[\phi_0E_ni^nE_{41}^{(1N)}\left(\alpha_Nr\right)+C_{nN}E_{41}^{(3N)}\left(\alpha_Nr\right)+M_{nN}E_{42}^{(3N)}\left(\beta_Nr\right)\right]\sin\left(n\theta\right)\mathrm{e}^{-i\omega t}$$

$$\sigma_{rrj}=2\mu_{0j}\left(1-M_{kj}\right)r^{-2}\sum_{n=0}^{\infty}\left[A_{nj}E_{11}^{(3j)}\left(\alpha_jr\right)+A_{nj}^{1}E_{11}^{(4j)}\left(\alpha_jr\right)+B_{nj}E_{12}^{(3j)}\left(\beta_jr\right)+B_{nj}^{1}E_{11}^{(4j)}\left(\beta_jr\right)\right]\cos\left(n\theta\right)\mathrm{e}^{-i\omega t}$$

$$\sigma_{\theta\theta j}=2\mu_{0j}\left(1-M_{kj}\right)r^{-2}\sum_{n=0}^{\infty}\left[A_{nj}E_{21}^{(3j)}\left(\alpha_jr\right)+A_{nj}^{1}E_{21}^{(4j)}\left(\alpha_jr\right)+B_{nj}E_{22}^{(3j)}\left(\beta_jr\right)+B_{nj}^{1}E_{22}^{(4j)}\left(\beta_jr\right)\right]\cos\left(n\theta\right)\mathrm{e}^{-i\omega t}$$

$$\sigma_{r\theta j} = 2\mu_{0j}\left(1-M_{kj}\right)r^{-2}\sum_{n=0}^{\infty}\Big[A_{nj}E_{51}^{(3j)}\left(\alpha_j r\right)+A_{nj}^{1}E_{61}^{(4j)}\left(\alpha_j r\right)$$
$$+B_{nj}E_{52}^{(3j)}\left(\beta_j r\right)+B_{nj}^{1}E_{52}^{(4j)}\left(\beta_j r\right)\Big]\sin\left(n\theta\right)\mathrm{e}^{-i\omega t}$$

where

$$E_{11}^{(kj)} = \left(n^2+n-\frac{\beta_j^2 r^2}{2}\right)Y_n^{(kj)}\left(\alpha_j r\right)-\alpha_j r Y_{n-1}^{(kj)}\left(\alpha_j r\right)$$

$$E_{12}^{(kj)} = n\Big[\left(n+1\right)Y_n^{(kj)}\left(\beta_j r\right)+\beta_j r Y_{n-1}^{(kj)}\left(\beta_j r\right)\Big]$$

$$E_{21}^{(kj)} = -\left(n^2+n+\frac{\beta_j^2 r^2}{2}-\alpha_j^2 r^2\right)Y_n^{(kj)}\left(\alpha_j r\right)+\alpha_j r Y_{n-1}^{(kj)}\left(\alpha_j r\right)$$

$$E_{22}^{(kj)} = n\Big[\beta_j r Y_n^{(kj)}\left(\beta_j r\right)-\left(n+1\right)Y_n^{(kj)}\left(\beta_j r\right)\Big]$$

$$E_{31}^{(kj)} = \left(\alpha_j^2 r^2-\frac{\beta_j^2 r^2}{2}\right)Y_n^{(kj)}\left(\alpha_j r\right)$$

$$E_{41}^{(kj)} = n\Big[\left(n+1\right)Y_n^{(kj)}\left(\alpha_j r\right)-\alpha_j r Y_{n-1}^{(kj)}\left(\alpha_j r\right)\Big]$$

$$E_{42}^{(kj)} = -\left(n^2+n-\frac{\beta_j^2 r^2}{2}\right)Y_n^{(kj)}\left(\beta_j r\right)+\beta_j r H_{n-1}^{(kj)}\left(\beta_j r\right)$$

$$E_{51}^{(kj)} = \Big[\alpha_j r Y_{n-1}^{(kj)}\left(\alpha_j r\right)-nY_n^{(kj)}\left(\alpha_j r\right)\Big]$$

$$E_{52}^{(kj)} = -nY_n^{(kj)}\left(\beta_j r\right)$$

$$E_{61}^{(kj)} = -nY_n^{(kj)}\left(\alpha_j r\right)$$

$$E_{62}^{(kj)} = \Big[nY_n^{(kj)}\left(\beta_j r\right)-\beta_j r Y_{n-1}^{(kj)}\left(\beta_j r\right)\Big],\quad k=1,2,3,4$$

where $Y_n^{(1j)} = J_n, Y_n^{(2j)} = N_n, Y_n^{(3j)} = H_n^{(1)}, Y_n^{(4j)} = H_n^{(2)}$.

The construction of a formal solution does not meet fundamental difficulties, but the study of such a solution requires a huge amount of computation. The tasks are reduced to solving inhomogeneous algebraic equations with complex coefficients

$$[C]\{q\} = \{p\}. \tag{16}$$

where $\{q\}$ is a vector column containing arbitrary constants; $\{F\}$—vector column of external loads; $[C]$ is a square matrix, the elements of which are expressed through the functions of Bessel and Henkel. Equation (13) is solved by the Gauss method with the selection of the main element. In the work of movement and stress is reduced in dimensionless types

$$u_{rj}^{*} = \frac{u_{rj}}{i\alpha\varphi_A};\quad u_{\theta j}^{*} = \frac{u_{\theta j}}{i\alpha\varphi_A};\quad \sigma_{rrj}^{*} = \frac{\sigma_{rrj}}{\sigma_0};$$

$$\sigma_{r\theta j}^{*} = \frac{\sigma_{r\theta j}}{\sigma_0};\quad \sigma_0 = -\overline{\mu}\beta^2\varphi_A.$$

In the case when $E_1 = E_2 = \cdots = E_N$, $\rho_1 = \rho_2 = \cdots = \rho_N$ and $\nu_1 = \nu_2 = \cdots = \nu_N$, we get holes ($r = R_0$) that are in infinitely elastic medium ($a_{\lambda N}(\omega) = 0$, $b_{\lambda N}(\omega) = 0$). The boundary ($r = R_0$) is stress free, *i.e.* no liquid. In this case, the circumferential voltage on the surface of the cavity is reduced to the following:

$$\sigma_{\theta\theta N}(R,\theta,t) = \frac{-4}{\pi}\beta_N^2\mu_N\phi_0\left(1-\frac{1}{k^2}\right)\sum_{n=0}^{\infty}(-1)^n \in_n H_n^{(1)}(\alpha_N Z)\overline{T}_{nN}\cos(n\theta)\mathrm{e}^{-i\omega t}, \quad (17)$$

where

$$\overline{T}_{nN} = T_{nN}(R_N) = \left[\alpha_N R_N H_{n-1}(\alpha_N R_N) - H_{n-1}(\alpha_N R_N) + Q_{nN}(\beta_N R_N)\right]^{-1}$$

$$Q_{nN}(\beta_N R_N) = \frac{\left(n^3 - n + \frac{1}{2}\beta_N^2 R_N^2\right)\beta_N R_N H_{n-1}(\beta_N R_N) - \left(n^2 + n - \frac{1}{4}\beta_N^2 R_N^2\right)\beta_N^2 R_N^2 H_n^{(1)}(\beta_N R_N)}{\left(n^2-1\right)\beta_N R_N H_{n-1}^{(1)}(\beta_N R_N) - \left(n^2 - n + \frac{1}{2}\beta_N^2 R_N^2\right)H_n^{(1)}(\beta_N R_N)}$$

$k_N^2 = C_{pN}^2 / C_{SN}^2$.

Now consider some limiting cases.

With $r \to 0$:

$$H_0^{(1),(2)}(z)\Big|_{r\to 0} = \pm\frac{2i}{\pi}\ln z - i\left(\frac{z}{2}\right)^2\left(1-\frac{2}{\pi}\ln z\right) + 0\left(z^4\ln z\right),$$

$$H_m^{(1),(2)}(z)\Big|_{r\to 0} = \mp\frac{i}{\pi}\left(\frac{z}{2}\right)^2\left\{(n-1)! + n!z^2 + 0\left(z^4\right)\right\}.$$

And $r \to \infty$: $H_m^{(1),(2)}(z) = \left(\frac{2}{\pi z}\right)^{1/2}\mathrm{e}^{\pm i(kz-\pi/4)}$, the asymptotic formulas of Hankel of the 1st and 2nd kind were used [17]. If in expression (17) Z tends to infinity, then we can use the asymptotic expansions of the Henkel function for large values of the argument [17] (α- is a finite)

$$\lim_{Z\to\infty}\sigma_{\theta\theta}^*\Big|_{r=R_N} \approx \frac{4}{4}\left[1-\frac{1}{k_N^2}\right]\sum_{n=0}^{\infty} i^{n+1}E_n T_{nN}\cos(n\theta)\mathrm{e}^{-i\omega t} \quad (18)$$

This expression completely coincides with the expressions obtained by [17] for a plane incident wave. If the wave number tends to zero, then the limiting process describes static solutions for long waves. This limiting process allows us to use approximating expressions for the Henkel functions for small values of the argument (Z is finite)

$$\lim_{\alpha\to 0}\sigma_{\theta\theta}\Big|_{r=R_1} \approx 4\left[1+\left(\frac{R_N}{Z}\right)^2 + \frac{4}{Z}\cos\theta\right] * \sum_{m=2}^{\infty}(-1)^{m-2}\left(-\frac{R_N}{Z}\right)^{m-2}(m-1)\cos(m\theta) \quad (19)$$

This solution exactly coincides with the solution of the static problem obtained in [18]. If the cylindrical cavity contains an ideal fluid, then the ring stresses take the form

$$\sigma_{\theta\theta}^{*}=-\frac{4}{\pi}\sum_{n=0}^{\infty}\frac{\in_n i^{n+1}}{\Delta_n}\left\{\left[\left(\frac{1}{\chi_N^2}-1\right)\left(\frac{n\beta_N^2R^2}{2}(n-1)-n^2\left(n^2-1\right)-n\frac{\beta_N^4R^4}{4}\right)\right.\right.$$
$$\left.+\frac{\beta_N^2R^3}{4}\eta\left(n(n+1)-\frac{1}{2}\beta_N^2R^2\right)\right]I_n(\alpha_0R)H_n(\beta_NR)$$
$$+\left[\left(\frac{1}{\chi_N^2}-1\right)\left(n^3-n^2-n\right)-\frac{1}{4}n\beta_N^2R^2\right]\beta_NRI_n(\alpha_0R)H_{n-1}(\beta_NR)$$
$$+\left(\frac{1}{\chi_N^2}-1\right)\left(n^3-n+\frac{1}{2}\beta_N^2R^2\right)\alpha_0RI_{n-1}(\alpha_0R)H_n(\beta_NR)$$
$$\left.+\left(\frac{1}{\chi_N^2}-1\right)\left(1-n^2\right)\alpha_0\beta_N^2R^2I_{n-1}(\alpha_0R)H_{n-1}(\beta_NR)\right\}\cos(n\theta)\mathrm{e}^{-i\omega t}$$

where $\chi_N^2=\frac{2(1-\nu_N)}{1-2\nu_N}=\frac{\beta_N^2}{\alpha_N^2};\eta=\frac{\rho_1}{\rho_N}$. At $\alpha_1R\to 0$, then it turns out the solution of a static problem

$$\sigma_{rr}^{*}=\frac{\lambda_1}{\lambda_1+\mu_N};\ \sigma_{\theta\theta}^{*}=\frac{1}{1-\nu_N}\left[\left(1-\frac{2\lambda_1(1-\nu_N)}{\lambda_1+\mu_N}\right)-(2-4\nu_N)\cos(2\theta)\right].$$

In the limiting processes in expressions (15) and (16) is described by physical results, is given in Table 1. The stress concentration coefficient $\sigma_{\theta\theta N}^{*}$ is determined by the following formulas

$$\sigma_{\theta\theta}^{*}\big|_{r=R_N}=\frac{\sigma_{\theta\theta}\big|_{r=R_N}}{\sigma_{\theta\theta}^{(p)}}. \tag{20}$$

where $\sigma_{\theta\theta}^{(p)}=i\pi\varphi_0\mu\alpha^2\left[\pi\varphi\mu H_2^{(1)}(\alpha\bar{r})+\left(1-k^2\right)H_0^{(1)}(\alpha\bar{r})\right]\mathrm{e}^{-i\omega t}$.

If we take the fluid into account, then using (2), (3) and (15) we can determine the corresponding stresses σ_{rrN}^{*} and $\sigma_{\theta\theta N}^{*}$. In the absence of an incident wave (6), the natural oscillations of an unsupported (or reinforced) hole located in the medium are considered.

At the boundary $r=R$, we set a voltage-free condition, *i.e.*

$$\sigma_{rr}\big|_{r=a}=\sigma_{r\theta}\big|_{r=a}=0. \tag{21}$$

Substituting (12) into (21), we obtain the frequency equation

$$Z_{1n}X_{2n}+Z_{2n}X_{1n}=0. \tag{22}$$

where

$$X_{1n}=\Omega_0H_{n+1}^{(1)}(\Omega_o)+\left(a_{n2}^1-d_1\Omega_0^2\right)H_0^{(1)}(\Omega_o);$$
$$X_{2n}=n\left[(n-1)H_n^{(1)}(\Omega_1)-\Omega_1H_{n+1}^{(1)}(\Omega_1)\right];$$
$$Z_{1n}=n\left[(1-n)H_n^{(1)}(\Omega_o)-\Omega_oH_{n+1}^{(1)}(\Omega_o)\right];$$
$$Z_{2n}=\left(a_{n2}^1-\Omega_1^2/2\right)H_n^{(1)}(\Omega_1)+\Omega_1H_{n+1}^{(1)}(\Omega_1);$$
$$d_1=(1-\nu_1)/(1-2\nu_1);\ a_{n2}=n^2;\ a_{n2}^1=n^2-n;\ \Omega_o=\Omega_1L_1;$$
$$l_1=(1-2\nu_1)/(2(1-\nu_1));\ \Omega_1=\omega a/C_{p1}$$

Table 1. Information on limiting processes.

Case 1	Case 2	Case 3	Case 4
$\lim_{Z\to\infty}\left\{\sigma^*_{\theta\theta}\big\vert_{r=R}\right\}$	$\lim_{\alpha\to 0}\left\{\sigma^*_{\theta\theta}\big\vert_{r=R}\right\}$	$\lim_{Z\to 0}\left\{\sigma_{\theta\theta}\big\vert_{r=R}\right\}$	$\lim_{\alpha\to 0}\left\{\lim_{r\to\infty}\sigma_{\theta\theta}\Big\vert_{r=R}\right\}$
α - arbitrary	z- of course	$\alpha\to 0$	α - of course
Dynamic solution for a plane wave.	Static solution, linear source of expansion waves.	Static solution, pure shear state.	The static problem of the flat deformed state.

Frequency Equation (22) is solved numerically, *i.e.* Muller method. The complex eigenfrequencies $\left(\omega_{nj}, j=1,2,3\right)$ are given $n\geq 0$ $\left(\nu_1=0.25\right)$ in Table 2. In the table of the first column correspond the complex frequency ω_{01}, second ω_{11}, third $\omega_{21},\omega_{22},\omega_{23}$ and fourth, columns $\omega_{31},\omega_{32},\omega_{33}$.

The partial equation, for differential Equations (6), under the condition of a sliding contact, takes the form:

$$\begin{vmatrix} h_2Y_{1n}-Z_o\left(\Omega_o\right)X_{1n} & h_2Y_{2n}-Z_o\left(\Omega_o\right)Z_{2n} \\ Z_{1n} & X_{2n}\end{vmatrix}=0 \tag{23}$$

where

$$h_2=h_o/R;\ Y_{1n}=nH_n^{(1)}\left(\Omega_1\right)-\Omega_1H_{n+1}^{(1)}\left(\Omega_1\right);$$

$$Z_{jn}=n\left[\left(1-n\right)H_n^{(1)}\left(\Omega_j\right)+\Omega_jH_{n+1}^{(1)}\left(\Omega_j\right)\right];$$

$$X_{1n}=\left(-d_1\Omega_1^2+\alpha_{n2}^1\right)H_n^{(1)}\left(\Omega_1\right)+\Omega_1H_{n+1}^{(1)}\left(\Omega_1\right);$$

$$X_{2n}=\left(\alpha_{2n}^1-\Omega_2^2/2\right)H_n^{(1)}\left(\Omega_2\right)+\Omega_2H_{n+1}^{(1)}\left(\Omega_2\right);$$

$$Y_{2n}=nH_n^{(1)}\left(\Omega_2\right),\ j=1,2$$

$$\nu_2=1-\nu_o;\ \alpha_{n1}=b^2\left(n^2-1\right)+1;\ \Omega_1=\alpha_1a;$$

$$\Omega_2=\beta_1\alpha=\Omega_1\left(C_{\rho1}/C_{s1}\right);\ \Omega_o=\alpha_oR;\alpha_o\quad a_0=\omega/C_o;$$

$$b^2=h^2/12R^2;\ b_1=E_1\left(1-\nu_0^2\right)/\left(E_o\left(1+\nu_1\right)\right);$$

$$a_{n2}^1=n^2;\ \beta_1=E_oh_o/\left(1-\nu_o^2\right);$$

$C_o=E_o/\rho_o$ —Rod wave velocity

$$Z_o\left(\Omega_o\right)=b_1/\left[\left(\Omega_0^2\nu_2-a_{n1}\right)-n^2/\left(\Omega_0^2\nu_2-a_{n2}\right)\right] \tag{24}$$

In this case, we obtain asymmetric vibrations of the cylindrical shell, which are described by the expression

$$h_2\left(\Omega_0^2\nu_2-a_{01}\right)+b_1-b_1d_1\Omega_1H_o^{(1)}\left(\Omega_1\right)/H_1^{(1)}\left(\Omega_1\right)=0. \tag{25}$$

where $\Omega_1=\Omega_oL_1;L_1=\eta E\left(1+\nu_1\right)\left(1-2\nu_1\right)/\left(1-\nu_1\right)$ (the index "0" corresponds to the shell, and "1" to the environment). If we use the asymptotic expression of the Henkel function with $l_1\gg 1$, then for the zero and first order we obtain the expression of the complex natural frequencies

Table 2. The dependence of the complex natural frequencies of the cylindrical hole.

	$n=0$	$n=1$	$n=2$	$n=3$
ω_1	0.4529D+00 −i0.47651D+00	0.10927D+01 −i0.76538D+00	0.19075D+01 −i0.89782D+00	0.27565D+01 −i0.99155D+00
ω_2			0.28621D+00 −i0.17852D+00	0.72325D+01 −i0.32283D+01
ω_3			0.404607D+00 −i0.178552D+00	0.12307D+00 −i0.22283D+00

$$\Omega_o = -i\frac{b_1 d_1 l_1}{2h_2 v_2} + \sqrt{\frac{a_{01}}{v_2} - \left(\frac{d_1}{h_2 v_2} + \left(\frac{d_1 l_1 b_1}{h_2 v_2}\right)^2\right)} \tag{26}$$

To obtain complex and imaginary natural frequencies, the following condition must be met

$$\Omega = \begin{cases} \Omega_R + i\Omega_I & \text{if } \left(a_{01}/v_1\right) > \left(b_1/h_2 v_2\right) + \left(d_1 l_1 b_1/h_2 v_2\right)^2 \\ \Omega_I & \text{if } \left(a_{01}/v_1\right) > \left(b_1/h_2 v_2\right) + \left(d_1 l_1 b_1/h_2 v_2\right)^2 \end{cases} \tag{27}$$

To fulfill the first condition, the modulus of elasticity E must satisfy the inequality

$$E > \left(1+v_1\right)\left(b^2+1\right)h_2^2\left(\left[h_2+\left(1-v_1\right)\right]\eta\left(1-2v_1\right)^{-1}\right)^{-1}\left(1-v_0^2\right)^{-1} \tag{28}$$

A similar condition is set for η:

$$\eta < h_2\left(1-2v_1\right)\left(1-v_1\right)^{-1}\left[h_2 a_{01}\left(1+v_1\right)\left(1-2v_1\right)^{-1}\left(E_o/E_1\right)-1\right]$$

The numerical values of asymmetric Ω ($n=0$) natural frequencies are given in Table 3 for different values of $E(E_1/E_0)$.

4. Numeric Results

For given incident wave, voltage and displacement are determined by the rows described by expressions (12) - (17) in the case of hard contact. The calculations were performed on the Mat lab computer program complex; the series were calculated with an accuracy of 10^{-8}. All expressions for stresses and displacements are:

$$\left(R+i\,\mathrm{Im}\right)\mathrm{e}^{-iwt} = \left(R^2+\mathrm{Im}^2\right)^{1/2}\mathrm{e}^{-i(wt-\gamma)}. \tag{29}$$

As can be seen, the solution of the problem is expressed through the special functions of the Bessel and Henkel of the 1st and 2nd kind. With the increase in their argument, the series (12) - (17) converges. Therefore, on the basis of numerical experiments, it has been established that the accuracy of 5 - 6 members of the series has reached 10^{-6} - 10^{-8}. As the relaxation core of a viscoelastic material, let's take a three-parameter core $R(t)=\dfrac{A\mathrm{e}^{-\beta t}}{t^{1-\alpha}}$ Rizhanitsen-Koltunova [19], which has a weak singularity, where A,α,β —parameters materials [19].

Table 3. The dependence of the complex natural frequencies of ax symmetric vibrations of cylindrical shells on *E*.

ω	$E=0.03$	$E=0.09$	$E=0.12$	$E=0.15$	$E=0.25$
ω_{01}	1.3308D-01 −i1.9767D-02	2.3976D-01 −i4.5891D-02	3.2670D-01 −i6.1776D-02	4.1665D-01 −i7.9394D-02	1.5270D-12 −i1.3691D-01

Take the following parameters: $A=0.048;\beta=0.05;\alpha=0.1$. To study the stress concentration on the free surface, we use the absolute values of the complex value and relations (18) and (19). The magnitude of the complex function depends on the wave number a, angle θ distances $\bar{r}$, Poisson's ratio, Young's module, densities, geometrical parameters R and Z. If all the characteristics (**Figure 1**) of the mechanical system are the same ($E_1=E_2=\cdots=E_n$; $\rho_1=\rho_2=\cdots=\rho_n$; $\nu_1=\nu_2=\nu_3=\cdots=\nu_n$), then the problem of the interaction of cylindrical waves with cylindrical cavities is considered. **Figure 2** shows the plot of the stress concentration factor $\sigma^*_{\theta\theta}\big|_{r=R_N}$ depending on θ at

$$A=0.048;\ \beta=0.05;\ \alpha=0.1;\ \nu=0.25;\ \frac{Z}{R}=3.0,30,50,\ \alpha R=0.1.$$

Figure 2 shows that the influence of the proximity of the source lies in moving the maximum value to the point where the line drawn from the source touches the boundary of the cavity.

For the stress concentration coefficients, we will use the absolute value of the complex value (21). **Figure 3** shows the change $\sigma^*_{\theta\theta}\big|_{r=R_N}$ depending on the wave number at different values $\frac{Z}{R}=6.0;12;20$, which quickly aim for a solution for a plane wave when $\alpha R \succ 0.16$. This means that when the source is at a distance of five radii from the cavity, the high frequency nature of the change $\sigma^*_{\theta\theta}$ can be approximated by a solution for a plane wave. Further, all values approach the same asymptote. The largest difference between the solution for a plane wave ($Z\to\infty$) and the solution under consideration is in the $0\le\alpha R\le 0.22$. Легко видеть, что когда $\alpha R\to 0$, dynamic solution for the case of a plane wave is reduced to a static value ($\nu=0.25,\theta=\pi/2$), *i.e.* $\sigma^*_{\theta\theta}=2.67$.

A similar but more pronounced change is noted for $\sigma^*_{\theta\theta}$ at ($\theta=\pi$) (**Figure 4**). When $\alpha R\ge 1.0$, solution for dynamic source with values $\frac{Z}{R}=5.0;10;20$ again reduced to a solution for a plane wave. When $Z/R=2$ (**Figure 3**) the dynamic concentration curve differs from static to 15%. When $\alpha R=2.0$ Static and dynamic stress state results are radically different at close source distances ($Z/R=2$). With $R/Z>50$ the impact of the cylindrical source unfolds as a plane wave, *i.e.* you can ignore the radius of curvature of the wave. Similar results were obtained for a cylindrical cavity with an ideal fluid [20]. The results of the calculations are shown in **Figure 5**. It can be seen from the figure that the voltage

values strongly depend on the parameter $\gamma = \frac{C_{p1}}{C_{p2}}$. And also there is a resonant phenomenon. Calculation results $n \geq 0$ ($\nu_1 = 0.25$) natural oscillations are shown in Table 2. As the table shows, with the increase in the number of waves around the circumference, the corresponding complex frequencies increase.

The complex frequencies consist of two parts, the real ($\mathrm{Re}\,\Omega$) and imaginary parts ($\mathrm{Im}\,\Omega$) which means natural frequencies and damping factors. Frequency equations (23) depends only on the parameter ν (Poisson's ratio). With increasing Poisson's ratio within $0 \leq \nu \leq 0.4$ real and imaginary parts of the complex frequency changes to 27%. With $\nu_1 = 0.5$ the environment becomes incompressible, the attenuation is naturally absent. The existence of an imaginary value of the natural frequency means that the oscillatory processes in the system are only damped. The imaginary natural frequencies turn out to depend on the longitudinal and transverse speeds, as well as the whole radius.

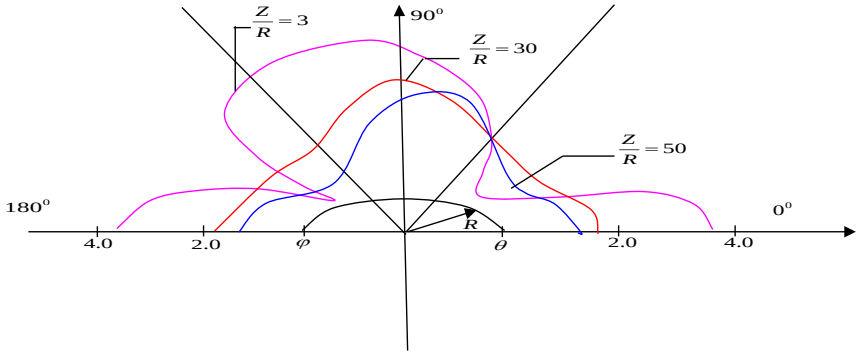

Figure 2. Effect of source proximity on voltages $\left|\sigma^*_{\theta\theta}\right|$ depending on the $\theta(\alpha R = 0.1)$ at different values of $\frac{Z}{R} = 3;30;50$.

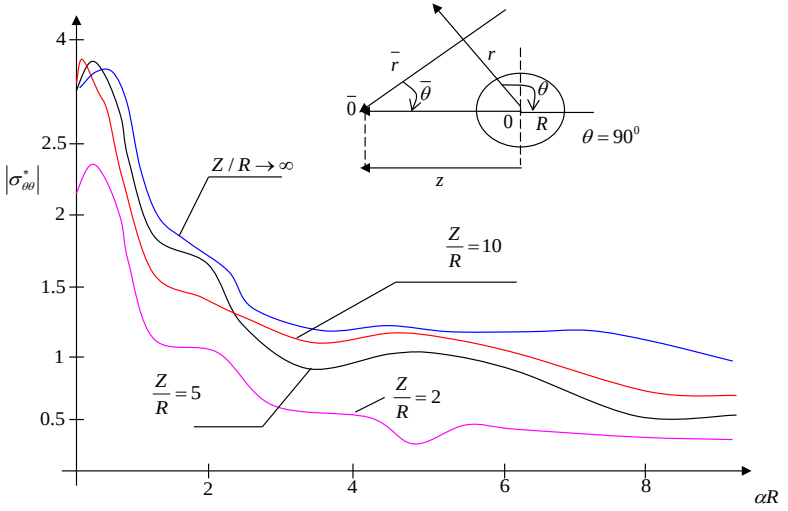

Figure 3. $\left|\sigma^*_{\theta\theta}\right|$ depending on the αR (wave number) when $\theta = 90^\circ; A = 0.048;$ $\alpha = 0.1; \beta = 0.5$.

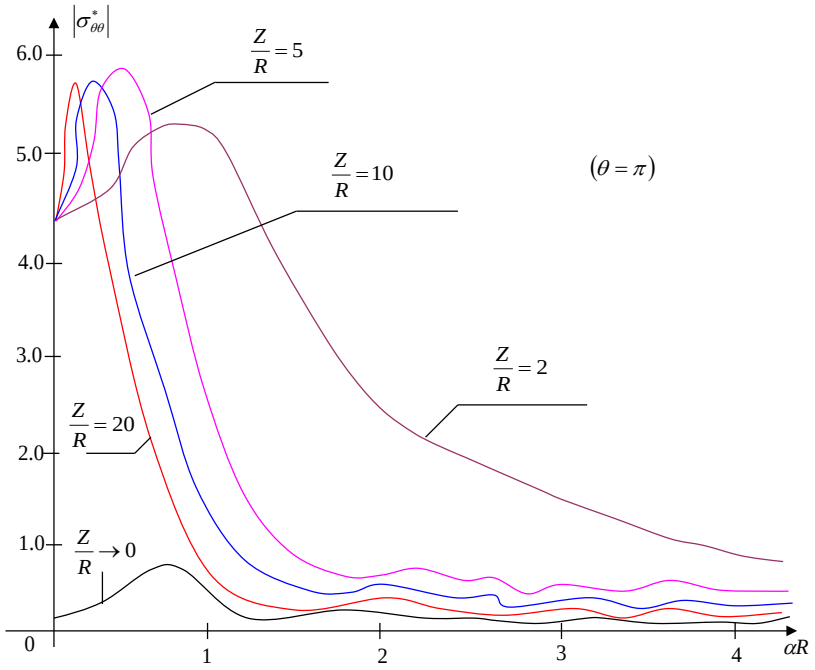

Figure 4. Value $|\sigma^*_{\theta\theta}|$ depending on the αR ($\theta=\pi$).

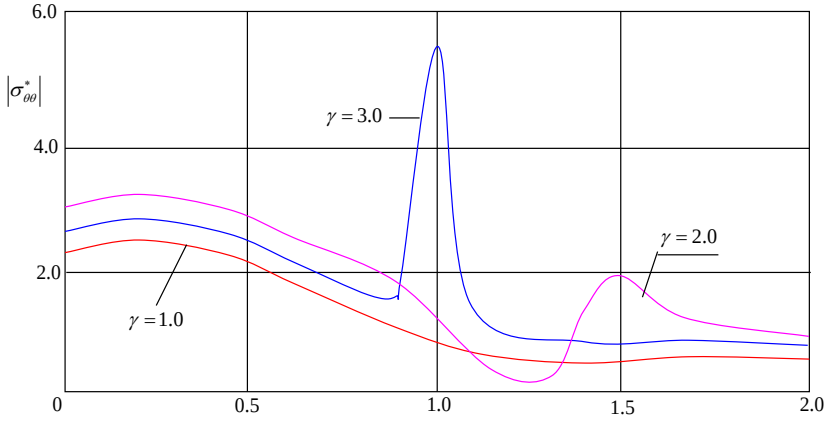

Figure 5. Dependency $|\sigma^*_{\theta\theta}|$ from $\alpha_N R$ (wave number).

The existence of a discrete frequency plays an important role for the calculation of underground pipelines located in the ground environment.

The obtained numerical results are presented in the form of tables and figures. The appearance of an additional free surface mainly thickens and reduces the Eigenvalue frequency by 10% - 16%. The existence of a natural frequency means that Rayleigh waves can occur in the vicinity of the free surface of a cylindrical hole. Thus, according to (28) with $E(E_1/E_0)\to 1$ the real part of the complex frequency does not exist.

As we see, $(E_1/E_o)\geq 0.21$ the real parts of the natural frequency vanish, and the behavior of the imaginary parts remains unchanged. The obtained numerical results are confirmed by the condition (25).

5. Conclusions

1) The task of diffraction of harmonic waves in a cylindrical body is solved in displacement potentials. Displacement potentials are determined from solutions of the Helmholtz equation. Arbitrary constants are determined from the boundary conditions that are put between the bodies. As a result, the task is reduced to a system of inhomogeneous algebraic equations with complex coefficients, which are solved by the Gauss method with the selection of the main element.

2) Contour stresses $\sigma_{\theta\theta}$ on the free surface of cylindrical bodies reach their maximum value in $\frac{\pi}{2}$—when exposed to longitudinal waves, and $\frac{\pi}{4}$—shear waves. Contour stresses $\sigma_{\theta\theta}$ when subjected to transverse harmonic waves, are 15% - 20% more than those when subjected to longitudinal waves.

3) When the source of harmonic waves is at a distance of five radii ($Z > 5R$) from a cylindrical body, the high-frequency nature of changes in loop stresses $\sigma_{\theta\theta}$ (on the inner free surface), is well approximated by the solution for a flat ($Z \to \infty$) waves. Further, all values approach the same asymptote.

4) Numerical results show that the dynamic stress concentration factors near cylindrical bodies depend on the distance between the source and the body, the wave number for the cylinder and the medium; physico-mechanical parameters of the environment and the body.

5) Consideration of the viscous properties of the material of the environment when calculating the effect of seismic waves reduces stress and displacement by 10% - 15%. Calculations show that for fixed values of the amplitudes and the duration of the incident wave with increasing acoustic parameters of the fluid, the deflections and efforts also moderately increase. In the region of the long waves, the stress distribution of a pipe with and without liquid differs by up to 15%, and in the region of short waves, in some values of frequency, they differ by up to 40%. With a hole with a lining, the stress in the soil will be less than for the case of a hole without reinforcement. On the other hand, the amplification will be subjected to stresses from seismic loads and must withstand them.

6) The statement of the problem is proposed: natural oscillations of cylindrical bodies being in a deformable medium. The task is to find those $\Omega = \Omega_R + i\Omega_i$ (Ω_R—real and Ω_i—imaginary parts of complex eigenfrequencies), in which the system of equations of motion and shortened radiation conditions have a nonzero solution in the class of infinitely differentiable functions. It is shown that the task has a discrete spectrum.

Conflicts of Interest

The authors declare no conflicts of interest regarding the publication of this paper.

References

[1] Guz, A.N., Kubenko, V.D. and Cherevko, M.A. (1978) Diffraction of Elastic Waves. Science Dumka, Kiev, 307 p.

[2] Safarov, I.I. and Umarov, A.O. (2014) The Impact of Longitudinal and Transverse Waves on Cylindrical Layers with a Liquid. *Perm University Bulletin. Mathematics. Mechanics. Informatics*, **3**, 69-75.

[3] Safarov, I.I., Akhmedov, M.Sh. and Umarov, A.O. (2014) Dynamic Stresses and Mixing near a Cylindrical Reinforced Cavity from a Plane Harmonic Wave. *Journal* "*Prospero*" (*Novosibirsk*), **3**, 57-61.

[4] Safarov, I.I., Teshaev, M.Kh. and Boltaev, Z.I. (2017) Distribution of Harmonic Waves in Expansion Plastic and Cylindrical Viscoelastic Bodies. Open Science Publishing, Raleigh, 218 p.

[5] Strelchuk, N.A., Slavin, O.K. and Shaposhnikov, V.N. (1971) Investigation of the Dynamic Stress State of Tunnel Lining under the Influence of Blast Waves. Building and Architecture, Moscow, No. 9, 129-136.

[6] Rashidov, T.R., Hozhimatov, G.Kh. and Mardonov, B.M. (1975) Oscillations of Structures Interacting with the Ground. Fan, Tashkent, 174 p.

[7] Rashidov, T.R., Sagdiev, H. and Safarov, I.I. (1989) On Two Main Methods for Studying the Seismic Stress State of Underground Structures under the Action of Seismic Waves. Reports of the Academy of Sciences, Tashkent, 6, 13-17.

[8] Muborakov, Ya.N. (1987) Seismic Dynamics of Underground Structures of the Shell Type. Fan, Tashkent, 192 p.

[9] Rashidov, T.R. (1973) Dynamic Theory of Seismic Resistance of Complex Systems of Underground Structures. Fan, Tashkent, 182 p.

[10] Rashidov, T.R., Dorman, I.Ya. and Ishanhodzhaev, A.A. (1975) The Seismic Resistance of Tunnel Structures of the Metro. Transport, M., 120 p.

[11] Muborakov, Ya.N. and Safarov, I.I. (1990) On the Basic Methods of Studying the Stress-Strain State of Underground Cylindrical Structures When Interacting with Elastic Waves. Collection: Durability of Engineering Structures under Seismic and Pulse Effects. Fan, Tashkent.

[12] Muborakov, Ya.N. and Safarov, I.I. (1988) Assessment of the Seismic State of Underground Structures by the Method of Wave Dynamics. In: *Seismodynamics of Buildings and Structures*, Fan, Tashkent, 114-122.

[13] Koltunov, M.A. (1976) Creep and Relaxation. Higher School, M., 277 p.

[14] Safarov, I.I. (1992) Collisions and Waves in Dissipatively Non-Fertile Environments and Constructions. Fan, Toshkent, 250 p.

[15] Mun, P. (1962) The Influence of the Curvature of Spherical Waves on the Concentration of Dynamic Stresses. *Applied Mechanics*, **2**, 93.

[16] Mente, M. (1963) Dynamic Stresses and Displacement in the Vicinity of a Cylindrical Discontinuity Surface from a Plane Harmonic Shear Wave. *Applied Mechanics*, **30**, 117-126.

[17] Ilyushin, A.A., Rashidov, T.R., *et al.* (1985) The Effect of Seismic Waves on Underground Pipelines. *Proceedings of the International Scientific Conference*: *Friction, Wear and Lubricants*, Tashkent, 22-26 May 1985, 128-132.

[18] Gorshkov, A.G. (1981) Non-Stationary Interaction of Plates and Shells with Continuous Media. RHDL Proceedings of the Academy of Sciences. Fur. Solids, No. 4, 177-189.

[19] Avliyakulov, N.N. and Safarov, I.I. (2007) Modern Problems of Statics and Dynamics of Underground Pipelines. Fan, Tashkent, 306 p.

[20] Bozorov, M.B., Safarov, I. and Shokin, Yu.I. (1996) Numerical Simulation of Oscillations of Dissipatively Homogeneous and Inhomogeneous Mechanical Systems. Novosibirsk, 189 p.

Scientific Research Publishing

Applied Mathematics, 2019, 10, 485-512
http://www.scirp.org/journal/am
ISSN Online: 2152-7393
ISSN Print: 2152-7385

A Full Asymptotic Series of European Call Option Prices in the SABR Model with Beta = 1

Z. Guo, H. Schellhorn

Claremont Graduate University, Claremont, California, USA
Email: henry.schellhorn@cgu.edu

How to cite this paper: Guo, Z. and Schellhorn, H. (2019) A Full Asymptotic Series of European Call Option Prices in the SABR Model with Beta = 1. *Applied Mathematics*, **10**, 485-512.
https://doi.org/10.4236/am.2019.106034

Received: May 21, 2019
Accepted: June 25, 2019
Published: June 28, 2019

Abstract

We develop two new pricing formulae for European options. The purpose of these formulae is to better understand the impact of each term of the model, as well as improve the speed of the calculations. We consider the SABR model (with $\beta = 1$) of stochastic volatility, which we analyze by tools from Malliavin Calculus. We follow the approach of Alòs *et al.* (2006) who showed that under stochastic volatility framework, the option prices can be written as the sum of the classic Hull-White (1987) term and a correction due to correlation. We derive the Hull-White term, by using the conditional density of the average volatility, and write it as a two-dimensional integral. For the correction part, we use two different approaches. Both approaches rely on the pairing of the exponential formula developed by Jin, Peng, and Schellhorn (2016) with analytical calculations. The first approach, which we call "Dyson series on the return's idiosyncratic noise" yields a complete series expansion but necessitates the calculation of a 7-dimensional integral. Two of these dimensions come from the use of Yor's (1992) formula for the joint density of a Brownian motion and the time-integral of geometric Brownian motion. The second approach, which we call "Dyson series on the common noise" necessitates the calculation of only a one-dimensional integral, but the formula is more complex. This research consisted of both analytical derivations and numerical calculations. The latter show that our formulae are in general more exact, yet more time-consuming to calculate, than the first order expansion of Hagan *et al.* (2002).

Keywords

SABR Model, Stochastic Volatility, Malliavin Calculus, Exponential Formula, Option Pricing

1. Introduction

European options are traditionally priced and hedged by Black-Scholes [1] (1973) model, one of the natural extensions of the Black-Scholes model to make volatility stochastic. The simplest stochastic volatility models assume that the volatility and the noise driving stock prices are uncorrelated. Moreover, the Hull-White formula [2] (1987) establishes that the European option price is the expectation of the Black-Scholes option pricing formula with a time-dependent volatility. An important success of this model is that it calculates European prices which implied volatilities smile. The development of local volatility models by Dupire and Derman (1994) was a major development in handling smiles and skews. However its predictions contradict empirical findings. Thus the SABR (stochastic alpha beta rho) model, a stochastic volatility model in which the asset price is correlated with its volatility was derived by Hagan *et al.* [3] (2002) to resolve this problem. Alòs [4] (2006) extended the classical Hull-White formula to the correlated case by means of Malliavin calculus. The new generalization decomposes option prices as the sum of the same derivative price if there was no correlation and a correction due by correlation. Another popular model is the Heston (1993) model. In that model, the volatility is mean-reverting. The general asymptotic method presented by Fouque, Papanicolau and Sircar (2000) [5] can be used to analyze Heston's model. For more information on stochastic volatility models, we refer the reader to Gatheral [6] (2006).

Nevertheless, there are still terms of conditional expectation of functions of non-adapted processes in the new generalization of Hull-White formula. Jin, Peng and Schellhorn [7] (2016) showed that under certain smoothness conditions, a Brownian martingale can be represented via an exponential formula when evaluated at a fixed time. It is a powerful tool similar to Clark-Ocone formula that allows us to work with the conditional expectation of a random variable instead of the random variable itself.

The main goal of this research was to obtain an option pricing formula for the special case of the SABR model with $\beta = 1$. We used two different approaches. Both approaches rely on the pairing of the exponential formula developed by Jin, Peng, and Schellhorn (2016) with analytical calculations, and start by conditioning on the path of the common noise term W. In the first approach, which we call "Dyson series in the return's idiosyncratic noise", we first apply a Dyson series in the idiosyncratic noise term Z and then apply Yor's [8] formula (1992) for the joint density of a Brownian motion and the time-integral of geometric Brownian motion to integrate with respect to the common noise term W. We note that Yor's formula is used for pricing Asian options, but it is ideally suited to analyze realized volatility in the SABR model with $\beta = 1$, since volatility is a geometric Brownian motion. Faà di Bruno's formula is used for analytical differentiation. The first approach yields a complete series expansion but necessitates the calculation of a 7-dimensional integral. Two of these dimensions come from the analytical expression of the joint density of a Brownian motion and the

time-integral of geometric Brownian motion. In the second approach, which we call "Dyson series in the common noise", we first integrate away the idiosyncratic noise term Z and then apply a Dyson series in the common noise term W. This results in a formula which necessitates the calculation of only a one-dimensional integral, but the formula is more complex, and we carried the calculation only of the first term of the series.

The organization of this paper is as follows. In Section 2 we present a brief introduction to Malliavin Calculus as well as a representation theorem for smooth Brownian Martingales. Section 3 is a review of basic option pricing theory and an extension to stochastic volatility models. In Section 4, we present several Hull-White formulas for European call option prices with different model assumptions. In Section 5, we derive the Dyson series in the return's idiosyncratic noise for the call price. In Section 6, we derive the Dyson series in the common noise for the call price, and compare numerically all approaches.

2. Preliminaries on Malliavin Calculus

The following section briefly reviews some basic facts of Malliavin Calculus required along the paper. For a complete exposition we refer to Nualart [9] (1995) and Øksendal [10] (2008). Let $\left(\Omega,\mathcal{F},\{\mathcal{F}_t\}_{t\geq 0},\mathbb{P}\right)$ be a complete filtered probability space where $\{\mathcal{F}_t\}$ is generated by a standard Brownian motion $\{W_t\}_{t\geq 0}$. In Section 2.4, we will enlarge our probability space to consider two standard Brownian motions.

2.1. Malliavin Derivative

Let $L^2\left([0,T]^n\right)$ be the standard space of square integrable Borel real functions on $[0,T]^n$ and let $\tilde{L}^2\left([0,T]^n\right)\in L^2\left([0,T]^n\right)$ be the space of symmetric square integrable Borel real functions on $[0,T]^n$, consider the set

$S_n=\left\{(t_1,\cdots,t_n)\in[0,T]^n:0\leq t_1\leq\cdots\leq t_n\leq T\right\}$.

Definition 2.1 If f is a deterministic function defined on $S_n\left(n\geq 1\right)$ such that $\|f\|^2_{L^2(S_n)}:=\int_{S_n}f^2(t_1,\cdots,t_n)\mathrm{d}t_1\cdots\mathrm{d}t_n<\infty$, then the n-fold iterated Itô integral is defined as

$$J_n(f):=\int_0^T\int_0^{t_n}\cdots\int_0^{t_3}\int_0^{t_2}f(t_1,\cdots,t_n)\mathrm{d}W_{t_1}\cdots\mathrm{d}W_{t_{n-1}}\mathrm{d}W_{t_n},\tag{1}$$

and if $g\in\tilde{L}^2\left([0,T]^n\right)$ we define

$$I_n(g)=\int_{[0,T]^n}g(t_1,\cdots,t_n)\mathrm{d}W_{t_1}\cdots\mathrm{d}W_{t_n}:=n!J_n(g).\tag{2}$$

Theorem 2.2 *The Wiener-Itô Chaos Expansion. Let F be an $\mathcal{F}_T$-measurable random variable in $L^2(P)$. Then there exists a unique sequence $\{f_n\}_0^\infty$ of functions $f_n\in\tilde{L}^2\left([0,T]^n\right)$ such that $F=\sum_0^\infty I_n(f_n)$.*

Definition 2.3 Let $u(t)$, $t\in[0,T]$, be a measurable stochastic process such that for all $t\in[0,T]$ the random variable $u(t)$ is $\mathcal{F}_T$-measurable and $E\left[\int_0^T u^2(t)\mathrm{d}t\right]<\infty$. Let its Wiener-Itô chaos expansion be

$$u(t)=\sum_0^\infty I_n\left(f_{n,t}\right)=\sum_0^\infty I_n\left(f_n(\cdot,t)\right). \tag{3}$$

Then we define the Skorohod integral of u by

$$\delta(u):=\int_0^T u(t)\delta W_t:=\sum_0^\infty I_{n+1}\left(\tilde{f}_n\right), \tag{4}$$

when converge in $L^2(P)$, we say that u is Skorohod integrable and we write $u\in Dom(\delta)$ if the series in (4) converges in $L^2(P)$.

The operator δ is an extension of the Itô integral, in the sense that the set $L^2(P)$ of square integrable and adapted processes is included in $Dom(\delta)$ and the operator δ restricted to $L^2(P)$ coincides with the Itô stochastic integral.

Theorem 2.4 *Let* $u=u(t),t\in[0,T]$, *be a measurable* $\mathbb{F}$ *-adapted stochastic process such that* $E\left[\int_0^T u^2(t)\mathrm{d}t\right]<\infty$. *Then* $u\in Dom(\delta)$ *and its Skorohod integral coincides with the Itô integral*

$$\int_0^T u(t)\delta W_t=\int_0^T u(t)\mathrm{d}W_t. \tag{5}$$

Definition 2.5 Let $F\in L^2(P)$ be $\mathcal{F}_T$ -measurable with chaos expansion $F=\sum_0^\infty I_n(f_n)$, where $f_\cdot\in\tilde{L}^2\left([0,T]^n\right)$, for $n=1,2,\cdots$, we say that $F\in\mathbb{D}_{1,2}$ if $\|F\|_{\mathbb{D}_{1,2}}^2:=\sum_0^\infty nn!\|f_n\|_{L^2([0,T]^n)}^2<\infty$. If $F\in\mathbb{D}_{1,2}$ we define the Malliavin derivative D_tF of F at time t as the expansion

$$D_tF=\sum_{n=1}^\infty nI_{n-1}\left(f_n(\cdot,t)\right),t\in[0,T]. \tag{6}$$

We will need the following results on the Malliavin derivative.

Theorem 2.6 ***Product rule for Malliavin derivative.*** *Suppose* $F_1,F_2\in\mathbb{D}_{1,2}^0$. *Then* $F_1,F_2\in\mathbb{D}_{1,2}$ *and also* $F_1F_2\in\mathbb{D}_{1,2}$ *with*

$$D_t\left(F_1F_2\right)=F_1D_tF_2+F_2D_tF_1. \tag{7}$$

Theorem 2.7 ***Chain rule.*** *Let* $G\in\mathbb{D}_{1,2}$ *and* $g\in\mathcal{C}^1(\mathbb{R})$ *with bounded derivative. Then* $g(G)\in\mathbb{D}_{1,2}$ *and*

$$D_tg(G)=g'(G)D_tG. \tag{8}$$

Example 2.1

$$D_t\left(\int_0^T f(s)\mathrm{d}W_s\right)^n=n\left(\int_0^T f(s)\mathrm{d}W_s\right)^{n-1}D_t\left(\int_0^T f(s)\mathrm{d}W_s\right)=n\left(\int_0^T f(s)\mathrm{d}W_s\right)^{n-1}f(t).$$

Theorem 2.8 ***The fundamental theorem of calculus.*** *Let* $u=u(s),s\in[0,T]$, *be a stochastic process such that* $E\left[\int_0^T u^2(s)\mathrm{d}s\right]<\infty$ *and assume that, for all* $s\in[0,T],u(s)\in\mathbb{D}_{1,2}$ *and that, for all* $t\in[0,T],D_tu\in Dom(\delta)$. *Assume also that* $E\left[\int_0^T\left(\delta(D_tu)\right)^2\mathrm{d}t\right]<\infty$. *Then* $\int_0^T u(s)\delta W_s$ *is well-defined and belongs to* $\mathbb{D}_{1,2}$ *and*

$$D_t\left(\int_0^T u(s)\delta W_s\right)=\int_0^T D_tu(s)\delta W_s+u(t). \tag{9}$$

2.2. Exponential Formula

A Brownian motion martingale can be represented via an exponential formula

when evaluated at a fixed time under certain smoothness conditions.

Definition 2.9 *Given* $\omega \in \Omega$, *a freezing operator* ω^t *is defined as*:

$$W\left(s,\omega^t(\omega)\right)=\begin{cases}W(s,\omega), & \text{if } s\le t;\\ W(t,\omega), & \text{if } t<s\le T.\end{cases} \tag{10}$$

The freezing operator ω^t is a mapping from Ω to Ω. The following equations show some properties of the freezing operator:

Proposition 2.10

1) *For* $p\in\mathcal{P}$, *space of polynomials, suppose* $F=p\left(W_{s_1},\cdots,W_{s_n}\right)$, *then* $F\left(\omega^t\right)=p\left(W_{s_1\wedge t},\cdots,W_{s_n\wedge t}\right)$;

2) $\left(\int_0^T f(s)\mathrm{d}W_s\right)\left(\omega^t\right)=\int_0^t f(s)\mathrm{d}W_s$;

3) $\left(\int_0^T W_s\mathrm{d}s\right)\left(\omega^t\right)=\int_0^t W_s\mathrm{d}s+W_t(T-t)$;

4) $\left(\int_0^T W_s\mathrm{d}W_s\right)\left(\omega^t\right)=\left(\frac{W_T^2-T}{2}\right)\left(\omega^t\right)=\frac{W_t^2-T}{2}$.

We denote the Malliavin derivative of order l of F at time t by $D_t^l F$, as a shorthand notation for $D_t\cdots D_t F$. We call $\mathbb{D}_\infty\left([0,T]\right)$ the set of random variables which are $\mathcal{F}_t$-measurable and infinitely Malliavin differentiable.

Definition 2.11 A random variable F is said to be infinitely Malliavin differentiable if for any integer n:

$$E\left[\left(\sup_{s_1,\cdots,s_n\in(t,T)}\left|\left(D_{s_n}^2\cdots D_{s_1}^2F\right)\right|\right)^2\right]<+\infty. \tag{11}$$

In particular, we denote by $\mathbb{D}^N\left([0,T]\right)$ the space of all random variables F which satisfy (14) for all $n\le N$.

The next theorem, or exponential formula, was obtained by Jin *et al.* (2016). The resulting series (12) is called a *Dyson series*.

Theorem 2.12 *Suppose* $F\in\mathbb{D}_\infty\left([0,T]\right)$ *satisfies the following condition*:

$$\frac{(T-t)^{2n}}{\left(2^n n!\right)^2}E\left[\left(\sup_{u_1,,u_n\in(t,T)}\left|\left(D_{u_n}^2\cdots D_{u_1}^2F\right)\left(\omega^t\right)\right|\right)^2\right]\xrightarrow[n\to\infty]{}0,$$

for fixed $t\in[0,T]$, *then*

$$E\left[F\mid\mathcal{F}_t\right]=\sum_{i=0}^{\infty}\frac{1}{2^i i!}\int_{[t,T]^i}\left(D_{s_i}^2\cdots D_{s_1}^2F\right)\left(\omega^t\right)\mathrm{d}s_i\cdots\mathrm{d}s_1. \tag{12}$$

Example 2.2 *An example of applying the Exponential formula*: *Let* $F=W_T^2$, *then for* $t\le s\le T$: $F\left(\omega^t\right)=W_t^2$ *and* $\left(D_s^2F\right)\left(\omega^t\right)=2$, *then by Theorem* 2.2 *we have*

$$E\left[F\mid\mathcal{F}_t\right]=F\left(\omega^t\right)+\frac{1}{2}\int_t^T\left(D_s^2F\right)\left(\omega^t\right)\mathrm{d}s=W_t^2+T-t. \tag{13}$$

2.3. Faà di Bruno's Formula

Lemma 2.13 ***Faà di Bruno's formula.*** *If f and g are functions with a sufficient*

number of derivatives, then

$$\frac{\mathrm{d}^n}{\mathrm{d}x^n} f\left(g(x)\right) = \sum \frac{n!}{\prod_{i=1}^{n} m_i!} f^{\left(\sum_{k=1}^{n} m_k\right)}\left(g(x)\right) \cdot \prod_{j=1}^{n} \left(\frac{g^{(j)}(x)}{j!}\right)^{m_j}, \tag{14}$$

where the sum is over all n-tuples of non-negative integers $(m_1, \cdots, m_n)$ *satisfying the constraint* $\sum_{k=1}^{n} k m_k = n$. *Combining the terms with the same value of* $\sum_{i=1}^{n} m_i = k$ *leads to a simpler formula expressed in terms of Bell polynomials* $B_{n,k}(x_1, \cdots, x_{n-k+1})$:

$$\frac{\mathrm{d}^n}{\mathrm{d}x^n} f\left(g(x)\right) = \sum_{k=1}^{n} f^{(k)}\left(g(x)\right) \cdot B_{n,k}\left(g'(x), g''(x), \cdots, g^{n-k+1}(x)\right). \tag{15}$$

Definition 2.14 Exponential Bell polynomials. The partial or incomplete exponential Bell polynomials are a triangular array of polynomials given by

$$B_{n,k}(x_1, x_2, \cdots, x_{n-k+1}) = \sum \frac{n!}{\prod_{i=1}^{n-k+1} j_i!} \prod_{i=1}^{n-k+1} \left(\frac{x_i}{i!}\right)^{j_i}, \tag{16}$$

where the sum is taken over all sequences $j_1, j_2, \cdots, j_{n-k+1}$ non-negative integers such that these two conditions are satisfied: $\sum_{i=1}^{n-k+1} j_i = k$ and $\sum_{i=1}^{n-k+1} i \cdot j_i = n$. The sum

$$B_n(x_1, \cdots, x_n) = \sum_{k=1}^{n} B_{n,k}(x_1, x_2, \cdots, x_{n-k+1}), \tag{17}$$

is called the n th complete exponential Bell polynomials.

The Faà di Bruno's formula can be generalized to Malliavin derivative in the following way:

Lemma 2.15 ***Faà di Bruno's formula for Malliavin derivative.*** *If f and g are functions with a sufficient number of derivatives, then for a random variable* $F \in \mathbb{D}^N([0,T])$ *and* $\forall n \le N$, *by theorem* 2.7 *and lemma* 15 *we have*

$$D_t^n f\left(g(F)\right) = \sum_{k=1}^{n} f^{(k)}\left(g(F)\right) \cdot B_{n,k}\left(g'(F), g''(F), \cdots, g^{n-k+1}(F)\right) D_t^n F, \tag{18}$$

where $B_{n,k}(x_1, \cdots, x_{n-k+1})$ *are the incomplete exponential Bell polynomials.*

2.4. Extension to Two Brownian Motions

In what follows, we work with two independent Brownian motions $\{W_t\}_{t\ge 0}$ and $\{Z_t\}_{t\ge 0}$ defined in a probability space $(\Omega, \mathcal{F}, \{\mathcal{F}_t\}_{t\ge 0}, \mathbb{P})$, let $\{\mathcal{F}_t^W\}$ and $\{\mathcal{F}_t^Z\}$ be the filtrations generated by the Brownian motion W_t and Z_t respectively. Let $\mathcal{F}_{t_1}^W \vee \mathcal{F}_{t_2}^Z := \sigma\{W_{s_1}, Z_{s_2}, s_1 \le t_1, s_2 \le t_2\}$ be the filtration generated by two Brownian motions W_t and Z_t. When $t_1 = t_2 = t$, we keep the symbol $\mathcal{F}_t := \mathcal{F}_t^W \vee \mathcal{F}_t^Z$ for the sigma-algebra generated by both Brownian motions.

Let D^W and D^Z be the Malliavin derivation operator w.r.t the Brownian motion W_t and Z_t, this implies that for a $\mathcal{F}_T$ measurable random variable $F(\omega)$, the 2-dimensional directional derivative of F at the point $\omega \in \Omega$ in the direction $\gamma(\gamma_1, \gamma_2) \in \Omega$ by:

$$D_\gamma F(\omega) := \lim_{\epsilon \to 0} \frac{F(\omega + \epsilon\gamma) - F(w)}{\epsilon} = \int_0^T D_s^W F(\omega) \frac{\mathrm{d}\gamma_1}{\mathrm{d}s} \mathrm{d}s + \int_0^T D_s^Z F(\omega) \frac{\mathrm{d}\gamma_2}{\mathrm{d}s} \mathrm{d}s. \tag{19}$$

The freezing operators ω_W^t and ω_Z^t follow the same definition 2.9 as the one dimension case. However, each random variable are depend on the the path of single Brownian motion indicated by its subscript.

3. Preliminaries on Option Pricing

Throughout this paper we shall operate in the context of a complete financial market. Options are an example of a broader class of assets called contingent claims. We will study European call option pricing under stochastic framework. The aim of this section is to review the basic objects, ideas and results of the classical Black-Scholes theory, stochastic volatility models of derivative pricing [11].

Definition 3.1

1) A contingent claim is any asset whose future payoff is contingent on the outcome of some uncertain event.

2) A European call option is a contract that gives its holder the right, but not the obligation, to buy one unit of an underlying asset for predetermined strike price K on the maturity date T.

3.1. The Black-Scholes Theory

The Black-Scholes model is widely used for the dynamics of a financial market containing derivative investment instruments. From the Black-Scholes equation, one can deduce the Black-Scholes formula, which gives a theoretical estimate of the price of European-style options. The Black-Scholes model with constant volatility under risk-neutral probability measure is that the stock price S_t satisfies the following stochastic differential equation:

$$\mathrm{d}S_t = rS_t\mathrm{d}t + \sigma S_t \mathrm{d}W_t, \tag{20}$$

where r and σ are constants. For reasons of convenience, we make the change of variable in the following sections, let $X_t = \ln S_t$ denote the logarithm of stock price, then

$$\mathrm{d}X_t = r - \frac{1}{2}\sigma^2 \mathrm{d}t + \sigma \mathrm{d}W_t, \tag{21}$$

the price V_t of an European call option with payoff $(X_T - K)_+$ at time t for this model with constant volatility σ, current stock price e^x, maturity time T and interest rate r, satisfy the risk-neutral pricing formula [12]:

$$V_t = \mathrm{e}^{-r(T-t)} E\left[(S_T - K)^+ \mid \mathcal{F}_t \right]. \tag{22}$$

And the closed-form solution of Black-Scholes PDE is the Black-Scholes-Merton formula:

$$V_t = BS(t,x,\sigma) := \mathrm{e}^x N(d_+) - K\mathrm{e}^{-r(T-t)} N(d_-), \tag{23}$$

where

$$d_\pm(t,\sigma) = \frac{X_t - \ln K + \left(r \pm \frac{\sigma^2}{2}\right)(T-t)}{\sigma\sqrt{T-t}}, \tag{24}$$

and

$$N(x) = \frac{1}{\sqrt{2\pi}} \int_{-\infty}^{x} \mathrm{e}^{\frac{-y^2}{2}} \mathrm{d}y = \frac{1}{\sqrt{2\pi}} \int_{-x}^{\infty} \mathrm{e}^{\frac{-y^2}{2}} \mathrm{d}y. \tag{25}$$

is the standard normal cumulative distribution function. The derivation consists of finding a self-financing investment strategy, that replicates the call option payoff structure and assume that one continuously adjusts the replicating portfolio over time.

3.2. Stochastic Volatility Models

That it might make sense to model volatility as a random variable should be clear to the most casual observer of equity markets. Nevertheless, given the success of the Black-Scholes model in parsimoniously describing market option prices, it's not immediately obvious what the benefit of making such a modeling choice might be.

3.2.1. SABR (Stochastic Alpha Beta Rho) Model with $\beta = 1$

Stochastic volatility models are useful because they explain in a self-consistent way why options with different strike and expiration have different Black-Scholes implied volatility. And moreover, stochastic volatility models assume realistic dynamics for the underlying. Specifically, the SABR model is an extension of the Black Scholes model in which the volatility parameter follows a stochastic process:

$$\mathrm{d}S_t = rS_t\mathrm{d}t + \sigma_t S_t^\beta \left(\rho \mathrm{d}W_t + \sqrt{1-\rho^2}\mathrm{d}Z_t\right), \tag{26}$$

$$\mathrm{d}\sigma_t = \alpha\sigma_t \mathrm{d}W_t. \tag{27}$$

The two Brownian motions, W_t and Z_t are independent. It can be shown by Lévy's Theorem that $M_t := \rho \mathrm{d}W_t + \sqrt{1-\rho^2}\mathrm{d}Z_t$ is a Brownian motion, thus $\mathrm{d}M_t \mathrm{d}W_t = \rho \mathrm{d}t$. Volatility does note mean revert in the SABR model, so it is only good for short expirations. Nevertheless the model has the virtue of having an exact expression for the implied volatility smile in the short-expiration limit $\tau := T - t \to 0$. The resulting functional form can be used to fit observed short-dated implied volatilities and the model parameters α, β and ρ thereby extracted.

Hagan *et al.* derived, with perturbation techniques, an approximating direct formula for this implied volatility under the SABR model in [3]:

$$\begin{aligned}&\sigma_{BS}(S_0,K)\\&=\frac{\sigma_0}{(S_0K)^{(1-\beta)/2}\left[1+\frac{(1-\beta)^2}{24}\ln^2\frac{S_0}{K}+\frac{(1-\beta)^4}{1920}\ln^4\frac{S_0}{K}+\cdots\right]}\frac{z}{x(z)}\\&\cdot\left[1+\left(\frac{(1-\beta)^2}{24}\frac{\sigma_0^2}{(S_0K)^{1-\beta}}+\frac{1}{4}\frac{\rho\beta\alpha\sigma_0}{(S_0K)^{(1-\beta)/2}}+\frac{2-3\rho^2}{24}\alpha^2\right)\tau+O(\tau^2)\right],\end{aligned}\tag{28}$$

where $z:=-\frac{\alpha}{\sigma_0}(S_0K)^{(1-\beta)/2}\log\left(\frac{S_0}{K}\right)$ and $x(z)=\ln\left(\frac{\sqrt{1-2\rho z+z^2}+z-\rho}{1-\rho}\right)$.

For the case of at-the money options, *i.e.* when $S_0=K$, this formula reduces to

$$\sigma_{BS}(S_0,S_0)=\frac{\sigma_0}{S_0^{1-\beta}}\cdot\left[1+\left(\frac{(1-\beta)^2\sigma_0^2}{24S_0^{2-2\beta}}+\frac{\rho\beta\alpha\sigma_0}{4S_0^{1-\beta}}+\frac{2-3\rho^2}{24}\alpha^2\right)\tau+O(\tau^2)\right].\tag{29}$$

In the special case $\beta=1$, the SABR implied volatility formula reduces to

$$\sigma_{BS}(S_0,K)=\sigma_0\frac{y}{f(y)}\left[1+\left(\frac{1}{4}\rho\alpha\sigma_0+\frac{2-3\rho^2}{24}\alpha^2\right)\tau+O(\tau^2)\right],\tag{30}$$

where $y:=-\frac{\alpha}{\sigma_0}\log\left(\frac{S_0}{K}\right)$ and $f(y)=\ln\left(\frac{\sqrt{1-2\rho y+y^2}+y-\rho}{1-\rho}\right)$.

3.2.2. Exponential Functions of Brownian Motion

Marc Yor's discovery (1992) of an integral formula for joint density of the distribution of a Brownian motion and the integral of exponential Brownian motion taken over a finite time interval has been computed in the case $\sigma=2$.

Proposition 3.2 ***Marc Yor's formula.*** *Applying Brownian motion rescaling* [13], *this joint density of* $\left(\int_0^t e^{\sigma W_s}ds, W_t\right)$, $\sigma>0$ *can be written for an arbitrary volatility parameter* σ *as*

$$\begin{aligned}\phi_{t,\sigma}(x,y)&:=\frac{1}{dxdy}\mathbb{P}\left(\int_0^t e^{\sigma W_s}ds\in dx, W_t\in dy\right)\\&=\frac{\sigma}{2x}e^{-\frac{2}{\sigma^2x}\left(1+e^{\sigma y}\right)}\cdot\theta\left(\frac{4e^{\sigma y/2}}{\sigma^2x},\frac{\sigma^2t}{4}\right),\end{aligned}\tag{31}$$

for $x>0, y\in R, t>0$, *where*

$$\theta(r,t)=\frac{r}{\sqrt{2\pi^3t}}e^{\frac{\pi^2}{2t}}\int_0^\infty e^{-\frac{\xi^2}{2t}}\cdot e^{-r\cosh\xi}\sinh\xi\sin\frac{\pi\xi}{t}d\xi,\ \ r,t>0.\tag{32}$$

By Lyasoff [14], (32) *is equivalent to the following*:

$$\theta(r,t)=\frac{r}{\sqrt{2\pi^3t}}e^{\frac{\pi^2}{2t}}\int_0^\infty e^{-\frac{\xi^2}{2t}}\cdot\cosh\xi\cos\left(r\sinh\xi-\frac{\pi\xi}{2t}\right)d\xi,\ \ r,t>0.\tag{33}$$

From computational point of view, the $\frac{\pi}{2}$-formula: (31) with $\theta(\cdot)$ defined

as (33), may be preferable to the π-formula: (31) with $\theta(\cdot)$ defined as (32).

Proposition 3.3 *A straightforward application of the Cameron-Martin-Girsanov theorem implies that the joint density of* $\left(\int_0^t e^{\sigma W_s - \mu s} ds, W_t\right)$, $\sigma > 0, \mu \in \mathbb{R}$, *which we denote by* $\phi_{t,\sigma,\mu}(x,y)$, $x > 0, y \in \mathbb{R}$, *can be connected with the density* $\phi_{t,\sigma}(x,y) = \phi_{t,\sigma,0}(x,y)$ *through the formula*

$$\phi_{t,\sigma,\mu}(x,y) = e^{-\frac{\mu}{\sigma}y + \frac{\mu^2 t}{2\sigma^2}} \phi_{t,\sigma,0}\left(x, y - \frac{\mu}{\sigma}t\right). \tag{34}$$

4. Hull and White Formula and Extension

The no-arbitrage price at time t using the risk-neutral theory for any derivatives with terminal time T and payoff function $h(x)$ is given by the risk-neutral formula below:

$$V_t = E\left[e^{-r(T-t)} h(X_T) \mid \mathcal{F}_t\right]. \tag{35}$$

Thus V_t is a no-arbitrage price for the contingent claim. In what follows, we consider the pricing of a call option, *i.e.*:

$$h(X_T) = \left(e^{X_T} - K\right)^+. \tag{36}$$

4.1. Hull-White Formula: Uncorrelated Volatility

Under the assumption that the volatility σ_t is uncorrelated with the asset price driven by another Brownian motion Z_t, *i.e.* when $\rho = 0$, the pricing formula (35) can be further simplified. By conditioning on the path of the volatility process and using the iterated conditioning property, the European call option price is given by

$$V(t, X_t, \sigma_t) = e^{-r(T-t)} E\left[E\left[\left(e^{X_T} - K\right)^+ \mid \mathcal{F}_t \vee \mathcal{F}_T^W\right]\right]. \tag{37}$$

The inner expectation is the Black-Scholes computation with a time-dependent volatility. Since σ_t is a Markov process, we can apply the Black-Scholes formula, and obtain:

$$V(t,x,y) = E\left[BS(t,x;K,T;v_t) \mid Y_t = y\right], \tag{38}$$

where

$$v_t^2 = \frac{1}{T-t}\int_t^T \sigma_s^2 ds, \tag{39}$$

is the root-mean-square time future average volatility.

4.2. Hull-White Formula: Correlated Volatility

In general, the situation is more complicated when volatility is correlated with the Brownian motion W_t driving the stock price. Again we can use iterated expectation to price a European call option.

$$V(t,x,y) = E\left[\xi_t BS\left(t,x;K\xi_t^{-1},T;\bar{\sigma}_\rho\right) \mid Y_t = y\right], \tag{40}$$

where

$$\xi_t = \exp\left(\rho\int_t^T \sigma_s \mathrm{d}\hat{Z}_s - \frac{1}{2}\rho^2\int_t^T \sigma_s^2 \mathrm{d}s\right), \tag{41}$$

$$\bar{\sigma}_\rho^2 = \frac{1}{T-t}\int_t^T \left(1-\rho^2\right)\sigma_s^2 \mathrm{d}s. \tag{42}$$

The Hull-White formula is of practical use for Monte Carlo simulation of prices in a correlated stochastic volatility model since only one Brownian motion path has to be generated. However, it does not directly reveal any information about the implied volatility curve like the uncorrelated case.

4.3. A Generalization of Hull-White Formula

The classical Hull-White formula for option pricing can be extended, by means of Malliavin Calculus, to the correlated case. The main problem is that average future volatility is not adapted, however, this issue can be resolved by anticipating stochastic calculus. And this method decomposes option prices as the sum of the same derivative price if there is no correlation and a correction due by correlation. The following theorem is due to Alòs *et al.* (2006).

Theorem 4.1 *Consider model* (26)-(27) *with* $\beta = 1$, *and assume the following hypotheses hold*:

1) *The payoff function* $h: \mathbb{R} \to \mathbb{R}_+$ *is continuous and piecewise* $\mathcal{C}^1$;

2) *There exists a positive real constant a such that* $a \le \sigma_t^2$ *for all* $t \in [0,T]$;

3) $\sigma^2 \in \mathcal{L}_W^{1,2}([0,T])$;

4) *For all* $t \in [0,T]$ *there exists a positive constant C such that for all* $s \in [0,T]$,

$$\left|E\left[\left(\int_s^T D_s^W \sigma_r^2 \mathrm{d}r\right)\sigma_s \mid \mathcal{F}_t\right]\right| \le C. \tag{43}$$

Then, for all $t \in [0,T]$,

$$V_t = E\left[BS\left(t, X_t, v_t\right) \mid \mathcal{F}_t\right] + \frac{\rho}{2}E\left[\int_t^T \mathrm{e}^{-r(s-t)} H\left(s, X_s, v_s\right)\Lambda_s \mathrm{d}s \mid \mathcal{F}_t\right], \tag{44}$$

where v_t^2 *is the future average volatility defined* (39) *in Subsection* 4.1 *and*

$$H\left(s, X_s, v_s\right) := \left(\frac{\partial^3}{\partial x^3} - \frac{\partial^2}{\partial x^2}\right) BS\left(s, X_s, v_s\right), \tag{45}$$

$$\Lambda_s := \left(\int_s^T D_s^W \sigma_r^2 \mathrm{d}r\right)\sigma_s. \tag{46}$$

Notice that formula (44) does not reduce the dimensionality of the problem but identifies the impact of correlation. When $\rho = 0$, it is the same as (38).

5. Dyson Series in the Return's Idiosyncratic Noise

5.1. Application of Marc Yor's Formula

Throughout this and next section we denote by $V_{t_1,t_2} := \int_{t_1}^{t_2} \sigma_u^2 \mathrm{d}u$ a cumulative time integral, from t_1 to t_2, of future volatility, *i.e.* $V_{s,T} = v_s^2(T-s)$. The aim

of this paper is to extend Theorem 4.1 to a deterministic form by specifically assuming the underlying asset and volatility process follow (26), then σ_t is a square integrable process adapted to $\left\{\mathcal{F}_t^W\right\}$.

Lemma 5.1 *The conditional probability density function of* $V_{s,T}$ *is* $\frac{1}{\sigma_s^2}\psi_{V_{s,T}}\left(\frac{v}{\sigma_s^2}\right)$.

where

$$y_{V_{s,T}}(v)=\int_{-\infty}^{\infty}\phi_{T-s,2\alpha,\alpha^2}(v,z)\mathrm{d}z. \tag{47}$$

One straightforward application of (47) is using the conditional density of $V_{t,T}$ to obtain the first conditional expectation in (44):

Theorem 5.2 *The conditional expectation of* $BS(t,X_t,v_t)$ *is*

$$E\left[BS(t,X_t,v_t)\,|\,\mathcal{F}_t\right]=\int_0^{\infty}BS\left(t,X_t,\sqrt{\frac{v}{T-t}}\right)\frac{1}{\sigma_t^2}\psi_{V_{t,T}}\left(\frac{v}{\sigma_t^2}\right)\mathrm{d}v. \tag{48}$$

5.2. Application of Exponential Formula

Theorem 5.3 *For* $t\le s$, *define* $G(s,X_s,v_s)=\sum_{n=0}^{\infty}\frac{1}{2^n n!}g_n(s,X_t,v_t)$, *where* $g_n(s,X_t,v_t)=\omega_Z^t\circ\int_{[t,T]^n}D_{\tau^{\otimes n}}^{2n,Z}H(s,X_s,v_s)\mathrm{d}\tau^{\otimes n}$. *Let* G_s,H_s *be the short notation for* $G(s,X_s,v_s)$ *and* $H(s,X_s,v_s)$, *then the option price* (44) *can be further simplified as the following*:

$$V_t=E\left[BS(t,X_t,v_t)\,|\,\mathcal{F}_t\right]+\frac{\rho}{2}\int_t^T\mathrm{e}^{-r(s-t)}E\left[\Lambda_s G_s\,|\,\mathcal{F}_t\right]\mathrm{d}s. \tag{49}$$

here $\otimes$ denotes the tensor power. In general, the tensor product $f\otimes g$ of two functions f,g is defined by $f\otimes g(x_1,x_2)=f(x_1)g(x_2)$. See [15] for more detail.

Now we use Malliavin calculus to deduce a full asymptotic series for $G(s,X_s,v_s)$ and use it to obtain $E\left[\Lambda_s G_s\,|\,\mathcal{F}_t\right]$ in (49), which gives us a deterministic formula for European option price. By (21) and (23),

$$\begin{aligned}X_s&=X_t+\int_t^s r-\frac{1}{2}\sigma_u^2\mathrm{d}u+\int_t^s\sigma_u\left(\rho\mathrm{d}W_u+\sqrt{1-\rho^2}\mathrm{d}Z_u\right)\\&=X_t+r(s-t)-\frac{1}{2}V_{t,s}+\frac{\rho}{\alpha}(\sigma_s-\sigma_t)+\sqrt{1-\rho^2}\int_t^s\sigma_u\mathrm{d}Z_u.\end{aligned} \tag{50}$$

Note that the volatility process in (26) is the differential notation for $\sigma_t-\sigma_0=\int_0^t\alpha\sigma_u\mathrm{d}W_u$, and obviously for $0<t<s$, $\sigma_s-\sigma_t=\int_t^s\alpha\sigma_u\mathrm{d}W_u$. And accordingly by (50) and (24), $d_{\pm}(s,X_s,v_s)=\dfrac{X_s-\ln K+\left(r\pm\frac{v_s^2}{2}\right)(T-s)}{\sqrt{V_{s,T}}}$.

Therefore by Theorem 2.7,

$$D_\tau^Z X_s=D_\tau^Z\int_t^s\sigma_u\sqrt{1-\rho^2}\mathrm{d}Z_u=\sigma_\tau\sqrt{1-\rho^2}\mathbb{1}_{\{\tau\le s\}}, \tag{51}$$

$$D_\tau^Z d_+ = D_\tau^Z d_- = \frac{D_\tau^Z X_s}{v_s\sqrt{T-s}} = \frac{\sigma_\tau\sqrt{1-\rho^2}\,\mathbb{1}_{\{\tau\le s\}}}{v_s\sqrt{T-s}}. \tag{52}$$

Lemma 5.4 *Let two real-valued functions* $p(t,x,\sigma)$ *and* $q(t,x,\sigma)$ *be defined as following*:

$$p(t,x,\sigma) = x - \frac{d_+^2(x,t)}{2} + \ln\left(-d_-(x,t)\right), \tag{53}$$

$$q(t,x,\sigma) = \frac{1}{\sqrt{2\pi\sigma^2(T-t)}}\mathrm{e}^x. \tag{54}$$

Then the $2n^{th}$ *order Malliavin derivative of* H_s *can be expressed as*:

$$D_{\tau\otimes n}^{2n,Z} H_s = \left(1-\rho^2\right)^n H_s B_{2n}\left(p'(\cdot), p''(\cdot), \cdots, p^{(2n)}(\cdot)\right)\prod_{i=1}^n \sigma_{\tau_i}^2 \mathbb{1}_{\{\tau_i\le s\}}, \tag{55}$$

where

$$p^{(j)}(s, X_s, v_s) = \begin{cases} \dfrac{(-1)^{j+1} - d_-^2}{\left(\sqrt{V_{s,T}}\,d_-\right)^j} & \text{when } j = 1,2; \\ \dfrac{(-1)^{j+1}(j-1)!}{\left(\sqrt{V_{s,T}}\,d_-\right)^j} & \text{for } j \ge 3. \end{cases} \tag{56}$$

for d_- *evaluated at* (s, X_s, v_s).

The second step to calculate $G(s, X_s, v_s)$ is to apply freezing operator ω_Z^t to $D_{\tau\otimes n}^{2n,Z} H_s$ for $n = 0,1,2,\cdots$. Let $\mathcal{X}$ be any random variable depend on Brownian motion $\{Z_t\}_{t\ge 0}$, denote $\mathcal{X}_Z^\omega := \omega_Z^t \circ \mathcal{X}$ be the random variable $\mathcal{X}$ applied by the freezing operator ω_Z^t, by Proposition 2.10,

$$\begin{aligned} X_s^\omega &:= X_t + r(s-t) - \frac{1}{2}\int_t^s \sigma_u^2 \mathrm{d}u + \frac{\rho}{\alpha}(\sigma_s - \sigma_t) + \omega_Z^t \circ \int_t^s \sigma_u\sqrt{1-\rho^2}\,\mathrm{d}Z_u \\ &= X_t + r(s-t) - \frac{1}{2}V_{t,s} + \frac{\rho}{\alpha}(\sigma_s - \sigma_t), \end{aligned} \tag{57}$$

and accordingly we have

$$d_\pm^\omega(s, X_s, v_s) = d_\pm\left(s, X_s^\omega, v_s\right) = \frac{X_s^\omega - \ln K + \left(r \pm \dfrac{v_s^2}{2}\right)(T-s)}{\sqrt{V_{s,T}}}, \tag{58}$$

$$H_s^\omega = \frac{\sqrt{V_{s,T}} - d_+^\omega}{\sqrt{2\pi V_{s,T}}}\mathrm{e}^{X_s^\omega - \frac{d_+^{\omega 2}}{2}} = \frac{-d_-^\omega}{\sqrt{2\pi V_{s,T}}}\mathrm{e}^{X_s^\omega - \frac{d_+^{\omega 2}}{2}}. \tag{59}$$

Therefore in general, for $n = 0,1,2,\cdots$,

$$\begin{aligned} &D_{\tau\otimes n}^{2n,Z} H_s^\omega \\ &= \omega_Z^t \circ \left[\left(1-\rho^2\right)^n H_s B_{2n}\left(p'(s, X_s, v_s), \cdots, p^{(2n)}(s, X_s, v_s)\right)\prod_{i=1}^n \sigma_{\tau_i}^2\right] \\ &= \left(1-\rho^2\right)^n H_s^\omega B_{2n}\left(p'\left(s, X_s^\omega, v_s\right), \cdots, p^{(2n)}\left(s, X_s^\omega, v_s\right)\right)\prod_{i=1}^n \sigma_{\tau_i}^2 \mathbb{1}_{\{\tau_i\le s\}}, \end{aligned} \tag{60}$$

where $p^{(j)}\left(s, X_s^\omega, v_s\right) := \omega_Z^t \circ p^{(j)}(s, X_s, v_s)$ is given by (56) except that d_- is

now evaluated at $\left(s, X_s^{\omega}, v_s\right)$. Thus, by (60), we are able to compute G_s in the following:

$$\begin{aligned} G_s &= \sum_{n=0}^{\infty} \frac{1}{2^n n!} \omega_Z^t \circ \int_{[t,T]^n} D_{\tau^{\otimes n}}^{2n,Z} H\left(s, X_s, v_s\right) \mathrm{d}\tau^{\otimes n} \\ &= \sum_{n=0}^{\infty} \frac{\left(1-\rho^2\right)^n}{2^n n!} H_s^{\omega} B_{2n}\left(p'\left(s, X_s, v_s\right), \cdots, p^{(2n)}\left(s, X_s, v_s\right)\right) \\ &\quad \cdot \int_{[t,T]^n} \prod_{i=1}^n \sigma_{\tau_i}^2 \mathbb{1}_{\{\tau_i \le s\}} \mathrm{d}\tau^{\otimes n} \\ &= H_s^{\omega} \sum_{n=0}^{\infty} \frac{\left(1-\rho^2\right)^n}{2^n n!} \left(V_{t,s}\right)^n B_{2n}\left(p'\left(s, X_s^{\omega}, v_s\right), \cdots, p^{(2n)}\left(s, X_s^{\omega}, v_s\right)\right). \end{aligned} \tag{61}$$

5.3. Option Pricing Formula for SABR Model

Lemma 5.5 *Let* $L_s^{\omega} = V_{s,T} H_s^{\omega} = \frac{-d_-^{\omega}}{\sqrt{2\pi}} \mathrm{e}^{X_s^{\omega} - \frac{d_+^{\omega 2}}{2}}$ *and* $f\left(s, X_s, v_s\right) = V_{s,T} G\left(s, X_s, v_s\right)$, *given that* G_s *is a function in terms of* X_s *and* $V_{s,T}$ *in* (61), *then conditional expectation of the product of* Λ_s *and* G_s *can be calculated as the following*:

$$E\left[\Lambda_s G_s \mid \mathcal{F}_t\right] = 2\alpha \int_0^{\infty} \int_{-\infty}^{\infty} h\left(\sigma_t^2 x, \sigma_s\left(y\right)\right) \phi_{s-t,2\alpha,\alpha^2}\left(x, y\right) \mathrm{d}y \mathrm{d}x, \tag{62}$$

where $h\left(V_{t,s}, \sigma_s\left(W_s - W_t\right)\right) = \frac{1}{\sigma_s} \int_0^{\infty} f\left(s, X_s\left(V_{t,s}, \sigma_s\right), \sqrt{\frac{v}{T-s}}\right) \psi_{V_{s,T}}\left(\frac{v}{\sigma_s^2}\right) \mathrm{d}v$.

Remark *Equation* (57) *shows that* X_s^{ω} *is a function depends only on two random variables*: $V_{t,s}$ *and* σ_s, *i.e.* $X_s^{\omega}\left(V_{t,s}, \sigma_s\right) = X_t + r\left(s-t\right) - \frac{1}{2}\int_t^s \sigma_u^2 \mathrm{d}u + \frac{\rho}{\alpha}\left(\sigma_s - \sigma_t\right)$. *While* σ_s *itself is a function of* $W_s - W_t$. *The joint density for* $\left(V_{t,s}, W_{s-t}\right)$ *is given by Marc Yor's formula, Proposition* (3.2) *in Section* 3, *with properly parameters.*

Remark $X_s^{x,y}$ *represent a real-valued function of* (s, x, y) *which mimic the definition of* X_s^{ω} *but replace* $V_{t,s}$ *and* $W_s - W_t$ *with x and y.*

Theorem 5.6 ***Full Dyson Series Expansion.*** *For SABR model* (26)-(27) *with* $\beta = 1$, *let* $c = \frac{(T-t)\sqrt{1-\rho^2}}{\sqrt{2}}$ *and assume that*

$$\frac{c^{2n}}{n!^2} E\left[\left(\sup_{\tau_i \in (t,T)} \left| H_s B_{2n}\left(p'\left(s, X_s, v_s\right), \cdots, p^{(2n)}\left(s, X_s, v_s\right)\right) \prod_{i=1}^n \sigma_{\tau_i}^2 \mathbb{1}_{\{\tau_i \le s\}} \right|\right)^2\right] \xrightarrow[n\to\infty]{} 0.$$

Let $p(\cdot)$ *and* $f(\cdot)$ *be defined in Lemma* 5.4 *and Lemma* 5.5, *respectively, then for all* $t \in [0,T]$,

$$\begin{aligned} V_t &= \int_0^{\infty} \int_{-\infty}^{\infty} \frac{1}{\sigma_t^2} BS\left(t, X_t, \sqrt{\frac{v}{T-t}}\right) \phi_{T-t,2\alpha,\alpha^2}\left(\frac{v}{\sigma_t^2}, z\right) \mathrm{d}z \mathrm{d}v \\ &\quad + \rho\alpha \int_t^T \int_0^{\infty} \int_{-\infty}^{\infty} \int_0^{\infty} \int_{-\infty}^{\infty} l\left(s, v, z, x, y\right) \mathrm{d}z \mathrm{d}v \mathrm{d}y \mathrm{d}x \mathrm{d}s, \end{aligned} \tag{63}$$

where

$$l(s,v,z,x,y)=\frac{\mathrm{e}^{-r(s-t)}}{\sigma_s(y)}\cdot f\left(s,X_s^{x,y},\sqrt{\frac{v}{T-s}}\right)\cdot\phi_{T-s,2\alpha,\alpha^2}\left(\frac{v}{\sigma_s^2},z\right)\cdot\phi_{s-t,2\alpha,\alpha^2}(x,y). \tag{64}$$

Example 5.1 First Order Approximation. Let $m>0$, define

$$f_m(s,X_s,v_s):=L_s^{\omega}\sum_{n=0}^{m}\frac{\left(\left(1-\rho^2\right)V_{t,s}\right)^n}{2^n n!}B_{2n}\left(p'\left(X_s^{\omega}\right),p''\left(X_s^{\omega}\right),\cdots,p^{2n}\left(X_s^{\omega}\right)\right), \tag{65}$$

then the first order approximation $f_1(s,v_s,X_s)$ is calculated as following:

$$\begin{aligned}f_1(s,X_s,v_s)&=L_s^{\omega}\left(1+\frac{\left(1-\rho^2\right)V_{t,s}}{2}\left[\left(p^{(1)}\left(X_s^{\omega}\right)\right)^2+p^{(2)}\left(X_s^{\omega}\right)\right]\right)\\&=L_s^{\omega}\left(1+\frac{\left(1-\rho^2\right)V_{t,s}}{2}\left[\left(\frac{1-d_-^2}{\sqrt{V_{s,T}}d_-}\right)^2+\frac{-1-d_-^2}{\left(\sqrt{V_{s,T}}d_-\right)^2}\right]\right)\\&=\frac{-d_-^{\omega}}{\sqrt{2\pi}}\mathrm{e}^{X_s^{\omega}-\frac{d_+^{\omega 2}}{2}}\left(1+\frac{\left(1-\rho^2\right)V_{t,s}}{2}\frac{d_-^{\omega 2}-3}{V_{s,T}}\right).\end{aligned} \tag{66}$$

6. Dyson Series in the Common Noise

6.1. First Order Approximation Pricing Formula for SABR Model

One obvious drawback of formula (66) is that the option price is a 7-dimensional integral when the volatility is correlated with underlying asset, which could be computationally expensive, even for the first order approximation. In this section, we reverse the order of the two major steps that have been used in previous section by first using the conditional probability density to solve one Brownian motion, then apply Exponential formula to the remaining. For simplicity, we denote $J=\frac{\rho}{2}E\left[\int_t^T\mathrm{e}^{-r(s-t)}H_s\Lambda_s\mathrm{d}s\,|\,\mathcal{F}_t\right]$ as the correlation correction term of option price (44) in Theorem 4.1. Therefore the option price is the sum of conditional expectation of Black-Scholes and the correction term: $V_t=E\left[BS(t,X_t,v_t)\,|\,\mathcal{F}_t\right]+J$.

Theorem 6.1 *Let* $C_1=\frac{1}{\sqrt{2\pi}}\rho\alpha K\mathrm{e}^{-r(T-t)}$, $Q_s=E\left[-d_-\mathrm{e}^{-\frac{d_-^2}{2}}\,|\,\mathcal{F}_T^W\cup\mathcal{F}_t^Z\right]$, *then the correction term can be written as* $J=C_1\int_t^T E\left[\sigma_s Q_s\,|\,\mathcal{F}_t\right]\mathrm{d}s$.

Lemma 6.2 *Let* $C_2=-\frac{1}{\left(2-\rho^2\right)^{3/2}}$, $C_3=-\frac{1}{2\left(2-\rho^2\right)}$, $\kappa=X_t-\ln K+r(T-t)$ *and define*

$$\gamma\left(V_{t,s},V_{s,T},\sigma_s\right):=\frac{\kappa+\frac{\rho}{\alpha}\left(\sigma_s-\sigma_t\right)-\frac{1}{2}\left(V_{t,s}+V_{s,T}\right)}{\sqrt{V_{s,T}}},$$ *for simplicity, we write* γ *in-*

stead of $\gamma\left(V_{t,s},V_{s,T},\sigma_s\right)$ *hereafter, then* Q_s *defined in the above theorem is calculated as* $Q_s = C_2\gamma \mathrm{e}^{C_3\gamma^2}$.

Theorem 6.3 *For* $\forall t \le s$, *define* $R\left(s,X_s,v_s\right)=\dfrac{\sigma_s Q_s}{C_2}$, *let* R_s *be the short notation for* $R\left(s,X_s,v_s\right)$, *define* $r_n\left(s,X_t,v_t\right)=\omega_W^t \circ \int_{[t,T]^n} D_{\tau\otimes n}^{2n,W} R_s \mathrm{d}\tau^{\otimes n}$. *Let* $c=\dfrac{T-t}{\sqrt{2}}$, *assume that* $\dfrac{c^{2n}}{n!^2}E\left[\left(\sup\limits_{\tau_i\in(t,T)} \left| D_{\tau\otimes n}^{2n,W} R_s\right|\right)^2\right] \xrightarrow[n\to\infty]{} 0$, *then the correction term of the option price in* (44) *can be further simplified as the following*:

$$J = C_1\int_t^T E\left[\sigma_s Q_s \mid \mathcal{F}_t\right]\mathrm{d}s = C_1C_2\int_t^T \sum_{n=0}^{\infty}\frac{1}{2^n n!} r_n\left(s,X_t,v_t\right)\mathrm{d}s. \tag{67}$$

Corollary 1 *By Theorem* 6.3, *let* $m>0$, *then the* m^{th} *order approximation for the correction term can be obtained by*

$$J \approx J_m = C_1C_2\int_t^T \sum_{n=0}^{m}\frac{1}{2^n n!} r_n\left(s,X_t,v_t\right)\mathrm{d}s. \tag{68}$$

Corollary 2 ***First order approximation by time integral.*** *For* $\forall s\in[t,T]$, *there exists two analytical functions* $p(s)$ *and* $q(s)$, (71) *and* (70), *such that the first order approximation for the correction term of the option price is a time integral of the sum of those two functions*:

$$J_1 = \frac{1}{2}C_1C_2\left[\int_t^T\left[p(s)+q(s)\right]\mathrm{d}s + 2(T-t)\right]. \tag{69}$$

$$q(s) = R_s^{\omega}\left[-2\alpha^2\left(2C_3^2\left(\gamma^{\omega 3}+\sqrt{V_{s,T}^{\omega}}\gamma^{\omega 2}\right)+1+\frac{\sqrt{V_{s,T}^{\omega}}}{\gamma^{\omega}}\right)+4\alpha^2 {V_{s,T}^{\omega}}^2 \mathcal{A}_3^{\omega}\right](T-s), \tag{70}$$

$$\begin{aligned}
p(s) = R_s^{\omega}\Bigg[\Bigg[&\frac{\rho\alpha^2\mathrm{e}^{-\frac{1}{2}\alpha^2(s-t)}(s-t)}{\sqrt{\mathrm{e}^{-\alpha^2(s-t)}-\mathrm{e}^{-\alpha^2(T-t)}}}-\frac{2\alpha\sigma_t\left(\frac{1}{\alpha^2}\left(1-\mathrm{e}^{-\alpha^2(s-t)}\right)-(s-t)\mathrm{e}^{-\alpha^2(s-t)}\right)}{\mathrm{e}^{-\alpha^2(s-t)}-\mathrm{e}^{-\alpha^2(T-t)}}\\
&-2\alpha^2\left(\sqrt{\frac{\sigma_t^2}{\alpha^2}\left(\mathrm{e}^{-\alpha^2(s-t)}-\mathrm{e}^{-\alpha^2(T-t)}\right)}+\gamma^{\omega}\right)\cdot\frac{\frac{1}{\alpha^2}\left(1-\mathrm{e}^{-\alpha^2(s-t)}\right)-(s-t)\mathrm{e}^{-\alpha^2(T-t)}}{\mathrm{e}^{-\alpha^2(s-t)}-\mathrm{e}^{-\alpha^2(T-t)}}\\
&+2\frac{\left(\rho\alpha^2\mathrm{e}^{-\frac{1}{2}\alpha^2(s-t)}+\alpha\sigma_t\mathrm{e}^{-\alpha^2(s-t)}\right)(s-t)-\frac{\sigma_t}{\alpha}\left(1-\mathrm{e}^{-\alpha^2(s-t)}\right)}{\sqrt{\mathrm{e}^{-\alpha^2(s-t)}-\mathrm{e}^{-\alpha^2(T-t)}}}\Bigg]\cdot\left(\frac{1}{\gamma^{\omega}}+2C_3\gamma^{\omega}\right)\\
&+\frac{\left(\rho\alpha\mathrm{e}^{-\frac{1}{2}\alpha^2(s-t)}+\sigma_t\mathrm{e}^{-\alpha^2(s-t)}\right)^2(s-t)-2\frac{\rho}{\alpha}\sigma_t\left(\mathrm{e}^{-\frac{1}{2}\alpha^2(s-t)}-\mathrm{e}^{-\frac{3}{2}\alpha^2(s-t)}\right)+\frac{\sigma_t^2}{2\alpha^2}\left(3\mathrm{e}^{-2\alpha^2(s-t)}-4\mathrm{e}^{-\alpha^2(s-t)}+1\right)}{\mathrm{e}^{-\alpha^2(s-t)}-\mathrm{e}^{-\alpha^2(T-t)}}\\
&\cdot\left(6C_3+4C_3^2\gamma^{2,\omega}\right)-2\sigma_t^3\frac{\rho}{\alpha}\mathrm{e}^{-\frac{1}{2}\alpha^2(s-t)}\left(\frac{1}{\alpha^2}\left(1-\mathrm{e}^{-\alpha^2(s-t)}\right)-(s-t)\mathrm{e}^{-\alpha^2(T-t)}\right)\mathcal{A}_1^{\omega}
\end{aligned}$$

$$+\frac{4\sigma_t^4}{\alpha^4}\left[\left(\frac{1}{2}\left(1-\mathrm{e}^{-2\alpha^2(s-t)}\right)+\left(\mathrm{e}^{-2\alpha^2(s-t)}+\mathrm{e}^{-2\alpha^2(s-t+T-t)}-\mathrm{e}^{-\alpha^2(s-t)}-\mathrm{e}^{-\alpha^2(T-t)}\right)+\alpha^2\mathrm{e}^{-\alpha^2(T-t+s-t)}(s-t)\right)\mathcal{A}_2^{\omega}\right.$$

$$\left.+\left(\frac{1}{2}\left(1-\mathrm{e}^{-2\alpha^2(s-t)}\right)+2\left(\mathrm{e}^{-\alpha^2(T-t+s-t)}-\mathrm{e}^{-\alpha^2(T-t)}\right)+\alpha^2\mathrm{e}^{-2\alpha^2(T-t)}(s-t)\right)\mathcal{A}_3^{\omega}\right]+\alpha^2(s-t)\Bigg], \tag{71}$$

where

$$\mathcal{A}_1^{\omega}=\frac{4C_3^2\gamma^{\omega 3}+4C_3^2\sqrt{V_{s,T}^{\omega}}\gamma^{\omega 2}+8C_3\gamma^{\omega}+6C_3\sqrt{V_{s,T}^{\omega}}}{\sqrt{V_{s,T}^{\omega\,3}}}$$
$$+\frac{1}{\sqrt{V_{s,T}^{\omega\,3}}\gamma^{\omega}}+\frac{\alpha}{\rho}\left(\frac{2C_3\gamma^{\omega 2}+2C_3\sqrt{V_{s,T}^{\omega}}\gamma^{\omega}+1}{\sigma_s^{\omega}V_{s,T}^{\omega}}+\frac{1}{\sigma_s^{\omega}\sqrt{V_{s,T}^{\omega}}\gamma^{\omega}}\right), \tag{72}$$

$$\mathcal{A}_2^{\omega}=\frac{2C_3^2\gamma^{\omega 3}+2C_3^2\sqrt{V_{s,T}^{\omega}}\gamma^{\omega 2}+C_3\left(V_{s,T}^{\omega}+3\right)\gamma^{\omega}+3C_3\sqrt{V_{s,T}^{\omega}}}{\sqrt{V_{s,T}^{\omega\,3}}}+\frac{1}{2\sqrt{V_{s,T}^{\omega}}\gamma^{\omega}}, \tag{73}$$

$$\mathcal{A}_3^{\omega}=\frac{C_3^2\gamma^{\omega 4}+2C_3^2\sqrt{V_{s,T}^{\omega}}\gamma^{\omega 3}+\left(C_3^2V_{s,T}^{\omega}+3C_3\right)\gamma^{\omega 2}+4C_3\sqrt{V_{s,T}^{\omega}}\gamma^{\omega}}{V_{s,T}^{\omega\,2}}$$
$$+\frac{6C_3V_{s,T}^{\omega}+3}{4V_{s,T}^{\omega\,2}}+\frac{1}{2\sqrt{V_{s,T}^{\omega\,3}}\gamma^{\omega}}, \tag{74}$$

$$V_{s,T}^{\omega}=\frac{\sigma_t^2}{\alpha^2}\left(\mathrm{e}^{-\alpha^2(s-t)}-\mathrm{e}^{-\alpha^2(T-t)}\right), \tag{75}$$

$$\gamma^{\omega}\left(V_{t,s},V_{s,T},\sigma_s\right)=\frac{\alpha\kappa+\rho\sigma_t\left(\mathrm{e}^{-\frac{1}{2}\alpha^2(s-t)}-1\right)-\frac{\sigma_t^2}{2\alpha}\left(1-\mathrm{e}^{-\alpha^2(T-t)}\right)}{\sigma_t\sqrt{\mathrm{e}^{-\alpha^2(s-t)}-\mathrm{e}^{-\alpha^2(T-t)}}}. \tag{76}$$

6.2. Numerical Approximation

In Tables 1-3 we compare the values of the approximate European call option prices approximated by different approaches with the corresponding estimation prices obtained by generalized Hull-White formula in Alòs (2006). The Monte Carlo Simulation (MCS) used number of simulation times by $N=10^6$ in order to achieve accuracy up to second decimal point. We have chosen $T-t=1, \ln X_t=100, r=0.1, \sigma_t=0.3, \alpha=1, \rho=0, \pm 0.5$ and varying values for the strike price K listed in the first column. Column 2-column 5 are corresponding option prices through MCS, Hagan's implied volatility formula (30), first order approximation by Full Dyson Series Expansion (63) and the one-dimensional time integral approximation formula (69), respectively.

The average calculation speed for each methods are listed in Table 4.

Although providing high accuracy, both Monte Carlo and Quasi Monte Carlo used in Dyson (63) is time-consuming. While Hagan (30) has a great advantage in calculation speed because the formula is analytic. Notice that it cost almost

same amount of time when comparing 1-Dim integral (69) and Uncorrelated pricing formula (48), which implies that not only (69) provides accuracy but also can be viewed as time efficiency.

Table 1. $\rho = 0$.

K	Monte Carlo	Hagan (30)	Uncorrelated pricing formula (48)
90	23.573138	23.415000	23.626726
95	20.440334	20.337570	20.457574
100	17.562962	17.624483	17.594033
105	15.066565	15.291032	15.063452
110	12.885739	13.322697	12.875527

Table 2. $\rho = -0.5$.

K	Monte Carlo	Hagan (30)	Formula I (63)	Formula II (69)
90	23.972526	22.025500	23.762565	23.704533
95	20.640584	19.229952	20.539753	20.772327
100	17.500136	16.889528	17.505670	17.792294
105	14.688296	14.952772	14.836533	14.581574
110	12.121686	13.353472	12.884976	11.002132

Table 3. $\rho = 0.5$.

K	Monte Carlo	Hagan (30)	Formula I (63)	Formula II (69)
90	22.352943	24.228522	22.979063	21.234073
95	20.035690	20.836574	20.304502	18.059835
100	17.186214	17.691469	17.555458	17.124973
105	15.172375	14.842598	14.965057	16.082605
110	13.080356	12.333288	12.802697	14.488551

Table 4. Methods comparison.

Methods	Time in seconds
Monte Carlo Simulation	29.117930
Hagan (30)	0.008773
Formula I (63)	27.315683
Formula II (69)	4.220214
Uncorrelated pricing formula (48)	4.172000

7. Conclusion

We derived that the European call option price for SABR model with $\beta = 1$ in two different approaches by means of Malliavin Calculus. The full Dyson series expansion is a high dimension integration with its integrand to be an infinite sum of asymptotic series. The second approach uses similar method as previous one but with different order; it yields to a first order approximation by time integral for the correction part of option price. A big advantage of the latter is that the integrand is analytic function. Besides, some partial results can be further extended to fractional Brownian motion case, which will be our future work.

Conflicts of Interest

The authors declare no conflicts of interest regarding the publication of this paper.

References

[1] Black, F. and Scholes, M. (1973) The Pricing of Options and Corporate Liabilities. *Journal of Political Economy*, **3**, 637-654. https://doi.org/10.1086/260062

[2] Hull, J. and White, A. (1987) The Pricing of Options on Assets with Stochastic Volatilities. *The Journal of Finance*, **42**, 281-300. https://doi.org/10.1111/j.1540-6261.1987.tb02568.x

[3] Hagan, P.S., Kumar, D., Lesniewski, A.S. and Woodward, D.E. (2002) Managing Smile Risk. *Wilmott*, **1**, 84-108.

[4] Als, E. (2006) A Generalization of Hull and White Formula with Applications to Option Pricing Approximation. *Finance and Stochastics*, **10**, 353-365. https://doi.org/10.1007/s00780-006-0013-5

[5] Fouque, J.-P., Papanicolaou, G. and Sircar, K.R. (2000) Derivatives in Financial Markets with Stochastic Volatility. Cambridge University Press, Cambridge.

[6] Gatheral, J. (2006) The Volatility Surface: A Practitioner's Guide. John Wiley & Sons, Hoboken.

[7] Jin, S., Peng, Q. and Schellhorn, H. ((2016)) A Representation Theorem for Expectations of Functionals of Brownian Motion. *Stochastics*, **88**, 651-679. https://doi.org/10.1080/17442508.2015.1116537

[8] Yor, M. (1992) On Some Exponential Functionals of Brownian Motion. *Advances in Applied Probability*, **24**, 509-531. https://doi.org/10.1017/S0001867800024381

[9] Nualart, D. (2008) The Malliavin Calculus and Related Topics. Springer, Berlin.

[10] Di Nunno, G., *et al.* (2008) Malliavin Calculus for Levy Process with Applications to Finance. Springer, Berlin. https://doi.org/10.1007/978-3-540-78572-9

[11] Bodie, Z., Cleeton, D. and Merton, R.C. (2008) Financial Economics. Pearson Prentice Hall, Upper Saddle River.

[12] Shreve, S.E. (2004) Stochastic Calculus for Finance II Continuous-Time Models. Springer, Berlin. https://doi.org/10.1007/978-1-4757-4296-1

[13] Pintoux, C. and Privault, N. (2011) The Dothan Pricing Model Revisited. *Mathematical Finance*, **21**, 355-363. https://doi.org/10.1111/j.1467-9965.2010.00434.x

[14] Lyasoff, A. (2016) Another Look at the Integral of Exponential Brownian Motion

and the Pricing of Asian Options. *Finance and Stochastics*, **20**, 1061-1096. https://doi.org/10.1007/s00780-016-0307-1

[15] Ito, K. (1951) Multiple Wiener Integral. *Journal of the Mathematical Society of Japan*, **3**, 157-169. https://doi.org/10.2969/jmsj/00310157

Appendix

Proof of Lemma 5.1

The conditional density of $\int_s^T \sigma_u^2 \mathrm{d}u$ can be obtained by integrating the joint probability density of $\left(\int_0^t \mathrm{e}^{\sigma W_s - \mu s}\mathrm{d}s, W_t\right), t > 0$. By Markov property of the volatility process σ_t and proposition 3.2 we have

$$\begin{aligned}\mathbb{P}\left(\int_s^T \sigma_u^2 \mathrm{d}u \le v \mid \sigma_s\right) &= \mathbb{P}\left(\int_0^{T-s} \mathrm{e}^{2\alpha(W_u)-\alpha^2 u}\mathrm{d}u \le \frac{v}{\sigma_s^2}, W_{T-s} < \infty\right) \\ &= \int_0^{\frac{v}{\sigma_s^2}} \int_{-\infty}^{\infty} \phi_{T-s,2\alpha,\alpha^2}(x,y)\mathrm{d}y\mathrm{d}x.\end{aligned} \quad \blacksquare \tag{77}$$

Proof of Theorem 5.3

Let $F = H(s, X_s, v_s)\Lambda_s$, recall that $\mathcal{F}_T^W \vee \mathcal{F}_t^Z := \sigma\{W_T, Z_t\}$ is the filtration generated by W_T and Z_t, using iterated conditioning we have, for $s \ge t$,

$$E[F \mid \mathcal{F}_t] = E\left[E\left[H_s\Lambda_s \mid \mathcal{F}_T^W \vee \mathcal{F}_t^Z\right] \mid \mathcal{F}_t\right] = E[\Lambda_s G_s \mid \mathcal{F}_t], \tag{78}$$

where $G_s = E\left[H_s \mid \mathcal{F}_T^W \vee \mathcal{F}_t^Z\right]$ is a random variable depending only on Brownian motion $\{Z_t\}_{t\ge 0}$, and we can apply exponential formula (12) to H_s. $\blacksquare$

Proof of Lemma 5.4

From the framework Black-Scholes Theory we know that

$\frac{\partial BS(t,x,\sigma)}{\partial x} = N(d_+)\mathrm{e}^x$, and accordingly

$H_s = \left(\frac{\partial^3}{\partial x^3} - \frac{\partial^2}{\partial x^2}\right) BS(s, X_s, v_s) = \frac{\sqrt{V_{s,T}} - d_+}{\sqrt{2\pi V_{s,T}}} \mathrm{e}^{X_s - \frac{d_+^2}{2}}$, for d_+ evaluated at (s, X_s, v_s).

It is obvious that $\frac{\mathrm{d}q^n}{\mathrm{d}x^n} = q$ for $\forall n \in \mathbb{N}$ and

$$\frac{\mathrm{d}p^n}{\mathrm{d}x^n} = \begin{cases} \dfrac{(-1)^{j+1} - d_-^2(x,t)}{\left(\sigma\sqrt{T-s}d_-(x,t)\right)^n} & \text{when } j = 1,2; \\ \dfrac{(-1)^{n-1}(n-1)!}{\left(\sigma\sqrt{T-s}d_-(x,t)\right)^n} & \text{for } j \ge 3. \end{cases} \tag{79}$$

Then $q(s, p(s, X_s, v_s), v_s) = \frac{-d_-}{\sqrt{2\pi V_{s,T}}} \mathrm{e}^{X_s - \frac{d_+^2}{2}} = H_s$, and by Lemma 2.15,

$$\begin{aligned} D_{\tau\otimes n}^{2n,Z} H_s &= D_{\tau\otimes n}^{2n,Z} q(s, p(s, X_s, v_s), v_s) \\ &= \sum_{k=1}^{2n} q^{(k)}(\cdot, p(\cdot)) \cdot B_{2n,k}\left(p'(\cdot), p''(\cdot), \cdots, p^{(2n-k+1)}(\cdot)\right) D_{\tau\otimes n}^{2n,Z} X_s \\ &= q(\cdot, p(\cdot)) \sum_{k=1}^{2n} B_{2n,k}\left(p'(\cdot), p''(\cdot), \cdots, p^{(2n-k+1)}(\cdot)\right) \prod_{i=1}^n \left(1-\rho^2\right)\sigma_{\tau_i}^2 \mathbb{1}_{\{\tau_i \le s\}} \\ &= \left(1-\rho^2\right)^n H_s B_{2n}\left(p'(\cdot), p''(\cdot), \cdots, p^{(2n)}(\cdot)\right) \prod_{i=1}^n \sigma_{\tau_i}^2 \mathbb{1}_{\{\tau_i \le s\}}. \end{aligned} \quad \blacksquare \tag{80}$$

Proof of Lemma 5.5

Note that the volatility in model (26) is an exponential martingale, thus Λ_s can be further simplified as $\Lambda_s := \left(\int_s^T D_s^W \sigma_r^2 \mathrm{d}r\right)\sigma_s = \left(\int_s^T 2\alpha\sigma_r^2 \mathrm{d}r\right)\sigma_s = 2\alpha V_{s,T}\sigma_s$. Then, for $t \le s \le T$, by Iterated conditioning property, we have

$$\begin{aligned} E\left[\Lambda_s G_s \mid \mathcal{F}_t\right] &= 2\alpha E\left[\sigma_s E\left[V_{s,T} G_s \mid \mathcal{F}_s\right] \mid \mathcal{F}_t\right] \\ &= 2\alpha E\left[\sigma_s E\left[f\left(s, X_s, v_s\right) \mid \mathcal{F}_s\right] \mid \mathcal{F}_t\right], \end{aligned} \tag{81}$$

where

$$f\left(s, X_s, v_s\right) = L_s^{\omega} \sum_{n=0}^{\infty} \frac{\left(\left(1-\rho^2\right)V_{t,s}\right)^n}{2^n n!} B_{2n}\left(p'\left(s, X_s^{\omega}, v_s\right), \cdots, p^{(2n)}\left(s, X_s^{\omega}, v_s\right)\right).$$

Recall that the conditional probability density of $V_{s,T}$ is given by (47), therefore the conditional expectation $E\left[f\left(s, X_s, v_s\right) \mid \mathcal{F}_s\right]$, through probabilistic approach, is $E\left[f\left(s, X_s, v_s\right) \mid \mathcal{F}_s\right] = \int_0^{\infty} f\left(s, X_s, \sqrt{\frac{v}{T-s}}\right) \frac{1}{\sigma_s^2} \psi_{V_{s,T}}\left(\frac{v}{\sigma_s^2}\right) \mathrm{d}v$, and

$$E\left[\Lambda_s G_s \mid \mathcal{F}_t\right] = 2\alpha E\left[\frac{1}{\sigma_s}\int_0^{\infty} f\left(s, X_s, \sqrt{\frac{v}{T-s}}\right) \psi_{V_{s,T}}\left(\frac{v}{\sigma_s^2}\right) \mathrm{d}v \mid \mathcal{F}_t\right]. \tag{82}$$

Denote $\sigma_s\left(W_s - W_t\right) = \sigma_t \mathrm{e}^{\alpha\left(W_s - W_t\right) - \frac{1}{2}\alpha^2(s-t)}$, $X_s^{x,y} = X_s^{\omega}\left(\sigma_t^2 x, \sigma_s\left(y\right)\right)$, define $h\left(V_{t,s}, \sigma_s\left(W_s - W_t\right)\right) = \frac{1}{\sigma_s}\int_0^{\infty} f\left(s, X_s\left(V_{t,s}, \sigma_s\right), \sqrt{\frac{v}{T-s}}\right) \psi_{V_{s,T}}\left(\frac{v}{\sigma_s^2}\right) \mathrm{d}v$, then again using proposition 3.2 we have

$$\begin{aligned} &E\left[\frac{1}{\sigma_s}\int_0^{\infty} f\left(s, X_s, \sqrt{\frac{v}{T-s}}\right) \psi_{V_{s,T}}\left(\frac{v}{\sigma_s^2}\right) \mathrm{d}v \mid \mathcal{F}_t\right] \\ &= E\left[h\left(V_{t,s}, \sigma_s\left(W_s - W_t\right)\right) \mid \mathcal{F}_t\right] \\ &= \int_0^{\infty}\int_{-\infty}^{\infty} h\left(\sigma_t^2 x, \sigma_s\left(y\right)\right) \phi_{s-t,2\alpha,\alpha^2}\left(x, y\right) \mathrm{d}y\mathrm{d}x. \end{aligned} \tag{83}$$

■

Proof of Theorem 5.6

This theorem is an extension result of Theorem 5.3, the proof is easily combine of Theorem 5.1 and Lemma 5.5, then Equation (49) becomes

$$\begin{aligned} V_t &= E\left[BS\left(t, X_t, v_t\right) \mid \mathcal{F}_t\right] + \frac{\rho}{2}\int_t^T \mathrm{e}^{-r(s-t)} E\left[\Lambda_s G_s \mid \mathcal{F}_t\right] \mathrm{d}s \\ &= E\left[BS\left(t, X_t, v_t\right) \mid \mathcal{F}_t\right] \\ &\quad + \rho\alpha\int_t^T \mathrm{e}^{-r(s-t)} E\left[\frac{1}{\sigma_s}\int_0^{\infty} f\left(s, X_s, \sqrt{\frac{v}{T-s}}\right) \psi_{V_{s,T}}\left(\frac{v}{\sigma_s^2}\right) \mathrm{d}v \mid \mathcal{F}_t\right] \mathrm{d}s \\ &= \int_0^{\infty} BS\left(t, X_t, \sqrt{\frac{v}{T-t}}\right) \frac{1}{\sigma_t^2} \psi_{V_{t,T}}\left(\frac{v}{\sigma_t^2}\right) \mathrm{d}v \\ &\quad + \rho\alpha\int_t^T \int_0^{\infty}\int_{-\infty}^{\infty} \mathrm{e}^{-r(s-t)} h\left(\sigma_t^2 x, \sigma_s\left(y\right)\right) \phi_{s-t,2\alpha,\alpha^2}\left(x, y\right) \mathrm{d}y\mathrm{d}x\mathrm{d}s \end{aligned}$$

$$
\begin{aligned}
&= \int_0^\infty \int_{-\infty}^\infty \frac{1}{\sigma_t^2} BS\left(t, X_t, \sqrt{\frac{v}{T-t}}\right) \phi_{T-t,2\alpha,\alpha^2}\left(\frac{v}{\sigma_t^2}, z\right) \mathrm{d}z\mathrm{d}v \\
&\quad + \rho\alpha \int_t^T \int_0^\infty \int_{-\infty}^\infty \int_0^\infty \int_{-\infty}^\infty l(s,v,z,x,y)\,\mathrm{d}z\mathrm{d}v\mathrm{d}y\mathrm{d}x\mathrm{d}s,
\end{aligned} \tag{84}
$$

where

$$
\begin{aligned}
&l(s,v,z,x,y) \\
&= \frac{\mathrm{e}^{-r(s-t)}}{\sigma_s(y)} \cdot f\left(s, X_s^{x,y}, \sqrt{\frac{v}{T-s}}\right) \cdot \phi_{T-s,2\alpha,\alpha^2}\left(\frac{v}{\sigma_s^2}, z\right) \cdot \phi_{s-t,2\alpha,\alpha^2}(x,y).
\end{aligned} \tag{85}
$$

Proof of Theorem 6.1

From Theorem 5.3 we see the expression of X_s and $d_\pm$, a straightforward algebra calculation shows that $X_s - \frac{d_+^2}{2} = -\frac{d_-^2}{2} + \left(\ln K - r(T-s)\right)$. Therefore we have the correction term as the following:

$$
\begin{aligned}
J &= \frac{\rho}{2}\int_t^T \mathrm{e}^{-r(s-t)} E\left[\frac{-d_-}{\sqrt{2\pi V_{s,T}}} \mathrm{e}^{X_s - \frac{d_+^2}{2}} 2\alpha V_{s,T}\sigma_s \mid \mathcal{F}_t\right]\mathrm{d}s \\
&= \frac{\rho}{2}\int_t^T \mathrm{e}^{-r(s-t)} \frac{2\alpha}{\sqrt{2\pi}} E\left[\sigma_s E\left[-d_- \mathrm{e}^{-\frac{d_-^2}{2} + (\ln K) - r(T-s)} \mid \mathcal{F}_T^W \vee \mathcal{F}_t^Z\right] \mid \mathcal{F}_t\right]\mathrm{d}s \\
&= C_1 \int_t^T E\left[\sigma_s Q_s \mid \mathcal{F}_t\right]\mathrm{d}s.
\end{aligned} \tag{86}
$$

Proof of Lemma 6.2

Recall that X_s by (50) is a linear function in $Z = \int_t^s \sigma_u \mathrm{d}Z_u$, where Z is conditional normal with zero mean and variance of $V_{t,s}$ *i.e.* $Z \sim \mathcal{N}(0, V_{t,s})$. Denote $\lambda(V_{s,T}) := \sqrt{\frac{1-\rho^2}{V_{s,T}}}$ and for simplicity we will write λ for $\lambda(V_{s,T})$ in all derivation following, thus

$$
d_-(s, X_s, v_s) = \frac{X_s + r(T-s) - \ln K - \frac{1}{2}V_{s,T}}{\sqrt{V_{s,T}}} = \lambda Z + \gamma, \tag{87}
$$

is also a linear function of Z. Substitute (87) into Q_s and use the normal probability density of Z we can solve for Q_s. For simplicity, we write $a = \lambda^2 V_{t,s} + 1$, $a = \lambda^2 V_{t,s} + 1$, $c = \frac{\gamma^2 V_{t,s}}{a}$, then

$$
\begin{aligned}
Q_s &= E\left[-(\lambda Z + \gamma)\mathrm{e}^{-\frac{(\lambda Z+\gamma)^2}{2}} \mid \mathcal{F}_T^W \vee \mathcal{F}_t^Z\right] \\
&= \int_{\mathbb{R}} -(\lambda z + \gamma)\mathrm{e}^{-\frac{(\lambda z+\gamma)^2}{2}} \frac{1}{\sqrt{2\pi V_{t,s}}} \mathrm{e}^{-\frac{z^2}{2V_{t,s}}}\mathrm{d}z
\end{aligned} \tag{88}
$$

$$= -\frac{1}{\sqrt{2\pi V_{t,s}}}\int_{\mathbb{R}}(\lambda z+\gamma)\mathrm{e}^{-\frac{a\left(z^2+2bz+c\right)}{2V_{t,s}}}\mathrm{d}z$$

$$= -\mathrm{e}^{\frac{a\left(b^2-c\right)}{2V_{t,s}}}\left(\frac{\gamma-\lambda b}{\sqrt{a}}\right) = -\frac{\gamma}{\left(2-\rho^2\right)^{3/2}}\mathrm{e}^{-\frac{\gamma^2}{2\left(2-\rho^2\right)}} = C_2\gamma\mathrm{e}^{C_3\gamma^2}$$

Notice that we used the fact that $\lambda^2 V_{t,s} = 1-\rho^2$ and $a = 2-\rho^2$ for the substitution in the second last equality.

Proof of Theorem 6.3

Since $R_s = \sigma_s\gamma\mathrm{e}^{C_3\gamma^2}$ is a random variable depends only on Brownian motion $\{W_t\}_{t\geq 0}$, we may apply exponential formula (12) to R_s such that:

$$E\left[R_s \mid \mathcal{F}_t\right] = \sum_{n=0}^{\infty}\frac{1}{2^n n!}r_n\left(s, X_t, v_t\right). \quad \blacksquare \tag{89}$$

Sketch of Proof of Corollary 6.2

The formal proof use no more techniques than calculating the first and second order Malliavin derivative of R_s based on the stochastic process of the volatility, and then apply freezing operator ω_W^t to Malliavin derivative of R_s for $t \leq s \leq T$, the integration result will be the correction term of the option price.

Step 1: Calculation of $D_\tau^{2,W}\gamma\left(V_{t,s}, V_{s,T}, \sigma_s\right)$

Denote γ as a short notation for $\gamma\left(V_{t,s}, V_{s,T}, \sigma_s\right)$ defined in lemma 6.2, and by chain rule (Theorem 2.7), $D_\tau^W\sqrt{V_{s,T}} = \frac{D_\tau V_{s,T}}{2\sqrt{V_{s,T}}} = \frac{\int_s^T D_\tau\sigma_u^2\mathrm{d}u}{2\left(\int_s^T\sigma_u^2\mathrm{d}u\right)^{\frac{1}{2}}}$, then we have

$$D_\tau^W\gamma = \frac{\sqrt{V_{s,T}}\left(\frac{\rho}{\alpha}D_\tau^W\sigma_s - \frac{1}{2}D_\tau^W V_{t,s}\right) - \frac{1}{2}\left(\sqrt{V_{s,T}}+\gamma\right)D_\tau^W V_{s,T}}{V_{s,T}}, \tag{90}$$

$$\begin{aligned}\left(D_\tau^W\gamma\right)^2 = &\frac{\left(\frac{\rho}{\alpha}D_\tau^W\sigma_s - \frac{1}{2}D_\tau^W V_{t,s}\right)^2}{V_{s,T}} + \frac{\left(\sqrt{V_{s,T}}+\gamma\right)^2}{4V_{s,T}^2}\left(D_\tau^W V_{s,T}\right)^2\\ &-\frac{\left(\frac{\rho}{\alpha}D_\tau^W\sigma_s - \frac{1}{2}D_\tau^W V_{t,s}\right)\left(\sqrt{V_{s,T}}+\gamma\right)}{\sqrt{V_{s,T}^3}}D_\tau^W V_{s,T}.\end{aligned} \tag{91}$$

$$\begin{aligned}D_\tau^{2,W}\gamma &= D_\tau^W\left(\frac{\frac{\rho}{\alpha}D_\tau^W\sigma_s - \frac{1}{2}D_\tau^W V_{t,s}}{\sqrt{V_{s,T}}}\right) - \frac{1}{2}D_\tau^W\left(\frac{\left(\sqrt{V_{s,T}}+\gamma\right)D_\tau^W V_{s,T}}{V_{s,T}}\right)\\ &= M - \frac{1}{2}N,\end{aligned} \tag{92}$$

where

$$M = \frac{\frac{\rho}{\alpha} D_\tau^{2,W}\sigma_s - \frac{1}{2} D_\tau^{2,W} V_{t,s}}{\sqrt{V_{s,T}}} - \frac{\frac{\rho}{\alpha} D_\tau^{W}\sigma_s - \frac{1}{2} D_\tau^{W} V_{t,s}}{2\sqrt{V_{s,T}^3}} D_\tau V_{s,T}, \tag{93}$$

$$N = \left(\frac{1}{2\sqrt{V_{s,T}^3}} - \frac{\sqrt{V_{s,T}}+\gamma}{V_{s,T}^2}\right)\left(D_\tau^W V_{s,T}\right)^2 + \frac{D_\tau^W \gamma}{V_{s,T}} D_\tau^W V_{s,T} + \frac{\sqrt{V_{s,T}}+\gamma}{V_{s,T}} D_\tau^{2,W} V_{s,T}. \tag{94}$$

Therefore, substitute M and N in (92) and combining like terms, we have

$$\begin{aligned} D_\tau^{2,W}\gamma = {} & \frac{\rho/\alpha}{\sqrt{V_{s,T}}} D_\tau^{2,W}\sigma_s - \frac{1}{2\sqrt{V_{s,T}}} D_\tau^{2,W} V_{t,s} - \frac{\sqrt{V_{s,T}}+\gamma}{2V_{s,T}} D_\tau^{2,W} V_{s,T} \\ & - \frac{\rho/\alpha}{\sqrt{V_{s,T}^3}} D_\tau^W \sigma_s D_\tau^W V_{s,T} + \frac{1}{2\sqrt{V_{s,T}}} D_\tau^W V_{t,s} D_\tau^W V_{s,T} \\ & + \frac{2\sqrt{V_{s,T}}+3\gamma}{4V_{s,T}^2}\left(D_\tau^W V_{s,T}\right)^2. \end{aligned} \tag{95}$$

Step 2: Calculation of $D_\tau^{2,W} R(s, X_s, v_s)$

Let $f(x,y) = yx\mathrm{e}^{C_3 x^2}$, then $R(s, X_s, v_s) = f(\gamma, \sigma_s)$ and $f_{yy} = 0$, by Product rule and Chain rule as well as Theorem 2.6 and 2.7,

$$\begin{aligned} D_\tau^{2,W} R_s = {} & f_x(\gamma,\sigma_s) D_\tau^{2,W}\gamma + f_{xx}(\gamma,\sigma_s)\left(D_\tau^W \gamma\right)^2 \\ & + f_y(\gamma,\sigma_s) D_\tau^{2,W}\sigma_s + 2 f_{xy}(\gamma,\sigma_s) D_\tau^W \gamma D_\tau^W \sigma_s \\ = {} & R_s\left[\left(\frac{1}{\gamma} + 2C_3\gamma\right) D_\tau^{2,W}\gamma + \left(6C_3 + 4C_3^2\gamma^2\right)\left(D_\tau^W\gamma\right)^2 \right. \\ & \left. + \frac{1}{\sigma_s} D_\tau^{2,W}\sigma_s + 2\left(\frac{1}{\gamma\sigma_s} + \frac{2C_3\gamma}{\sigma_s}\right) D_\tau^W\gamma D_\tau^W\sigma_s\right] \\ = {} & R_s\left[\frac{1}{\sigma_s} D_\tau^{2,W}\sigma_s + \left(\frac{1}{\gamma} + 2C_3\gamma\right)\left(\frac{\rho/\alpha}{\sqrt{V_{s,T}}} D_\tau^{2,W}\sigma_s \right.\right. \\ & \left. - \frac{1}{2\sqrt{V_{s,T}}} D_\tau^{2,W} V_{t,s} - \frac{\sqrt{V_{s,T}}+\gamma}{2V_{s,T}} D_\tau^{2,W} V_{s,T}\right) \\ & + 2\left(\frac{1}{\gamma\sigma_s} + \frac{2C_3\gamma}{\sigma_s}\right)\left(\frac{\frac{\rho}{\alpha}\left(D_\tau^W\sigma_s\right)^2 - \frac{1}{2} D_\tau^W\sigma_s D_\tau^W V_{t,s}}{\sqrt{V_{s,T}}}\right) \\ & + \left(6C_3 + 4C_3^2\gamma^2\right)\frac{\left(\frac{\rho}{\alpha} D_\tau^W\sigma_s - \frac{1}{2} D_\tau^W V_{t,s}\right)^2}{V_{s,T}} \\ & \left. - \frac{\rho}{\alpha}\mathcal{A}_1 D_\tau^W\sigma_s D_\tau^W V_{s,T} + \mathcal{A}_2 D_\tau^W V_{t,s} D_\tau^W V_{s,T} + \mathcal{A}_3\left(D_\tau^W V_{s,T}\right)^2\right], \end{aligned} \tag{96}$$

where

$$\mathcal{A}_1 = \frac{4C_3^2\gamma^3 + 4C_3^2\sqrt{V_{s,T}}\gamma^2 + 8C_3\gamma + 6C_3\sqrt{V_{s,T}}}{\sqrt{V_{s,T}^3}} \tag{97}$$

$$+\frac{1}{\sqrt{V_{s,T}^3}\gamma}+\frac{\alpha}{\rho}\left(\frac{2C_3\gamma^2+2C_3\sqrt{V_{s,T}}\gamma+1}{\sigma_s V_{s,T}}+\frac{1}{\sigma_s\sqrt{V_{s,T}}\gamma}\right),$$

$$\mathcal{A}_2=\frac{2C_3^2\gamma^3+2C_3^2\sqrt{V_{s,T}}\gamma^2+C_3\left(V_{s,T}+3\right)\gamma+3C_3\sqrt{V_{s,T}}}{\sqrt{V_{s,T}^3}}+\frac{1}{2\sqrt{V_{s,T}}\gamma}, \tag{98}$$

$$\mathcal{A}_3=\frac{4\left(C_3^2\gamma^4+2C_3^2\sqrt{V_{s,T}}\gamma^3+\left(C_3^2V_{s,T}+3C_3\right)\gamma^2+4C_3\sqrt{V_{s,T}}\gamma\right)+6C_3V_{s,T}+3}{4V_{s,T}^2}+\frac{1}{2\sqrt{V_{s,T}^3}\gamma}. \tag{99}$$

Step 3: Apply freezing operator ω_W^t to $D_\tau^{2,W}R\left(s,X_s,v_s\right)$ to obtain an analytical expression

Recall that the volatility process σ_t for $t\in[0,T]$ is defined by (27), which implies that for $0<t<s<T$, $\sigma_s=\sigma_t\mathrm{e}^{-\frac{1}{2}\alpha^2(s-t)+\alpha(W_s-W_t)}$. By the structure of σ_t for $t\in[0,T]$, we have the following results:

$$D_\tau^W\sigma_s=\alpha\sigma_s\mathbb{1}_{\{\tau\le s\}},\quad D_\tau^{2,W}\sigma_s=\alpha^2\sigma_s\mathbb{1}_{\{\tau\le s\}}, \tag{100}$$

$$D_\tau^W V_{s,T}=2\alpha V_{\tau\wedge s,T},\quad D_\tau^{2,W}V_{s,T}=4\alpha^2V_{\tau\wedge s,T}, \tag{101}$$

$$D_\tau^W V_{t,s}=2\alpha V_{\tau,s}\mathbb{1}_{\{\tau\le s\}},\quad D_\tau^{2,W}V_{t,s}=4\alpha^2V_{\tau,s}\mathbb{1}_{\{\tau\le s\}}. \tag{102}$$

The following results can be obtained by applying freezing operator ω_W^t to each integral of square of volatility for $t\le s\le T$,

$$\sigma_s^\omega:=\omega_W^t\circ\sigma_s=\sigma_t\mathrm{e}^{-\frac{1}{2}\alpha^2(s-t)}, \tag{103}$$

$$V_{t,s}^\omega:=\omega_W^t\circ V_{t,s}=\frac{\sigma_t^2}{\alpha^2}\left(1-\mathrm{e}^{-\alpha^2(s-t)}\right), \tag{104}$$

$$V_{s,T}^\omega:=\omega_W^t\circ V_{s,T}=\frac{\sigma_t^2}{\alpha^2}\left(\mathrm{e}^{-\alpha^2(s-t)}-\mathrm{e}^{-\alpha^2(T-t)}\right), \tag{105}$$

$$V_{t,T}^\omega:=\omega_W^t\circ V_{t,T}=\frac{\sigma_t^2}{\alpha^2}\left(1-\mathrm{e}^{-\alpha^2(T-t)}\right). \tag{106}$$

Thus, it is straightforward to calculate $\gamma^\omega\left(V_{t,s},V_{s,T},\sigma_s\right):=\omega_W^t\circ\gamma\left(V_{t,s},V_{s,T},\sigma_s\right)$ which we write γ^ω and $\mathcal{A}_k^\omega:=\omega_W^t\circ\mathcal{A}_k$, for $k=1,2,3$.

$$\begin{aligned}\gamma^\omega\left(V_{t,s},V_{s,T},\sigma_s\right)&=\omega_W^t\circ\frac{\kappa+\frac{\rho}{\alpha}\left(\sigma_s-\sigma_t\right)-\frac{1}{2}\left(V_{t,s}+V_{s,T}\right)}{\sqrt{V_{s,T}}}\\&=\frac{\alpha\kappa+\rho\sigma_t\left(\mathrm{e}^{-\frac{1}{2}\alpha^2(s-t)}-1\right)-\frac{\sigma_t^2}{2\alpha}\left(1-\mathrm{e}^{-\alpha^2(T-t)}\right)}{\sigma_t\sqrt{\mathrm{e}^{-\alpha^2(s-t)}-\mathrm{e}^{-\alpha^2(T-t)}}}.\end{aligned} \tag{107}$$

Combine these results with (96), we have for $\tau>s$,

$$
\begin{aligned}
D_\tau^{2,W} R_s^\omega &:= \omega_W^t \circ D_\tau^{2,W} R_s \\
&= R_s^\omega \left[\left(\frac{1}{\gamma^\omega} + 2C_3^2 \gamma^{\omega 2} \right) \left(-2\alpha^2 \left(\sqrt{V_{s,T}^\omega} + \gamma^\omega \right) \right) + \mathcal{A}_3^\omega \left(2\alpha V_{s,T}^\omega \right)^2 \right].
\end{aligned} \tag{108}
$$

Notice that when $\tau > s$, $D_\tau^W \sigma_s = D_\tau^W V_{t,s} = 0$. When $\tau \le s$,

$$
\begin{aligned}
& D_\tau^{2,W} R_s^\omega \\
&= R_s^\omega \left[\alpha^2 + \left(\frac{1}{\gamma^\omega} + 2C_3 \gamma^\omega \right) \left(\frac{\rho/\alpha}{\sqrt{V_{s,T}^\omega}} \alpha^2 \sigma_s^\omega - \frac{1}{2\sqrt{V_{s,T}^\omega}} 4\alpha^2 V_{\tau,s}^\omega \right. \right. \\
&\quad \left. - \frac{\sqrt{V_{s,T}^\omega} + \gamma^\omega}{2V_{s,T}^\omega} 4\alpha^2 V_{\tau,T}^\omega + 2 \left(\frac{\frac{\rho}{\alpha} \left(\alpha \sigma_s^\omega \right)^2 - \frac{1}{2} \alpha \sigma_s^\omega 2\alpha V_{\tau,s}^\omega}{\sigma_s \sqrt{V_{s,T}^\omega}} \right) \right) \\
&\quad + \left(6C_3 + 4C_3^2 \gamma^{2,\omega} \right) \frac{\left(\frac{\rho}{\alpha} \alpha \sigma_s^\omega - \frac{1}{2} 2\alpha V_{\tau,s}^\omega \right)^2}{V_{s,T}^\omega} \\
&\quad \left. - \frac{\rho}{\alpha} \mathcal{A}_1^\omega \alpha \sigma_s^\omega 2\alpha V_{\tau,T}^\omega + \mathcal{A}_2^\omega 2\alpha V_{\tau,s}^\omega 2\alpha V_{\tau,T}^\omega + \mathcal{A}_3^\omega \left(2\alpha V_{\tau,T}^\omega \right)^2 \right] \\
&= R_s^\omega \left[\alpha^2 + \left(\frac{1}{\gamma^\omega} + 2C_3 \gamma^\omega \right) \left(\frac{\rho \alpha^2 \mathrm{e}^{-\frac{1}{2}\alpha^2 (s-t)}}{\sqrt{\mathrm{e}^{-\alpha^2(s-t)} - \mathrm{e}^{-\alpha^2(T-t)}}} - \frac{2\alpha\sigma_t \left(\mathrm{e}^{-\alpha^2(\tau-t)} - \mathrm{e}^{-\alpha^2(s-t)} \right)}{\sqrt{\mathrm{e}^{-\alpha^2(s-t)} - \mathrm{e}^{-\alpha^2(T-t)}}} \right. \right. \\
&\quad - 2\alpha^2 \left(\sqrt{\frac{\sigma_t^2}{\alpha^2} \left(\mathrm{e}^{-\alpha^2(s-t)} - \mathrm{e}^{-\alpha^2(T-t)} \right)} + \gamma^\omega \right) \cdot \frac{\mathrm{e}^{-\alpha^2(\tau-t)} - \mathrm{e}^{-\alpha^2(T-t)}}{\mathrm{e}^{-\alpha^2(s-t)} - \mathrm{e}^{-\alpha^2(T-t)}} \\
&\quad \left. + 2 \frac{\rho \alpha^2 \mathrm{e}^{-\frac{1}{2}\alpha^2(s-t)} - \alpha\sigma_t \left(\mathrm{e}^{-\alpha^2(\tau-t)} - \mathrm{e}^{-\alpha^2(s-t)} \right)}{\sqrt{\mathrm{e}^{-\alpha^2(s-t)} - \mathrm{e}^{-\alpha^2(T-t)}}} \right) \\
&\quad + \left(6C_3 + 4C_3^2 \gamma^{2,\omega} \right) \frac{\left(\rho\alpha \mathrm{e}^{-\frac{1}{2}\alpha^2(s-t)} - \sigma_t \left(\mathrm{e}^{-\alpha^2(\tau-t)} - \mathrm{e}^{-\alpha^2(s-t)} \right) \right)^2}{\mathrm{e}^{-\alpha^2(s-t)} - \mathrm{e}^{-\alpha^2(T-t)}} \\
&\quad - 2\sigma_t^3 \frac{\rho}{\alpha} \mathrm{e}^{-\frac{1}{2}\alpha^2(s-t)} \left(\mathrm{e}^{-\alpha^2(\tau-t)} - \mathrm{e}^{-\alpha^2(T-t)} \right) \mathcal{A}_1^\omega \\
&\quad + \frac{4\sigma_t^4}{\alpha^2} \left[\left(\mathrm{e}^{-\alpha^2(\tau-t)} - \mathrm{e}^{-\alpha^2(s-t)} \right) \left(\mathrm{e}^{-\alpha^2(\tau-t)} - \mathrm{e}^{-\alpha^2(T-t)} \right) \mathcal{A}_2^\omega \right. \\
&\quad \left. \left. + \left(\mathrm{e}^{-\alpha^2(\tau-t)} - \mathrm{e}^{-\alpha^2(T-t)} \right)^2 \mathcal{A}_3^\omega \right] \right]
\end{aligned} \tag{109}
$$

Step 4: A time integral formula for the correction term of option price

Let $p(s) := \int_t^s D_\tau^{2,W} R_s^\omega \mathrm{d}\tau$ and $q(s) := \int_s^T D_\tau^{2,W} R_s^\omega \mathrm{d}\tau$ be the integration of $D_\tau^{2,W} R(s, X_s, v_s)$ for both $\tau \le s$ and $\tau > s$ case, respectively. By Corollary 1, the first order approximation for the correction term is

$$J_1 = C_1 C_2 \int_t^T 1 + \frac{1}{2} \int_t^T D_\tau^{2,W} R_s^\omega \mathrm{d}\tau \mathrm{d}s = \frac{1}{2} C_1 C_2 \left[\int_t^T p(s) + q(s) \mathrm{d}s + 2(T-t) \right]. \quad (110)$$

The detail integration calculation for $p(s)$ and $q(s)$ is omitted here, a remark for $q(s)$ is that when $\tau > s$, $D_\tau^{2,W} R_s^\omega$ does not depend on τ, which yields an simpler expression of $q(s)$ than $p(s)$. ■

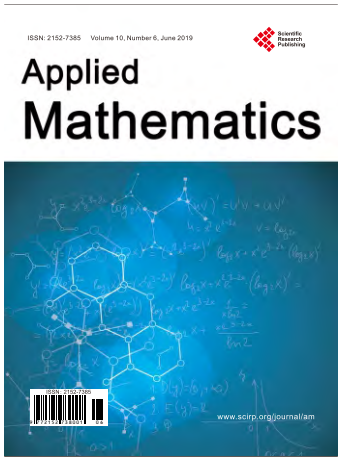

Call for Papers

Applied Mathematics (AM)

ISSN Print: 2152-7385 ISSN Online: 2152-7393
http://www.scirp.org/journal/am

Applied Mathematics **(AM)** is an international journal dedicated to the latest advancement of applied mathematics. The goal of this journal is to provide a platform for scientists and academicians all over the world to promote, share, and discuss various new issues and developments in different areas of applied mathematics.

Subject Coverage

All manuscripts must be prepared in English, and are subject to a rigorous and fair peer-review process. Accepted papers will immediately appear online followed by printed hard copy. The journal publishes original papers including but not limited to the following fields:

- Applied Probability
- Applied Statistics
- Approximation Theory
- Chaos Theory
- Combinatorics
- Complexity Theory
- Computability Theory
- Computational Methods in Mechanics and Physics
- Continuum Mechanics
- Control Theory
- Cryptography
- Discrete Geometry
- Dynamical Systems
- Elastodynamics
- Evolutionary Computation
- Financial Mathematics
- Fuzzy Logic
- Game Theory
- Graph Theory
- Information Theory
- Inverse Problems
- Linear Programming
- Mathematical Biology
- Mathematical Chemistry
- Mathematical Economics
- Mathematical Physics
- Mathematical Psychology
- Mathematical Sociology
- Matrix Computations
- Neural Networks
- Nonlinear Processes in Physics
- Numerical Analysis
- Operations Research
- Optimal Control
- Optimization
- Ordinary Differential Equations
- Partial Differential Equations
- Probability Theory
- Statistical Finance
- Stochastic Processes
- Theoretical Statistics

We are also interested in: 1) Short Reports—2-5 page papers where an author can either present an idea with theoretical background but has not yet completed the research needed for a complete paper or preliminary data; 2) Book Reviews—Comments and critiques.

Notes for Intending Authors

Submitted papers should not have been previously published nor be currently under consideration for publication elsewhere. Paper submission will be handled electronically through the website. All papers are refereed through a peer review process. For more details about the submissions, please access the website.

Website and E-mail

http://www.scirp.org/journal/am **E-mail: am@scirp.org**

What is SCIRP?

Scientific Research Publishing (SCIRP) is one of the largest Open Access journal publishers. It is currently publishing more than 200 open access, online, peer-reviewed journals covering a wide range of academic disciplines. SCIRP serves the worldwide academic communities and contributes to the progress and application of science with its publication.

What is Open Access?

All original research papers published by SCIRP are made freely and permanently accessible online immediately upon publication. To be able to provide open access journals, SCIRP defrays operation costs from authors and subscription charges only for its printed version. Open access publishing allows an immediate, worldwide, barrier-free, open access to the full text of research papers, which is in the best interests of the scientific community.

- High visibility for maximum global exposure with open access publishing model
- Rigorous peer review of research papers
- Prompt faster publication with less cost
- Guaranteed targeted, multidisciplinary audience

Scientific Research Publishing

Website: http://www.scirp.org

Subscription: sub@scirp.org

Advertisement: service@scirp.org